The mechanism of action and physiological role of PLCζ at fertilisation



Alaa Hachem
Department of Pharmacology
Worcester College

A thesis submitted for the degree of
Doctor of philosophy
Hilary 2018

Acknowledgements

I must firstly thank my supervisor Professor John Parrington for all his guidance and encouragement that helped me during the time of research and writing of this thesis. I am also very grateful to the previous and current lab members of Parrington's lab who have provided me with a good companion throughout my journey both in research and in life.

My sincere thanks also go to members of the academic staff of the Department of Pharmacology and their lab members, including, but not limited to Prof. Antony Galione, Prof. Fran Platt, Prof. Grant Churchill, Prof. Daniel Anthony and Dr. Ming Lei, who gave me access to their labs and research facilities. Without their precious support it would not be possible to conduct this research.

I have also benefited greatly from help given by the sponsor of my DPhil study in Oxford. This work would not have been possible without the financial support of the Higher Committee for Education Development in Iraq.

Special mention goes to Cath Frasier, Paula Savin, Hilary Long, Clive Garnham, Angela Curran, and to all staff members of Level-2 Biomedical Services for their constant help and support.

I would like also to express my greatest gratitude to all those including James Bae, Danni Zhu, and Faizzan Ahmad, who have provided me with great companionship throughout my time in Oxford. Special thanks should go to my cousin Tamer Alchemmari and his wife Zainab who have provided me with unlimited support and help. To the both of you I am deeply indebted; I thank you from the bottom of my heart.

Last but not least, I would like to thank my family for all their love and encouragement. Thank you for all the support you offered me.

Alaa Hachem
April, 2018
Oxford.

Publications

- **Hachem, A.**, Godwin, J., Ruas, M., Lee, H.C., Ferrer Buitrago, M., Ardestani, G., Bassett, A., Fox, S., Navarrete, F., de Sutter, P., Heindryckx, B., Fissore, R., Parrington, J. (2017) PLCζ is the physiological trigger of the Ca^{2+} oscillations that induce embryogenesis in mammals but offspring can be conceived in its absence. *Development*. 15;144(16):2914-2924.

  *Abstract accepted for poster presentation at the European Society of Human Reproduction and Embryology Annual meeting, Geneva, Switzerland. July 2017.

  *Abstract accepted for oral presentation at the 28th mammalian genetics and development workshop, UCL Institute of Child Health, London. November 2017.

- Parrington, J., Lear, P., and **Hachem, A.** (2015) Calcium signals regulated by NAADP and two-pore channels - their role in development, differentiation and cancer. *Int. J. Dev. Biol.* 59: 341-355.

Interview

The people behind the papers: Alaa Hachem & John Parrington, Posted by the Node Interviews (The community site for and by developmental biologists) on August 16th, 2017. http://thenode.biologists.com/people-behind-papers-alaa-hachem-john-parrington/interview/

List of abbreviations

PGC	Primordial germ cells
LH	Luteinising hormone
cAMP	Cyclic adenosine monophosphate
MPF	Maturation promoting factor
GVBD	Germinal vesicle breakdown
ER	Endoplasmic reticulum
PLC	Phospholipase C
IP_3	Inositol trisphosphate
PIP_2	Phosphatidylinositol 4,5-bisphosphate
DAG	Diacylglycerol
PKC	Protein kinase C
BAPTA	1,2-bis(o-aminophenoxy)ethane-N,N,N′,N′-tetraacetic acid
SERCA	Sarco-endoplasmic reticulum Ca^{2+} ATPases
CGE	Cortical granule exocytosis
MII	Second meiotic phase
CaMKII	Calmodulin-dependent protein kinase II
MI	First meiotic phase
ICSI	Intracytoplasmic sperm injection
CDK1	Cyclin-dependent kinase 1
MAPK	Mitogen-activated protein kinase
$SrCl_2$	Strontium chloride
cRNA	Complementary RNA
PH	Pleckstrin homology
domain	domain
NLS	Nuclear localisation signal
ART	Assisted reproductive technologies
FF	Fertilization failure
CAPZA3	Actin-capping protein gene
PAWP	WW domain-binding protein
YAP	Yes-associated protein
AOA	Assisted oocyte activation
TRP	Transient receptor potential

2-APB	2-aminoethoxydiphenyl borate
CRISPR	Clustered regularly interspaced short palindromic repeats
Cas9	CRISPR-associated protein 9
ZFN	Zinc finger nucleases
TALEN	Transcription activator-like effector nucleases
ESCs	Embryonic stem cells
tracrRNA	Transactivating CRISPR RNA
crRNAs	CRISPR RNAs
DSB	Double strand break
NHEJ	Nonhomologous end joining
HDR	Homology-directed repair
Indels	Insertions/deletions
ssODNs	Single-stranded DNA oligonucleotides
sgRNA	Single guide RNA
PAM	Protospacer adjacent motif
HRM	High resolution melting
PMSG	Pregnant mare's serum gonadotropin
hCG	Human Chorionic Gonadotropin
HTF	Human tubal fluid
RT-PCR	Reverse transcription-PCR
TIDE	Tracking of Indels by Decomposition
CASA	Computer-assisted semen analysis
VAP	Average pathway velocity
VSL	Straight-line velocity
VCL	Curvilinear velocity
ALH	Lateral head displacement
BCF	Beat cross frequency
LIN	Linearity
STR	Straightness
cADPr	Cyclic adenosine diphosphate-ribose
NAADPH	Nicotinic acid adenine dinucleotide phosphate
SOCE	Store-operated calcium entry

Abstract

Activation of the egg by the sperm is a key developmental event that in mammals triggered by the sperm-induced calcium oscillations. This has been proposed to be caused by the sperm-factor phospholipase C isoform zeta (PLCζ), although this remained a matter of debate for nearly 15 years.

The first part of this thesis demonstrates the successful use of the novel CRISPR/Cas9 gene editing technology in targeting the coding sequence of PLCζ gene in mouse embryos that subsequently has led to the creation of the first mouse model lacking the functional expression of PLCζ.

The main part of the thesis investigates the phenotype of the produced homozygous knockout male mutants. Functional analysis showed no adverse effects from the mutation on spermatogenesis, and normal sperm functional parameters. Although PLCζ-null sperm failed to trigger Ca^{2+} oscillations following ICSI procedures, experiments involving *in vitro* fertilisation, or fertilisation *in vivo* by natural mating, revealed that live offspring can still be conceived, albeit at greatly reduced efficiency and after a significant time delay. These findings suggest a yet-to-be identified PLCζ-independent route in mammalian egg activation that is completely dependent on sperm-egg membranes interactions.

Lastly, oocytes fertilised *in vivo* and *in vitro* by PLCζ-null sperm were found to be polyspermic. The significant finding supports the role of PLCζ protein in generating the standard Ca^{2+} oscillations that which govern the cortical and zonal reactions and membrane establishment following fertilisation. Oolemmal membrane localisation of Juno proteins post fertilisation showed complete dependency on sperm-oocyte interaction. However, Juno shedding mechanism failed to block the polyspermic fertilisation caused by lacking the expression of PLCζ. Thus, contradicting the proposed roles of Juno in establishing oocyte membrane block to supernumerary fertilisation in mammals.

Contents

1 **INTRODUCTION** ---- 1

1.1 GENERAL INTRODUCTION ---- 1
1.2 CALCIUM IONS AS A SECOND MESSENGER IN FERTILISATION: ---- 3
1.3 SOURCE OF CALCIUM IN OOCYTE ACTIVATION ---- 10
1.4 PHOSPHOLIPASE C - ZETA (PLCZ) ---- 14
1.4.1 PLCζ as a putative oocyte activation factor ---- 14
1.4.2 PLCζ structure ---- 21
1.4.3 Mammalian sperm PLCζ localisation ---- 24
1.5 OOCYTE ACTIVATION FAILURE AND MALE-FACTOR INFERTILITY ---- 28
1.6 FERTILISATION FAILURE AND ASSISTED OOCYTE ACTIVATION ---- 30
1.7 PLCZ AS A THERAPEUTIC AGENT IN ART ---- 33
1.8 AIM OF THE STUDY ---- 34

2 **GENERATION OF PLCZ MUTANTS BY CRISPR/CAS9 GENE EDITING TECHNOLOGY** ---- 35

2.1 BACKGROUND ---- 36
2.2 MATERIALS AND METHODS ---- 40
2.2.1 Animals ---- 40
2.2.2 sgRNA design ---- 40
2.2.3 sgRNA Production ---- 41
2.2.4 Generation of PLCζ-null mice by CRISPR/Cas9 microinjection ---- 42
2.2.5 Identification of PLCζ mouse knockouts at the DNA level ---- 44
2.2.5.1 PCR primer design ---- 44
2.2.5.2 Genomic DNA isolation ---- 44
2.2.5.3 Polymerase Chain Reaction (PCR) and Agarose gel electrophoresis ---- 45
2.2.5.4 Agarose gel electrophoresis ---- 46
2.2.5.5 DNA sequencing by Sanger sequencing ---- 46
2.2.5.6 High Resolution Melt (HRM) analysis ---- 46
2.2.5.7 TIDE analysis ---- 48
2.2.5.8 Identification of somatic mosaicism and DNA subcloning ---- 48
2.2.6 Identification of PLCζ mouse knockouts at the RNA level ---- 51
2.2.6.1 RNA extraction from mouse testes ---- 51
2.2.6.2 RNA agarose gel electrophoresis ---- 51

2.2.6.3 Reverse transcription primers design ---- 52
2.2.6.4 Single-step reverse transcription-PCR (RT-PCR) and sequencing---- 52
2.2.6.5 Real-time qRT-PCR ---- 53
2.2.7 Identification of PLCζ mouse knockouts at the protein level---- 55
2.3 RESULTS---- 56
2.3.1 Identification of mouse PLCζ knockouts at the DNA level ---- 56
2.3.1.1 Screening for indels in the transgenic founder (F0) mice ---- 56
2.3.1.2 DNA subcloning and traces from selected founders (F0) ---- 63
2.3.1.3 Generation and identification of PLCζ-null F1 animals ---- 65
2.3.2 Identification of mouse PLCζ knockouts at the RNA level ---- 67
2.3.3 Identification of mouse PLCζ knockouts at the protein level---- 68
2.4 DISCUSSION---- 69
2.4.1 Is it convenient, efficient and reliable to use CRISPR/Cas9 gene editing technology to target the coding sequence of PLCζ in mice? ---- 69
2.4.2 What is the best approach to identify the desired mutant alleles in F0 mosaic animals? -- 72
2.4.3 Is homozygous PLCζ deletion a lethal mutation?---- 74
2.5 CONCLUSION---- 75
3 **PLCZ MUTANT FUNCTIONAL ANALYSIS**---- 76
3.1 BACKGROUND ---- 77
3.2 MATERIALS AND METHODS ---- 77
3.2.1 Animals ---- 77
3.2.2 Histology---- 78
3.2.3 Sperm viability ---- 78
3.2.4 Sperm motility and hyperactivation ---- 79
3.2.5 Acrosome reaction---- 80
3.2.6 Calcium imaging post sperm injection ---- 80
3.2.7 Calcium imaging post IVF---- 81
3.2.8 Sperm penetration---- 82
3.2.9 Generation of recombinant PLCζ RNA---- 82
3.2.10 Microinjection of PLCζ cRNA---- 83
3.2.11 Calcium imaging---- 83
3.2.12 In vitro development of in vivo fertilized oocytes ---- 84
3.2.13 Analysis of Wbp2nl/PAWP mRNA expression in testis---- 84
3.2.14 Immunoblot analysis of PAWP in sperm ---- 85
3.2.15 Statistical Analyses---- 85
3.3 RESULTS---- 86
3.3.1 Spermatogenesis and sperm functional parameters of PLCζ knockouts ---- 86
3.3.1.1 Spermatogenesis analysis ---- 86
3.3.1.2 Sperm viability analysis ---- 88
3.3.1.3 Sperm motility and hyperactivation analysis---- 90

3.3.1.4 Acrosome reaction ---- 94
3.3.2 The effect of PLCζ-null sperm on triggering calcium oscillations in mouse eggs ---- 96
3.3.2.1 Sperm-PLCζ is required to trigger calcium oscillations in wildtype mouse oocytes – A sperm injection study. ---- 96
3.3.2.2 Sperm PLCζ is required to trigger calcium oscillations in wildtype mouse oocytes – in vitro fertilisation study. ---- 102
3.3.3 In vivo fertilisation and development with PLCζ^{em2Jparr} sperms. ---- 103
3.3.4 In vivo animal mating and live offspring development. ---- 105
3.3.5 Sperm penetration analysis ---- 107
3.3.6 In vitro fertilisation and blastocyst formation with PLCζ-null sperm ---- 108
3.3.7 PAWP expression analysis ---- 109
3.4 DISCUSSION ---- 110
3.4.1 Does PLCζ deletion compromise spermatogenesis and sperm quality parameters? ---- 110
3.4.2 Does the lack of PLCζ expression abolish the sperm's ability to induce Ca^{2+} rise post-fertilisation? ---- 114
3.5 CONCLUSION ---- 117
4 **POLYSPERMY AND JUNO SHEDDING** ---- 118
4.1 BACKGROUND ---- 119
4.2 MATERIALS AND METHODS ---- 122
4.2.1 In vivo fertilized eggs and sperm DNA staining ---- 122
4.2.2 In vitro fertilized eggs immunostaining against Juno and sperm DNA ---- 122
4.3 RESULTS ---- 124
1.1.1 Increased polyspermy in oocytes fertilized in vivo by PLCζ-null sperm ---- 124
1.1.2 Increased polyspermy in oocytes fertilized in vitro by PLCζ-null sperm ---- 126
1.1.3 Juno shedding post fertilisation is PLCζ-independent ---- 128
4.4 DISCUSSION ---- 131
4.4.1 Does sperm PLCζ contribute to block polyspermy? ---- 131
4.4.2 Does Juno's shedding mechanism contribute to oocyte membrane establishment? ---- 133
4.5 CONCLUSION ---- 135
5 **GENERAL DISCUSSION** ---- 136
5.1 CIRPSR/CAS9 APPROACH AND CREATING THE FIRST PLCZ KNOCKOUTS ---- 137
5.2 THE ROLE OF PLCZ IN MAMMALIAN FERTILITY ---- 139
5.3 THE ROLE OF PLCZ IN ZP BLOCKS AND MEMBRANE ESTABLISHMENT ---- 142
5.4 THEORIES OF THE ALTERNATIVE PATHWAY IN EGG ACTIVATION. ---- 144
5.5 GENERAL CONCLUSION ---- 150
6 **REFERENCE LIST** ---- 152

List of figures

Figure 1-1: Ca^{2+} responses following fertilisation in oocytes of various species. ---------- 6
Figure 1-2: The proposed models of egg activation ---------- 12
Figure 1-3: Intracellular Ca^{2+} oscillations in mouse oocytes measured by the fluorescence of Ca^{2+} sensitive dye. ---------- 15
Figure 1-4: Proposed role/mechanism of PLCζ in mammalian oocyte activation ---------- 20
Figure 1-5: Schematic representation of PLC isoenzyme domain structures. ---------- 23
Figure 1-6: Schematic drawing of a model for the functional structure of PLCζ ---------- 23
Figure 1-7: PLCζ localisation patterns in mouse sperm ---------- 25
Figure 1-8: PLCζ localisation patterns in human sperm from published studies ---------- 26
Figure 2-1: Generation of PLCζ mutants by CRISPR-Cas9 targeted disruption ---------- 43
Figure 2-2: Multiple DNA sequence alignment of PCR products on exon 3. ---------- 58
Figure 2-3: High-resolution melting curves shows that there are a variety of different melt curves for twelve PCR fragments from animals 8-20. ---------- 58
Figure 2-4: TIDE software is used to analyse the spectrum and frequency of indels formation in six F0 animals generated by targeting the same sequence on exon 3 with a pair of sgRNAs. ---------- 59
Figure 2-5: Multiple DNA sequence alignment of PCR products on exon 5 of mouse PLCζ for ten animals produced with wildtype Cas9 and a single gRNA activity. ---------- 60
Figure 2-6: Left, (1.5%) (w/v) agarose gel electrophoreses of PCR products from animals 1 to 6 which were produced by targeting exon 5 of PLCζ with wildtype Cas9 and single gRNA. Right, HRM analysis of animal number 2 against wildtype traces. ---------- 61
Figure 2-7: High-resolution melting curves show that there are a variety of different melt curves for twenty PCR fragments from animals 1-8 and animals from 21-33 produced with targeting exon 5 of PLCζ by wildtype Cas9 with a single gRNA. ---------- 62
Figure 2-8: The TIDE software is used to analyse the spectrum and frequency of indels formation in five animals generated by targeting the same region on exon 5 with a wildtype Cas9 and single gRNAs. ---- 62
Figure 2-9: Genomic characteristics of mouse PLCζ ^{em1Jparr} mutant allele ---------- 65
Figure 2-10: Genomic characteristics of mouse PLCζ ^{em2Jparr} mutant allele ---------- 66
Figure 2-11: PLCζ expression analysis in testes of PLCζ^{WT}, PLCζ ^{em1Jparr} and PLCζ ^{em2Jparr} ---------- 67
Figure 2-12: PLCζ immunoblot analysis of sperm samples from PLCζ^{WT}, and PLCζ ^{em1Jparr} ---------- 68
Figure 3-1: Histological analysis of testes sections stained with hematoxylin and eosin ---------- 87
Figure 3-2: Sperm viability analysis ---------- 89
Figure 3-3: Sperm progressive motility of wildtype and PLCζ$^{-/-}$ spermatozoa. ---------- 91

Figure 3-4: Sperm motility and hyperactivation parameters of wildtype and PLCζ$^{-/-}$ spermatozoa ------- 93
Figure 3-5: Induced acrosome reaction in PLCζ$^{-/-}$ and wildtype spermatozoa ---------- 95
Figure 3-6: Representative Ca^{2+} responses of wildtype mouse oocytes (n=13) fertilised with microinjected PLCζ ^{wt} sperm.---------- 97
Figure 3-7: Representative Ca^{2+} responses of wildtype mouse oocytes fertilised with microinjected PLCζ$^{-/-}$ spermatozoa. ---------- 97
Figure 3-8: Rescue of failed fertilisation with PLCζ cRNA (2µg/µl) microinjection. ---------- 98
Figure 3-9: In vitro produced embryos with ICSI in the absence of Ca2+ oscillations. ---------- 99
Figure 3-10: Ca^{2+} responses elicited by intracytoplasmic sperm injection (ICSI) into mouse oocytes. --- 100
Figure 3-11: Rescue of PLCζ$^{-/-}$ phenotype by cRNA injection ---------- 101
Figure 3-12: Ca^{2+} responses elicited by IVF into mouse oocytes ---------- 102
Figure 3-13: Analysis of mouse embryos produced in vivo ---------- 104
Figure 3-14: Images of heterozygous male and heterozygous female at 7-week old, produced from in vivo mating between homozygous PLCζ^{em1Jparr} male and PLCζ^{wt} female---------- 106
Figure 3-15: Mean percentage of oocytes showing sperm penetration as indicative of fertilization------- 107
Figure 3-16: Show IVF and embryo development rate with PLCζ^{em1Jparr} sperm---------- 108
Figure 3-17: Expression levels of Wbp2nl/PAWP in PLCζ mutant lines. ---------- 109
Figure 4-1: Polyspermic oocytes produced with natural mating ---------- 125
Figure 4-2: Increased polyspermy in oocytes fertilized by PLCζ^{em1Jparr} sperm ---------- 127
Figure 4-3: Presents oocytes inseminated in vitro with (A) PLCζ^{wt} and (B) PLCζ^{em1Jparr} spermatozoa---- 127
Figure 4-4: Representative confocal images of mouse oocytes exhibiting characteristic localisation of Juno proteins on the oolemma before and after incubation with sperm ---------- 130
Figure 5-1: Schematic represents the proposed mechanisms of egg activation following fertilisation with PLCζ-null sperm. ---------- 149

List of tables

Table 2-1: sgRNA targeting sequences on the mouse PLCζ gene---------- 40
Table 2-2: Genotyping primer sequences---------- 44
Table 2-3: PCR reaction setup---------- 45
Table 2-4: Thermocycling conditions for PCR---------- 45
Table 2-5: HRM reaction setup ---------- 47
Table 2-6: Thermocycling conditions for HRM ---------- 47
Table 2-7: RT-PCR primers sequence---------- 52
Table 2-8: RT-PCR reaction mix---------- 52
Table 2-9: Thermocycling conditions for RT-PCR ---------- 53
Table 2-10: One-step real time RT-PCR reaction mix---------- 53
Table 2-11: Thermocycling conditions for one step real time RT-PCR---------- 54
Table 3-1: Ca^{2+} oscillations following ICSI with PLCζ$^{-/-}$ and wildtype spermatozoa. ---------- 98
Table 3-2: Mating pairs and fertility parameters---------- 106

1 Introduction

1.1 General introduction

Sexual reproduction in mammals is maintained by a permanent syngametic fusion between sperm and oocyte in the female reproductive tract. The process requires formation of highly specialised haploid gametes, capable of restoring the diploid number of the chromosomes in the newly formed individual. The resulting offspring's genome consists of a combination of the parental DNA with a slight alteration through a naturally occurring genetic recombination during meiosis.

In *Homo sapiens* and in *Mus musculus*, gonadogenesis starts at the time of embryonic gastrulation when a population of primary undifferentiated cells (the primordial germ cells - PGCs) migrate from the epiblast layer of the embryo to the future position of the gonads at the gonadal ridge (Nikolic et al., 2016). Upon arrival, the PGCs start to differentiate according to the sexual and gonadal determination system to spermatogonia if the embryos' sex chromosomes are XY, if XX the cells will then be differentiated to oogonia (Sadler and Langman, 2012).

In males, spermatogenesis takes place near the time of puberty in the seminiferous tubules of the testes. The process includes formation of the haploid spermatozoa from the diploid spermatogonial stem cells. During meiosis, the cells undergo single DNA replication and two cell divisions, before entering the critical stage of cytodifferentiation and maturation (Griswold, 2016). Sperm maturation involves transforming the round spermatid into a fertilisation-competent cell; this includes formation of the acrosomal cap, condensation of the nucleus, shedding most of the cytoplasm, and formation of the neck, middle piece, and the tail of the spermatozoon (Sadler and Langman, 2012; O'Donnell *et al.*, 2011). The mature spermatozoa are released from the supporting Sertoli cells into the seminiferous tubules, and then pushed by the peristaltic movement of the smooth muscles towards the epididymis where the last part of the sperm maturation process take place.

The epididymal lumens and ducts help the maturation process by providing a cocktail of essential materials for the sperm to acquire the ability to swim in the female genital tract by the propulsive movement of the tail (Dacheux *et al.*, 2005; Arrotéia *et al.*, 2012).

Unlike spermatogenesis in the male, the formation and differentiation of the oocytes start much earlier, while the female is still at the neonatal stage. It begins when a group of PGCs start to differentiate into oogonia with most of them entering the first meiotic (MI) division and forming the primary oocyte (Sadler and Langman, 2012). However, most of the oocytes remain naturally arrested at the dictyate/diplotene stage of prophase I, and do not complete their first meiotic division until puberty (Jones, 2005; Celik *et al.*, 2015). The meiosis arrest can last for months in mice and years in women, and is maintained by the inhibitory follicular environment of the somatic supporting cells surrounding the oocyte (Jones, 2004). At the time of puberty and in response to the luteinising hormone (LH) surge near the mid-cycle, the primary oocyte exits the first meiosis and enters the metaphase of MII where it remains arrested until fertilisation (Arur, 2017). It is believed that the collagenase activity of the LH on the mature follicles during ovulation causes a physical discontinuity between the supporting cells and the oocyte leading to a sudden increase in maturation promoting factor (MPF) (Krisher, 2013). This increase in MPF levels might happen directly or indirectly due to the reduction in the oocyte's cyclic adenosine monophosphate (cAMP) levels, which at this stage triggers the resumption of the MI and breakdown of the germinal vesicle (GVBD) (Senthilkumaran, 2011; Tsafriri *et al.*, 1994; Jones, 2004).

At fertilisation, a sperm is responsible for providing half of the genetic material to the new individual, and also to trigger a temporally ordered series of events collectively known as egg activation. The process involves a multitude of cellular changes include cortical and zona reactions to prevent polyspermy, resumption of the MII, and metabolic activation of the egg that precedes the first embryonic cell division (Kline and Kline, 1992; Stricker, 1999; Rauh *et al.*, 2005; Ducibella *et al.*, 2006; Parrington *et al.*, 2007; Swann and Yu, 2008).

1.2 Calcium ions as a second messenger in fertilisation:

Cells generate intracellular signalling cascades to adapt to environmental changes, and calcium (Ca^{2+}) is the most universal carrier of signals (Berridge and Galione, 1988). In most of the biological systems found in nature, changes in the concentration of intracellular free Ca^{2+} can regulate a wide range of physiological processes as diverse as cell proliferation, muscle contraction, synaptic plasticity, secretion, and cell death.

Needless to say that fertilisation is not an exception and the process relies heavily on Ca^{2+} as a universal second messenger in controlling oocyte maturation, egg activation, and embryo development (Parrington *et al.*, 2015). The proposal that Ca^{2+} signal is fundamental for every fertilisation event is supported by the fact that sperm-oocyte fusion triggers Ca^{2+} release from the oocyte's internal stores, leading to release of the oocyte from MII arrest, and kick-starting male and female pronuclei formation (Miyazaki *et al.*, 1992). Artificially manipulating Ca^{2+} ions can also induce the same activating events that can lead to embryonic development. For instance, introducing Ca^{2+} ions directly by microinjection was found to be sufficient to oocyte activation and trigger embryonic development to the blastocyst stage in mice (Kline and Kline, 1992; Swann and Yu, 2008; Ozil *et al.*, 2005). Moreover, inhibiting the Ca^{2+} rise by buffering its action with Ca^{2+} chelators, such as 1,2-bis(o-aminophenoxy)ethane-N,N,N′,N′-tetraacetic acid (BAPTA), blocks all oocyte activation events (Kline and Kline, 1992), affecting the membrane block to polyspermy (Gardner *et al.*, 2007b) and inhibiting the first mitotic cycle division (Kono *et al.*, 1996). Furthermore, manipulating the Ca^{2+} release from the egg's internal stores by utilising the Ca^{2+} ionophore-A23187, induced parthenogenetic egg activation in complete independence of the ionic composition of the external environment (Steinhardt *et al.*, 1974). These phenomena were observed in several species widely separated phylogenetically, signifying the importance of the Ca^{2+} signalling for every fertilisation event in most of the studied species.

One of the key contributors to the dynamics of the Ca^{2+} signal in eggs is the endoplasmic reticulum (ER). The luminal structure of the ER is the main storage site for the bound calcium that is released into the cytosol in response to certain stimuli (Stricker, 2006). In almost all species studied so far, it has been found that inducing Ca^{2+} rise by sperm-oocyte fusion or by using a variety of agonists, was always accompanied by a wave of Ca^{2+} in the

cytosol, followed by a rapid decline in the ER's content then by a gradual recovery (Wakai and Fissore, 2013; Takahashi *et al.*, 2013).The spatio-temporal organisation of the Ca^{2+} rises vary between species and can act as a signal that regulates a wide spectrum of cellular activities. In medaka fish, sea urchin, starfish and frog, a single Ca^{2+} wave originates at the site of sperm entry was found to traverse the entire egg leading to initiate the series of egg activation (Ridgway *et al.*, 1977; Steinhardt *et al.*, 1977; Eisen and Reynolds, 1984; Busa and Nuccitelli, 1985). In mammalian oocytes, however, the Ca^{2+} rises following sperm entry involve a pattern of periodical increases, known as Ca^{2+} oscillations, and the persistence of these transients appears to be critical for resumption of MII and embryo development (Cuthbertson and Cobbold, 1985; Miyazaki *et al.*, 1986; Ducibella *et al.*, 2006) (See figure 1.1).

It was found that local Ca^{2+} rise due to a fertilisation-like event could contribute directly or indirectly to more Ca^{2+} being released periodically from the ER by a positive feedback mechanism of Ca^{2+}-induced Ca^{2+} release (CICR) (Berridge and Galione, 1988; Galione *et al.*, 1993a). CICR is triggered by the opening of the ryanodine receptor which plays a central role in globalising the Ca^{2+} signal, through initiating a regenerative wave capable of sweeping through the cytoplasm (Berridge, 1997). A transmembrane influx of Ca^{2+} was also found to be essential to refill the ER in order to sustain the persistency of the oscillatory rises. In a medium devoid of extracellular Ca^{2+}, a reduction in intraluminal ER Ca^{2+} levels was observed with each releasing event leading to a total cessation of the oscillations over time (Bernhardt *et al.*, 2017). Consequently, depleting the ER content or inhibiting Ca^{2+} reuptake via the sarco-endoplasmic reticulum Ca^{2+} ATPases (SERCA) would always prematurely terminate the Ca^{2+} rise (Berridge *et al.*, 2000).

Sperm entry in mammals causes the cytoplasmic Ca^{2+} concentration of the oocyte to oscillate periodically between increase and decrease in a repetitive manner which lasts for several hours (Kline and Kline, 1992; Swann and Ozil, 1994; Jones, 1998a; Miyazaki and Ito, 2006). In contrast, eggs from non-mammalian species such as medaka fish, sea urchins, and frogs require only a single Ca^{2+} transient (wave-like propagation) which last only for several minutes (Swann and Whitaker, 1986; Nuccitelli, 1987; Galione *et al.*, 1994).

It is not clear why there is an observable difference between species in the pattern of Ca^{2+} release (wave-like vs oscillations). However, Jones (1998a) hypothesized that the reasons

for the long-lasting Ca^{2+} oscillations in animals with internal fertilisation is possibly due to the time that is required for ovulation, cortical granule exocytosis (CGE), resumption of MII, and the first cell division. In contrast, animals with external fertilisation such as in frogs, medaka fish, and sea urchin, the egg is usually shed with already completed meiosis which then almost instantaneously interacts with sperm. Thus, a single Ca^{2+} wave would then be sufficed to induce embryonic development in no more than a few tens of minutes.

It has been long recognised that Ca^{2+} oscillations and waves play a central role in egg activation in almost all the species studied so far (Homa and Swann, 1994). However, the nature, amplitude, and duration of the transients are largely species-specific (Jones, 1998a; Stricker, 1999; Ducibella *et al.*, 2002). Nevertheless, each Ca^{2+} transient was found to last for about 1-2 minute in mammals, and 10-minutes intervals between each of the transients of the oscillations (Swann and Ozil, 1994). Oscillations were also observed in non-mammalian species, such as molluscs, nemertean worms, and ascidians (Speksnijder *et al.*, 1989; Deguchi and Osanai, 1994; Stricker, 1999). However, in those systems the oscillations tend to be different from mammals in terms of their amplitude, frequency, and the time that is required for signal termination after sperm entry.

In most species, it has been found that the site of the first Ca^{2+} transient initiation was always originated at the site of sperm entry, and then it changes spatially for the following transients. In ascidians, for example, the initiation site moves gradually toward the vegetal pole of the oocyte (Carroll *et al.*, 2003), whereas in mice, the subsequent transients were reported to translocate from the site of sperm entry to the cortex of the vegetal pole (Deguchi *et al.*, 2000), which then come to a total cessation at the time of pronuclear formation (Marangos *et al.*, 2003).

The spatial and temporal organisation of the cytosolic free Ca^{2+} that traverses the entire cytoplasm appears to be very important in activating different events in different regions within the oocyte. It appears that the oscillatory signal in mammals encodes specific information with each pulse that can be efficiently transmitted through the cytosol (Smedler and Uhlen, 2014).

Manipulating the oscillatory signal experimentally with electric field pulses, circumvents the difficulties in studying the endogenous oscillations without causing detrimental effects

to development. A study by Ducibella et al. (2002) found that initiating the early events of oocyte activation, such as in CGE, was found to require a lower number of oscillations compare to the later events of meiosis and maternal mRNA recruitment. Indeed, from a physiological point of view, CGE is initiated before MII resumption, and the benefit of the early initiation is important in membrane establishment to block polyspermy (Ozil et al., 2006). On the other hand, the spatial organization of Ca2+ changes appears to be depend on the strategic distribution of Ca2+ stores and the targeted effectors within the cell (Thomas et al., 1996). For example, CGE occurs near to the cortex of the oocyte, whereas the completion of MII takes place at the pole opposite to the site of sperm entry (Talansky et al., 1991; Mehlmann et al., 1995).

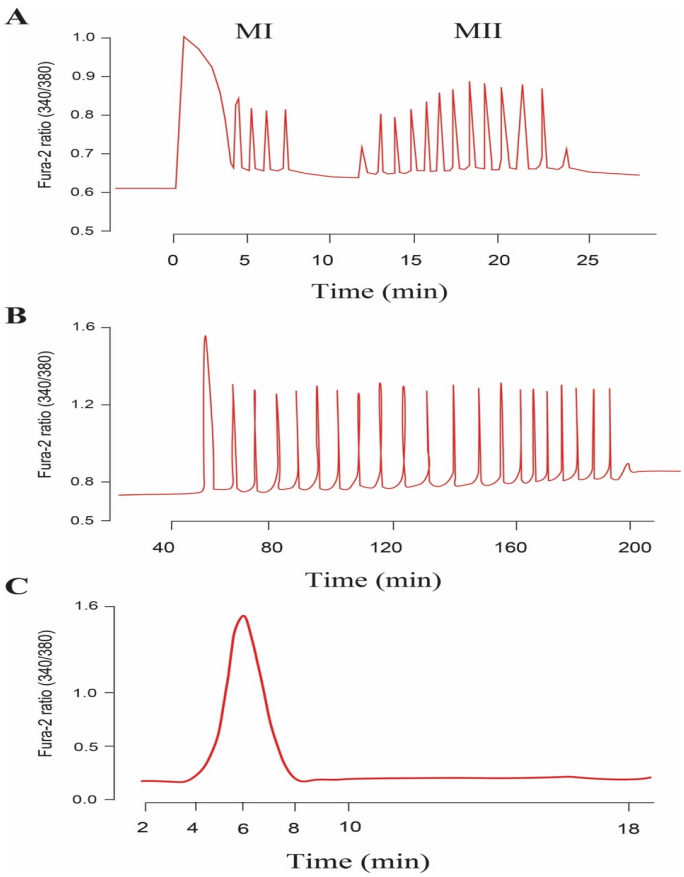


Figure 1-1: Ca^{2+} responses following fertilisation in oocytes of various species.

A. Adapted from (McDougall and Levasseur, 1998)
B. Adapted from (Saunders et al., 2002)
C. Adapted from (Busa and Nuccitelli, 1985)

Several studies have shed light on the role of the Ca^{2+} increase in alleviating the MII arrest and pronuclear formation in mammals. It has been found that an elevated Ca^{2+} concentration in a fertilisation-like event could trigger the resumption of MII through a CaMKII-mediated down-regulation of MPF activity. The cell metaphase arrest in mammals is maintained by the activity of oocyte MPF and the activity of its mediator early mitotic inhibitor 2 (Emi2) (Masui and Markert, 1971; Duesbery and Vande Woude, 1998). High MPF activity was found to be responsible for maintaining the oocyte's chromatin in a condensed state and stabilizes the meiotic spindle (Whitaker, 1996), while Emi2 regulates metaphase II arrest by inhibiting the anaphase-promoting complex/cyclosome (APC/C). MPF is composed of two subunits: cyclin-dependent kinase (CDK), and cyclin B1; CDK was found to utilise cellular ATP to phosphorylate specific serine and threonine residues of target proteins, whereas cyclin B1 works as a regulatory subunit for CDK.

The periodic increases in intracellular Ca^{2+} levels upon fertilization results in periodic increases in Ca^{2+}/calmodulin-dependent protein kinase II (CaMKII) activity (Ducibella *et al.*, 2006). Active form of CaMKII phosphorylates Emi2 at a specific residue (Rauh *et al.*, 2005), which then create a docking site for further phosphorylation by a protein kinase Polo-like kinase 1 (PLK1), that subsequently targets Emi2 for destruction (Suzuki *et al.*, 2010a; Ohe *et al.*, 2010). Lifting the inhibitory effect of Emi2 activates the APC/C that in turn stimulates the proteolysis of cyclin B (Clift and Schuh, 2013). Cyclin B degradation was found to be triggered by an increase in the activity of an E3 ubiquitin ligase leading to a decrease in MPF activity, and resumption of meiosis as the oocyte enters anaphase (Hyslop *et al.*, 2004). It was also found that CDK phosphorylation by Wee1B is required for MPF inactivation in the CaMKII-driven exit from meiosis (Oh *et al.*, 2011). In mammals, a brief Ca^{2+} rise was found to be sufficient to transiently degrade MPF; however, the normal levels were rapidly restored. Therefore, it is likely to highlight that the purpose of the repetitive transients is to maintain an effective suppression on the MPF levels for enough time for the oocytes to escape MII without damaging the oocytes by excessive Ca^{2+} or depleting ATP levels (Ozil and Swann, 1995; Miao *et al.*, 2012).

On the other hand, it was shown by number of studies that mitogen-activated protein kinases (MAPK) is responsible for the oocyte late activation events, such as PNs formation (Verlhac *et al.*, 1994). Two isoforms of MAPK were found to be expressed widely in mammalian oocytes; extracellular signal-regulated (ERK1 and ERK2) kinases, which are

usually activated by the upstream protein kinases Mos, and MEK1 and MEK2 (Gonzalez-Garcia *et al.*, 2014). However, Mos was found not to be required for maintaining MII in mammals (Suzuki *et al.*, 2010a).

Exiting from miosis and entering into the interphase was also shown to be dependent on the levels of MAPK and CDK1/Cyclin B. MPF downregulation is usually preceding the reduction of MAPK; Whereas, MAPK activity gradually decreases at the beginning of the Ca^{2+} oscillations, and never reaches total cessation until PNs formation (Gonzalez-Garcia *et al.*, 2014) (See figure 1.4).

The mechanism by which the Ca^{2+} oscillations can regulate MAPK activity is still poorly understood. Gonzalez-Garcia and colleagues (2014) found that a premature termination of the Ca^{2+} oscillations by BAPTA after the initial Ca^{2+} rise delays MAPK inactivation by roughly two hours. It appears that the numbers of the Ca^{2+} oscillations, and the duration of each single Ca^{2+} transient may contribute to modulating the MAPK inactivation (Ducibella *et al.*, 2002). Over expressing the upstream MEK in mouse oocytes has led to a sustained level of MAPK after fertilisation, which has prevented PNs formation (Moos *et al.*, 1996). Inhibiting MEK with a specific inhibitor (U0126) led to de-phosphorylation of ERK1 and ERK2 and parthenogenetic activation of mouse oocytes with no observable effects on MPF levels (Phillips *et al.*, 2002). Similarly, PNs formation was found to be accelerated in oocytes treated with a kinase inhibitor (DMAP), which has found be associated with a rapid reduction in MAPK activity (Liu and Yang, 1999). Thus, the timing for MAPK inactivation is crucial both in preventing premature formation of the PNs and premature termination of the Ca^{2+} oscillations (Day *et al.*, 2000).

In a study by Phillips and colleagues, a CDK inhibitor (Roscovitine) was found to induce eggs parthenogenesis via MPF inactivation, and subsequent MAPK decline similar to that following fertilisation (Phillips *et al.*, 2002). Studying the luminescence activities of the luciferase-tagged ERK1 and ERK2, Gonzalez-Garcia and colleagues highlighted the importance of MPF levels on the MAPK inactivation, suggest that the two pathways are somehow in a linked-state from the MPF side only. In this sense, MPF levels appears to act on safeguarding the oocyte from any premature termination of the Ca^{2+} oscillations by an abnormal MAPK decline.

In contrast to Ca^{2+} rise following fertilisation, intracellular Zn^{2+} levels have been reported by several studies to be central in regulating the meiotic maturation and MII resumption in oocyte (Kim *et al.*, 2011; Duncan *et al.*, 2016; Zhang *et al.*, 2016; Que *et al.*, 2015). It was found that disturbing the zinc homeostasis during MI by utilising the zinc chelator (TPEN), perturbed MPF re-establishment and blocked MI progression in oocyte (Kim *et al.*, 2010; Bernhardt *et al.*, 2011). Moreover, activating MII oocyte with a fertilising sperm or parthenogenetically, triggers Zn^{2+} fluxes to the extracellular space which were found to be associated with the first Ca^{2+} transients, in a secretory event termed as the "zinc spark". Furthermore, zinc fluxes can also be triggered artificially with TPEN. A Zn^{2+} chelator was found to be efficient in releasing the oocyte from MII arrest and development to term, in the absence of the Ca^{2+} transients (Suzuki *et al.*, 2010b). However, inhibiting the Ca^{2+} transients with BAPTA blocked the Zn^{2+} fluxes, and all the associated events with oocyte activation (Kim *et al.*, 2011). The findings suggest that Zn^{2+} dynamics is required for normal development of the oocyte, and is sufficient to induce egg activation and to conceive live offspring in a complete independency on Ca^{2+} rise.

The precise signalling mechanism that involves Zn^{2+} in egg activation remains unclear, and a Zn^{2+} dependent pathways has not been established. However, a possible explanation is that Zn^{2+} fluxes are activating the downstream effectors of the Ca^{2+} oscillations, and Ca^{2+} rise in this sense is only required to initiate the Zn^{2+} spark. For example, Zn^{2+} fluxes may modulate Emi2 expression following MII arrest. The fact that Emi2 activity can be abolished by a single point mutation on the Zn^{2+}-binding region, has led to the notion that a Zn^{2+} binding site may directly modulate Emi2 (Schmidt *et al.*, 2005). Similarly, the reduction in Zn^{2+} levels have also been suggested to modulate the phosphatase activity of cdc25c, which in turn phosphorylates MPF/CDK and induces cell cycle resumption (Sun *et al.*, 2007).

1.3 Source of calcium in oocyte activation

Three main models were hypothesised to explain the mechanism which triggers a Ca^{2+} signal in response to sperm entry:

The first model - The Ca^{2+} conduit model - proposed that sperm-egg/oocyte fusion works by introducing a small amount of Ca^{2+} into the egg/oocyte's cytoplasm via channels on the surface membrane of the sperm leading to CICR and egg/oocyte activation (Jaffe, 1983) (See figure 1.2A). However, findings from Steinhardt *et al.* (1974) and Schmidt *et al.* (1982) invalidated this model as they demonstrated that successful fertilisation can still be achieved in sea urchin eggs in the absence of the extracellular Ca^{2+}. Moreover, a single Ca^{2+} rise has been shown to be incapable of triggering the repetitive Ca^{2+} transients that normally accompany fertilisation in mammals (Swann and Ozil, 1994). This model did not pass the test of time, as it was later found that Ca^{2+} influx take place after the first Ca^{2+} transient, and its role was found to be to replenish the demand from the ER to sustain the repetitive release of Ca^{2+} (Miao *et al.*, 2012).

The second model - the membrane receptor model - was the dominant hypothesis for many years (Swann and Jones, 2002; Parrington *et al.*, 2007). This proposed that the Ca^{2+} rise and egg activation processes are mediated by a sperm- oocyte surface interaction (See figure 1.2B). A binding site on the oocyte's membrane would trigger a signalling cascade similar to the mechanism of cell signalling in somatic cells via the G-protein coupled receptor and/or receptor tyrosine kinase pathways, which triggers Ca^{2+} release in response to sperm binding (Evans and Kopf, 1998; Machaty, 2013). However, numerous studies provided evidence against this pathway by showing that inhibiting the G-protein coupled or tyrosine kinase pathways failed to block Ca^{2+} oscillations or activation in mammalian oocytes after sperm entry (Swann and Jones, 2002). In fact, sperm-oocyte fusion in mice always precede the onset of the first Ca^{2+} rise by 1-3 min, suggesting that the trigger for the Ca^{2+} transients is independent of the sperm binding (Lawrence *et al.*, 1997; Wassarman *et al.*, 2005). Other evidence against this proposal came from a procedure developed in the late 1980s to address fertilisation failure in patients with poor sperm quality (Palermo *et al.*, 2017). The procedure of by-passing the gametes' membrane interaction step by injecting the sperm directly into the oocyte, intracytoplasmic sperm injection (ICSI), led to successful fertilisation in most of the species studied. This cast a

significant doubt over this proposal since Ca^{2+} oscillations are triggered after ICSI, in the absence of a surface interaction between oocyte and sperm (Palermo *et al.*, 2017).

The third model - The soluble sperm factor model – proposed that the egg's Ca^{2+} rise is triggered by a sperm-born factor following gamete fusion. The first evidence came from studies in which sea urchin eggs were induced to undergo CGE in response to sperm extract injection (Dale *et al.*, 1985). Later, far more conclusive evidence came from microinjecting a mammalian sperm or a sperm extract into unfertilised oocytes. This was found to trigger Ca^{2+} oscillations similar to those seen at fertilisation, and to initiate embryonic development (Swann, 1990; Tesarik *et al.*, 1994; Palermo *et al.*, 1996). Swann (1990) found that increasing the quantity of the sperm cytosolic (soluble) fractions injected into hamster oocytes, increased the frequency of the Ca^{2+} transients but not the amplitude. Interestingly, injecting heat-denaturated soluble fractions, or sperm extracts treated with trypsin failed to trigger the Ca^{2+} oscillations, suggesting that the activation factor is a protein. However, adding the sperm extracts to the oocyte's extracellular surroundings have also failed to elicit a Ca^{2+} response. These observations are consistent with the idea that the sperm is the source of the activating factor and is responsible for deploying it upon fusion with oocytes (See figure 1.2C). It has also been reported that soluble sperm extracts from tilapia fish can induce Ca^{2+} oscillations in mouse oocytes (Coward *et al.*, 2003). Suggests the existence of a similar mechanism throughout a wide spectrum of species.

The soluble sperm factor proposal, however, received a great deal of criticism and was very controversial for a considerable period of time. Firstly, this was due to that oocyte activation in the previously mentioned studies was not due to a sperm factor, but was as a result of injecting the Ca^{2+}-rich culture medium along with the sperm (Machaty, 2013). Secondly, the inability to identify the activation factor at the molecular level (Parrington *et al.*, 2007). The first point was conclusively refuted by Tesarik et al. (1994) and Ozil and Swann (1995), while the second point was still an issue until the identification the first mammalian sperm factor as a sperm-specific phospholipase C, and later specifically as PLC-zeta (PLCζ) (Saunders *et al.*, 2002).

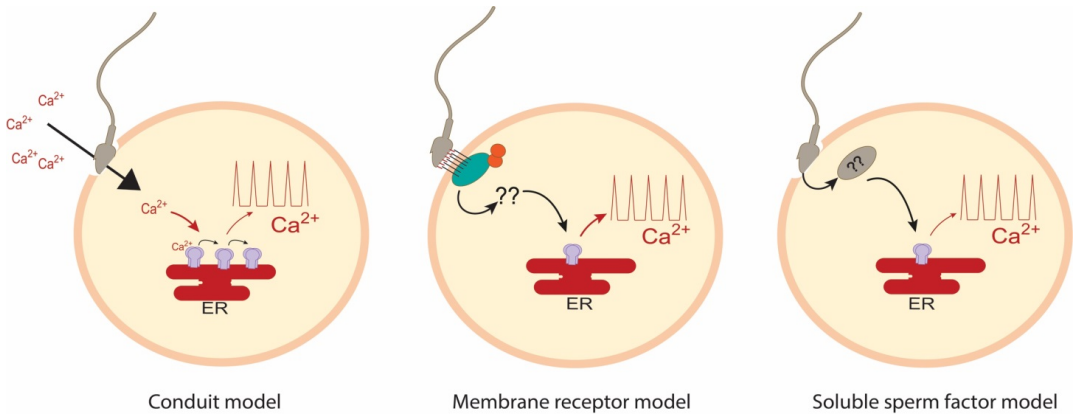


Figure 1-2: The proposed models of egg activation

Schematic representation of the three main hypotheses explaining the mechanism whereby the sperm induces intracellular Ca^{2+} increase in the egg/oocyte post fertilisation.
In the **sperm conduit model**, the sperm facilitates Ca^{2+} entry from the extracellular environment. The **membrane receptor model** suggests that upon fusion of the sperm with the egg/oocyte, a receptor on the oolemma is activated and transduces a signal which initiates Ca^{2+} release. The **soluble sperm factor model** suggests that sperm deliver a molecule upon fusion which initiates a Ca^{2+} release pathway.

A considerable body of research showed that Ca^{2+} released from the ER in response to a sperm or sperm extract was via activation of the phospholipase C (PLC) pathway (Miyazaki *et al.*, 1993; Xu *et al.*, 1994; Stachecki and Armant, 1996; Jones *et al.*, 1998). PLCs are a family of membrane-associated enzymes, that catalyse the hydrolysis of phosphatidylinositol 4,5-bisphosphate (PIP_2) within the membrane of a cell to generate the two by-products of diacylglycerol (DAG) and inositol 1,4,5-triphosphate (IP_3) (Berridge, 1981). The generated IP_3 binds to its receptor on the ER, causing Ca^{2+} to be periodically released from the ER to the cytosol of the egg in the form of Ca^{2+} spikes. Diacylglycerol, on the other hand, is a very potent stimulant of protein kinase C (PKC) (Castagna et al., 1982).

A very interesting series of findings during the 1980s and late 1990s helped to shed light on the role of PLCs in inducing Ca^{2+} release and the egg activation process in diverse animal groups, including mammals. The first was from Turner and colleagues (1984) who witnessed a significant increase in polyphosphoinositide metabolism in sea urchin eggs at fertilisation. That led to discover that IP_3 can artificially activate sea urchin eggs via single IP_3 microinjections, while in mammals it was found that maintaining injection

of IP_3 or an IP_3 analogue (adenophostin) was able to induce Ca^{2+} oscillations in oocytes (Whitaker and Irvine, 1984; Swann and Jones, 2002; Jones and Nixon, 2000; Galione *et al.*, 1994). Similarly, inhibiting the IP_3-receptor on the ER by the competitive antagonist (heparin) was found to inhibit the sperm-induced Ca^{2+} rise and egg activation in most of the species studied (Fissore *et al.*, 1995; Stricker, 1999). Furthermore, microinjecting the active form of an anti IP_3-receptor antibody into hamster oocytes, was shown to block Ca^{2+} release from the ER (Miyazaki *et al.*, 1992); similar studies in mouse oocytes have shown the same finding (Xu *et al.*, 1994). Further studies also showed that inhibiting the IP_3 production mechanism with the potent PLC inhibitor (U73122) inhibits the Ca^{2+} rise in mouse oocytes and sea urchin egg homogenates (Dupont *et al.*, 1996; Lee *et al.*, 1998; Jones *et al.*, 2000), indicating that the sperm factor might be a member of the PLC family.

According to protein structure, the PLC family is currently made up of 13 isoenzymes classified into six isotypes (β-beta, γ-gamma, δ-delta, ε-epsilon, ζ-zeta, and η-eta) (Kadamur and Ross, 2013) (See figure 1.5). All PLC isotypes contain two separated catalytic domains, the X and Y domains, that together form the binding pocket and the active site for cleaving PIP_2. They also contain various combinations of regulatory domains, including pleckstrin homology (PH domains), four EF-hands domains, Src homology 2/3 domains (SH2/SH3,), and C2 domains (Machaty, 2016).

Mammalian spermatozoa express several PLC isoforms including PLCβ, -γ and –δ (Mehlmann et al., 2001). However, none of the known PLC isotypes was able to induce Ca^{2+} release in sea urchin egg homogenates, or to mimic the repetitive Ca^{2+} signature seen at mammalian fertilisation when injected into a mouse oocyte (Jones *et al.*, 2000; Parrington *et al.*, 2002; Kashir *et al.*, 2017). The specific identity of the PLC isoform that induced a dynamic Ca^{2+} response similar to that generated by sperm-oocyte fusion, remained a mystery for some time. The breakthrough came from the analysis of mouse expressed sequence tag (EST) databases when Saunders and colleagues identified a novel PLC isoform expressed only in mammalian testis and sperm cells, termed PLC-zeta (PLCζ) (Saunders *et al.*, 2002) (See figure 1.4).

1.4 Phospholipase C - Zeta (PLCζ)

1.4.1 PLCζ as a putative oocyte activation factor

The testes-specific member of the PLC family was found to be the smallest known mammalian PLC, being ~74 KDa in mice, and ~70 KDa in humans. Several studies have also identified the putative oocyte activation factor (PLCζ) in other mammalian species, including hamster, pig, bovine, monkey, and horse (Cox *et al.*, 2002; Saunders *et al.*, 2002; Yoneda *et al.*, 2006; Parrington *et al.*, 2007; Schrimpf *et al.*, 2014; Cooney *et al.*, 2010).

Numerous studies have found that injecting the human or mouse complementary RNA (cRNA) of PLCζ, or recombinant PLCζ protein, into mouse oocytes triggers a pattern of Ca^{2+}oscillations very similar to those seen at fertilization, and supported PN formation and embryonic development to blastocyst stage (Saunders *et al.*, 2007; Cox *et al.*, 2002; Kouchi *et al.*, 2004) (See figure 1.3). However, the human version of PLCζ exhibits far greater potency in terms of generating the Ca^{2+} oscillations than the PLCζ from mice, when injected into mouse oocytes (Cox *et al.*, 2002). In addition, injecting human oocytes with human PLCζ cRNA was found to induce Ca^{2+} oscillations in unfertilised oocytes, and embryo development, by triggering parthenogenetic activities (Rogers *et al.*, 2004). Conversely, immunodepletion of PLCζ in sperm extracts prevents those extracts from inducing Ca^{2+} release in mouse oocytes (Saunders *et al.*, 2002). Injecting PLCζ cRNA into mouse oocytes was found to cause a down-regulation of IP_3 receptors similar to that seen at fertilization, suggesting that PLCζ generates IP_3 in the oocyte's cytoplasm similar to that proposed by the sperm soluble factor model (Lee *et al.*, 2010). In fact, the amount of cRNA that was required to induce Ca^{2+} oscillations similar to those observed at fertilisation was found to correlate significantly with the expected amount of the endogenous PLCζ within a single sperm (~40fg per oocyte) (Saunders *et al.*, 2002; Swann and Lai, 2016). In contrast, the closest homologue PLCδ induces a low Ca^{2+} oscillations only at much higher amounts (>1pg per oocyte) (Kashir *et al.*, 2014).

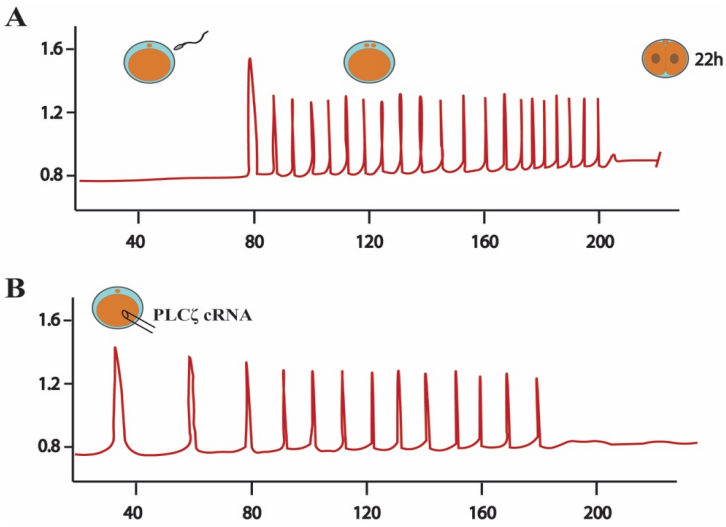


Figure 1-3: Intracellular Ca^{2+} oscillations in mouse oocytes measured by the fluorescence of Ca^{2+} sensitive dye.
A: Ca^{2+} oscillations post fertilisation *in vitro*
B: Ca^{2+} oscillations following PLCζ cRNA microinjection.
Adapted from (Saunders *et al.*, 2002)

A further finding in support of the role of PLCζ in mammalian oocyte activation came from a study by Knott and colleagues (2005), who showed that when the oocyte was fertilised with sperm from transgenic mice expressing short hairpin RNAs targeting PLCζ, the oocyte exhibited a shortened duration of Ca^{2+} release, resulting in a lower rate of oocyte activation. However, PLCζ was only partially depleted in this model.

Furthermore, PLCζ was also found in non-mammalian species such as chicken, newt, medaka fish, and quail (Coward *et al.*, 2005; Ito *et al.*, 2008; Mizushima *et al.*, 2009). Recombinant PLCζ from chicken and medaka was found to induce Ca^{2+} oscillations when injected into mouse oocytes (Coward *et al.*, 2005). Microinjecting recombinant PLCζ from quail along with quail sperm improves fertilisation and the development potential as well (Shimada *et al.*, 2014). The findings support the sperm factor model and the physiological role of PLCζ in non-mammalian species, however, the molecular mechanism that controls PLCζ activity in non-mammalian oocytes is still unknown.

Interestingly, PLCζ isoforms from non-testicular tissue were found in the brain and ovaries of pufferfish (Coward *et al.*, 2011). Those isoforms were found to share a close similarity with medaka fish and mammalian orthologs, specifically in the regions that are responsible for PLCζ enzymatic activity, and that regulates Ca^{2+} binding. However, injecting the pufferfish PLCζ cRNA into mouse oocytes did not induce Ca^{2+} oscillations, suggesting that this isoform might be physiologically inactive in mouse oocytes. It is worth noting that pufferfish and medaka species are lacking the first 60 amino acids at the N-terminal, compromising the first EF hand domain and part of the second. Previous studies confirmed the importance of this region for PLCζ activity, indicating that the pufferfish PLCζ inactivity might be due to the missing EF domain (Kouchi *et al.*, 2005; Coward *et al.*, 2011). Yet, microinjecting medaka cRNA into mouse oocyte induces Ca^{2+} oscillations very similar to the mammalian version but at a lower amplitude (Coward *et al.*, 2011). The findings suggest that PLCζ isoforms might still be expressed in non-testicular tissue, but PLCζ activity inside the pufferfish egg still requires other factors or molecules in order to activate the Ca^{2+} release through this pathway (Coward *et al.*, 2011).

Similarly, Yoshida and colleagues (2007) reported a preliminary finding regarding expression of PLCζ mRNA in the brain (telencephalon) of male and female mice, with a suspected motor function defect when PLCζ was overexpressed ectopically. Since that report, however, no further claims have been made from the same group or from other groups in support of finding.

It is worth noting that in the study by Coward and colleagues (2011) an interesting link was noted between PLCζ gene location and the testes-specific gene actin-capping protein gene (CAPZA3). PLCζ was found to share a bidirectional promotor with CAPZA3. A missense mutation in the CAPZA3 protein was found to cause sperm structural abnormality and infertility in mice (Geyer *et al.*, 2009). Meanwhile in clinical studies the two genes were found to correlate significantly in patients with globozoospermia, being associated with infertility at low expression, suggesting the two genes might be involved in this phenomenon (Javadian-Elyaderani *et al.*, 2016). Indeed, a study has shown a positive correlation between genetic variants which occur as a result of changes in the promoter region of PLCζ (the 5′-flanking region of the PLCζ gene that is located back-to-back with that of CAPZA3) and regulation of PLCζ activity and semen quality in Holstein bulls (Pan *et al.*, 2013). Further studies are still required to unravel the link between the

two genes, and the influence of the promoter region of PLCζ on normal sperm morphology as well as on the capacity of the sperm for oocyte activation.

Despite these findings in support of PLCζ being the physiological agent of oocyte activation, a number of studies have also questioned the physiological relevance of PLCζ for this process (Sette *et al.*, 1997; Wu *et al.*, 2007; Harada *et al.*, 2007; Aarabi *et al.*, 2012).

Sette and colleagues proposed tr-kit as an alternative candidate for the oocyte activation factor, this being a 23-kDa truncated fragment of the 150-kDa c-kit, the latter being found to play an important role in spermatogonial differentiation (Zhang *et al.*, 2011; Swann and Jones, 2002). Tr-kit is expressed during the haploid stages of mouse spermatogenesis, and was found to be localised to the cytoplasmic droplet, midpiece and the post-acrosomal region of the mouse epididymal spermatozoa (Sette *et al.*, 1997). In human sperm tr-kit was found to localize to both the equatorial segment and the sub-acrosomal region (Muciaccia *et al.*, 2010). Microinjecting the recombinant form of tr-kit was found to induce all stages of oocyte activation and development up to morula stage. It was proposed that tr-kit mediates parthenogenetic oocyte activation via interaction with Fyn (a Src-like kinase), Sam68, and activation of phospholipase Cγ1 within the oocyte cytoplasm (Sette *et al.*, 2002; Paronetto *et al.*, 2003). In line with this, microinjecting tr-kit into mouse oocytes and COS cells generates IP_3, and its action can also be inhibited with U73122, suggesting involvement of PLC activation via this pathway. Nevertheless, tr-kit activity can be inhibited by bovine PLCγ SH3 constructs (Sette *et al.*, 1997), which has been shown to have no effect on sperm-induced Ca^{2+} oscillations (Mehlmann *et al.*, 1998). Additionally, there has been no evidence showing that tr-kit can induce the repetitive Ca^{2+} oscillations similar to that seen following fertilisation or PLCζ microinjection (Machaty, 2016).

In non-mammalian species, citrate synthase from newt sperm extract was found to induce a Ca^{2+} wave and oocyte activation upon injection into newt oocytes. Citrate synthase in newts seems likely to play dual roles, first as a mitochondrial enzyme, and second as a sperm factor for oocyte activation. Injecting porcine citrate synthase protein, or the corresponding cRNA, into unfertilised oocytes, was found to trigger a Ca^{2+} rise (Harada *et al.*, 2007). Treating the oocytes with anti-citrate synthase antibody reduces oocyte activation events, while inhibiting enzymatic activity abolishes oocyte activation not only by the sperm extract but also by the fertilizing sperm (Iwao, 2012). However, newt sperm

extract did not induce a Ca^{2+} rise in Xenopus oocytes (Harada *et al.*, 2011), indicating that these oocytes do not contain the same signalling cascades that are required for oocyte activation by a sperm soluble extract. Further investigation is still required to understand the precise molecular mechanism that controls the Ca^{2+} rise in this species.

The other possible candidate for mammalian oocyte activation came from Wu and colleagues (2007). The study reported a sperm-specific expression of WW domain-binding protein (PAWP) on the postacrosomal sheath of the perinuclear theca of matured mammalian sperm, and this was found to be expressed and assembled as well in the elongating spermatids. WW domains generally regulate specific interactions with protein ligands, and some bind to phosphoserine- phosphothreonine-containing motifs (Chen and Sudol, 1995). The molecular mechanism that controls PAWP activity in mammalian and non-mammalian oocytes, was proposed to involve an interaction with WW domain-containing proteins, such as the yes-associated protein (YAP), which may in turn activate PLCγ via its SH3 domain, in oocytes (Machaty, 2016; Kashir *et al.*, 2015), similar to the activation mechanisms that are present in Xenopus oocytes and human neurons (Kashir *et al.*, 2017).

It was found that microinjection of recombinant PAWP protein in porcine, bovine, macaque, and Xenopus oocytes, triggers a high rate of pronuclear formation (Wu *et al.*, 2007; Aarabi *et al.*, 2010). In addition, microinjection of recombinant PAWP into human and mouse oocytes, induced Ca^{2+} oscillations and PNs formation, which was prevented by co-injecting a competitive inhibitor (Aarabi *et al.*, 2014). The same authors have also reported a significant correlation between PAWP expression levels and fertilization rates in infertile patients, with high levels of PAWP being associated with higher fertilization rates and embryonic development. Moreover, Kennedy and colleagues (2014) reported a positive correlation between PAWP expression levels and bovine sperm quality and infertility, suggesting a potential role for PAWP in sperm structural and functional integrity. Furthermore, a clinical finding from patients with globozoospermia showed accompanying low mRNA levels of the three oocyte activation candidates (PLCζ, PAWP, and tr-kit) with the structural changes in the sperm from these globozoospermic patients (Tavalaee and Nasr-Esfahani, 2016). Finally, Ferrer-Vaquer et al. (2016) showed that PLCζ levels might not necessarily correlate positively with semen characteristics and fertilization rates after ICSI, suggesting a role for other factors to contribute to fertilisation

failure in clinical studies, and that PLCζ expression alone is not sufficient to guarantee the standard oocyte activation (Ferrer-Vaquer *et al.*, 2016).

However, a number of studies have challenged the validity of these findings that favour an activation role for PAWP. For instance, a study of recombinant PAWP protein revealed ineffectiveness of the protein in catalysing PIP_2 to generate IP_3-induced Ca^{2+} release, and no capacity to activate or modulate the PLC pathway (Nomikos *et al.*, 2014a). It was also found that human PAWP protein and cRNA were unable to induce the Ca^{2+} oscillations similar to that generated by microinjecting PLCζ into mouse oocytes (Nomikos *et al.*, 2015).

A particularly damning finding came from a mouse knockout model lacking PAWP. This showed no effect of the knockout on sperm structure; and injecting a single PAWP knockout spermatozoon into the oocyte was sufficient to trigger Ca^{2+} oscillations. Suggests that sperm-specific PAWP is neither sufficient nor required for initiation of the Ca^{2+} oscillations and embryonic development in mammals (Satouh *et al.*, 2015). More recent findings from the clinical field have also shown no clear correlation between PAWP expression and fertilisation outcome in ICSI studies (Freour *et al.*, 2017; Escoffier *et al.*, 2016). Thus, the accumulated evidence is currently against the proposed role of PAWP as an oocyte activation factor in mammals, and the recognition of PAWP as a sperm-born oocyte activation factor still requires further verification. Therefore, the issue of whether PLCζ truly is the endogenous oocyte activation factor remains a crucial matter to be resolved. Consequently, a mouse model in which PLCζ function is totally abolished is still required to test the hypothesis that PLCζ is the physiological agent of oocyte activation.

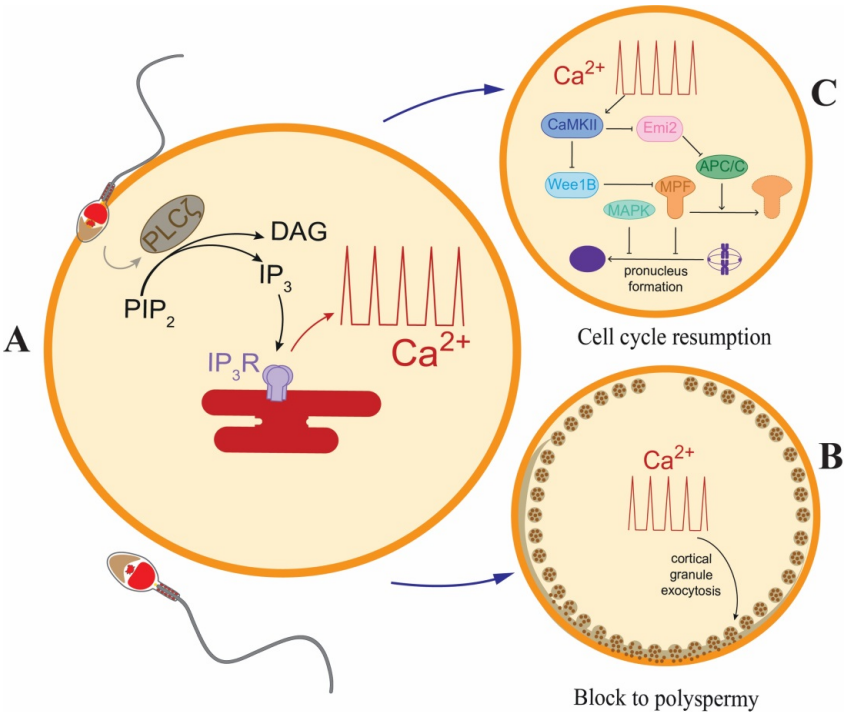


Figure 1-4: Proposed role/mechanism of PLCζ in mammalian oocyte activation

(**A**) Delivery of PLCζ by the sperm, induces an increase in IP3 levels in the oocyte, leading to release of $Ca^{2+}$from the endoplasmic reticulum (via IP3Rs) and triggering a series of cytosolic Ca^{2+} oscillations.
(**B**) Ca^{2+} oscillations lead to a block to polyspermy, via the cortical reaction. This involves the exocytosis of the cortical granules.
(**C**) Ca^{2+} oscillations lead to release of the oocyte from metaphase II arrest. Re-initiation of the cell cycle involves the initial activation of CaMKII leading to phosphorylation and inactivation of Emi2 and increased activity of APC/C (anaphase promoting complex/cyclosome), which in turns promotes degradation of MPF (M-phase promoting factor). Reduced levels of MPF and MAPK allow re-entry to anaphase and pronucleus formation.

1.4.2 PLCζ structure

Unlike other isoforms of the PLC family, PLCζ was found to be lacking the N-terminal pleckstrin homology (PH) domain. This domain was found to be responsible for binding the other isoforms of PLCs to the biological membranes in preparation for the signal transduction pathway. On the other hand, the PLCζ structure possess similarities to the other PLC isoforms in including four EF hands, an XY catalytic domain, and a C2 domain (Kadamur and Ross, 2013; Parrington *et al.*, 2007). The EF hands were found to be responsible for the specific sensitivity of PLCζ to Ca^{2+} (Yoda *et al.*, 2004). Deletion or mutation of the EF hands were found to cause a decrease in the maximal activity of PLCζ (Kouchi *et al.*, 2004). Several reports showed that PLCζ's sensitivity to Ca^{2+} is tenfold higher than a typical mammalian PLC, and is half maximal even when Ca^{2+} levels are at normal resting cellular concentrations (Nomikos *et al.*, 2005).

The XY domains are highly conserved among PLCs and are responsible for PIP_2 catalysis, and naturally occurring point mutations in this domain in infertile men can cause a loss of the enzyme activity of PLCζ in catalysing PIP_2 to IP_3 and DAG (Kashir *et al.*, 2012; Heytens *et al.*, 2009).

PLCζ was also found to differ from other PLC isoforms in containing a positively charged, poorly conserved X-Y linker peptide. This X-Y linker has been proposed to be involved in binding to the negatively charged head group of the substrate, as well as regulating the enzymatic activity of the protein (Saunders *et al.*, 2007). The length of the X-Y linker was found to vary amongst species, and this may underlie the species-specific pattern of Ca^{2+} oscillations in mammals (Yeste *et al.*, 2016; Saunders *et al.*, 2007; Swann *et al.*, 2006; Nomikos *et al.*, 2011a). Although human PLCζ possesses the shortest X-Y linker amongst most of the species studied so far, human PLCζ was found to be the most potent in generating Ca^{2+} oscillations when injected into mouse oocytes (Nomikos *et al.*, 2014b). The shorter sequence of the human X-Y linker was found to produce a higher positive charge region that may correlate with a higher rate of binding to PIP_2, and increased IP_3 production (Swann and Lai, 2016). Deletion of the linker causes a severe reduction in PLCζ enzymatic activity (Nomikos *et al.*, 2011b) (See figure 1.6).

Mouse PLCζ was also found to contain a nuclear localisation signal (NLS) near the end of the X-Y linker peptide, suggesting a role in binding to the nuclear transport receptor during protein translocation to the pronucleus. As PLCζ leaves the cytoplasm to enter the pronucleus, the Ca^{2+} transients gradually cease to termination after PN formation in mice (Kadamur and Ross, 2013; Saunders *et al.*, 2007; Kuroda *et al.*, 2006). A mutation on the NLS prevents pronuclear translocation of PLCζ and prolonged Ca^{2+} oscillations for hours (Larman *et al.*, 2004), whereas blocking PN formation causes Ca^{2+} oscillations to go on indefinitely (Jones, 2007).

Although all PLCζ orthologs were found to induce Ca^{2+} oscillations when injected into mouse oocytes, the pronuclear translocation of PLCζ seems to be a mouse-specific phenomenon. The translocation has only been reported for the mouse isoform and in mouse oocytes only, and to a lesser degree for the medaka ortholog (Ito *et al.*, 2008). Injecting other PLCζ orthologs (human, rat, and bovine), did not result in PLCζ translocation to the PN (Cooney *et al.*, 2010; Ito *et al.*, 2008). This might be the reason why Ca^{2+} oscillations evoked by such PLCζs continue far beyond the time of PN formation (Yeste *et al.*, 2016).

C2 domain was found to bind to phospholipids and to Ca^{2+} in order to regulate PLC enzymatic activities (Machaty, 2016; Ito *et al.*, 2011). However, the C2 domain of PLCζ did not show any predicted Ca^{2+} binding sites, suggesting that the PLCζ-C2 domain binds to lipids in a Ca^{2+}-independent manner (Saunders *et al.*, 2007). Deletion of the domain did not affect the enzymatic activities of PLCζ, but rather abolished the ability to induce Ca^{2+} oscillations, suggesting a role for C2 in maintaining the structural integrity of PLCζ (Nomikos *et al.*, 2005). Virtual 3-D homology modelling of PLCζ reveals a close interaction between the C2 and EF hand domains, indicating that this may be important for the enzymatic activity and the nuclear translocation (Kouchi *et al.*, 2005).

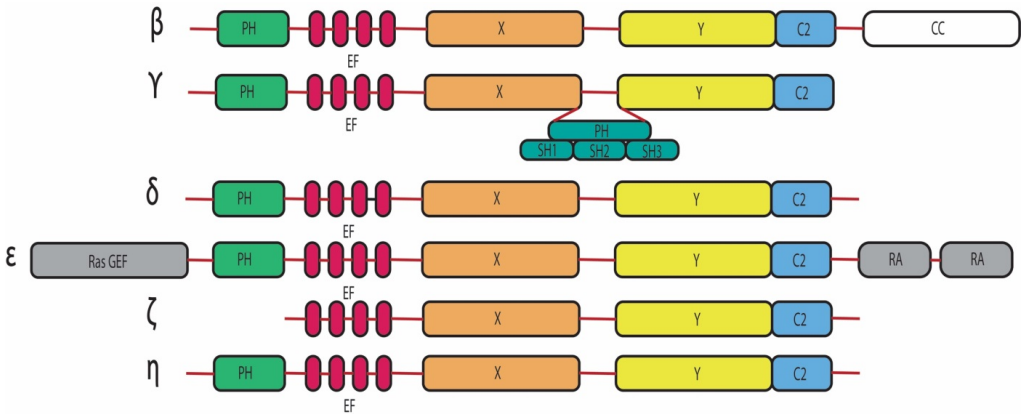


Figure 1-5: Schematic representation of PLC isoenzyme domain structures.
Adapted from (Kadamur and Ross, 2013)

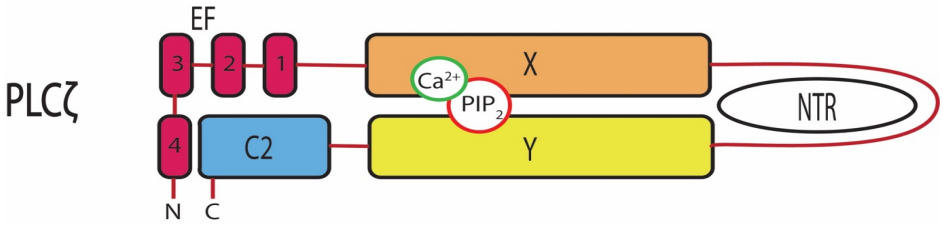


Figure 1-6: Schematic drawing of a model for the functional structure of PLCζ
Adapted from (Kuroda *et al.*, 2006)

1.4.3 Mammalian sperm PLCζ localisation

Mammalian sperm can be functionally dissected into two parts: the propulsive mechanism of the tail, which is responsible for the aggressive movement of the sperm; and the payload of the head of the sperm, which in this case is the paternal DNA, sperm-born RNAs, and according to the sperm content model - the egg activation factor. The proposed location of the sperm factor suggests the sperm factor should be located within the sperm head compartments in order to gain easy and rapid entry into the cytoplasm upon sperm-oocyte fusion. Thus, the sperm factor ought to reside in a location that provides easy access to the ooplasm, and the equatorial segment, the postacrosomal region on the sperm perinuclear theca were thought to be the best candidate locations for harbouring the sperm factor.

However, PLCζ has been found to localise to different regions in the sperm head (See figures 1.7 and 1.8). Immunofluorescence studies on mouse spermatozoa localised PLCζ on both the acrosome, and the postacrosomal region (Fujimoto *et al.*, 2004; Young *et al.*, 2009); whereas in human sperm, PLCζ was found in the area surrounding the equatorial segment, with subsidiary expression in the acrosome and the postacrosomal regions (Escoffier *et al.*, 2015; Heytens *et al.*, 2009; Grasa *et al.*, 2008; Yoon *et al.*, 2008; Ferrer-Vaquer *et al.*, 2016). Suggesting different functional roles for each location.

However, number of studies on human, mouse, and bull spermatozoa found that PLCζ could also reside in the acrosomal area with a possible contribution to the acrosome reaction (Kashir *et al.*, 2013; Bi *et al.*, 2009; Yoon and Fissore, 2007; Grasa *et al.*, 2008; Mejia-Flores *et al.*, 2017). Moreover, the principle piece of the flagellum was also found to harbour PLCζ in capacitated and uncapacitated equine sperm. Injecting this sperm region into mouse oocytes was found to trigger Ca^{2+} oscillations (Bedford-Guaus *et al.*, 2011). Further investigation is still required to elucidate the physiological relevance of multiple localisations of PLCζ in mammalian sperm.

The absence of an animal model lacking PLCζ, and a highly-specific antibody against PLCζ protein have been some of the main reasons for the contradictory conclusions in different studies. For instance, studying the PLCζ localisation in human samples was found to be even trickier, as it's even more common with seemingly healthy individuals

to have high levels of abnormal sperm morphology, and variable mRNA expression profiles (World Health Organization., 2010; Menkveld *et al.*, 2001; Garrido *et al.*, 2009). Such facts would create misleading conclusions regarding the true localisation of PLCζ within the structure of the human sperm.

Multiple localisation of PLCζ in sperm of the same species may affect the way sperm induce oocyte activation. In fact, the equatorial area of the sperm is the first part that comes in contact with the oocyte's membrane prior to fusion, and it would be physiologically relevant for the oocyte activation factor to be located in this area in order for easy access and fast release into the oocyte (Kashir *et al.*, 2014). The sperm postacrosomal region contains highly condensed cytosolic proteins surrounding the nucleus, and PLCζ localised to this area might be subjected to a slower rate of release. However, this could rather be beneficial at for the oocyte late activation events (Yanagimachi, 1998; Escoffier *et al.*, 2015; Fujimoto *et al.*, 2004).

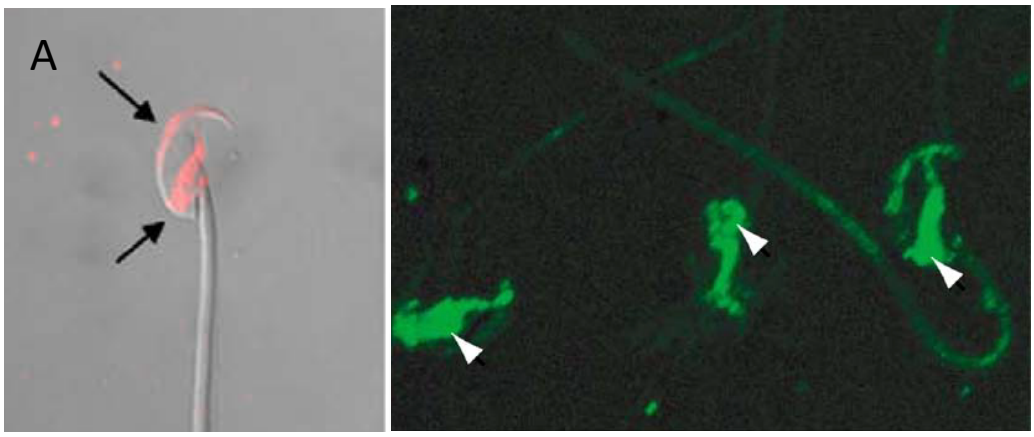


Figure 1-7: PLCζ localisation patterns in mouse sperm
Mouse sperm showing the acrosomal and post-acrosomal populations (arrow heads).
A: Adapted from (Young *et al.*, 2009)
B: Adapted from (Fujimoto *et al.*, 2004)

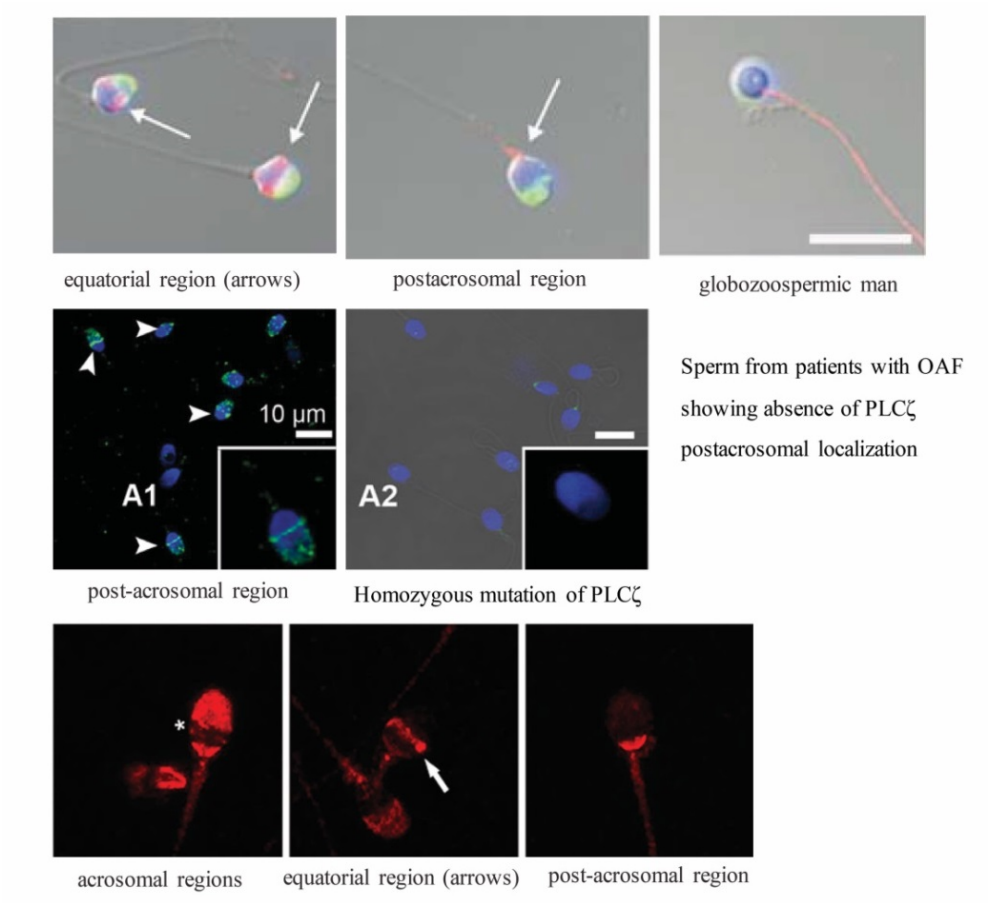


Figure 1-8: PLCζ localisation patterns in human sperm from published studies

Adapted from (Heytens *et al.*, 2009; Escoffier *et al.*, 2016; Ferrer-Vaquer *et al.*, 2016)

In addition, oocyte activation factor localisation might be subjected to slight modifications among different species, and that could be due to number of anatomical and structural variations. It was observed that these variations may influence the release of the oocyte activation factor and diffusion inside the ooplasm. In hamster, for example, the initial Ca^{2+} transient starts within seconds after sperm-oocyte fusion (Swann, 1990; Miyazaki *et al.*, 1992), while in mice, a latency of several minutes was reported after sperm-oocyte fusion and before the appearance of the initial Ca^{2+} rise (Swann and Ozil, 1994). This suggests that PLCζ proteins from different species of mammals could have different factors of solubility and require an additional period of time to be released from the sperm head and to diffuse throughout the ooplasm (Machaty, 2016). Here, the differences in the diffusion ability might be directly related to the mode of packaging and localisation within the sperm, and thus it is judicious to suggest that sperm from different species may release the activation factor into the oocyte at different rates.

Studies suggest that PLCζ protein post-fertilisation is distributed uniformly within the ooplasm (Swann and Lai, 2016). Thus, a study of fluorescently tagged recombinant PLCζ injected into the oocyte showed this to be localised to PIP_2-rich vesicles distributed throughout the ooplasm and not to the plasma membrane as might have been expected (Yu *et al.*, 2012). The finding has raised significant number of questions regarding the targeted site of PLCζ activity inside the oocyte, and the feasibility of PIP_2 at the membrane site. Since all other PLC family members catalyse PIP_2 at the plasma membrane, PLCζ was also assumed to follow the same scenario in catalysing PIP_2 on the plasma membrane. Surprisingly, PIP_2 concentration within the plasma membrane was found to be increased instead of decreased following fertilisation and PLCζ microinjection (Halet *et al.*, 2002). Depleting PIP_2 levels at the plasma membrane did not produce any effects on PLCζ activity, while it completely abolishes the ability of PLCδ1 to induce Ca^{2+} release (Yu *et al.*, 2012). DAG, on the other hand, was not found to be detectable at the plasma membrane (Yu *et al.*, 2008; Halet *et al.*, 2002). This suggests that PLCζ after all may not be targeting the PIP_2 anchored to the plasma membrane, but an intracellular source distributed evenly throughout the cytoplasm (Kashir *et al.*, 2014).

It appears that what makes PLCζ the perfect candidate for the oocyte activation factor is not only being solely expressed in sperm cells, but also its unique enzymatic activity that is only active in the ooplasm. Overexpressing PLCζ in adherent somatic cells did not produce any alteration in resting or induced Ca^{2+} release, even when the overexpression level was 1000-times higher than in the oocyte (Phillips *et al.*, 2011). Yet, injecting cell extracts from these cell lines into mouse oocytes induced Ca^{2+} oscillations similar to those observed after fertilisation by sperm (Phillips *et al.*, 2011). The same phenomenon was also observed when PLCζ was expressed ectopically in all tissues of transgenic mice where it did not produce any phenotypic alteration, except in the ovaries where the animals started to develop ovarian teratomas (Yoshida *et al.*, 2007). Based on these findings Swann and Lai (2016) have suggested that the absence of PLCζ activity in non-ovarian tissues was highly likely due to the absence of the PIP_2-rich vesicles which have only been reported in mammalian oocytes. It is possible that these vesicles might provide a larger surface area per oocyte for more PIP_2 for PLCζ to bind to in the lipid layers of the vesicles, thereby generating more IP_3 by completely bypassing the plasma membrane. Further investigation is therefore still required to unravel the mechanism by which PLCζ binds to these vesicles and initiates IP_3 production and oocyte activation.

1.5 Oocyte activation failure and male-factor infertility

Infertility is considered to be a complex and multi-factorial condition affecting both men and women of reproductive age in very different ways. Generally, it can be defined as the inability to achieve a clinical pregnancy after one year of regular unprotected sexual intercourse (Zegers-Hochschild *et al.*, 2009). The disease, as described by WHO, affects 8-12% of couples worldwide, with 40-50% of all infertility cases being due to male-factor infertility (Kumar and Singh, 2015). Along with the technical advancements in this field, the use of infertility treatment in the form of assisted reproductive technology (ART) has increased steadily for the past three decades (Palermo *et al.*, 2017). Currently in the UK up to 1.5% of all births are a result of assisted reproduction interventions (Kashir *et al.*, 2010), and the most extensively used procedure of ART is IVF.

Human *in vitro* fertilisation was initially developed by Patrick Steptoe and Robert Edwards in the late 1970s to treat a woman with a uterine tubes defect (Kamel, 2013). Since then the technique has offered an effective treatment globally to treat most of the causes of infertility, except in severe cases of male factor infertility where this technique was found to be ineffective (Nasr-Esfahani *et al.*, 2010; Wilkes *et al.*, 2009). One of the main causes of this type of infertility is related to sperm structural abnormalities, such as azoospermia, oligozoospermia, asthenozoospermia and teratozoospermia, and some yet to be understood factors (Amdani *et al.*, 2013). In these cases, an alternative approach of, intracytoplasmic sperm injection (ICSI) has offered an effective method for bypassing the structural abnormalities by injecting the sperm directly into the ooplasm. To date ICSI procedures have decreased the impact of male factor infertility significantly, achieving 70% to 80% successful fertilization rates, and resulting in millions of pregnancies (Palermo *et al.*, 2017; ESHRE, 2012).

However, injecting a sperm successfully into an oocyte does not always create an embryo, as 1% to 5% of every ICSI cycles in every ART clinic fails due to what is known as fertilization failure (FF) (Esfandiari *et al.*, 2005; Nasr-Esfahani *et al.*, 2010; Yanagida, 2004; Palermo *et al.*, 2017). The underlying cause of total FF is likely to be complex and may rely both on sperm-related and/or oocyte-related factors (Swain and Pool, 2008; Esfandiari *et al.*, 2005; Heindryckx *et al.*, 2008). An interesting link between post-ICSI oocyte FF and abnormal sperm morphology was found in human patients with a clinical

condition known as globozoospermia (Dam *et al.*, 2007). Globozoospermia is a rare clinical disorder characterised by round-headed spermatozoa with absence of the acrosomal area (Heytens *et al.*, 2010; Heindryckx *et al.*, 2005). Injecting sperm from such patients by ICSI yielded very low fertilisation success, which was found later to be rescued by the addition of Ca^{2+} ionophore (Dam *et al.*, 2007; Heytens *et al.*, 2009). The clinical finding linked for the first-time patients with sperm structural abnormalities and the inability to induce Ca^{2+} release in human oocytes. This indicates that most of the ICSI failure that are witnessed clinically is actually a result of a deficiency in the physiological mechanism that controls oocyte activation. Since, PLCζ was found to be the best candidate for oocyte activation in mammals, a deficiency or abnormality of PLCζ protein may be associated with the reduction in oocyte activation capacity in humans.

Two experimental studies from 2008 and 2009 showed that sperm from infertile men who suffered recurrent IVF and ICSI failure, fail to induce Ca^{2+} oscillations following injection into mouse oocytes (Heytens *et al.*, 2009; Yoon *et al.*, 2008). The ICSI procedure was shown previously to elicit Ca^{2+} oscillations in mouse oocytes via the IP_3 signalling pathway (Swann, 1990; Sousa *et al.*, 1996; Sato *et al.*, 1999). In addition, immunofluorescence and immunoblot analysis of sperm PLCζ expression, revealed a significant reduction or complete diminishment of PLCζ expression in those patients. Moreover, co-injecting PLCζ cRNA was found to rescue the activation failure when such human sperm were injected into mouse oocytes and to allow PN formation (Yoon *et al.*, 2008), providing a significant support to the potential use of recombinant PLCζ as a therapeutic agent (Yamaguchi *et al.*, 2017).

Further evidence for an important physiological role for PLCζ came from identification of an infertile man with two mutations – PLCζ ^{H398P} and PLCζ ^{H233L} – one in each allele of his PLCζ gene, that result in dysfunctional PLCζ proteins and thus could be the cause of this man's infertility problem (Heytens *et al.*, 2009; Kashir *et al.*, 2012). Microinjection of PLCζ cRNA harbouring the mutation PLCζ^{H398P} or PLCζ^{H233L} into mouse oocytes failed to induce Ca^{2+} oscillations; instead injecting the recombinant PLCζ protein containing either of these mutations resulted in either no Ca^{2+} oscillations or a grossly abnormal pattern of Ca^{2+} transients. A more recent study identified two infertile brothers each with the mutation PLCζ^{I489P} in both alleles leading to the absence of the protein in sperm (Escoffier *et al.*, 2016). However, despite these indirect pieces of evidence implicating PLCζ as the physiological agent of oocyte activation in human, this issue has

become controversial, with doubts raised about a role for PLCζ in this process (Aarabi *et al.*, 2012; Ferrer-Vaquer *et al.*, 2016).

1.6 Fertilisation failure and assisted oocyte activation

The ICSI procedure is currently a highly effective method of ART in the war against male factor infertility. However, 1–5% of all ICSI treatments result in FF, and the main cause for this was shown to be a defect in the process of oocyte activation (Liu *et al.*, 1995). Taking the fundamental role of PLCζ into the account, it is possible therefore to consider any abnormal functional activity of PLCζ that might be the underlying cause of FF in post-ICSI procedures (Aarabi *et al.*, 2014; Heytens *et al.*, 2009; Yoon *et al.*, 2008). Rescuing fertilisation with assisted oocyte activation (AOA) has been increasingly applied both experimentally and clinically to restore fertilization and pregnancy rates.

On the experimental side, the oocyte activation failure can be addressed artificially by using a variety of stimuli such as Ca^{2+} ionophore, ethanol, and strontium, leading to induction of one or more Ca^{2+} transients in the ooplasm (Santella and Dale, 2015). Although treatment with ionophores fail to stimulate the standard Ca^{2+} oscillations in mammals, flooding the oocytes with Ca^{2+} has been shown to induce parthenogenetic activation and embryo development to term.

Clinically, post-ICSI fertilisation failure has been successfully overcome by the application of AOA. Which involves manipulating the intracellular Ca^{2+} influx with a variety of physical, mechanical or chemical activation stimuli, such as electrical pulses (Yanagida et al., 1999), a modified ICSI procedure (Tesarik et al., 2002), or Ca^{2+} ionophores and $SrCl_2$ (Nasr-Esfahani et al., 2010) to mimic the initial physiological conditions during oocyte activation.

Despite the availability of different AOA technologies, number of labs reported lower fertilization and pregnancy rates after using different AOA protocols (Montag et al., 2012) compared to others (Heindryckx et al., 2008), or no obvious differences in fertilization rate after the application of AOA compared to routine ICSI (Borges et al., 2009). The differences in the efficiency of AOA protocols might be due to the patients' fertility background, and the lack of diagnostic tests or the specific AOA protocols used (Vanden

Meerschaut et al., 2014). However, the effect of specific culture components, such as the mineral concentration and other culture conditions have not been considered yet during the application of AOA technology to overcome FF (Ozil *et al.*, 2017; Casser *et al.*, 2017).

The most widely used artificial activation agents for human oocytes are the Ca^{2+} selective ionophores, ionomycin and calcimycin (Ebner *et al.*, 2015; Vanden Meerschaut *et al.*, 2014). Ca^{2+} ionophores was found to induce oocyte activation by increasing the Ca^{2+} flux to the oocyte from the extracellular environment, and to some degree trigger Ca^{2+} influx from the internal stores (Dedkova et al., 2000). However, $SrCl_2$ in mouse studies was found with to induce Ca^{2+} oscillations similar to that of PLCζ (Ma et al., 2005). It has also been found to be very effective in inducing artificial activation of mouse oocytes following somatic cell nuclear transfer or round spermatid microinjection (Loren and Lacham-Kaplan, 2006).

Similarly, $SrCl_2$ has been applied as an effective AOA agent in clinics to overcome FF after ICSI (Kyono *et al.*, 2008). Although successful pregnancies were reported following ICSI by using $SrCl_2$ in cases with low fertilization rates (Kim *et al.*, 2014; Kyono *et al.*, 2008), the efficiency of $SrCl_2$ as an activating agent for human oocytes is still under debate. This is mainly due to the fact that the exact mechanism by which $SrCl_2$ induces egg activation is still unknown.

A possible explanation is that $SrCl_2$ might induce Ca^{2+} oscillations by sensitizing Ca^{2+}-induced Ca^{2+} release mechanisms, causing Ca^{2+} release from the ER through the IP_3 receptor (Jellerette et al., 2000). Sanders *et al.* (2018) recently reported that PLCζ and $SrCl_2$ triggers Ca^{2+} oscillations in mouse eggs via fundamentally different mechanisms. It was found that $SrCl_2$ sensitised IP_3R to IP_3 to induce Ca^{2+} oscillations from the internal stores, while Ca^{2+} levels were found to be essential in PLCζ-dependent IP_3 production.

Importantly, however, Ca^{2+} influx from the extracellular milieu was found to be required for maintaining the Ca^{2+} oscillations. Stimulating transient receptor potential (TRP)V3 $Ca2^{+}$ channel was found to promote Ca^{2+} entry and egg activation via mediating $SrCl_2$ induced Ca^{2+} oscillations in mouse eggs (Carvacho et al., 2013). Generally, TRPV3 channels are modulated by a variety of stimuli and ligands, including various natural compounds like carvacrol, thymol and eugenol (Xu et al., 2006). Remarkably, activation of TRPV3 channels by 2-APB and carvacrol promotes Ca^{2+} entry and provokes mouse

oocyte activation without temperature sensitization, whereas the absence of TRPV3 channels in mouse oocytes led to a failure of $SrCl_2$ induced activation (Carvacho et al., 2013). Recently, TRPV3 have been identified at the plasma membrane of human oocytes. However, $SrCl_2$ failed to induce Ca^{2+} release and egg activation (Lu *et al.*, 2018). The finding challenges number of clinical reports highlighted the effectiveness of $SrCl_2$ on overcoming activation failure in human oocyte (Kyono *et al.*, 2008; Kim *et al.*, 2014).

Moreover, it has even been possible to bypass the Ca^{2+} rise at fertilization by bypassing this normal physiological signal and inducing Zn^{2+}-dependent exit from meiosis, resulting in development to term, albeit 50% less efficiently (Bernhardt et al., 2012). However, against the idea that the precise nature of the Ca^{2+} signal at fertilization is not important, studies by Ozil and colleagues have shown that the number and the frequency of Ca^{2+} transients affect both embryonic gene expression and development to term (Ozil *et al.*, 2006; Ducibella *et al.*, 2006). Addressing this issue is not only important from the point of view of understanding a fundamental developmental process, but it also has practical implications. Thus, stimuli such as Ca^{2+} ionophore, ethanol, and $SrCl_2$, have all been used successfully to generate live human offspring; such children appear normal but there has been no detailed assessment of whether they have any long-term health problems, subtle differences in gene expression, epigenetic changes, etc.

1.7 PLCζ as a therapeutic agent in ART

In mammals, sperm-oocyte fusion triggers the Ca^{2+} oscillations that induce the oocyte-to-embryo transitional process. The spatial and temporal organisation of the cytosolic free Ca^{2+} that traverses the entire ooplasm seems to be very important in activating different events in different regions within the oocyte. It appears that the Ca^{2+} oscillations in mammals encode specific information with each pulse that can be efficiently transmitted through the oocyte without damaging the oocyte itself. Absence of, or abnormal, Ca^{2+} oscillations following sperm entry contributes to oocyte activation failure and low fertilisation, respectively.

Currently, cases of post-ICSI failure are routinely resolved through artificial approaches such as ionophores, Ca^{2+} injections, and electrical pulses, which only induce oocyte activation, pregnancy and live birth via non-physiological Ca^{2+} transients. This has led to a debate about whether the precise pattern of Ca^{2+} signals at fertilization is important. It is worth noting that altering the fertilising Ca^{2+} signal may have long-term effects on both gene expression during the preimplantation stage and development to term. Consequently, the abnormal Ca^{2+} signals induced by AOAs represent a potential threat to subsequent development with potential impacts on epigenetic processes (Ciapa and Arnoult, 2011).

Thus, the main goal of AOA then is to mimic the Ca^{2+} characteristics that occur during fertilisation as closely as possible in relation to the normal physiological cues. Since PLCζ protein or cRNA have shown promising therapeutic capabilities to overcome low activation capacity in globozoospermic patients, recombinant PLCζ may represent a viable method to clinically treat cases of post-ICSI failure.

However, the therapeutic use of PLCζ cRNA is not yet a viable option as the uncontrollable transcription of PLCζ may hinder normal embryo development through gene expression irregularities. Therefore, the availability of purified, active recombinant human PLCζ protein instead of cRNA appears to represent both a highly practical and the most physiologically relevant therapeutic agent for overcoming failed ICSI cases.

1.8 Aim of the study

Despite the advancement in the general understanding of the signalling pathways that lie downstream of the sperm-induced Ca^{2+} oscillations, exactly how the sperm triggers such Ca^{2+} oscillations in the mammalian oocyte has remained controversial. Thus, this thesis aims to investigate the physiological relevance of the mammalian sperm PLCζ in a mouse model lacking PLCζ expression through gene knockout technique. Such animal model will provide an ideal system for the following research aims:

- Investigation of the specificity and efficiency of using the novel gene editing technique clustered regularly interspaced short palindromic repeats (CRISPR)-CRISPR-associated protein 9 (Cas9) to target the coding sequence of the PLCζ gene in C57bl/6j mice, and thereby create the first mouse model lacking expression of this gene.

- Study of the effects of the resulting phenotype on normal sperm functional parameters, the ability of the sperm to induce Ca^{2+} oscillations upon entry into mouse oocytes, and on resumption of MII and embryonic development.

- Study of the effects of the PLCζ deletion on the oocyte's membrane establishment to block polyspermy, via examining localisation and the shedding mechanism in the oocyte of folate receptor 4 (Juno) post fertilisation.

2 Generation of PLCζ mutants by CRISPR/Cas9 gene editing technology

Part of the material presented in this chapter was published in Development (Hachem *et al.*, 2017) ©The Company of Biologists Ltd.

2.1 Background

Genetically modified mice are used extensively in research for understanding gene function and for modelling human disease. In the first approach to generating gene-targeted mice, these were generated by introducing the desirable mutations into a gene through homologous recombination (HR) in mouse embryonic stem (ES) cells. The targeted ES cells injected into wild-type mouse blastocysts can contribute to the germ line of chimeric mice, which, when transmitted through the germ line, generate progeny containing the targeted gene (Capecchi, 2005). However, the generation of mutant mice by HR in ES cells is costly and time-consuming, as gene-targeted ES cell clones need to be selected and injected into blastocysts to generate chimeric mice, which then have to be bred extensively in order to generate single-gene homozygous mutant offspring, a procedure that usually takes 9–12 months (Yang et al., 2014).

A novel approach to gene targeting involves so-called 'gene editing'. This first employed custom nucleases designed for specific loci, such as zinc finger nucleases (ZFNs) or transcription activator-like effector nucleases (TALENs) (Gerlai, 2016; Carroll, 2011). More recently, gene editing has used a bacterial CRISPR-associated protein-9 nuclease (Cas9) that has been adapted from *Streptococcus pyogenes*; this has provided a much simpler and more economic method for gene-targeted modification (Doudna and Charpentier, 2014). Importantly, all the gene-editing approaches can be used to target genes in the fertilised egg, thereby meaning that ES cells do not need to be used for the creation of gene-targeted mice, although gene editing can also be used to target genes in ES cells. A variety of prokaryotes utilise Cas proteins, which are RNA guided endonucleases, as an intracellular defence against bacteriophage DNA infections (Horvath and Barrangou, 2010). The adaptive immune system in these prokaryotes acts by integrating short DNA sequences from the exogenous DNA into the CRISPR locus of the bacterial DNA, allowing the cell to remember, recognize and clear infections (Rath *et al.*, 2015). The integrated DNA fragments are transcribed from the bacterial CRISPR repeats into CRISPR RNAs (crRNAs) that match the invasive DNA sequence. crRNAs hybridize with an endogenous RNA termed the transactivating CRISPR RNA (tracrRNA) to form

a crRNA-tracrRNA duplex, which directs *Streptococcus pyogenes* Cas9 endonuclease to specific sites on the DNA, allowing the Cas9 to generate a double strand break (DSB) (Cong *et al.*, 2013; Jiang and Doudna, 2017).

The breaks activate a repair mechanism through error-prone nonhomologous end joining (NHEJ) or homology-directed repair (HDR). In the absence of a DNA template, the DSBs are re-ligated through the NHEJ process, which leaves scars in the form of insertion/deletion (indels) mutations. NHEJ can be used to generate gene knockouts, as indels occurring within the coding sequence of a gene can lead to frameshift mutations and premature stop codons (Chu *et al.*, 2015). In the presence of a donor template with homology to the targeted locus (e.g. insertion of an epitope or a fluorescent tag), the HDR pathway operates, allowing for precise knock-in changes to be made. The repair template can either be in the form of conventional double-stranded DNA targeting constructs with homology arms flanking the insertion sequence, or single-stranded DNA oligonucleotides (ssODNs).

The targeting specificity is determined by 20 nucleotide sequences at the 5'-end of the sgRNA (a simplified two component system has been described that fuses the tracrRNA and crRNA into a single synthetic guide RNA (sgRNA)), which can be altered to match any desired sequence in the DNA. The only limitation of this targeting is that the 20 nucleotides guide sequence has to be followed by a protospacer adjacent motif (PAM) of NGG in the DNA in order for efficient cleavage to occur (Shah *et al.*, 2013). For Cas9 to bind to DNA the target sequence in the genomic DNA must be complementary to the sgRNA sequence; in addition, it must be immediately followed by the correct protospacer adjacent motif (PAM) sequence, a 3-bp NGG motif present in the target sequence (Jinek *et al.*, 2013; Hsu *et al.*, 2013).

Unlike ZFNs and TALENs, the CRISPR/Cas9 system does not require the manufacturing of specific protein pairs for each target site (Lockyer, 2016). The targeting ability of Cas9 to a specific sequence is based on RNA-DNA base-pairing rules, with the ability to multiplex mutations in the same system to produce the combined effects (Hsu *et al.*, 2014). The simplicity of the CRISPR/Cas9 system has revolutionized genome engineering in a variety of cells and organisms, with huge potential for using this technology to create *in–vivo* and *in-vitro* platforms for better understanding of different gene functions and various sub-cellular pathways (Dow, 2015). Since 2013,

CRISPR/Cas9 technology has been used enormously to carry out genome engineering in a vast variety of animal species, including fruit flies (Bassett *et al.*, 2014), frogs (Wang *et al.*, 2015), mice (Cong *et al.*, 2013), rats (Shao *et al.*, 2014), pigs (Su *et al.*, 2015), primates (Niu *et al.*, 2014), humans (Ma *et al.*, 2017), and in plants as well. It is also not a total surprise to see that this technology has been heavily embraced by the transgenic mouse community in the approach to create different mouse animal models for different conditions and also in mimicking pathogenic gene mutations in humans (Ma *et al.*, 2017).

Although the increasingly popular CRISPR/Cas9 has profoundly changed the way we do gene editing, the system has several inherent potential limitations. Recent studies have questioned the specificity of Cas9 in targeting specific sequence after discovering that the system can tolerate multiple mismatches between an sgRNA and the sequence of the complementary target DNA, leading to potential off-target DSBs and indel formation (Ran et al., 2013). These undesirable mutations can potentially cause genomic instability, and pose a significant limitation for the usability of Cas9 as a gene editing tool in a field that requires high levels of precision (Zhang et al., 2015). To address this problem, Cong and colleagues created a mutated version of the wildtype Cas9 system with a single DNA strand nickase activity, called Cas9D10A-Nickase. The new system is designed to utilise a pair of offset sgRNAs complementary to the opposite strands of the targeted site (Cong *et al.*, 2013; Ran *et al.*, 2013), and individual nicks on each side of the double strand are mainly repaired by the high-fidelity base excision repair pathway (Zhang *et al.*, 2015). Choosing unique target sequences for each of the sgRNAs, the two double-strand nicks were found to have higher specificity than the wildtype Cas9 and with significant reduction in the off-target mutations (Cho *et al.*, 2014).

In addition to this limitation, it has been found that the founder mice (F0) that are generated by CRISPR/Cas9 microinjection into the fertilised egg, frequently show mosaicism for indel mutations and are riddled with somatic allele complexity. The prolonged expression and activity of Cas9 RNA injected into the zygotes, or the delay in activity beyond the single-stage embryo may contribute to mosaicism in DNA mutations by producing multiple DNA cuts with every cell cycle (Yen *et al.*, 2014). As the ultimate goal for every gene editing is to generate a desirable mutation on a specific sequence, and to establish stable breeding lines that faithfully transmit the desired mutant alleles, it is essential therefore to define the criteria for reporting "successful mutagenesis", as the genotyping findings are highly variable between founder mice derived from Cas9

injections that possess detectable indels in the tissue biopsies, and those that can truly transmit these alleles through the germline (Oliver *et al.*, 2015). Such waiting for genotyping results for the second generation to confirm mutation transmission can cost precious time, and increase animal care costs.

Regardless of the notable limitations in this system, CRISPR/Cas9 is still considerably easier, cheaper and more versatile than previous technologies. Addressing every limitation with better understanding about the way CRISPR/Cas9 works could provide us with the capabilities to harness its full potential.

This study utilised CRISPR/Cas9 in two different approaches to achieve an efficient way of targeting of PLCζ gene in the C57BL/6j strain of mice. The first approach includes using $Cas9^{wt}$ endonuclease with a single gRNA that targets exon five of PLCζ gene to create a knockout effect in a mouse line later known as $Plcz1^{em2Jparr}$, and the other approach utilises the $Cas9^{D10A}$ (double nickase) with a pair of guides RNA to target exon three of PLCζ gene in a knockout mouse line later known as $Plcz1^{em1Jparr}$. The rationale for utilising the two approaches on different animals was to confirm the specificity of CRISPR/Cas9 gene editing, and to assess the phenotypic alteration in the resulting offspring.

2.2 Materials and methods

2.2.1 Animals

Mice of the C57BL/6j strain were housed in individual ventilated cages at constant optimal temperature and humidity with 12 hours of light per day in the Biomedical Science Building, or the Dunn School of Pathology, both part of the University of Oxford, and fed with standard dry pellets and water *ad libitum*. Animal use was approved by the University of Oxford's Local Ethical Review Committee and permitted by a licence from the UK Home Office in accordance with UK law (Animals [Scientific Procedures] Act 1986).

2.2.2 sgRNA design

The CRISPR single guide RNAs (sgRNAs) were designed using the online design tool, called the CRISPR design tool (crispr.mit.edu) (Cong *et al.*, 2013). The web-based tool locates viable DNA targets (20 bp, immediately upstream of a PAM sequence) within the mouse PLCζ sequence (NM_054066.4) and ranks them based on their predicted capacity for off-target effects. The selected oligonucleotide sequences were then cloned into either pX459 ($Cas9^{WT}$) or pX461 (Cas^{9D10A}) vectors (gifts from Prof. Feng Zhang, Massachusetts Institute of Technology) and tested for efficacy by transfection into N2A mouse neuroblastoma cells (obtained from ATCC-UK) by using Fugene®6 transfection reagent (Promega-UK) followed by high resolution melting (HRM) analysis with RotorGene Q (Qiagen) (Bassett and Liu, 2014a). Based on the HRM results, a pair of targeting sequences in exon three with Cas^{9D10A}, and a single targeting sequencing in exon five with $Cas9^{WT}$ were chosen for production of sgRNAs; details are shown in table (2-1).

Table 2-1: sgRNA targeting sequences on the mouse PLCζ gene

Cas^{9D10A}	PLC_3A	AAGGTTCAGGATGATTTTAG**AGG**
	PLC_3B	GTATGAAGCACGaGAAGTTA**AGG**
$Cas9^{WT}$	PLC_5	ACTCGGTCCCAATATTTGAT**CGG**

2.2.3 sgRNA Production

According to (Bassett and Liu, 2014b), sgRNAs were produced by *in vitro* transcription using a PCR template generated by Phusion polymerase extension of a pair of overlapping primers, which adds a T7 polymerase promoter to the 5' end and the common sgRNA sequence to the 3' end:

PLCZ1_exon3A(F):
5' gaaattaatacgactcactataggAGGTTCAGGATGATTTTAGgttttagagctagaaatagc 3'

PLCZ1_exon3B(F):
5' gaaattaatacgactcactataggTATGAAGCACGaGAAGTTAgttttagagctagaaatagc 3'

PLCZ1_exon5(F):
5' gaaattaatacgactcactataggCTCGGTCCCAATATTTGATgttttagagctagaaatagc 3'

sgRNA (R):
5'aaaagcaccgactcggtgccacttttcaagttgataacggactagccttattttaacttgctatttctagctctaaaac 3'

Products were purified using a PCR purification kit (Qiagen), and *in vitro* transcribed using the T7 MEGAscript kit (Ambion) at 37°C for 4 hours. sgRNAs were purified by phenol:chloroform extraction and precipitation using isopropanol followed by quantification by measuring absorbance at 260 nm (Implen-USA). 5 μg total sgRNA was mixed with 10 μg capped and polyadenylated $Cas9^{WT}$ or $Cas9^{D10A}$ mRNA (Trilink-USA) and 0.1 volumes 3M sodium acetate (pH 5.2), and co-precipitated using 3 volumes ethanol. RNA was washed twice in 70% ethanol and re-suspended in 15 μl water to a concentration of 1 mg/ml. Integrity of mRNA and sgRNA was confirmed by agarose gel electrophoresis.

2.2.4 Generation of PLCζ-null mice by CRISPR/Cas9 microinjection

3–4-week old C57Bl/6J female mice (Charles River UK) were injected intraperitoneally with 5 IU of pregnant mare's serum gonadotropin (PMSG) (Intervet) and 48 hours later with 5 IU of human chorionic gonadotropin (hCG) (Intervet), and were paired with C57BL/6J (Charles River, UK) male mice. Zygotes were retrieved from oviductal ampullae at 20 hours post-hCG. Cumulus-enclosed zygotes were denuded by exposure to 1 mg/ml hyaluronidase (Sigma) in modified human tubal fluid (HTF) (Zenith Biotech) for 3–6 minutes, washed through fresh modified HTF, and cultured in HTF in the presence of 5% CO_2 at 37°C. Two hours after release from the cumulus mass, zygotes with normal morphology were microinjected into the cytoplasm in 30 µl drops of modified HTF media using a PMM-150FU Piezo impact drive (Primetech) with homemade glass capillaries with ~5–10 pl of CRISPR/Cas9-sgRNA mix at a final concentration of 150 ng/µl (100 ng/µl Cas9 cRNA and 50 ng/µl sgRNA). Injected zygotes were cultured overnight in KSOMaa (Zenith Biotech) in the presence of 5% CO_2 at 37°C and checked for 2-cell division the next day. B6CBF1 females (Charles River) were mated to a vasectomised male and females showing the presence of a copulatory plug were surgically prepared to receive zygotes with a normal 2-cell morphology using a bilateral implantation. The resulting F0 offspring were biopsied, and genomic DNA isolated and analysed by PCR, sequencing, and HRM analysis. PCR products were also cloned into PGEM-T vector and individual clones sequenced for mosaicism detection. Based on the genotyping findings, founder F0 mice with mutant alleles were bred to C57BL/6J mice and offspring tested for inheritance of mutant alleles by DNA sequencing. Heterozygote progeny ($PLC\zeta^{+/-}$) were mated for production of homozygote mice ($PLC\zeta^{-/-}$) and a colony for each of the Cas9 approaches ($Plcz1^{em1Jparr}$ and $Plcz1^{em2Jparr}$) was maintained by mating pairs using $PLC\zeta^{-/-}$ females and $PLC\zeta^{+/-}$ males.

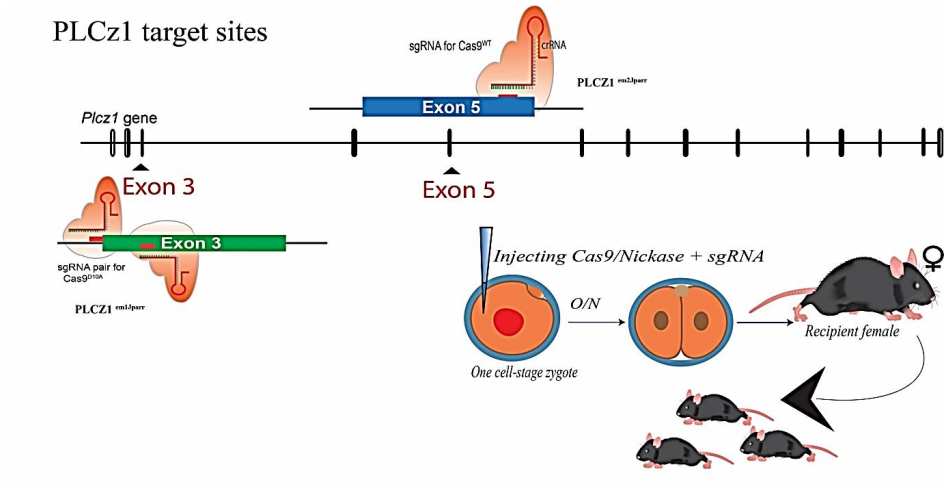


Figure 2-1: Generation of PLCζ mutants by CRISPR-Cas9 targeted disruption

CRISPR/Cas9 gene editing technology was used to knockout the PLCζ gene in mice and zygote microinjection was used as a route of delivery. Two strategies were employed targeting two exons of PLCζ: one used $Cas9^{WT}$ endonuclease with a single sgRNA, the second used $Cas9^{D10A}$ nickase with a pair of sgRNAs. From selected F0 animals showing frameshift-producing deletions, two mutant PLCζ mouse lines were produced: $Plcz1^{em1Jparr}$ generated by using the Cas9D10A nickase (22-nucleotide deletion), and $Plcz1^{em2Jparr}$ generated by using Cas9WT endonuclease (17-nucleotide deletion).

2.2.5 Identification of PLCζ mouse knockouts at the DNA level

2.2.5.1 PCR primer design

NCBI-Nucleotide was used to acquire the full-length nucleotide sequence of the mouse PLCζ gene (NCBI reference sequence: NC_000072.6). A sequence record format (FASTA) file was uploaded on Snapgene software and the primer binding sites were selected to span across the CRISPR recognition sites (Snapgene, 2016). The design of primers to amplify specific regions on the PLCζ gene was performed by using a web-based BLAST analysis at (https://www.ncbi.nlm.nih.gov/tools/primer-blast/); details are shown in table (2-2). All primer sequences used in this thesis were synthesised by Invitrogen.

Table 2-2: Genotyping primer sequences

Plcz1^{em1Jparr}	PLC_HRM_Fa	acaggcagggaaagggttt
	PLC_HRM_Rb	tgtctgagcacaggatagatga
Plcz1^{em2Jparr}	PLC_HRM_5Fa	agaaagaagggaggggaatcttc
	PLC_HRM_5Rc	tgatggtatatctgcatccttctt

2.2.5.2 Genomic DNA isolation

Genomic DNA was extracted from tail or ear biopsies by digestion with proteinase K overnight at 65°C with agitation in 0.1 ml lysis buffer (100 mM Tris-HCl pH 8, 5 mM EDTA, 200 mM NaCl, 0.1 % SDS, 0.5 mg/ml proteinase K (Roche)). Extracts were centrifuged at 17000 x g for 4 minutes, and supernatants diluted 6.5x into water prior to inactivation of the proteinase K at 95°C for 10 minutes.

2.2.5.3 Polymerase Chain Reaction (PCR) and Agarose gel electrophoresis

PCR reactions were performed in 0.2 ml tubes (Starlab) in an Eppendorf thermal cycler. The standard set up of solutions for PCR using *Taq* DNA Polymerase with Standard *Taq* Buffer from (Neb-USA) are summarised in table (2-3) in accordance with the manufacturer's instructions.

Table 2-3: PCR reaction setup

Reagent	**25 µl reaction**	**Final concentration**
10X Standard Taq Reaction Buffer	2.5 µl	1X
10 mM dNTPs	0.5 µl	200 µM
10 µM Forward Primer	0.5 µl	0.5 µM
10 µM Reverse Primer	0.5 µl	0.5 µM
Template DNA	Variable	1µg
Taq DNA Polymerase	0.125 µl	
Nuclease-free water	to 25 µl	

Samples were then subjected to a single round of thermal-cycling as summarised in table (2-4).

Table 2-4: Thermocycling conditions for PCR

Step	**Temp**	**Time**
Initial Denaturation	95°C	30 seconds
40 Cycles	95°C 58°C 68°C	30 seconds 45 seconds 60 seconds
Final Extension	68°C	5 minutes

PCR products were then analysed by gel electrophoresis and by DNA sequencing.

2.2.5.4 Agarose gel electrophoresis

PCR products were mixed with 6x DNA loading buffer (Neb-USA) and analysed using horizontal 2% (w/v) agarose gels in TAE buffer (40 mM Tris-acetate, 5 mM sodium acetate, 1 mM EDTA; pH 7.6) containing ethidium bromide (0.5 µg/ml), and then were electrophoresed at 70 V in TAE buffer. A 2-Log DNA Ladder which ranged from 0.1-10 kb (Neb-USA) was used to provide size markers. DNA was visualized using a UV transilluminator and when required, fragments of interest were excised for further purification and sequencing.

2.2.5.5 DNA sequencing by Sanger sequencing

The resultant PCR products were treated with ExoSAP-IT (PCR product cleanup reagent) in accordance with the manufacturer's instructions. In brief, 5 µl of a PCR reaction product was mixed with 2 µl of ExoSAP-IT reagent to give a combined 7 µl reaction volume. The mixture was then incubated at 37°C for 15 minutes to degrade remaining primers and nucleotides. The final step is to incubate the mixture at 80°C for 15 minutes to inactivate the ExoSAP-IT reagent before sending for sequencing. Purified PCR samples (~30 ng) plus 5 pM selected forward primer in a final volume of 5 µl per sample were sent for sample sequencing by GATC using an automated Sanger method. All the returned sequences were analysed using Snapgene software, and the built-in sequence alignment tool was used to align the PCR products sequences against the wildtype sequence. The findings were analysed by eye to check for the corresponding mutations.

2.2.5.6 High Resolution Melt (HRM) analysis

Melting curve analysis is an assessment of the dissociation-characteristics of double-stranded DNA during heating. HRM utilises PCR in the presence of a fluorescent DNA dye (LC Green). Indel mutations cause a change in melting profile of the product, which can be identified by the loss of fluorescent signal with increasing temperature.

HRM analysis is considered to be a very robust technique for detecting indel formation, polymorphisms and epigenetic differences in double-stranded DNA samples. The technique can also be used to detect mosaic mutations in a population of cells mutated with CRISPR/Cas9 (Bassett and Liu, 2014b).

HRM reactions were performed in 0.1 ml tubes (Starlab) in a RotorGeneQ thermal cycler (Qiagen). A standard set up for melting curve determination of genomic DNA was performed by using Hotshot Diamond PCR mix (Clent Lifescience) with LCGreen plus dye (BioFire Diagnostics). The reaction mix is summarised in table (2-5).

Table 2-5: HRM reaction setup

Reagent	**10 µl reaction**
2x Hotshot Diamond PCR mix	5 µl
10 µM forward primer (200 nM final)	0.2 µl
10 µM reverse primer (200 nM final)	0.2 µl
10x LC Green	1 µl
Nuclease-free water	2.6 µl
Template DNA	1 µl

Table 2-6: Thermocycling conditions for HRM

Step	**Temp**	**Time**
Initial Denaturation	95°C	5 minutes
45 Cycles	95°C 58°C 72°C	20 seconds 30 seconds 30 seconds
Melt curve	70-98°C	hold 2 seconds per cycle

Sample controls of mock-transfected cells, no template control, and control primers at non-targeted locus were included with every melt reaction. Fluorescent intensity and temperature shift of the melting curves were normalised and analysed with RotorGeneQ software.

2.2.5.7 TIDE analysis

For analysis of CRISPR activity, the web tool TIDE (Tracking of Indels by DEcomposition) from the Netherlands Cancer Institute was utilized. TIDE is a very simple and reliable tool that helps in identifying the frequency of the targeted mutations generated in a population of cells by CRISPR/Cas9. The process requires providing a CRISPR single guide RNA sequence (excluding the PAM), a sample sequence, and a control sequence (the wildtype sequence in this study). The web-based tool uses a specific algorithm to accurately reconstruct the spectrum of indels from the sequence traces. A final report provides details about the detectable indels with their frequencies.

It is worth noting that TIDE analysis depends heavily on the purity of the PCR products and the quality of the sequencing data. Highly repetitive regions of DNA around the target site of CRISPR/Cas9 can skew the results and so care must be taken to adjust the decomposition window accordingly.

2.2.5.8 Identification of somatic mosaicism and DNA subcloning

DNA subcloning by plasmid vector was performed on DNA from ear biopsies of founder mice generated by CRISPR/Cas9 injection into zygotes. In this study DNA subcloning was necessary to fully determine the level of mutagenesis in the founders and to identify the frequency of the targeted mutations when PCR and Sanger sequencing result in a convoluted spectrum with overlapping peaks that was difficult to delineate with TIDE analysis. The analysis process includes the following:

2.2.5.8.1 Purification of DNA from agarose gel

Gel fragments of PCR products were purified from agarose using QIAquick spin columns (QIAGEN) using the buffers provided, as per the manufacturer's instructions. Briefly, a gel slice containing the DNA fragment of interest was solubilized and applied to a silica-gel membrane of the spin column. DNA was adsorbed to the silica-membrane in the presence of high salt whilst agarose and other contaminants passed through the column. Bound DNA was washed and then eluted in distilled, deionised water.

2.2.5.8.2 Ligation

A linearized pGEM-T vector (Promega) was used in this study to incorporate the DNA fragments from the PCR step, in accordance with the manufacturer's recommendation. In brief, DNA fragments were added in a 1:3 vector to DNA fragment ratio. The enzyme used to ligate the DNA fragments is an enzyme from bacteriophage T4 called T4 DNA ligase; this was added at a final concentration of 3 units per 10 µl of the reaction volume together with the supplied ligation buffer. The reaction mixes were then incubated at room temperature for one hour.

2.2.5.8.3 Transformation of bacteria by heat-shock

The bacterial strain JM109 (Promega) was used to propagate DNA constructs. 50 µl of JM109 was thawed on ice, mixed with 2 µl of the ligation reaction, and then the mixture was incubated on ice for 20 min. Ligated DNA was introduced into bacteria via heat-shock by placing the mixture in a water bath set at 42°C for 50 seconds, immediately followed by replacing on ice for 2 minutes. Transformed bacteria were diluted with 950 µl of LB medium and incubated for 1.5 hours at 37°C with shaking at a 45° alignment. 100 µl of the transformed bacteria were directly plated out on LB-agar containing Ampicillin antibiotic selection. Agar plates were incubated overnight at 37°C to allow colonies to form.

2.2.5.8.4 Small scale preparation of plasmid DNA (Minipreps)

Plasmid DNA was prepared using the QIAprep Miniprep system (QIAGEN) following the manufacturer's instructions and using the solutions provided. Successfully transformed bacterial colonies were cultured overnight in 4 ml LB containing the selective antibiotic. The bacteria were pelleted and subsequently lysed under alkaline conditions. Upon neutralisation, genomic DNA, proteins and lipids were precipitated and the lysates were cleared by centrifugation. The resulting supernatant was run through a silica-gel membrane QIAprep column. DNA was adsorbed onto the silica under the high salt composition of the buffers; all other contaminants were washed through. Salt was

removed by washing the column with 80% (v/v) ethanol. The purified plasmid DNA was then eluted from the QIAprep column with distilled, deionised water.

DNA samples were then sent for sequencing, and all the returned sequences were analysed using Snapgene software, and the built-in sequence alignment tool was used to align the PCR product sequences against the wildtype sequence. The findings were analysed by eye and checked for the corresponding traces of mutations.

2.2.6 Identification of PLCζ mouse knockouts at the RNA level

2.2.6.1 RNA extraction from mouse testes

Testes from 8-week-old wildtype and mutant animals were collected and directly snap-frozen in liquid nitrogen and stored at -80°C for later processing. On the day of RNA extraction, the testes were mechanically homogenised using a Precellys tissue homogenizer (Bertin Instruments) in 1.5ml tubes containing 0.5mm bashing beads and 1ml of RNAzol RT (Sigma-USA). RNAzol RT is a mixture of guanidine thiocyanate and phenol in a monophase solution, that effectively dissolves DNA, RNA, and protein from homogenised tissue samples.

The addition of 0.4 ml of RNase-free water per 1 ml of RNAzol RT to the mixture allows precipitation of DNA, proteins, polysaccharides and other molecules, which can be removed by centrifugation at12,000 x g for 15 minutes at 4°C. For total RNA isolation, the supernatants were collected in fresh tubes and mixed with equal volume of 100% isopropanol (Sigma) to precipitate RNA. The precipitated RNA pellets were washed twice with 0.6 ml 75% ethanol (v/v) per 1ml of supernatant used for precipitation, and excess ethanol was removed with a micropipette. The RNA pellets were then solubilised in RNase-free water, aliquoted in 0.2 ml tubes and kept at -80°C at a concentration of 1-2 µg/ml for later use.

2.2.6.2 RNA agarose gel electrophoresis

This method has been used extensively to check for RNA integrity by examining the intensity of the ribosomal RNA bands (28S and 18S rRNA), and the absence of any genomic DNA contamination. A total amount of 0.5 ug of RNA per sample was loaded in a 1.5 % non-denaturing agarose gel stained with ethidium bromide, and then electrophoresed at 70 V in TAE buffer. Ribosomal RNA bands were visualized by using a UV transilluminator and analysed by eye to check for RNA integrity and purity from any DNA contamination.

2.2.6.3 Reverse transcription primers design

Mouse PLCζ cDNA sequences were downloaded from Ensemble (www.ensembl.org), and RT-PCR primers were either designed with Snapgene or with Primer-Blast from NCBI. In both of the approaches, primers were chosen to span across the CRISPR recognition sites. Primers were provided by Invitrogen.

Table 2-7: RT-PCR primers sequence

Plcz1^{em1Jparr}	PLC_RT_Fa	aagccaacttcatgagctcg
	PLC_RT_Rb	tcaatggtgattcttccttggt
Plcz1^{em2Jparr}	PLC_RT_5Fa	gagaactgtaaaaccgtgtacca
	PLC_RT_5Rc	cccagcagtcaatttccaga

2.2.6.4 Single-step reverse transcription-PCR (RT-PCR) and sequencing

For PLCζ mRNA expression analysis, conventional RT-PCR was performed on RNA samples using OneTaq One-Step RT-PCR (New England Biolabs, USA). One-Step RT-PCR utilises RNA templates to reverse transcribe cDNA synthesis and PCR amplification in one step and with a single reaction mix. The reaction mix is summarised in table (2-8):

Table 2-8: RT-PCR reaction mix

Reagent	**50 µl reaction**
OneTaq One-Step Reaction Mix (2X)	25 µl
OneTaq One-Step Enzyme Mix (25X)	2 µl
Forward Primer (10 µM)	2 µl
Reverse Primer (10 µM)	2 µl
Nuclease-free water	18 µl
RNA template	1 µl

Table 2-9: Thermocycling conditions for RT-PCR

Step	Temp	Time
Reverse Transcription	48°C	15 minutes
Initial denaturation	94°C	1 minutes
45 Cycles	94°C 58°C 68°C	20 seconds 30 seconds 30 seconds
Final Extension	68°C	5 minutes
Hold	4°C	∞

Products were analysed by gel electrophoresis and by DNA sequencing.

2.2.6.5 Real-time qRT-PCR

Quantitative real-time RT-PCR was performed in a 20 ul reaction volume on a 384-well plate (Starlab) designed for compatibility with the LightCycler thermal cycler (Roche). RNA samples from testes of wildtype and mutant animals (n=3) were reversely transcribed and amplified in a one-step reaction by using OnestepPLUS qRT-PCR MasterMix SYBR Green (Primerdesign, UK). The reaction mix setup and amplification protocol were applied as recommended by the manufacturer, see table (2-10 and 2-11). Non-template controls in the form of nuclease-free water in duplicate wells were always included. A gene expression profile was created by LightCycler included software based on the DNA fluorescence reporter. The RNA expression levels (Ct values) were then normalized to the beta actin mRNA level and calculated using the relative quantification approach compared to wildtype RNA samples.

Table 2-10: One-step real time RT-PCR reaction mix

Reagent	20 µl reaction
Precision®PLUS OneStep qRT-PCR Master Mix	10 µl
RT-PCR primers mix (6pmols forward and reverse)	2 µl
SYBR Green	1 µl
Template RNA (25ng)	1 µl
Nuclease-free water	6 µl

Table 2-11: Thermocycling conditions for one step real time RT-PCR

Step	Temp	Time
Reverse Transcription	55°C	10 minutes
Enzyme activation	95°C	2 minutes
45 Cycles	95°C	10 seconds
	60°C	1 minutes

2.2.7 Identification of PLCζ mouse knockouts at the protein level

Immunoblotting against sperm PLCζ protein was performed at Prof. Rafael Fissore's lab at the University of Massachusetts as previously described in Kurokawa's paper (Kurokawa *et al.*, 2005). Mouse sperm were diluted to appropriate concentrations, 2X sample buffer added and samples kept at −80°C until use. Thawed samples were boiled for 3 minutes, mixed well and loaded onto 7.5% SDS-PAGE gels and resolved polypeptides were transferred onto PVDF membranes (Millipore, Billerica, MA) using a Mini Trans-Blot Cell (Bio-Rad, Hercules, CA). The membranes were blocked in 6% non-fat dry milk in PBS–0.1% Tween and incubated overnight at 4°C with 1/1000 dilution of a custom-made anti-PLCζ rabbit sera (raised against a 19-mer sequence (GYRRVPLFSKSGANLEPSS) at the C-terminus of mouse PLCζ (mPLCζ) (accession no. NP_473407); this was followed by 1 hour of incubation with 1/2000 of a goat anti-rabbit horseradish peroxidase–labelled secondary antibody (Bio-Rad: #1662408EDU). Immunoreactivity was detected by using chemiluminescence per the manufacturer's instructions (PerkinElmer, Waltham, MA) using a Kodak Image Station 440CF.

2.3 Results

2.3.1 Identification of mouse PLCζ knockouts at the DNA level

2.3.1.1 Screening for indels in the transgenic founder (F0) mice

Several molecular-based approaches have been used to identify CRISPR/Cas9 mutagenesis outcomes in living animals. Their range can vary in sophistication from simple localisation of a PCR reaction on a gel, to the building of a barcoded library and next generation sequencing. Choosing the suitable method depends on the availability of that method and on the stage at which the animals are within the process of characterisation, i.e. as F0 (founders) or as a subsequent generation (F1), and also depends on the type of the desired allele mutagenesis (indels formation or point mutation).

F0 animals (born from microinjecting a zygote with CRISPR/Cas9 constructs) and F1 animals (obtained by crossing between F0 and a wildtype mice) represent very different challenges in terms of identifying their precise genotyping. As F0 animals are often mosaic, we approached their genotypic characterisation as a screen for the presence of an allele of interest by electrophoretic analysis of PCR products, HRMA analysis, Sanger sequencing, Tide analysis for deconvoluting mixed sequencing traces and DNA subcloning. On the other hand, alleles that can be definitively transmitted and characterised at the F1 generation were analysed by PCR and Sanger sequencing.

As a result of targeting the coding sequence of PLCζ gene with wildtype Cas9 and Cas9 nickase constructs by microinjection into the zygotes, a total of 33 mice were born, 14 animals (7 males and 7 females) were produced as a result of targeting exon 3 with a pair of sgRNA along with the double nickase, and 19 animals (5 males and 14 females) were produced as a result of targeting exon 5 with wildtype Cas9 and single guide RNA.

From targeting exon 3 with the double nickase, PCR analysis of tail DNA and Sanger sequencing showed that from 14 animals produced with this approach, 4 animals (2 males and 2 females) were wildtypes, 6 animals (3 males and 3 females) were mosaic, and 4 animals (2 males and 2 females) failed to generate PCR products suggesting that the nickase mutagenesis and the NHEJ pathway might have mutated the PCR primer amplification sites. DNA integrity was verified with primers targeting an independent locus.

Six animals have been identified with possible multiple allele complexity, IDs #8 (m), #11 (m), #14 (f), #16 (m), #19 (f), #20 (f), as shown in figures **2-2, 2-3, 2-4**. Multiple sequence alignment on Snapgene revealed formation of various indels on the targeted sequence of exon 3 in each of the six animals. Allele deconvolution analysis identified animal #8 (m) as a mosaic animal with a 27nt deletion on one allele and an 11nt insertion via the HDR pathway on another allele. There were also small traces of an additional wildtype allele at nearly 8.4%, and a 24nt deletion at 7.5%. An 11nt insertion can cause a frameshift mutation and loss of function of PLCζ if the animal is homozygous for this mutation, but due to the presence of the 27nt deletion (non-frameshift deletion) and the level of allele complexity, we could not use this animal to transmit the mutated allele through the germline, nor to study the phenotypic alteration of the mutation on the mature male.

- ✓ Animal #11 (m), was also identified as a mosaic animal of two mutated alleles, one with a 13nt deletion, and a 2nt deletion on another allele, making it highly likely that this is a null frameshift mutant.

- ✓ Animal #14 (f), had a 22nt deletion on both alleles, and was highly likely to be a homozygous frameshift mutant.

- ✓ Animal #16 (m), was very hard to deconvolute. It appears that a large deletion (~23nt) is covering the splice site.

- ✓ Animal #19 (f), was very hard to deconvolute.

- ✓ Animal #20 (f), was recognised to have 12nt and 28nt insertions; one allele would just remove 4 amino acids, the other should cause a frameshift.

At this stage, and for all types of indel formation, all founder F0 animals should be considered mosaic. In fact, even if only two alleles were identified during analysis of the founder ear biopsy DNA, the possibility of additional undetected alleles in these animals cannot be dismissed. These hidden alleles can be present in any part of the body including the germline, potentially resulting in the transmission of novel alleles not previously characterised at the screening step.

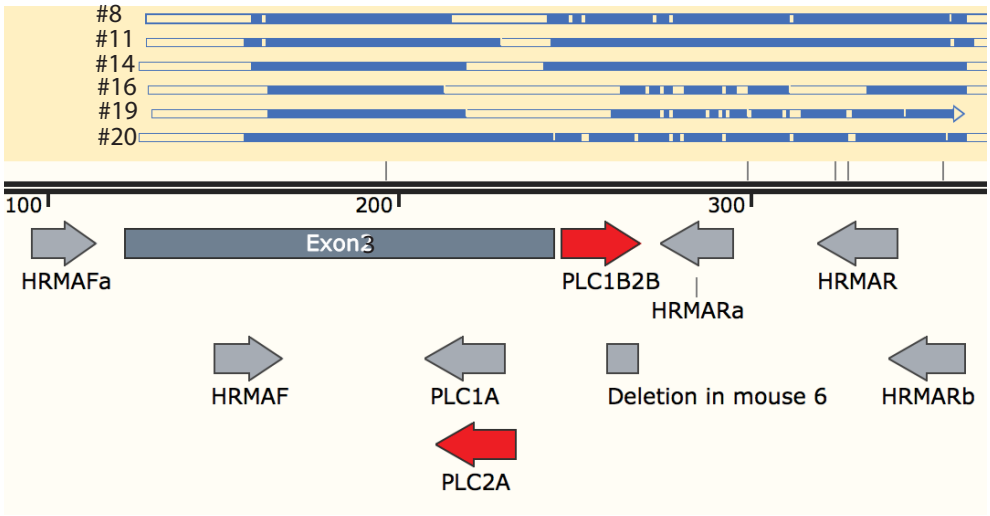


Figure 2-2: Multiple DNA sequence alignment of PCR products on exon 3.

For six animals (#8, #11, #14, #16, #19, and #20) produced with CRISPR nickase activity.

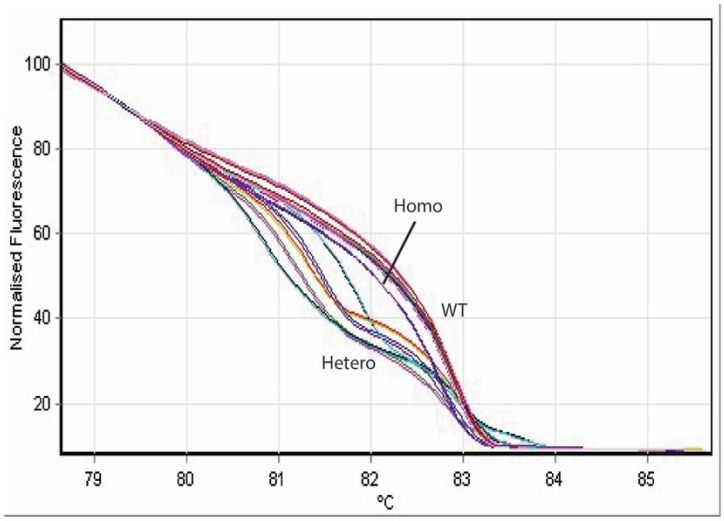


Figure 2-3: High-resolution melting curves shows that there are a variety of different melt curves for twelve PCR fragments from animals 8-20.

Produced with targeting exon 3 of PLCζ by double nicking the coding sequence with a pair of sgRNAs. Note: the irregular profiles of these curves are explained by mosaic heteroduplex PCR fragments formed because of the random mutations induced by CRISPR-Nickase mutagenesis

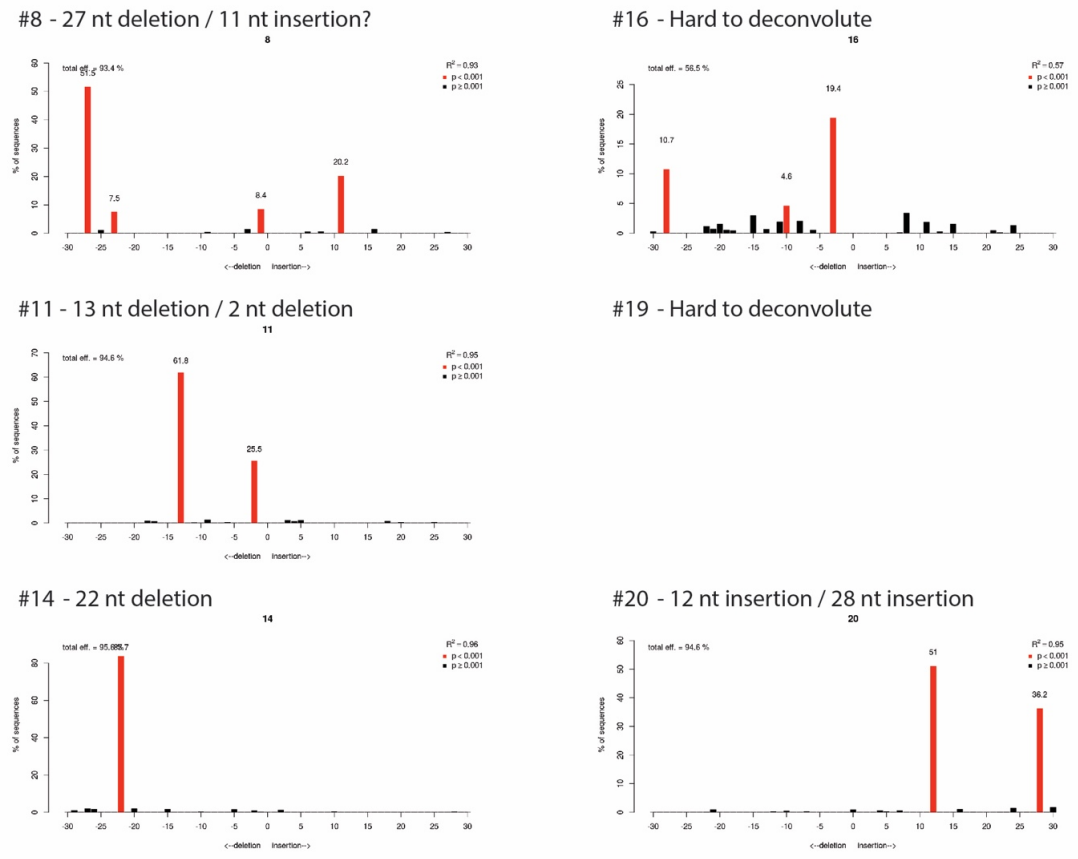


Figure 2-4: TIDE software is used to analyse the spectrum and frequency of indels formation in six F0 animals generated by targeting the same sequence on exon 3 with a pair of sgRNAs.

From targeting exon 5 with wildtype Cas9 and a single guide RNA, PCR analysis of tail DNA and Sanger sequencing showed that from 19 animals produced with this approach, 11 animals (2 males and 9 females) were wildtypes, 6 animals (2 males and 4 females) were mosaic, and 2 animals (2 females) failed to generate PCR products suggesting that the nickase mutagenesis and the NHEJ pathway might have mutated the PCR primer amplification site. DNA integrity was verified with primers targeting an independent locus.

Here, we identified six animals with possible multiple allele complexity, IDs #2 (m), #3 (f), #5 (f), #6 (f), #23 (m), #27 (f), as shown in figures **2-5, 2-7, 2-8**.

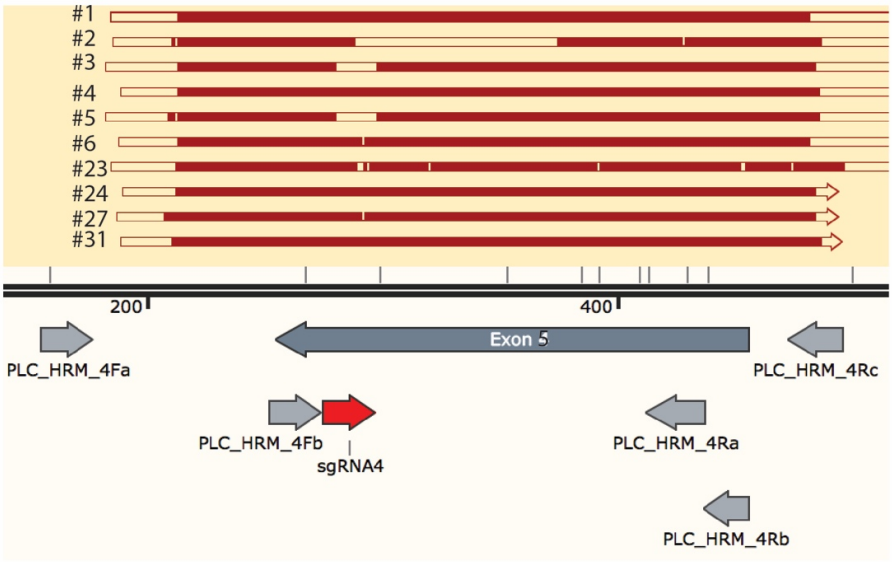


Figure 2-5: Multiple DNA sequence alignment of PCR products on exon 5 of mouse PLCζ for ten animals produced with wildtype Cas9 and a single gRNA activity.
Notice: traces from animals 1, 4, 24, and 31 are wildtypes.

Multiple DNA sequences alignment on Snapgene revealed various indel formation on the targeted sequence of exon 5 in each of the six animals. Allele deconvolution analysis identified animal #2 (m) as a mosaic animal with the largest deletion recorded in this study of 86nt on one allele and possible of 2nt deletion on the other allele (figure 2-7).

- ✓ Animal #3 (f), was also identified as a mosaic animal of two mutated alleles, one with a 17nt deletion, and a 5nt deletion on another allele, making it highly likely that this is a null frameshift mutant.

- ✓ Animal #5 (f), had a 17nt deletion on both alleles, and is highly likely to be a homozygous frameshift mutant.

- ✓ Animal #6 (f), had a 1nt insertion on both alleles, but different bases inserted on each allele (C on one, T on the other), and was highly likely to be a homozygous frameshift mutant.

- ✓ Animal #23 (m), had a 2nt deletion on one allele, and the other allele showed wildtype traces, 1nt insertion, and 8nt insertion. Further subcloning and sequencing was performed here to identify the level of the allele complexity.

- ✓ Animal #27 (f), had a 1nt deletion on both alleles, and highly likely to be homozygous frameshift mutant.

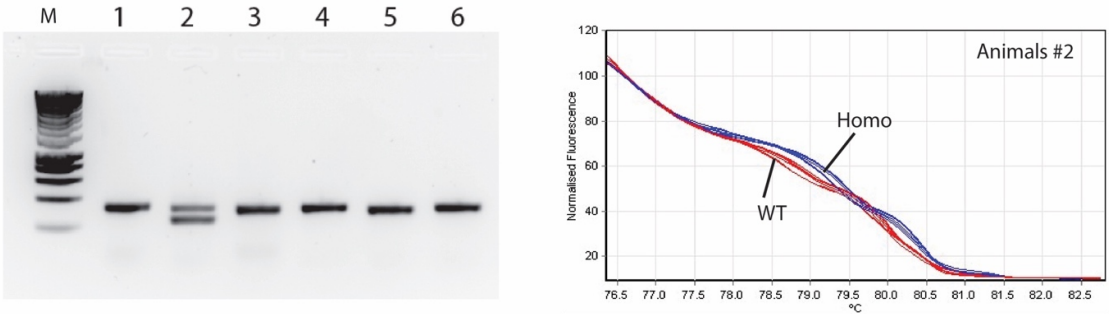


Figure 2-6: Left, (1.5%) (w/v) agarose gel electrophoreses of PCR products from animals 1 to 6 which were produced by targeting exon 5 of PLCζ with wildtype Cas9 and single gRNA. Right, HRM analysis of animal number 2 against wildtype traces.

Note: #2 is a mutant with quite a large deletion (it also shows the biggest shift in the HRMA), and the other samples vary in size considerably, consistent with the HRMA results (figure 2-8).

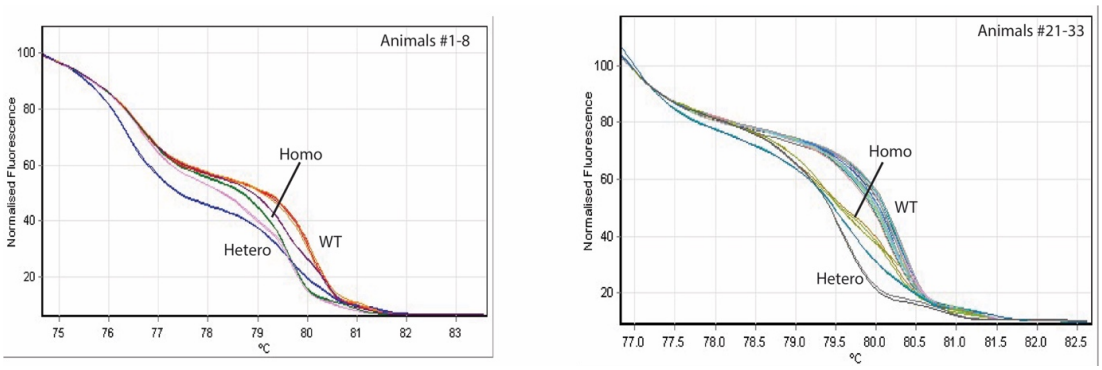


Figure 2-7: High-resolution melting curves show that there are a variety of different melt curves for twenty PCR fragments from animals 1-8 and animals from 21-33 produced with targeting exon 5 of PLCζ by wildtype Cas9 with a single gRNA.

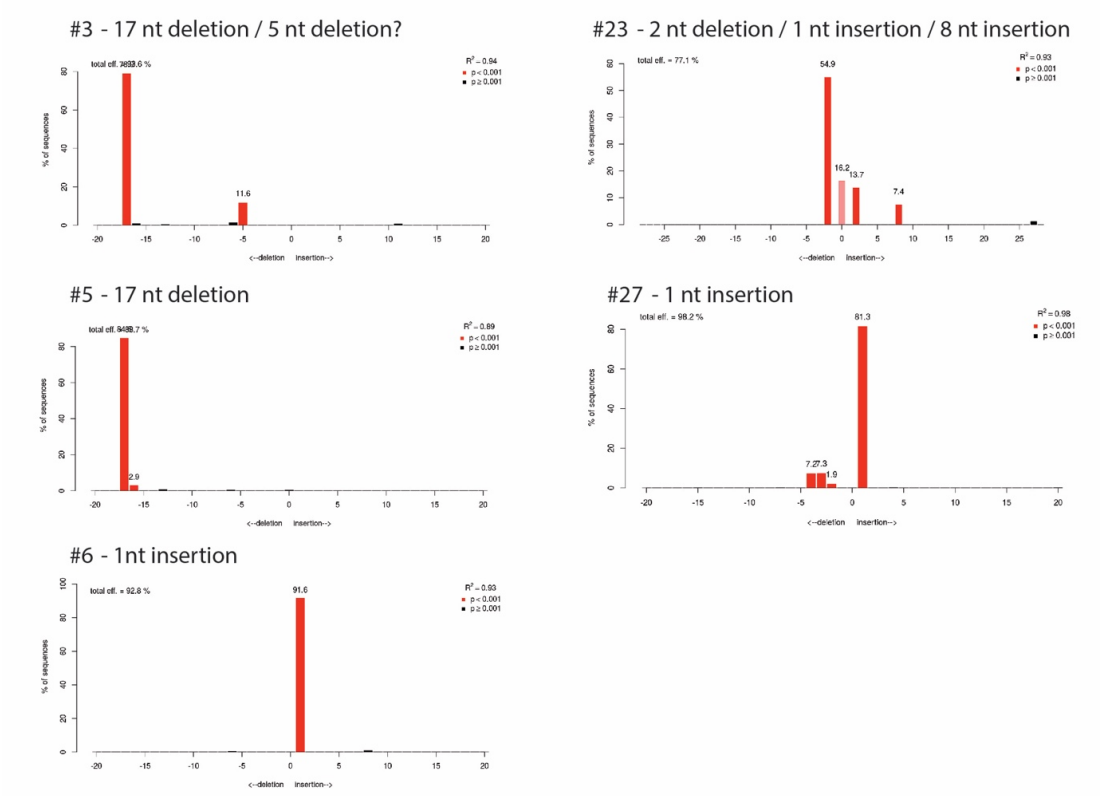


Figure 2-8: The TIDE software is used to analyse the spectrum and frequency of indels formation in five animals generated by targeting the same region on exon 5 with a wildtype Cas9 and single gRNAs.

Notice: the DNA traces in this approach appears less complicated to deconvolute than traces from double nicking with a pair of sgRNAs.

2.3.1.2 DNA subcloning and traces from selected founders (F0)

In order to characterise at least one desirable allele that can be transmitted to F1 mice from a F0 mosaic founder, we needed firstly to resolve the dilemma of the alleles' complexity in F0 animals, otherwise crossing F0 animals based on the findings from Tide analysis alone is not enough to establish a stable mouse line. We found that DNA subcloning and later sequencing individual traces would be ideal for identifying at least one candidate animal that can be responsible for transmitting the characterised allele to F1.

However, a number of selection criteria must be fulfilled before making any early decision regarding the candidate F0 animal:

1. Choosing the type of desirable indels (in this study, indels that are non-divisible by three nucleotides to create a knockout effect).

2. Size of the deletion (large deletions make it easier to identify heterozygous and homozygous mutants by routine PCR and gel electrophoresis).

3. Sex of the animal (in this study we desired females to be responsible for transmitting the alleles by crossing with wildtype males, as a mosaic F0 male might be infertile)

4. Level of alleles' complexity (animals with more complex traces are less faithful in transmitting the only desirable allele, while animals with only one visible mutated allele tend to transmit that allele via their germline).

Based on the mentioned selection criteria, we found that animal #14 (f) from the double nickase approach, and the animal #3 (f) from the wildtype Cas9 approach, were the best candidate animals to faithfully transmit the 22nt deletion and 17nt deletion, respectively, into two different colonies of F1 animals.

DNA subcloning and traces from selected founders (F0)



DNA subcloning and multiple sequences of PCR products from animals 11 (m), 14 (f), 16 (m) were aligned against wildtype traces, and mutation by indels formation were analysed by comparing different traces from each mutation site. This group of animals, were produced with double nicking exon 3 of PLCz1 with pair of sgRNAs, resulting that animal #11 contains a single type of a mutated sequence of 13nt deletion on alleles that examined with subcloning. Animal #14 was also shown single type of a mutated sequence of 22nt deletion on alleles. Animal #16 traces were very hard to deconvolute with Tide analysis due to the complexity of relatively large deletions that almost landed at the same location, first one was with 32nt deletion, and the second one was with 25nt.
Animals from targeting exon 5 with wildtype Cas9, Animal #2 (m) as expected, traces show 86nt deletion and 2nt deletion on the second allele. Traces from animal #3 (f) show 17nt.

2.3.1.3 Generation and identification of PLCζ-null F1 animals

Indeed, mouse #14 was mated with a wildtype male from the same background (C57BL/6j), and out of 14 mice produced from this mating, 3 (2 females, 1 male) were heterozygous for the 22nt deletion. The findings were confirmed by PCR, sequencing, and Tide analysis (See figure 2-9). Animals from this mouse line that contain the allele with a 22nt deletion will be hereafter referred to as PLCζ ^{em1Jparr}.

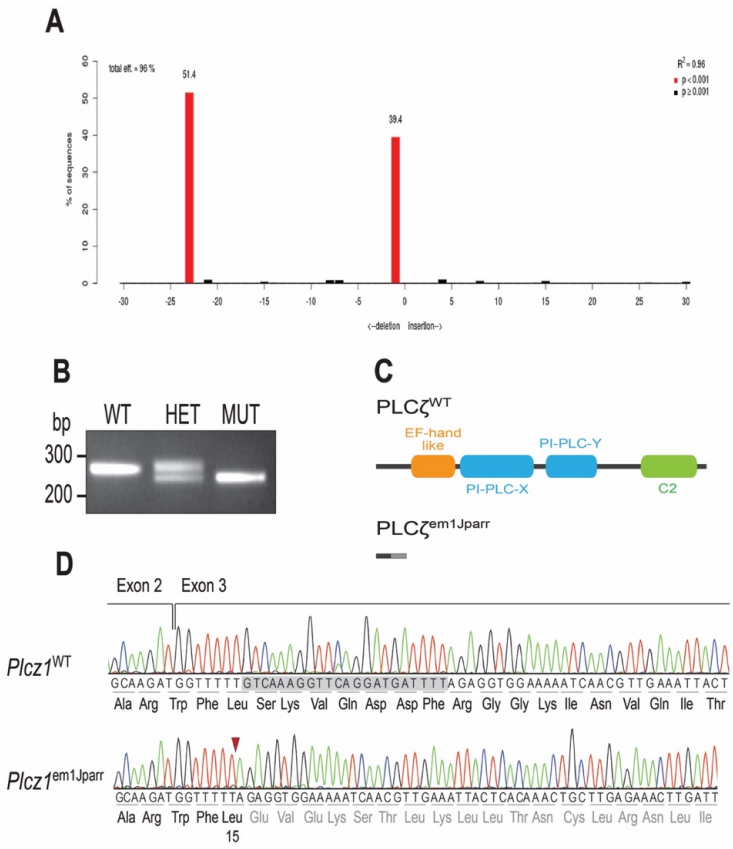


Figure 2-9: Genomic characteristics of mouse PLCζ ^{em1Jparr} mutant allele

(**A**) Melt analysis showing heterozygous F1 progeny resulting from crossing between mice #14 and BL/6j male.
(**B**) Results from a genotyping PCR reaction for 22nt deletion mutant line: HET = PLCζ $^{+/em1Jparr}$; MUT= homozygote PLCζ ^{em1Jparr}; WT = homozygote PLCζ ^{WT}.
(**C**)Predicted protein-domain structures for wildtype mouse PLCζ protein (PLCζ^{WT}) and truncated proteins resulting from expression of mutant PLCζ ^{em1Jparr} allele.
(**D**) Comparison of genomic sequences from the wildtype PLCζ^{WT} allele and 22nt-mutant PLCζ allele harbouring nucleotide deletions (deleted sequence shaded grey in PLCζ^{WT} sequence). Capital letters correspond to exonic sequences and lower-case letters to intronic sequences.

On other hand, mouse #3 was mated with a wildtype male from the same background (C57BL/6j), and out of 19 mice produced from this mating, 9 (3 females, 6 male) were heterozygous with the 17nt deletion. The findings were also confirmed by PCR, sequencing, and Tide analysis (See figure 2-10). Animals from this mouse line that contain the allele with the 17nt deletion will be referred to hereafter as PLCζ ^{em2Jparr}.

Heterozygous animals from PLCζ$^{+/em1Jparr}$ and PLCζ$^{+/em2Jparr}$ were then crossed between each other to create PLCζ^{em1Jparr} and PLCζ^{em2Jparr} homozygous mutants harbouring the frameshift-producing deletion. Homozygous males were used for sperm-PLCζ functional analysis, whereas homozygous females along with heterozygous females were used to expand the colonies by mating with PLCζ^{wt} males.

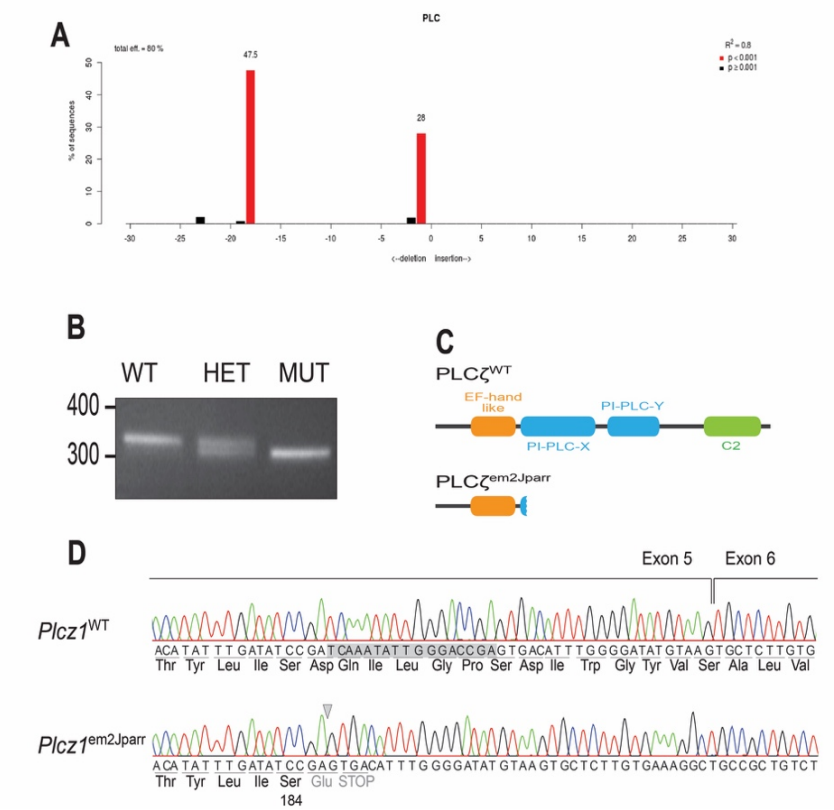


Figure 2-10: Genomic characteristics of mouse PLCζ ^{em2Jparr} mutant allele

(**A**) Melt analysis showing heterozygous F1 progeny resulting from crossing between mice #3 and BL/6j male.
(**B**) Results from a genotyping PCR reaction for 17nt deletion mutant line: HET = PLCζ $^{+/em2Jparr}$; MUT= homozygote PLCζ ^{em2Jparr}; WT = homozygote PLCζ ^{WT}.
(**C**) Predicted protein-domain structures for wildtype mouse PLCζ protein (PLCζ^{WT}) and truncated proteins resulting from expression of mutant PLCζ ^{em2Jparr} allele.
(**D**) Comparison of genomic sequences from the wildtype PLCζ^{WT} allele and 17nt-mutant PLCζ allele harbouring nucleotide deletions (deleted sequence shaded grey in PLCζ^{WT} sequence). Capital letters correspond to exonic sequences and lower-case letters to intronic sequences.

2.3.2 Identification of mouse PLCζ knockouts at the RNA level

Sequence analysis of RT-PCR products from testis mRNA obtained from homozygous males of PLCζ ^{em1Jparr} and PLCζ ^{em2Jparr} confirmed the presence of the mutations that are correspondent to the predicted mutant cDNA sequences with no observable residual wildtype sequence contamination (figure 2-9 d, 2-10 d), suggesting a complete lack of PLCζ^{WT} expression in these mutant lines. The truncated proteins that could be produced from the two mutant PLCζ alleles (figure 2-9 c, 2-10 c) are correspondent to small N-terminal portions, X-domain respectively are lacking the regions necessary for enzymatic activity of PLCζ.

A qualitative analysis of PLCζ gene expression levels in testes of PLCζ^{WT}, PLCζ ^{em1Jparr} and PLCζ ^{em2Jparr}, revealed a significant reduction (PLCζ^{WT} vs PLCζ ^{em1Jparr}, P >0.05), (PLCζ^{WT} vs PLCζ ^{em2Jparr}, P >0.01), but not complete cessation of PLCζ mRNA production (figure 2-11).

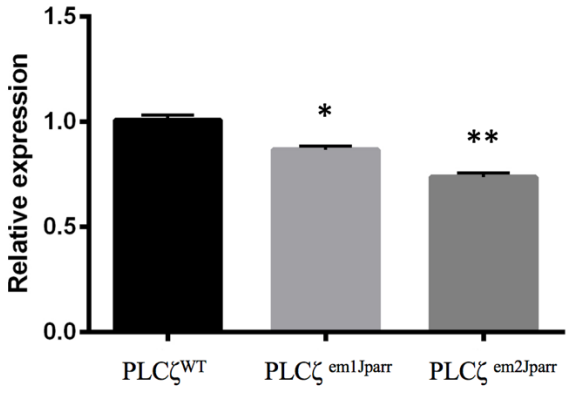


Figure 2-11: PLCζ expression analysis in testes of PLCζ^{WT}, PLCζ ^{em1Jparr} and PLCζ ^{em2Jparr}

*RT-PCR primer sets were chosen to anneal upstream to the locations of the CRISPR mutation.

2.3.3 Identification of mouse PLCζ knockouts at the protein level

Studying protein loss of function following site-specific mutagenesis is usually a very effective technique to elucidate the effect of a mutation on a specific phenotype. The non-divisible by three nucleotide deletion mutation can yield a non-functional protein sequence caused by the shift of the reading frame of a gene leading to formation of premature stop codons in the new frame. Nonsense-mediated decay can then eliminate the aberrant mRNA and thereby prevents a potentially toxic protein from being made.

A polyclonal anti-PLCζ antibody against the C-terminus region was used to validate the frameshift mutation and loss of function of PLCζ protein in sperm samples collected from PLCζ^{WT}, and PLCζ ^{em1Jparr}. The absence of full-length PLCζ was confirmed by performing the immuno-blotting analysis of sperm derived from PLCζ ^{em1Jparr} mice in triplicate with identical results.

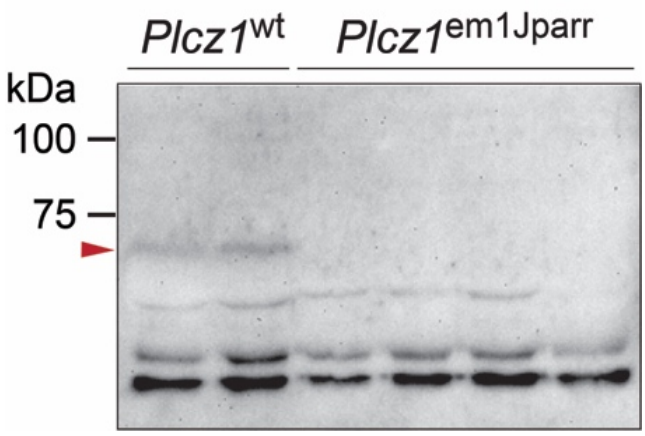


Figure 2-12: PLCζ immunoblot analysis of sperm samples from PLCζ^{WT}, and PLCζ ^{em1Jparr}

Immunoblotting analysis of PLCζ in sperm from PLCζ ^{WT} (n=2) and PLCζ ^{em1Jparr} (n=4) using a custom made anti-PLCζ antibody. Immuno-reactive band corresponding to PLCζ^{wt} is indicated by a red arrow.

2.4 Discussion

2.4.1 Is it convenient, efficient and reliable to use CRISPR/Cas9 gene editing technology to target the coding sequence of PLCζ in mice?

Generation of knockout mouse models is essential for understanding complex biological pathways within a biological system. Studying mammalian reproduction for instance, has been particularly facilitated through generation of knockout mice lacking certain genes expression thought to be involved in specific cellular processes. However, generation of such cellular or animal models with specific types of genetic alterations has for a very long time been both tedious and sometimes fallible (Lander, 2016).

Recently, a revolutionary tool from a bacterial adaptive immunity process (CRISPR/Cas9) was discovered in prokaryotes with the ability on targeting almost any bacteriophagic DNA sequences leading to formation of double-strand breaks. Harnessing the prokaryotic tool to directly target specific DNA sequences in eukaryotes has opened exciting new pathways in probing gene function in virtually any model system, including mice. The simplicity of this tool comes from its ability to target any genomic sequence by introducing short guide RNAs and the Cas9 protein or RNA into cells of interest, leading to DSBs at the targeted locus and random formation of indels at the NHEJ repair site. The result is a frame-shift mutation of the DNA sequence, subsequently targeting the mRNA with the new stop codon for degradation by the mechanism of nonsense-mediated decay. Moreover, utilising CRISPR/Cas9 system in the one-cell stage embryo has revolutionized the speed, simplicity and efficiency in generating genetically modified mice. Thus, providing a new platform for the generation of transgenic animals, not only in determining gene function in cellular processes, but also in gaining important insights into the mechanisms that underline normal physiology and diseases.

Investigating the physiological relevance of the sperm specific PLCζ during stages of mammalian oocyte activation and early embryo development was hampered for a long time due to the lack of a mutant mouse model that is deficient of PLCζ expression. Therefore, it was imperative in this study to explore the true capability of this novel tool on targeting the coding sequence of PLCζ gene in mice, with great anticipation on creating the first animal model lacking functional expression of PLCζ for further phenotypic analysis.

However, number of points needed to be taken into consideration before starting CRISPR/Cas9 microinjection into mouse single cell embryos. One regards the potential off-target mutations that may accompany the use of CRISPR, and the undesired genetic modifications that could be inserted anywhere in the genome. Such alteration would raise a major concern regarding the efficiency and the reliability of this tool, as this could eventually lead to disrupt the function of certain genes and pathways in the cell. Yet, the specificity of the CRISPR system is largely determined by the specificity of the sgRNA on targeting a genomic sequence compared to the rest of the genome. For instance, off-target effects can be achieved at sites that bear high similarity to the on-target sites, whereas at low similarity regions, nucleases have affinity near to zero due to a relatively large number of mismatches between guide RNAs and genomic DNA.

Thus, several online-based tools have been developed to search for any potential off-target based on a given genomic sequence. In this study, a web-based software designed by Feng Zhang's group at MIT has been used to generate high fidelity sgRNAs both for the wildtype Cas9 and the mutant nickases. Providing the PLCζ query sequence, the CRISPR-design tool program first fetched all the possible regions in the length range of 15 to 25 nucleotides, with PAM either on the 5' or 3' side. Two best candidate locations have been revealed, one at the exon3 for the nickases activity, and the second on the exon5 for $Cas9^{wt}$. These regions were then evaluated and filtered to show low/no off-target activity across the whole genome of C57BL6 mouse strain.

In ideal situations, the best approach to investigate any possible off-target mutation is by performing whole genome sequencing analysis pre and post injection of CRISPR/Cas9. The deep gene analysis would help to identify any presence of indels formation, SNPs, structural variants such as chromosomal inversion, rearrangements and deletions in any type of cells with great accuracy. However, this method was not possible to utilise in this study for cost reasons. It is worth noting that utilising Cas9 protein, instead of Cas9 RNA, was showed to offer less incidents of off-target mutation and enhanced the alleles complexity in each clone (Kouranova *et al.*, 2016). However, at the time of applying this technology in this study, the availability of Cas9 protein was substantially limited. Therefore, Cas9 RNA from a commercial provider was selected to follow the mutagenesis approach. Remarkably, there were number of available approaches to follow in this study to minimize the frequency of off-target mutations. One is to improve the targeting specificity of Cas9 by applying the mutant $Cas9^{(D10A)}$. By applying the paired nickase and

two separate gRNAs targeting opposite strands on the same targeted locus of PLCζ, led to generating two nicks in close proximity, which in turn were processed as double-stranded breaks within the targeted location. Although, a single nick on the DNA can easily be repaired by the base excision repair system (Caldecott, 2008), a pair of nicks on the opposite strands would drastically reduce any potential off-target effects of Cas9 (Cho *et al.*, 2014). Second is to target a different region on PLCζ, exon5, by utilising the wildtype Cas9, then any subsequent differences in the phenotypic alterations of the homozygous from the two approaches will be considered as undesired changes due to the off-target effect.

In the first approach to target the coding sequence of PLCζ, included microinjecting mouse zygotes with the wildtype Cas9 with a single guide RNA targeting exon five of PLCζ, produced six live animals with various indel formation on the coding sequence. The second approach, however, included microinjecting mouse zygotes with the mutant Cas9 (nickase) with a pair of guides RNAs targeting exon three of PLCζ, also produced six live animals with formation of various indels in the targeted sequence.

However, introduction of Cas9 and the mutant nickase cRNAs along with the sgRNAs into one-cell embryos, resulted in multicellular embryos and offspring with mosaic alleles in individual cells. Sequencing analysis revealed that the F0 animals have suffered from a certain level of mosaicism and allele complexity, leading to noticeable difficulties in determining the actual genotyping and allele variation in each animal. In both of the approaches, however, the formation of desired genetic alteration on PLCζ coding sequence was observed by DNA genotyping and sequencing the F0 offspring.

In conclusion, CRISPR/Cas9 as a gene editing tool has provided this study with an exceptional approach to target the coding sequence of PLCζ in mouse lines with mutagenesis. Thereby, two mouse lines harbouring various mutations on the targeted locus of PLCζ were generated with high efficiency, and were therefore used for the phenotypic analysis described in the next chapter.

2.4.2 What is the best approach to identify the desired mutant alleles in F0 mosaic animals?

Introducing CRISPR/Cas9 constructs into mouse zygotes in this study has successfully altered the wildtype genomic sequence of the PLCζ gene, producing number of homozygous and heterozygous animals with certain level of allele complexity in each trace. Decoding the allele complexity in each clone of the F0 animals was very crucial in determining the desired allele that needed to be transmitted to a subsequent progeny for the ultimate formation of homozygous males. Based on findings from PCR gel electrophoresis, HRMA, sequencing and Tide analysis, it was found that the outcomes of the allele complexity in each clone can drastically be increased in cases where more than one sgRNA was introduced with the Cas9.

In fact, all F0 animals produced with the aid of CRISPR/Cas9 RNA injection should be considered mosaic, this is due to the relatively longer time that it is required for the RNA to be transcribed, then to get degraded by the cellular process. Which in this case the active form of Cas9 RNA along with the gRNA would be carried by the first or the second cell division to the next embryonic cell, and thus creating multiple cuts with each cell division. However, the exact distribution of the multiple alleles in each clone was difficult to determine. This observation was witnessed in this study during investigating the PCR products from ear clips and tail tips of the founders. It was shown on the gel electrophoresis that most of the founders have one or two alleles that were altered by the mutation, yet, the possibility of additional undetected alleles in these animals could not be dismissed. Indeed, HRMA, DNA sequencing, and Tide analysis revealed that in almost all the F0 animals there were certain level of allele complexity that cannot be detected by the gel electrophoresis alone. Thus, it was essentially required in this part of the study to uncover the hidden alleles as it can potentially resulting in the transmission of uncharacterised sequence to the F1 that does not fit the selection criteria.

It is very clear that utilising the powerful Cas9-nickase with a pair of sgRNA targeting two regions on the same locus has increased the number of mutant alleles in each produced animal (Figure 2-2, 2-4). Varying from a single point mutation to relatively large sizes of deletion or insertion, the nickase activity has clearly increased the diversity of the mutant alleles when compared with $Cas9^{wt}$ (Figure 2-5, 2-8). Such findings would

be considered as disadvantageous and tricky to analyse; however, the documented on-target effect of this approach has outweighed any disadvantages. Consequently, screening the founders for mosaic alleles has to be comprehensive and part of a carefully planned approach beforehand. In fact, it has been found that sub-cloning of PCR products and trace sequencing to disentangle the alleles' complexity, was very important and required in cases of clones with difficult to deconvolute traces. Findings from this part helped to identify two potential candidate that fits the selection criteria with high likelihoods for transmitting the desirable alleles to the next generation. Indeed, a female mouse with a 22nt deletion from the nickase approach, and a female with a 17nt deletion from the wildtype Cas9 approach, were chosen to transmit the mutant alleles through the germline by crossing with wildtype male mice. This has led to efficient generation of number of heterozygous animals (F1), $PLC^{em1Jparr}$ and $PLC\zeta^{+/em2Jparr}$, which were later chosen to generate two mouse lines harbouring the PLCζ knockout mutation. Towards this end, DNA analysis, testes RNA and protein expression studies confirmed the transmission of the desired alleles through the germline in both of the colonies, with no visible evidence suggesting otherwise. PLCζ homozygous knockout males were generated from crossing between the heterozygous animals from each line, and the protein loss of function was confirmed by the frameshift mutation, and immunoblot analysis.

2.4.3 Is homozygous PLCζ deletion a lethal mutation?

The ultimate goal of this part of this study was to create the first animal model that is completely lacking the functional activity of the PLCζ gene. However, no previous reports have highlighted if such a mutation would create a detrimental effect on the life of homozygous mutants. Lethal gene deletions can be a type of mutation that either cause total embryonic agenesis, or foetal death during intrauterine life. In other cases, death can happen not immediately but during the adult's life. In such circumstances, if a mutation results in lethality, then this is indicative that the affected gene has a fundamental function in the growth, development, and survival of the organism.

Crossing between heterozygous animals of $PLC\zeta^{+/em1Jparr}$ and $PLC\zeta^{+/em2Jparr}$ produced animals at a rate very close to Mendelian proportions (table 3-1), plus all the homozygous mice from $PLC\zeta^{em1Jparr}$ and $PLC\zeta^{em2Jparr}$ colonies either were males or females showed a standard life-span that is similar to the $PLC\zeta^{wt}$ with no recorded consequence of the mutation on development or the normal physiology of the animals. Moreover, the findings also indicate to some extent the validity and the safety of using the endonuclease Cas9 and nickase on generating stable mouse lines harbouring a genetic mutation. Any presence of any off-target mutations thus would lead to further phenotypic alteration beyond the desired target. However, no further detectable phenotypic alteration at all the stages of the colony's expansion, apart from the alterations that has been reported with PLCζ mutation. Thus, two mouse lines of $PLC\zeta^{em1Jparr}$ and $PLC\zeta^{em2Jparr}$ lacking the expression of PLCζ gene have successfully been created with the twin approach of CRISPR/Cas9 or Cas9 nickase. Genotyping-based studies, PLCζ gene expression analysis, and immunoblot analysis all confirmed the frameshift mutation and loss of function of sperm-PLCζ protein in both of the mutant mouse lines.

2.5 Conclusion

Although the first successful application of CRISPR/Cas9 in mammalian cells was reported one-year before the establishment of this study, CRISPR/Cas9 has proved to offer a simple and a convenient platform for the generation of transgenic animals, with the possibility of considerable therapeutic potential in human diseases. Although, the editing efficiency and the outcome of CRISPR-aided mutagenesis can partially be unpredictable and hold a major concern to researchers in the field, it is essential therefore to adapt new and defined approaches to eliminate any off-target tendencies, less allele complexity to improve the capacity to characterise the transgenic animals to sufficient standards. The observations presented in this chapter provide a strong support for the role of the wildtype Cas9 and the mutant Cas9-nickase for targeting the coding sequence of PLCζ gene via a mouse zygote microinjection route. Generation of such stable transgenic animal lines lacking the functional expression of PLCζ gene has proved that CRISPR/Cas9 is a rapid, convenient, and efficient tool for one-step production of knockout mice.

3 PLCζ mutant functional analysis

Part of the material presented in this chapter was published in Development (Hachem *et al.*, 2017) ©The Company of Biologists Ltd.

3.1 Background

3.2 Materials and methods

3.2.1 Animals

In Oxford, mice of the C57BL/6j strain were housed in individual ventilated cages at constant optimal temperature and humidity with 12 hours of light per day in the Biomedical Science Building, or the Dunn School of Pathology, both part of the University of Oxford, and fed with standard dry pellets and water *ad libitum*. Animal use was approved by the University of Oxford's Local Ethical Review Committee and permitted by a licence from the UK Home Office in accordance with UK law (Animals [Scientific Procedures] Act 1986).

At the University of Massachusetts and the University of Ghent Hospital Medical School, mice were also used as a source of oocytes for ICSI, IVF, and microinjection experiments. Sperm used in these experiments were cryopreserved using straws at Oxford University and sent to the Massachusetts and Ghent labs where they were thawed before use in the experiments. Mice used for oocyte collection in Massachusetts were 8–10-week-old CD1 females and these were handled following the US National Research Council's Animal Care and Welfare Guidelines. These procedures were approved by the Institutional Animal Care and Use Committee at the University of Massachusetts.

In Ghent, mice used for oocyte collection were 8–10-week-old B6D2F1 females (a cross between female C57BL/6 and male DBA/2 mice). All procedures involving live animal handling and euthanasia were approved by the Ghent University Hospital Ethical Committee for Laboratory Animals (EC number 09/15).

3.2.2 Histology

Testes were fixed in 4% paraformaldehyde (PFA), dehydrated in increasing concentrations of ethanol, kept for 24 hours in Histo-Clear II (National Diagnostics, UK), then embedded in paraffin wax. Sections of 5 μm thickness were cut and mounted on superfrost plus slides (Fisher Scientific, USA). The sections were deparaffinised in Histo-Clear II, rehydrated in decreasing concentrations of ethanol, then stained with Harris hematoxylin (Sigma-Aldrich, USA) for 5 minutes. The sections were counterstained with eosin B solution (Sigma-Aldrich, USA) and visualized under a Leica DM5000B microscope.

3.2.3 Sperm viability

Spermatozoa were collected from the cauda epididymis and vas deferens of 8-week-old mice and incubated in HEPES-buffered saline solution containing 4 mg/ml bovine serum albumin at 37°C for 30 minutes, and assayed using the LIVE/DEAD Sperm Viability Kit (Molecular Probes) following manufacturer's instructions. In brief, the samples were incubated for 5 minutes with SYBR14 (Em 516 nm; labels live cells) at a final concentration of 100 nM, and then with PI (Em 617 nm; labels dead cells) at a final concentration of 12 μM for another 5 minutes. Stained samples were analysed using a BD FACS Canto II flow cytometer equipped with BD FACSDiva software version 6.1, collecting a minimum of 10000 gated sperm cells for the log of the fluorescence. Samples within the SYBR14+/PI– quadrant were considered viable, and within the SYBR14–/PI+ quadrant as non-viable. Events within the SYBR14–/PI– quadrant were considered as debris. Data were analysed for the relative fluorescence of SYBR14/PI by using FlowJo software v10.6 (FlowJo, LLC). Sperm viability was calculated by the percentage of live cells relative to the total number. Images of fluorescently-labelled sperm were obtained from samples loaded onto a microscope slide coated with 0.1% Poly-D-Lysine and imaged using an Olympus BX40 microscope.

3.2.4 Sperm motility and hyperactivation

Epididymal spermatozoa were collected and washed in a complete pre-warmed HTF medium supplemented with 4% BSA at 37°C under 5% CO_2. After two hour incubation with HTF medium (Zenith Biotech), 30 µl of the recovered sperm suspension (~2 x 10^5 sperm/ml) was loaded into a pre-warmed Leja slide chamber by capillary action on an Olympus CX41 microscope. Sperm motility and hyperactivation parameters were analysed using computer-assisted sperm analysis (CASA) with HTM-CEROS software (version12.3, Hamilton Thorne, MA, USA). Recordings of at least 800 mouse sperm/slide for each group was performed. The image-acquiring settings were: 60 frames per second, minimum contrast (50), minimum cell size (10 pixels), VAP cutoff (7.5 µm/s), VSL cutoff (6 µm/sec), cell intensity (80). Different progressive sperm motility grading scores (rapid, medium, slow, static) were recorded according to the Average Path Velocity (VAP) and Straight Line Velocity (VSL) parameters, while sperm hyperactivation (vigour) values were evaluated by Curvilinear Velocity (VCL), Amplitude of Lateral Head displacement (ALH) and Beat Cross Frequency (BCF).

3.2.5 Acrosome reaction

Spermatozoa were collected as before, washed, and then capacitated in complete HTF medium supplemented with 4 % BSA for one hour at 37°C and 5% CO_2. The samples were then divided into three groups at a sperm density of 3 x 10^6 sperm/ml: the first group was treated with ionomycin at a final concentration of 10 µM in DMSO, the second group was treated with progesterone at a final concentration of 20 µM in DMSO, and the third group was only treated with DMSO as a control. At different time points, spermatozoa were collected and pipetted onto a microscope slide coated with 0.1% Poly-D-Lysine, then fixed with acetone/methanol (1:1) on ice for 10 minutes. The slides were then washed twice with phosphate buffer saline before incubating with lectin PNA-Alexa Fluor 594 conjugate (Life Technologies, USA) for 30 minutes in the dark. Slides were washed twice with H_2O before mounting with ProLong Gold antifade reagent with DAPI for sperm DNA staining. The slides were assessed for acrosomal status (lectin PNA+ = unreacted, lectin PNA– = reacted) using an Olympus BX40 microscope. The percentage of acrosome-reacted spermatozoa was calculated as percentage of total numbers.

3.2.6 Calcium imaging post sperm injection

ICSI was carried out both at the University of Ghent Hospital Medical School and at the University of Massachusetts. Briefly, hybrid female mice were stimulated using pregnant mare serum gonadotrophin (PMSG). MII oocytes were obtained from the oviducts 12 to 14 hours after injection of hCG. After treatment with hyaluronidase to remove cumulus cells, MII oocytes were washed and transferred into KSOM (Potassium Simplex Optimized Medium) under culture conditions (37°C, 6% CO_2, 5% O_2). Sperm microinjection was performed by piezo-drilling following protocols previously described (Yoshida and Perry, 2007; Yoon and Fissore, 2007). All manipulations were carried out using HEPES-buffered medium at 37°C, under light mineral oil at room temperature. Sperm heads were separated from the tail and microinjected by applying Piezo pulses of different intensity to penetrate the zona pellucida and plasma membrane of the oocyte. The sperm head was then released into the ooplasm and the pipette carefully withdrawn from the oocyte.

3.2.7 Calcium imaging post IVF

In vitro fertilization was carried out and and zona pellucida-free mouse oocytes were collected as above and as previously described, the latter following standard superovulation procedures. Up to 4 cumulus-oocyte complexes (COCs) were placed into a 90µl drop of media (TYH standard medium) covered with mineral oil and previously equilibrated in an incubator with 5% CO2 at 37°C. Fertilization drops containing 20-30 oocytes were inseminated with sperm from each group incubated as described above in medium supporting capacitation (final concentration of 1 x 10^6 sperm/ml). Fertilization and polyspermy were evaluated using Hoechst staining at different hours post insemination. In the case where Ca^{2+} monitoring was performed, following oocyte collection the zonae pellucidae were removed using acidic Tyrode's solution (pH 1.6). Zona free oocytes were adhered to Cell-Tak (MatTek Corp., Ashland, USA)-treated glass-bottom dishes in 90 µl BSA-free TYH, and sperm were added to a final concentration of 10^5 sperm/ml, along with 4 µl TYH containing 30 mg/ml BSA for a final concentration of approximately 1.5 mg/ml BSA. Imaging began immediately after sperm addition and was performed essentially as described below. Because the sperm from both PLCζ-null males was cryopreserved, the control sperm was also cryopreserved and it was collected from a transgenic mouse line originally generated by Dr. G.S. McKnight, University of Washington (Morgan et al., 2008). Sperm penetration was confirmed by the presence of Ca^{2+} responses; as the large number of frozen sperms needed to achieve fertilization made it impossible to assess sperm entry.

3.2.8 Sperm penetration

Sperm-oocyte penetration analysis was performed six hours post *in vitro* fertilization. Briefly, C57BL/6J female mice at 3 – 4 weeks old (Charles River, UK) were stimulated using 5 IU pregnant mare serum gonadotrophin (PMSG, Folligon, Intervet, Boxmeer, The Netherlands). Ovulation was induced 46 – 48 hours later by 5 IU hCG (Chorulon, Intervet, Boxmeer, The Netherlands). Oocyte-granulosa cell complexes (MII oocytes) were collected 13-14 hours following hCG administration in a complete pre-warmed HTF medium (Zenith Biotech, USA), and then inseminated with precapacitated sperm from each animal group under mineral oil (Zenith Biotech, USA) at 37°C and 5% CO_2. Six hours later, oocytes were washed and treated for 60 seconds with acid Tyrode's solution to remove the extra sperm attached to the zona pellucida. The oocytes were then fixed in 3.7% paraformaldehyde for 30 minutes, washed and permeabilized in 0.5% Triton 100 before DNA staining with Hoechst 33324. Sperm DNA was detected using a 358/461 (ex/em.) laser line on a LSX8 Leica confocal scanning laser microscope. A high-resolution image series on z plane was generated in order to build 3-dimensional (3D) images of the embryos. Counting of sperm heads inside the oocytes, confirmed by the DNA staining method, was carried out on 3D projections. Processing and analysis of the digital images were performed using Image-J/Fiji.

3.2.9 Generation of recombinant PLCζ RNA

A synthetic mouse PLCζ cDNA (GeneArt Gene Synthesis, ThermoFisher Scientific) was subcloned into a pRNA vector for production of polyA+ / capped recombinant mRNA, using T3 RNA polymerase in an *in vitro* transcription reaction; capped transcripts were produced with the cap analog m7G(5')ppp(5')G, following manufacturer's instructions (mMessage mMachine, Ambion). Mutant PLCζ cDNA versions were obtained by swapping internal fragments within wild type PLCζ cDNA, with corresponding synthetic sequences harbouring the deletions present in PLCζ ^{em1Jparr} or PLCζ ^{em2Jparr}. The quality of the recombinant mRNA was assessed by agarose gel electrophoresis.

3.2.10 Microinjection of PLCζ cRNA

Microinjections were performed as described previously (Lee *et al.*, 2016). cRNA was delivered into oocytes and/or zygotes by pneumatic pressure (PLI-100 picoinjector, Harvard Apparatus, Cambridge, MA). Each oocyte received 5–10 pl, approximately 1–3 % of the total volume of the oocyte. Injection of cRNA into zygotes was performed 3 hours after completion of ICSI.

3.2.11 Calcium imaging

This was carried out in two different ways. In one approach, oocytes were pre-incubated for 30 minutes at 37°C in KSOM containing the Ca^{2+}-sensitive fluorescent dye Fura-2 acetoxymethyl ester (7.5 µM) (Fura-2 AM, Invitrogen, Merelbeke, Belgium). After ICSI, oocytes were transferred to a 10 µl KSOM droplet in a glass dish (MatTek Corp., Ashland USA) for Ca^{2+} analysis. Imaging was performed on an inverted epifluorescence microscope (Nikon Eclipse TE 300, Analis Ghent, Belgium) using a 20x objective and filter switch (Lambda DG-4 filter switch, Sutter Instrument Company, Novato, CA, USA), for excitation at 340 and 380 nm corresponding to Fura-2 AM spectrum. Images were acquired every 5 seconds for a duration of 2 hours and intracellular Ca^{2+} changes were registered as the ratio of fluorescence (340/380 nm). In another approach, Ca^{2+} monitoring was performed as previously described (Lee *et al.*, 2016) also using Fura 2-AM.

3.2.12 *In vitro* development of *in vivo* fertilized oocytes

3–4-week old C57Bl/6J female mice (Charles River UK) were injected intraperitoneally with 5 IU of PMSG (Intervet) and 48 hours later with 5 IU of hCG (Intervet), and paired with male mice. Zygotes were retrieved from oviductal ampullae at 18 hours post-hCG. Cumulus-enclosed zygotes were denuded by exposure to 1 mg/ml hyaluronidase (Sigma) in modified HTF (Zenith Biotech) for 3–6 minutes, washed through fresh modified HTF, and cultured in KSOMaa in the presence of 5% CO2 at 37°C. For assessment of polyspermy, denuded and washed zygotes were cultured in KSOMaa in the presence of 5% CO_2 at 37°C for 30 minutes. The zygotes were then placed in fresh modified HTF containing 1µg/ml Hoechst 33342 and incubated for 20 – 30 minutes. They were washed in fresh modified HTF and imaged using a fluorescence microscope.

3.2.13 Analysis of Wbp2nl/PAWP mRNA expression in testis

Wbp2nl mRNA expression levels were quantified in testes RNA by the same approach in section (2.2.6.5) using OnestepPLUS qRT-PCR MasterMix SYBR Green (Primerdesign, UK). The primers used for Wbp2nl mRNA detection were:

PAWP_RT_F: GGCAGCTCCAGACGGTGGCT

PAWP_RT_R: GCCCATCCAGAAGCTTGCAACTCG

Wbp2nl mRNA expression levels were normalized to beta actin mRNA expression levels, and calculated using the relative quantification approach. Real-time qPCR was performed on a Roche LightCycler 480.

3.2.14 Immunoblot analysis of PAWP in sperm

Immunoblot analysis of WPB2NL/PAWP was performed in a similar way to sperm PLCζ in section (2.2.7), using overnight incubation at 4°C with 1/1000 dilution of an anti-WPB2NL/PAWP rabbit polyclonal antibody (Proteintech-22587-1-AP, USA); this was followed by 1 hour of incubation with 1/15000 dilution of a goat anti-rabbit IRDye-800CW secondary antibody (Li-Cor #926-32211) and fluorescence imaged using a Li-Cor Odyssey imaging system (Li-Cor, USA). Immunoblotting procedures were repeated at least 3 times per sample.

3.2.15 Statistical Analyses

Where indicated data are presented as average ± sem and analysed by a one-way ANOVA with Bunnett's or Tukey's multiple comparison tests, or Student's t-test, as appropriate. In some Figures, data are presented as the proportion of total oocytes examined showing a specific characteristic from combined experiments; contingency tables with a Fisher's exact test were used in these cases. Graphs were annotated with the following conventions: $p > 0.05$ = ns; $p < 0.05$ = *; $p < 0.01$ = **; $p < 0.001$ = ***.

3.3 Results

3.3.1 Spermatogenesis and sperm functional parameters of PLCζ knockouts

3.3.1.1 Spermatogenesis analysis

The process of spermatogenesis in PLCζ$^{-/-}$ testes was evaluated with hematoxylin and eosin-stained paraffin-embedded sections (5μm thickness) from 8-week-old wildtype and PLCζ knockout mice. In all the animals studied, there was no visible structural testicular variance at any stage between the wildtypes and the mutants; all the testicular tissue sections show the seminiferous tubules lined by the seminiferous epithelium. At the base of this epithelium are, at regular intervals, the Sertoli cells, which have light-stained large oval nuclei. The seminiferous epithelium further shows cells undergoing spermatogenesis. Spermatogonia lie in the periphery of the seminiferous tubule and appear as dark stained cells (Figure 3-1). More mature cells directed toward the lumen include various stages of developing male germ cells, spermatocytes, round spermatids, elongated spermatids and matured spermatozoa which are in the process of being released into the lumen. Leydig cells are located adjacent to seminiferous tubules.

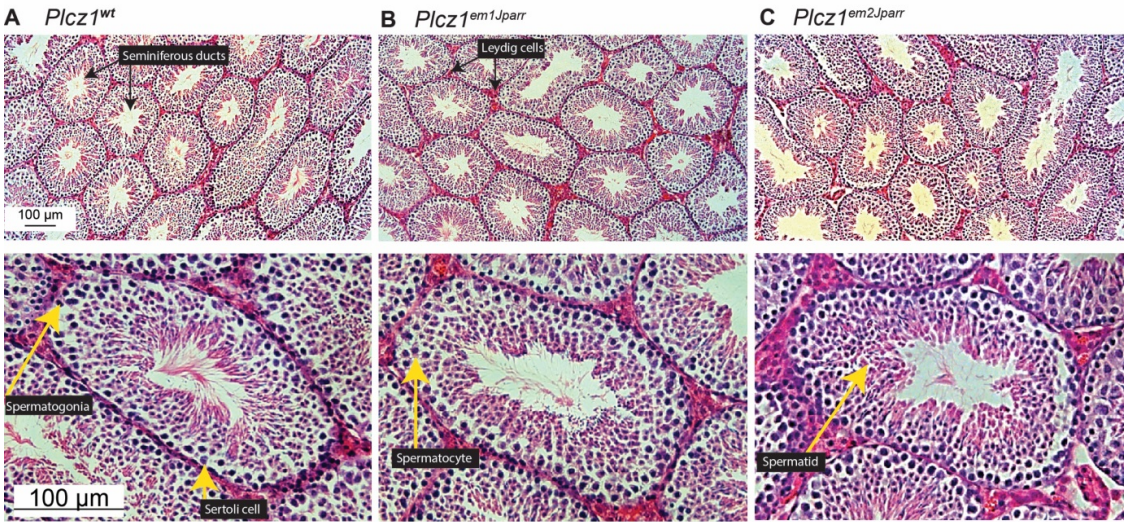


Figure 3-1: Histological analysis of testes sections stained with hematoxylin and eosin

Present cut-sections through paraffin-embedded testes from 8-week-old PLCζ^{wt} and PLCζ-null mice showing different stages of spermatogenesis in the seminiferous tubules.

3.3.1.2 Sperm viability analysis

In order to confirm the viability of the sperm generated by the above spermatogenesis process, epididymal sperm samples from wildtype and PLCζ knockouts were collected and examined with a fluorescence-based assay for analysing the viability and fertilizing potential of sperm by flow cytometry and fluorescence microscopy. The LIVE/DEAD sperm viability kit contains the membrane-permeant SYBR® 14 nucleic acid stain that labels live sperm with green fluorescence, and membrane-impairment propidium iodide which labels the nucleic acids of membrane-compromised sperm with red fluorescence (Figure 3-2).

The main advantage of this dye combination is that both fluorochromes have the same intracellular target (DNA), and since most DNA is found in the sperm head (and less in the mid-piece in the mitochondria), the assay indicates the integrity of the plasma membrane of the head domain only (Hossain *et al.*, 2011). Moreover, the probe mentioned above will not assess the integrity of the plasmalemma covering either the acrosome, the mid-piece, or the rest of the tail. For this reason, further sperm functional parameters, such as sperm motility, sperm hyperactivation, and capacity to undergo the acrosome reaction, were investigated in order to fully evaluate the plasma membrane integrity and the fertilisation potential of the PLCζ$^{-/-}$ spermatozoa.

It was very interesting to see that loss of PLCζ protein did not appear to have an adverse effect on the percentage of the viable sperm produced in each sample. Analysis of the emitted fluorescence light for each gated-quadrant of the flow cytometry charts showed that there is no significant difference ($P>0.05$) between wildtype and PLCζ mutant groups where the mean percentage of the viable sperm is between 34% and 40% of the total samples studied ($n=3$) (See figure 3-6).

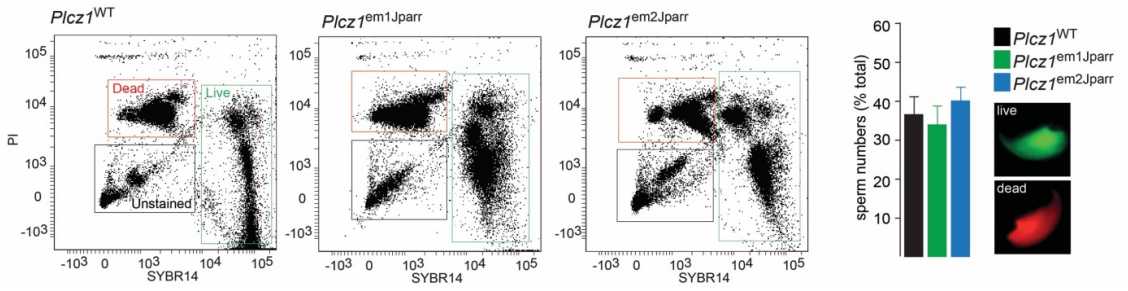


Figure 3-2: Sperm viability analysis

Density plots of sperm stained with SYBR14 (live sperm) and propidium iodide (PI; dead sperm) and analysed by flow cytometry. A total of 10000 of cellular events were collected for each group. (C) Quatification of data from (B). Representative fluorescence stained sperm were obtained using an Olympus BX40 microscope.

3.3.1.3 Sperm motility and hyperactivation analysis

Computer-assisted semen analysis (CASA) has been developed as a specific instrument for evaluating sperm motion characteristics and to make the assessment of semen quality more objective and thorough (Agarwal et al., 1992). In addition, the classification into motile and immotile spermatozoa can be based on well-defined velocity thresholds with CASA. Progressive motility (sperm moving in more or less a straight line) is a vital functional characteristic of spermatozoa that governs their ability to pass through the physical barriers of the female reproductive tract, and to penetrate the layers surrounding the oocyte (Mortimer and Mortimer, 2013). Applying CASA analysis to study the progressive motility of wildtype and PLCζ$^{-/-}$ spermatozoa did not show any significant differences among the mean percentages of the rapid progressive motility (Wildtype: 37.25%, Plcz1^{em1Jparr}: 33.25%, Plcz1^{em2Jparr}: 39.25%, P>0.05, n=3 samples from each group) (See figure 3-3). Similarly, other categories of sperm progressive motility (medium progressive, slow progressive, and static sperm) were also analysed by CASA in the same setups and they were as follows:

- Medium progressive (Wildtype: 12%, Plcz1^{em1Jparr}: 16.5%, Plcz1^{em2Jparr}: 14.75%, P>0.05, n=3 samples from each group).

- Slow progressive (Wildtype: 2%, Plcz1^{em1Jparr}: 1.75%, Plcz1^{em2Jparr}: 2%, P>0.05, n=3 samples from each group).

- Static sperm (Wildtype: 49.25%, Plcz1^{em1Jparr}: 48.25%, Plcz1^{em2Jparr}: 43.5%, P>0.05, n=3 samples from each group).

Statistical analysis of the findings from medium progressive, slow progressive, and static sperm showed no detectable difference between wildtype and PLCζ$^{-/-}$ spermatozoa.

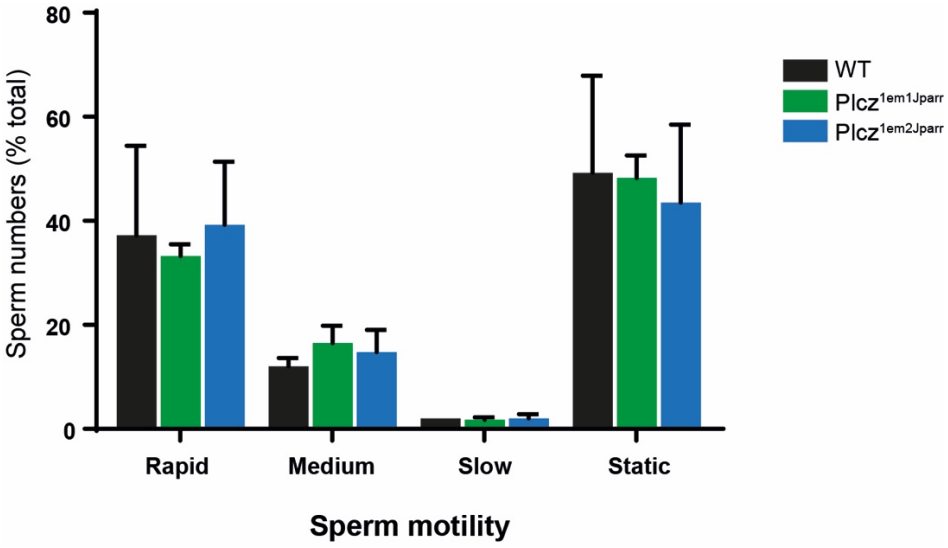


Figure 3-3: Sperm progressive motility of wildtype and PLCζ$^{-/-}$ spermatozoa.

Mean percentage of sperm motility ± SEM in n=3 samples from each group.

Since neither the sperm concentration nor the actual percentage of total motile spermatozoa in the samples fully reflects the fertilisation potential of a spermatozoon, further sperm functional parameters are still required for full and accurate sperm motility evaluation (Nikolettos *et al.*, 1999). Sperm velocity represents the ability of sperm to utilise ATP produced by the mitochondria for generating the purposive movement of the tail of the sperm in a medium. Sperm velocity in this study was measured in three different ways for every spermatozoon (linear, curvilinear, and straight line). Average pathway velocity (VAP), straight-line velocity (VSL) and curvilinear velocity (VCL) are the three most commonly used measures of sperm movement with CASA. VAP is the smoothed average position of a spermatozoon, VSL is the straight-line distance between the beginning and the end of the cell path, and VCL is the total distance travelled by the sperm cell including every point in the cell path all divided by the time elapsed and expressed in micrometre per second. Statistical analysis of sperm samples revealed no significant differences in the sperm velocities between wildtype and PLCζ$^{-/-}$ spermatozoa (see figure 3-4).

- VAP (Wildtype: 123.6 µm/s, Plcz1^{em1Jparr}: 117.1 µm/s, Plcz1^{em2Jparr}: 106.1 µm/s, P>0.05, n=3 samples from each group).

- VSL (Wildtype: 90.6 µm/s, Plcz1^{em1Jparr}: 82.4 µm/s, Plcz1^{em2Jparr}: 76.2 µm/s, P>0.05, n=3 samples from each group).

- VCL (Wildtype: 225.3 µm/s, Plcz1^{em1Jparr}: 216.1 µm/s, Plcz1^{em2Jparr}: 199.5 µm/s, P>0.05, n=3 samples from each group).

Moreover, sperm hyperactivation, a concomitant of capacitation and the ability of a sperm to pass through the cumulus cells of the oocyte, can also be evaluated by CASA. Sperm hyperactivation can be characterised by the amplitude of lateral head displacement (ALH) and the asymmetrical beating pattern of the sperm tail (beat cross frequency (BCF)), which are both measures of cell oscillation and are based on each specific sperm cell path (Mortimer *et al.*, 2015). Amplitude of lateral head displacement is the measurement of the maximum value of the distance, in µm, of any point on the cell track from the average path (figure 3-4). BCF measures the frequency with which the cell track crosses the average cell path in either direction and is expressed in Hz (Farrell *et al.*, 1998). Sperm samples from wildtype and PLCζ$^{-/-}$ spermatozoa did not show any significant variation in these parameters (figure 3-4):

- ALH (Wildtype: 10 µm, Plcz1^{em1Jparr}: 9.5 µm, Plcz1^{em2Jparr}: 9.4 µm, P>0.05, n=3 samples from each group).

- BCF (Wildtype: 27.9 Hz, Plcz1^{em1Jparr}: 27.35 Hz, Plcz1^{em2Jparr}: 27.9 Hz, P>0.05, n=3 samples from each group).

Other factors, such as linearity (LIN), and straightness (STR), are all ratios of the velocity parameters (VSL/VCL, VSL/VAP, respectively) used for looking at progressiveness on a relative scale and are expressed as a percentage.

- LIN (Wildtype: 41%, Plcz1^{em1Jparr}: 39.25 %, Plcz1^{em2Jparr}: 39.75 µm, P>0.05, n=3 samples from each group).

- STR (Wildtype: 70 %, Plcz1^{em1Jparr}: 68 %, Plcz1^{em2Jparr}: 69.2 µm, P>0.05, n=3 samples from each group).

To sum up, CASA findings in this study provided conclusive evidence that all the epididymal sperm that were involved in this study from PLCζ$^{-/-}$ spermatozoa did not show any significant difference when compared to the wildtype samples, suggesting that PLCζ knockout has no detrimental effect on sperm functional parameters of morphology, viability, and motility.

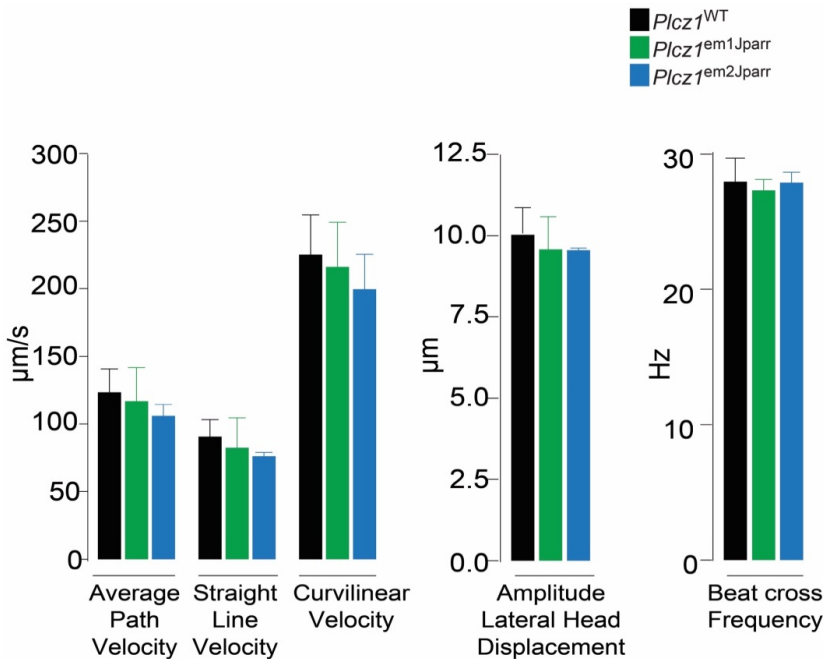


Figure 3-4: Sperm motility and hyperactivation parameters of wildtype and PLCζ$^{-/-}$ spermatozoa

Analysis of sperm motility parameters using computer assisted sperm analysis (CASA).

3.3.1.4 Acrosome reaction

A fully-functioning spermatozoon is naturally equipped with lytic enzymes designed to break through the layers surrounding the oocyte once it comes in contact with the outermost layer of zona pellucida. Structural abnormalities in the acrosomal segment can cause a severe reduction in the capability of a sperm to undergo the acrosome reaction, leading to a reduction in the fertilisation ability of a sperm and infertility in humans.

As mentioned before, several immunofluorescence studies have identified expression of PLCζ protein on the acrosome region of mouse spermatozoa, leading to proposals of yet-to-be-confirmed physiological roles associated with the acrosome reaction. A spliced variant of PLCζ protein (NYD-SP27) was also found in the sperm acrosome with intrinsic decapacitation activities, that is both necessary and sufficient for sperm capacitation and the acrosome reaction (Bi *et al.*, 2009). It is therefore imperative to examine whether PLCζ$^{-/-}$ spermatozoa have inherited any structural abnormalities in the acrosomal area as a result of the PLCζ deletion, or if the loss of sperm-PLCζ has reduced the ability to undergo acrosome reaction when the sperm comes into contact with the zona layers.

We have found that the best approach to study the acrosome reaction in PLCζ$^{-/-}$ spermatozoa is by incubating the sperm in a capacitation medium supplemented with progesterone (20 μM), or ionomycin (10 μM) (in different setups), and then to stain the sperm with lectin PNA-Alexa Fluor 594 conjugate to visualise the reacted acrosome on slides. It is worth noting that ionomycin can induce the acrosome reaction in a non-physiological activation pathway that does not require capacitation beforehand, while progesterone have been shown to only promote the acrosome reaction in capacitated mouse sperm (Brucker *et al.*, 1994). For this reason, progesterone was used in this experiment to examine its ability to induce the acrosome reaction in PLCζ$^{-/-}$ spermatozoa in a more physiological manner.

Different time intervals of incubation with ionomycin (10 μM), or progesterone (20 μM) induced the acrosome reaction in PLCζ$^{-/-}$ spermatozoa in a manner similar to that found with wildtype sperm. Statistical analysis of the findings showed no significant difference in the mean percentage of acrosome reacted sperm between the PLCζ$^{-/-}$ and wildtype groups.

In detail, 30, 60, or 90 minutes incubation with ionomycin (10 µM) induced the acrosome reaction as follows:

- 30min (Wildtype: 42.2 %, Plcz1^{em1Jparr}: 45.6 %, Plcz1^{em2Jparr}: 46.2 %, P>0.05, n=3 samples from each group).
- 60min (Wildtype: 55.2 %, Plcz1^{em1Jparr}: 54.6 %, Plcz1^{em2Jparr}: 58.1 %, P>0.05, n=3 samples from each group).
- 90min (Wildtype: 66 %, Plcz1^{em1Jparr}: 66.1 %, Plcz1^{em2Jparr}: 68.3 %, P>0.05, n=3 samples from each group).

In comparison, 30, 60, or 90 minutes incubation with progesterone (20 µM) induced the acrosome reaction as follows:

- 30min (Wildtype: 26 %, Plcz1^{em1Jparr}: 26.6 %, Plcz1^{em2Jparr}: 25.4 %, P>0.05, n=3 samples from each group).
- 60min (Wildtype: 41.6 %, Plcz1^{em1Jparr}: 39.2 %, Plcz1^{em2Jparr}: 40.9 %, P>0.05, n=3 samples from each group).
- 90min (Wildtype: 45 %, Plcz1^{em1Jparr}: 44.5 %, Plcz1^{em2Jparr}: 43.3 %, P>0.05, n=3 samples from each group).

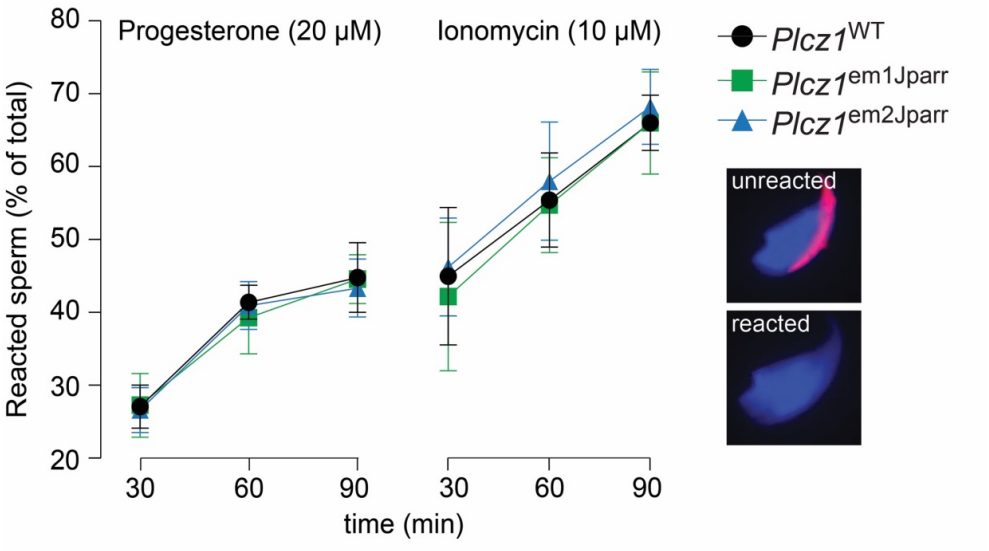


Figure 3-5: Induced acrosome reaction in PLCζ$^{-/-}$ and wildtype spermatozoa

Acrosome reaction was induced either by treatment with progesterone or ionomycin and reacted sperm were assessed by lack of reactivity towards fluorescently labelled lectin PNA. Representative images of reacted and unreacted sperm are shown. Data are presented as average ± sem followed by a one-way ANOVA analysis.

3.3.2 The effect of PLCζ-null sperm on triggering calcium oscillations in mouse eggs

Live-cell Ca^{2+} imaging on mouse oocytes were performed at both Dr Rafael Fissore's lab at the University of Massachusetts and at Dr Petra de Sutter's lab at Ghent University Hospital.

Epididymal spermatozoa from wildtype and PLCζ mutant animals were collected in sperm cryoprotective agent (Raffinose pentahydrate 180mg/ml, skimmed milk 30mg/ml, L-glutamine 14.6 mg/ml), and cryopreserved by plunging the semen straws in liquid nitrogen. A number of semen samples from wildtype and PLCζ-null mice were loaded into a dry-shipper and sent by a carrier from Oxford to either Massachusetts or Ghent.

3.3.2.1 Sperm-PLCζ is required to trigger calcium oscillations in wildtype mouse oocytes – A sperm injection study.

1. Sutter's lab findings:

To verify the Ca^{2+} releasing and activating ability of $PLC\zeta^{wt}$ spermatozoa, a total of 13 mouse oocytes were microinjected with $PLC\zeta^{wt}$ spermatozoa. Following microinjection, Ca^{2+} oscillations were recorded by Ca^{2+} imaging and were found symptomatic of those seen at fertilization in 11/13 (85%) of the injected oocytes (Figure 3-6). In contrast, $PLC\zeta^{-/-}$ spermatozoa failed to induce Ca^{2+} oscillations in all the injected oocytes within a duration of 120 minutes (Figure 3-7): $PLC\zeta^{em1Jparr}$ sperm (21/0) 0% Ca^{2+}oscillations; $PLC\zeta^{em2Jparr}$ sperm (21/0) 0% Ca^{2+}oscillations).

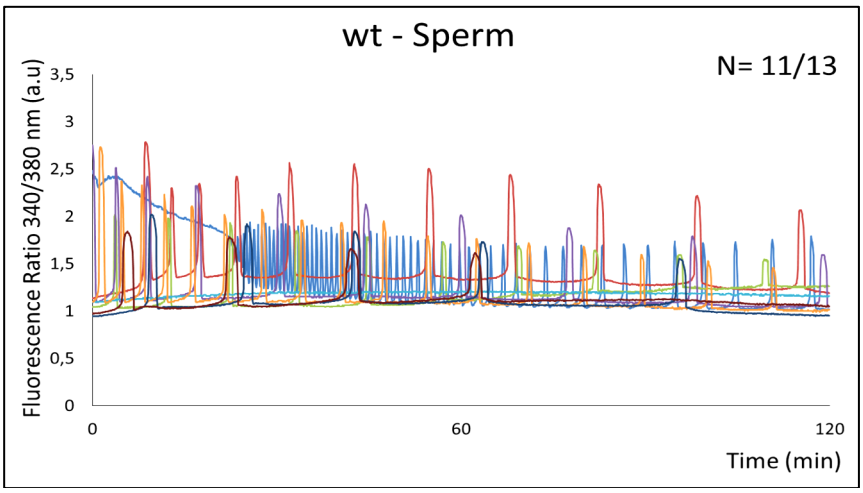


Figure 3-6: Representative Ca^{2+} responses of wildtype mouse oocytes (n=13) fertilised with microinjected PLCζ ^{wt} sperm.

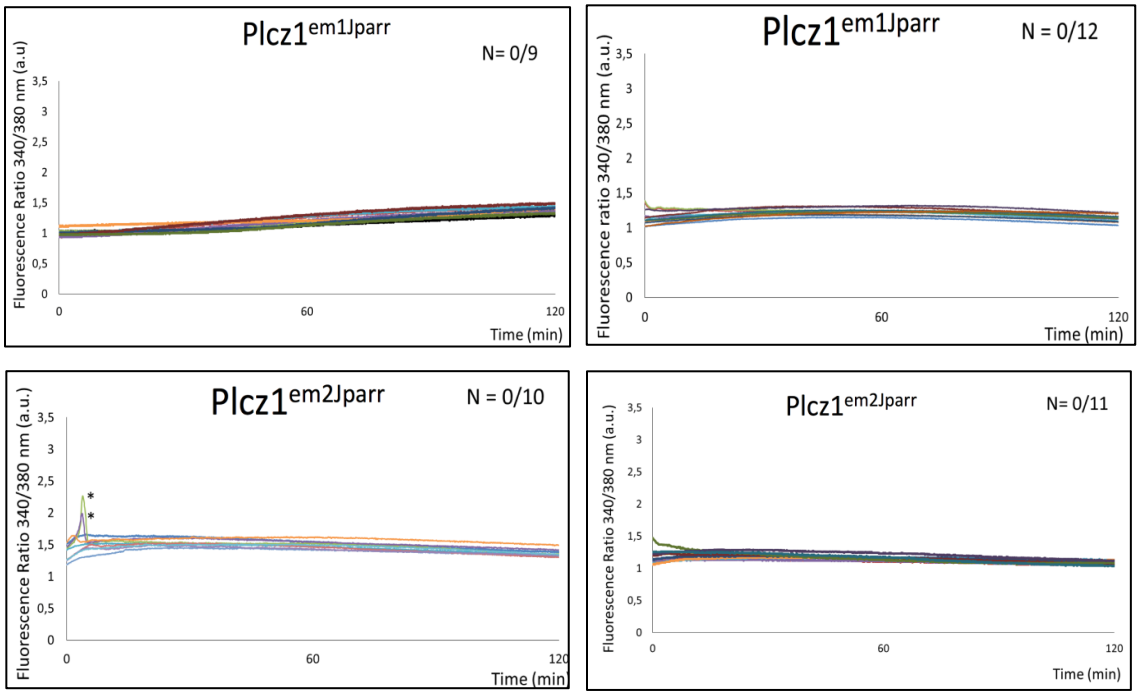


Figure 3-7: Representative Ca^{2+} responses of wildtype mouse oocytes fertilised with microinjected PLCζ$^{-/-}$ spermatozoa.

Table 3-1: Ca^{2+} oscillations following ICSI with PLCζ$^{-/-}$ and wildtype spermatozoa.

Animal group	Number of eggs injected (total)	Number of eggs showing Ca^{2+} oscillation (%)
PLCζ ^{wt} sperm	13	11 (85%)
PLCζ ^{em1Jparr} sperm	21	0 (0%)
PLCζ ^{em2Jparr} sperm	21	0 (0%)

*results are from three replicates

Wildtype mouse oocytes preincubated with Fura-2 fluorescence ratio, responding to microinjection of either PLCζ^{wt} or PLCζ – null spermatozoa.

A rescue of oocytes microinjected with PLCζ–null spermatozoa, was performed by microinjecting full length PLCζ cRNA (2µg/µl) 120 minutes post sperm injection. A total of six oocytes were injected with PLCζ cRNA, and six of them showed cytoplasmic Ca^{2+} oscillations matching those observed after microinjection of PLCζ^{wt} spermatozoa (Figure 3-9).

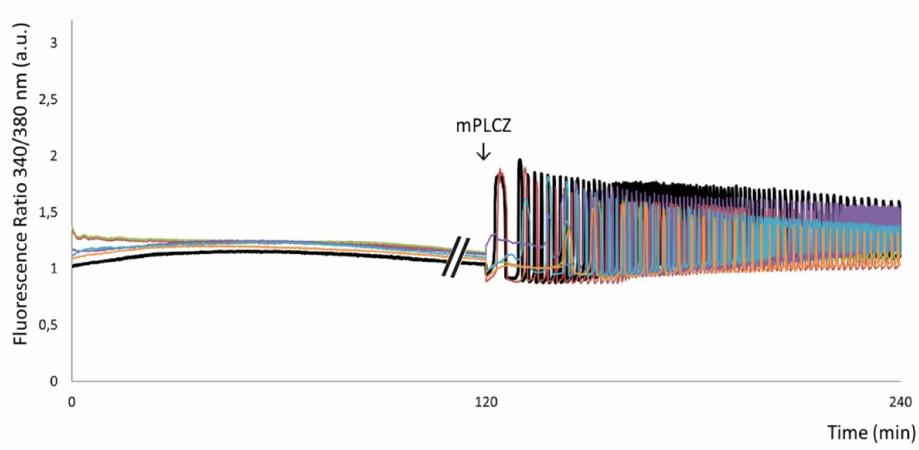


Figure 3-8: Rescue of failed fertilisation with PLCζ cRNA (2µg/µl) microinjection.

Representative Ca^{2+} responses of (n=6) wildtype oocytes injected with the full length PLCζ cRNA, 120 min post PLCζ ^{em1Jparr} sperm microinjection.

Since Ca^{2+} oscillations are considered to be the physiological trigger of mammalian oocyte activation, we assessed the ability of PLCζ-null sperm to trigger this process. Following ICSI using PLCζ^{wt} sperm, 35/40 of zygotes reached the two-cell stage, and 27/40 developed to the blastocyst stage. In contrast, PLCζ-null sperm largely failed to trigger activation, with only a few oocytes reaching the two-cell stage (PLCζ^{em1Jparr}: 2/36 and PLCζ^{em2Jparr}: 1/47) and only one reaching the blastocyst stage (PLCζ^{em1Jparr}: 1/36 and PLCζ^{em2Jparr}: 0/47). This inability of PLCζ-null sperm to trigger consistent oocyte activation was rescued by injection of PLCζ^{wt} cRNA 3-hour after ICSI with a significant proportion of oocytes now developing to the 2-cell stage (PLCζ^{em1Jparr}: 16/20 and PLCζ^{em2Jparr}: 6/9) (figure 3-10).

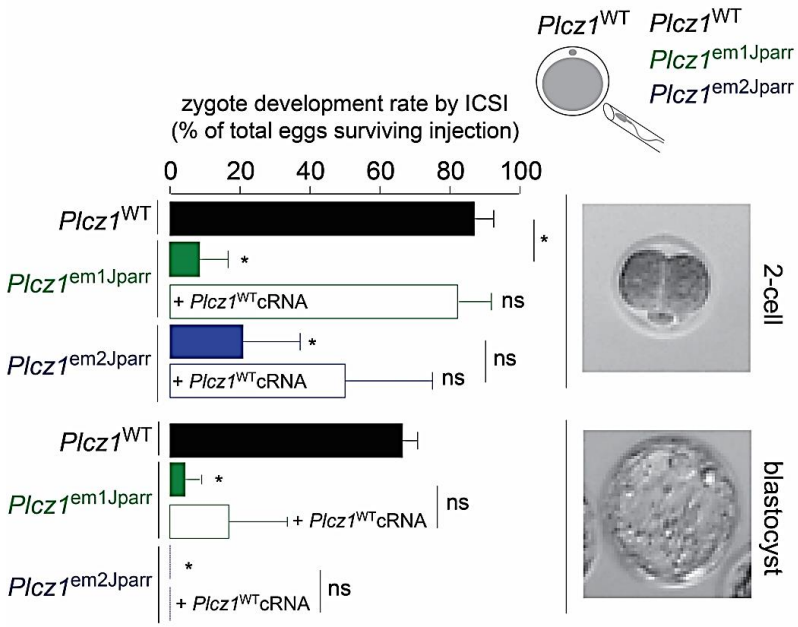


Figure 3-9: *In vitro* produced embryos with ICSI in the absence of Ca2+ oscillations.

Proportion of 2-cell and blastocyst embryos, 2 days or 5 days post ICSI, respectively (PLCζ^{wt}: 40 oocytes, 3 males; PLCζ^{em1Jparr}: 36 oocytes, 1 male; PLCζ^{em2Jparr}: 47 oocytes, 3 males). PLCζ^{wt} cRNA was injected after ICSI (PLCζ^{em1Jparr}: 20 eggs, 1 male; PLCζ^{em2Jparr}: 9 oocytes, 2 males). Data are presented as average ± sem of 3 – 6 experiments and exemplar embryos are shown.

2. Fissore's lab findings:

Rafael Fissore's lab confirmed the findings from Belgium regarding the inability of PLCζ-null sperm to trigger Ca^{2+} oscillations in wildtype mouse oocytes. Ca^{2+} imaging of oocytes injected with $PLC\zeta^{wt}$ sperm showed 15/19 (78%) Ca^{2+} oscillations, while sperm from either PLCζ-null line failed to trigger Ca^{2+} release during a duration of 240 minutes.

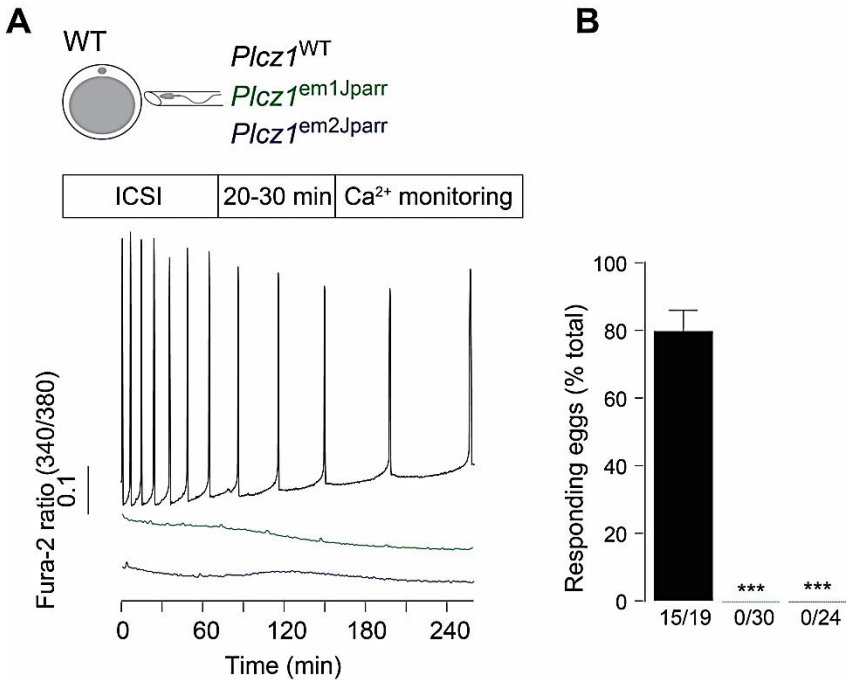


Figure 3-10: Ca^{2+} responses elicited by intracytoplasmic sperm injection (ICSI) into mouse oocytes.

(A) Representative traces of Ca^{2+} responses, monitored by fluorescence ratio (excitation 340/380 nm) of Fura-2, in wild-type mouse oocytes, elicited by ICSI with sperm from homozygote $PLC\zeta^{wt}$, $PLC\zeta^{em1Jparr}$ or $PLC\zeta^{em2Jparr}$ males.
(B) Compilation of results from all oocytes subjected to ICSI. Data are presented as average ± sem followed by a one-way ANOVA analysis; numbers shown underneath each bar indicate proportion of responding oocytes; the following number of animals were used for each group in a total of 4–5 experiments: $PLC\zeta^{wt}$ (3), $PLC\zeta^{em1Jparr}$ (2), $PLC\zeta^{em2Jparr}$ (4).

A rescue of failed fertilisation with full length PLCζ cRNA microinjection, induced Ca^{2+} oscillations in all of the injected oocytes after 3 hours incubating the oocytes with the injected PLCζ-null sperm (figure 3-12).

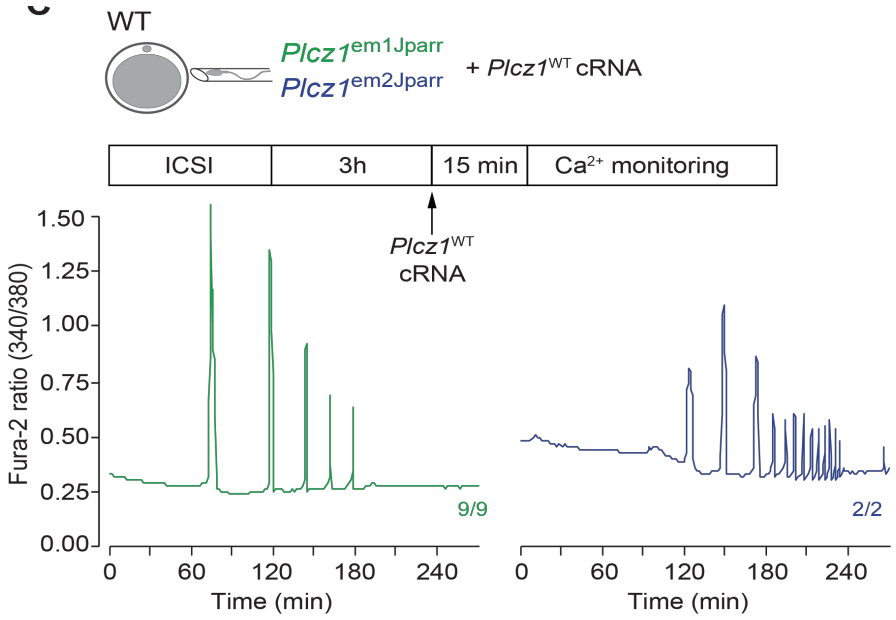


Figure 3-11: Rescue of PLCζ$^{-/-}$ phenotype by cRNA injection

Representative traces of Ca^{2+} responses, monitored by fluorescence ratio (excitation 340/380 nm) of Fura-2, in wildtype mouse oocytes, elicited by injection of PLCζ^{wt} cRNA after ICSI with sperm from homozygote PLCζ^{em1Jparr} and PLCζ^{em2Jparr} males. Numbers shown next to traces indicate proportion of responding oocytes subjected to ICSI and cRNA injection.

3.3.2.2 Sperm PLCζ is required to trigger calcium oscillations in wildtype mouse oocytes – *in vitro* fertilisation study.

To confirm that the absence of Ca^{2+} oscillations with PLCζ-null sperm is due to the absence of PLCζ and not as a result of the microinjection step, live-cell Ca^{2+} imaging was conducted to study the Ca^{2+} oscillations during *in vivo* fertilisation in wildtype zona pellucida-free oocytes. While 16/34 oocytes showed Ca^{2+} oscillations following IVF with PLCζ^{wt} sperm, none of the 40 oocytes subjected to IVF with PLCζ^{em1Jparr} -derived sperm showed such oscillations, with one oocyte showing a single Ca^{2+} transient at around 100 minutes (figure 3-13).

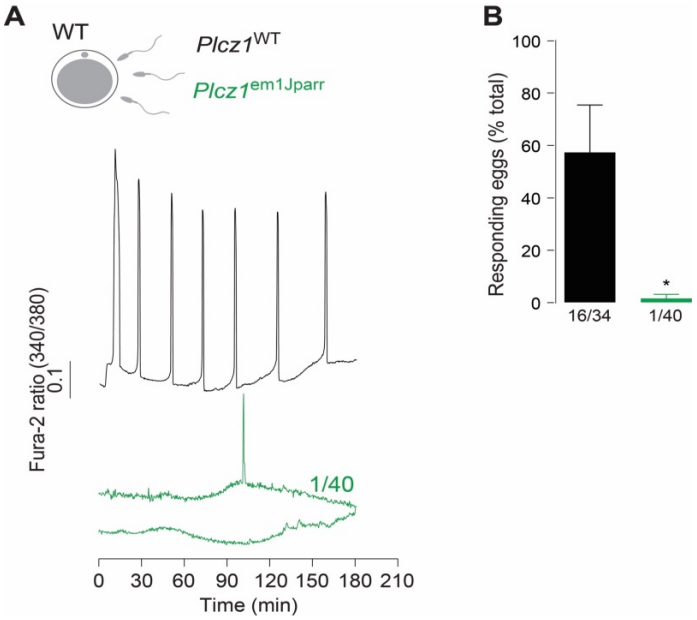


Figure 3-12: Ca^{2+} responses elicited by IVF into mouse oocytes

(A) Representative traces of Ca^{2+} responses, in wildtype mouse oocytes, elicited by IVF with sperm from PLCζ^{wt} and PLCζ^{em1Jparr} males; the PLCζ^{wt} control sperm were from a transgenic line of the same strain background as the PLCζ^{em1Jparr} sperm.

(B) Compilation of results from all oocytes subjected to IVF. Data are presented as average ± sem followed by a Student's t-test; numbers shown underneath each bar indicate proportion of responding oocytes; the following number of animals were used for each group in a total of 4–5 experiments: PLCζ^{wt} (5), PLCζ^{em1Jparr} (1).

3.3.3 *In vivo* fertilisation and development with PLCζ^{em2Jparr} sperms.

The unexpected, albeit greatly reduced, ability of some oocytes injected with sperm from PLCζ-null males to undergo oocyte activation and development after ICSI could be caused by the injection protocol, or the IVF medium of the culturing system. To bypass this possible artefact, and others associated with ICSI or *in vitro* fertilization procedures, we directly examined fertilization and embryo development of wildtype oocytes from females fertilized *in vivo* by PLCζ^{wt} and PLCζ-null males. Oocytes/zygotes were collected at 18 hours post hCG and allowed to develop *in vitro* during which time they were routinely examined. At the early time point of 18 hours, differences in activation events were already obvious, as PLCζ^{wt} fertilized eggs displayed significant differences in pronuclei formation compared to the PLCζ-null fertilized eggs, the former showing mostly condensed sperm head(s) (Figure 3-14 A). Thus, PLCζ-null sperm induced oocyte activation much less efficiently and protractedly, as further observed at subsequent time points (Figure 3-14 B): oocytes fertilized by PLCζ^{wt} sperm showed a high rate of 2 pronuclei formation (19/25) by 22 hours and cleavage to 2-cells (18/25) by 32 hours post hCG-treatment, whereas oocytes fertilized by PLCζ-null sperm only displayed 2 pronuclei formation (PLCζ^{em1Jparr}: 6/120 and PLCζ^{em2Jparr}: 1/43) by 25 hours and cleavage to the 2-cell stage (PLCζ^{em1Jparr}: 23/120 and PLCζ^{em2Jparr}: 9/43) after 38 hours post hCG-treatment (Figure 3-14 B).

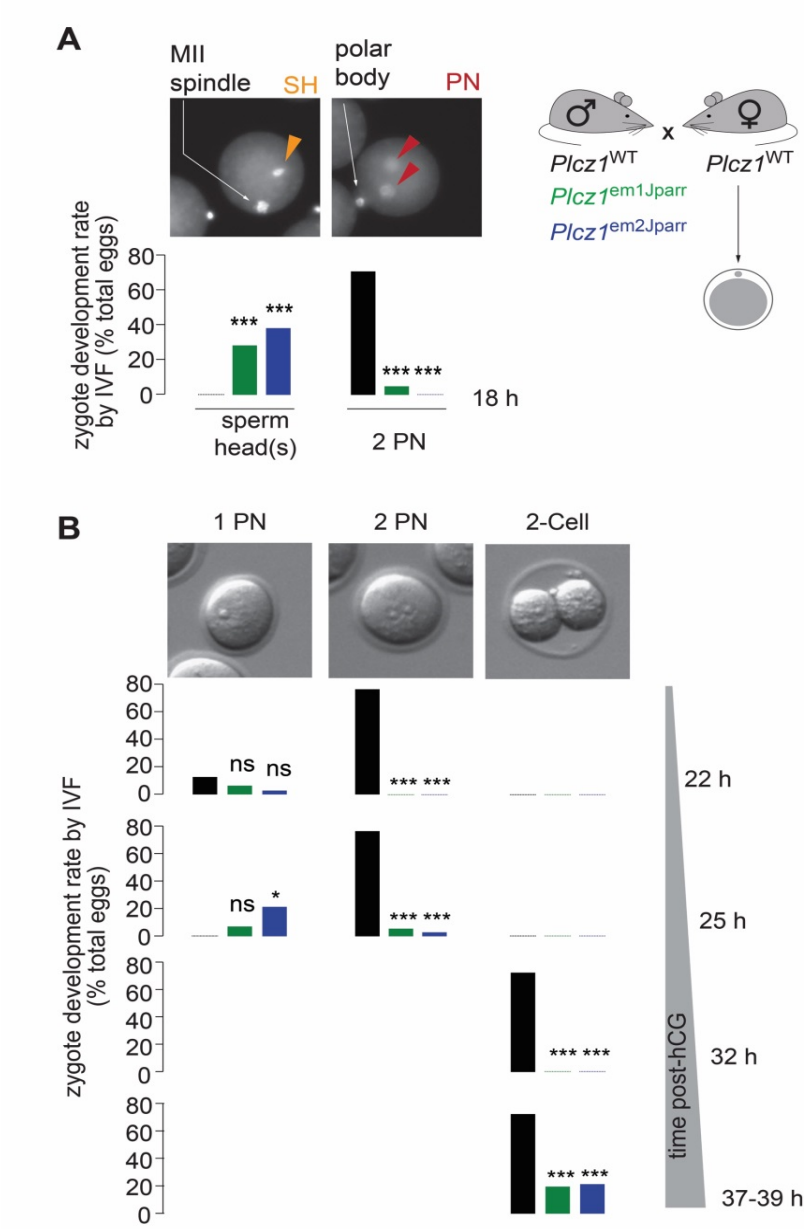


Figure 3-13: Analysis of mouse embryos produced *in vivo*

(A) Oocytes from super-ovulated females treated with hCG were fertilized *in vivo*, collected between 18 to 22 hours post hCG, and allowed to develop *in vitro*. The proportion of oocytes showing sperm head(s) (SH), 1 pronucleus (1PN), 2 pronuclei (2PN), 2-cell embryos and blastocysts at the indicated times. Exemplar embryonic development stages are shown (A) Data for 18 hours was obtained from Hoeachst-stained oocytes (PLCζ^{wt}: 37 oocytes, 2 males; PLCζ^{em1Jparr}: 111 oocytes, 3 males; PLCζ^{em2Jparr}: 82 oocytes, 2 males). **(B)** Data from 22 hours onwards was obtained from (PLCζ^{wt}: 25 oocytes, 2 males; PLCζ^{em1Jparr}: 120 oocytes, 3 males; PLCζ^{em2Jparr}: 43 oocytes, 1 male). For all panels, statistical significance was performed by a one-way ANOVA analysis.

3.3.4 *In vivo* animal mating and live offspring development.

The inability of PLCζ-null sperm to trigger Ca^{2+} oscillations could affect the capacity of PLCζ-null males to produce live offspring. Table 3-1 shows the compilation of results from various *in vivo* crosses. The study found that unlike crosses between PLCζ-heterozygous males and females, or between PLCζ-null females and PLCζ heterozygotes, which resulted in offspring similar in number to $PLC\zeta^{wt}$ crosses in close similarity to Mendelian proportions; PLCζ-null males was found to produce offspring, but at a much lower efficiency compared to $PLC\zeta^{wt}$ males.

Indeed, while crossings between wildtypes produced average litter sizes of 7.8 ± 0.8 and an average of 12.7 ± 1.8 pups per female over the initial mating period of 10 weeks, wildtype females crossed with homozygote $PLC\zeta^{em1Jparr}$ or $PLC\zeta^{em2Jparr}$ males produced significantly smaller litter sizes (4.2 ± 0.6; 3.2 ± 1.2; respectively) with an average pups per female (4.9 ± 1.2 and 2.3 ± 1.0, respectively) over the same time period. The finding is the first in demonstrating that natural mating in mammals can result in living offspring without the standard physiological trigger of oocyte activation (Figure 3-15). Although, Ca^{2+} imaging studies failed to detect Ca^{2+} increase following sperm introduction, the *in vivo* mating setups have uncovered an alternative pathway in egg activation that is not dependent on PLCζ.

Table 3-2: Mating pairs and fertility parameters

Crosses			litters born	Litter size	pups/female	genotype ratio (%)
Male	x	Female	(10 week period)	(average ± sem)	(10 week period)	(WT/MUT/HET)
WT (n=7)	x	WT (n=8)	13	7.8 ± 0.8	12.7 ± 1.8	
HET(em1Jparr) (n=3)	x	HET(em1Jparr) (n=4)	9	4.7 ± 1.1 (ns)	10.5 ± 0.9 (ns)	21.1/23.1/55.8
HET(em2Jparr) (n=4)	x	HET(em2Jparr) (n=6)	13	7.1 ± 0.5 (ns)	15.3 ± 0.9 (ns)	27.6/25.8/46.4
HET(em1Jparr) (n=4)	x	MUT(em1Jparr) (n=8)	17	5.7 ± 0.6 (ns)	12.1 ± 2.5 (ns)	
HET(em2Jparr) (n=3)	x	MUT(em2Jparr) (n=4)	8	4.9 ± 0.7 (ns)	9.7 ± 2.3 (ns)	
MUT(em1Jparr) (n=4)	x	WT (n=7)	8	4.2 ± 0.6 (*)	4.9 ± 1.2 (**)	
MUT(em2Jparr) (n=6)	x	WT (n=7)	5	3.2 ± 1.2 (*)	2.3 ± 1.0 (***)	

Mating pairs or trios were set up between males and females with genotypes as indicated. Data refer to pups born during the initial 10 weeks of mating and are presented as average ± sem followed by one-way ANOVA analysis. HET = PLCζ$^{+/em1Jparr}$ or PLCζ$^{+/em1Jparr}$; MUT = homozygote PLCζ^{em1Jparr} or PLCζ^{em1Jparr}; WT = homozygote PLCζ^{wt}

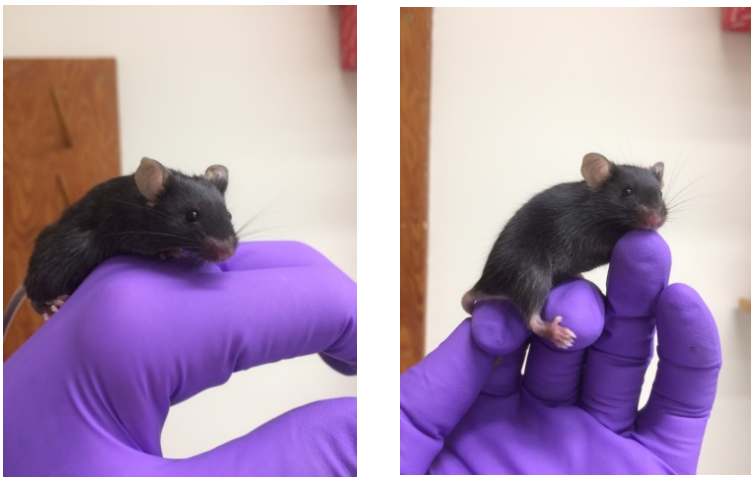


Figure 3-14: Images of heterozygous male and heterozygous female at 7-week old, produced from *in vivo* mating between homozygous PLCζ^{em1Jparr} male and PLCζ^{wt} female

3.3.5 Sperm penetration analysis

Although sperm functional analysis shows no structural or behavioural changes of the PLCζ-null spermatozoa when compared with PLCζ^{wt} sperm, the ability to bind and penetrate the oocyte at the same level of PLCζ^{wt} still needed to be established. This vital point is very important to show that the conclusive findings from the *in vivo* animal production (section 3.4.4) and from Ca^{2+} imaging after IVF (section 3.4.2.2) was due to the lack of sperm PLCζ and not because of an unknown factor that affected the sperm-oocyte binding and fusion.

Sperm DNA staining with Hoechst and 3-D projections of confocal microscopy images helped in localising the sperm heads within the inseminated PLCζ^{wt} oocytes. The findings provided a substantial confirmation of the ability of PLCζ-null sperm to penetrate the mouse oocytes at the same rate as sperm derived from PLCζ^{wt} males. No significant difference was recorded in this experiment, and the mean percentage of the penetration rates for PLCζ^{wt} and PLCζ^{em1Jparr} were 77.6% and 78.2%, respectively (Figure 3-16).

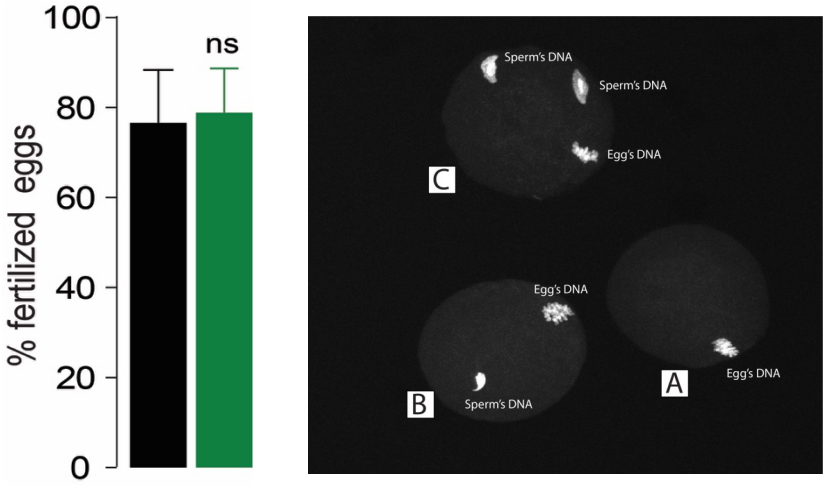


Figure 3-15: Mean percentage of oocytes showing sperm penetration as indicative of fertilization

Wildtype oocytes were stained with Hoechst 6 hours post IVF with PLCζ^{wt}- and PLCζ^{em1Jparr}-derived sperm (PLCζ^{wt}: 193 oocytes, 3 male; PLCζ^{em1Jparr}: 132 oocytes, 3 male), and examined with confocal laser microscopy for sperm head(s) DNA localisation inside the oocytes. Picture show exemplar oocytes (A) unpenetrated, (B) penetrated with single sperm, (C) penetrated with two sperm.

3.3.6 *In vitro* fertilisation and blastocyst formation with PLCζ-null sperm

For further examination of PLCζ-null spermatozoa fertilising ability and oocyte activation *in vitro*, a series of IVF experiments were performed on PLCζ^{wt} oocytes collected 14 hours post hCG, then inseminated either with PLCζ^{wt}, or PLCζ^{em1Jparr} sperm in separated setups at a final sperm concentration of 1x10^{6} sperm/ml in HTF medium. Two-cell stage embryo formation was recorded 24 hours post IVF, and embryo culture was extended to 96 hours post insemination for monitoring four-cell, morula, and blastocyst formation. The findings show a highly significant decrease in the mean percentage of embryo development *in vitro* from oocytes inseminated with PLCζ^{em1Jparr} sperm (Two-cell: 16.8%; Four-cell: 12.3%; Morula: 12.3%; Blastocyst: 9.6%) ($p<0.001$), when compared to oocytes inseminated with PLCζ^{wt} (Two-cell: 90.8%; Four-cell: 85.9%; Morula: 77.2%; Blastocyst: 71.4%) (figure 3-17). There was no significant difference in the number of the collected oocytes for each fertilisation dish for either the wildtype or PLCζ-null spermatozoa.

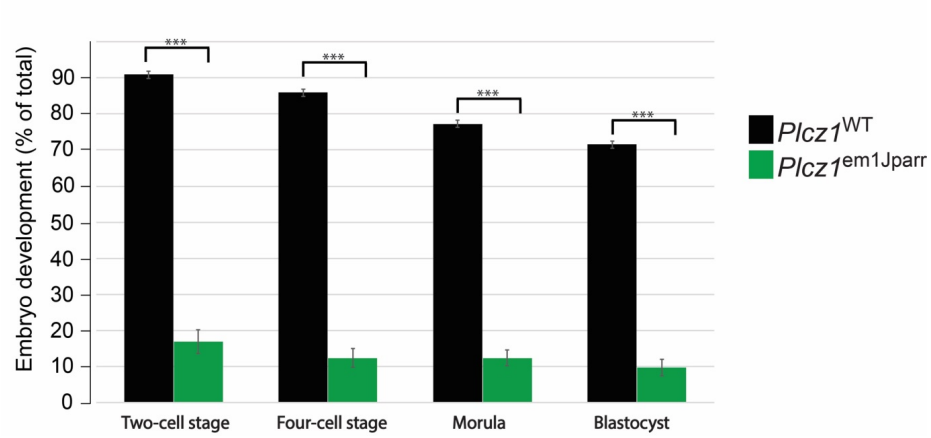


Figure 3-16: Show IVF and embryo development rate with PLCζ^{em1Jparr} sperm

Data refer to IVF resulting embryos during four days of embryo culture in KSOM-aa medium and are presented as average ± sem followed by one-way ANOVA analysis.

3.3.7 PAWP expression analysis

It has been previously suggested that the postacrosomal WW domain-binding protein (Wbp2nl/PAWP), could function as the physiological agent of oocyte activation. Thus, to ensure that the Wbp2nl/PAWP gene was not affected by the CRISPR/Cas9 induced mutagenesis, number of experiments were carried out to investigate the status of Wbp2nl/PAWP expression in PLCζ mutant lines. RT-qPCR analysis for Wbp2nl mRNA revealed that the neither CRISPR/Cas9, nor the PLCζ mutations have yielded any detrimental effects upon Wbp2nl mRNA expression in testis (figure 3-18 A). Furthermore, immuno-blotting analysis for PAWP showed no apparent differences in the level of PAWP protein between PLCζ^{wt}- and PLCζ^{em1Jparr} -derived sperm (figure 3-18 B).

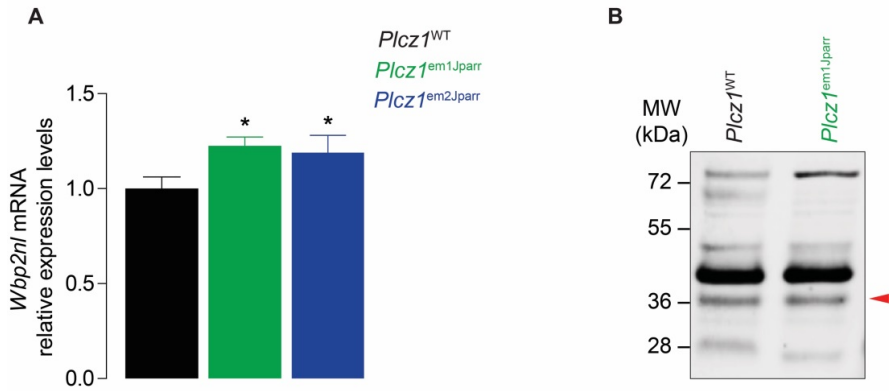


Figure 3-17: Expression levels of Wbp2nl/PAWP in PLCζ mutant lines.

(A) Levels of Wbp2nl mRNA in testis were determined by RT-qPCR using expression of ß-actin as the reference housekeeping gene. Relative levels were determined by ΔΔCt analysis and are shown as average ± SEM of three different animals in triplicate, followed by a one-way ANOVA test.
(B) Whole sperm samples from PLCζ^{WT} and PLCζ^{em1Jparr} males were used in immunoblot analysis for PAWP (anti-PAWP antibody; ProteinTech). The immunoreactive band corresponding to the predicted size of mouse PAWP (37.5 kDa) is indicated by a red arrow.

3.4 Discussion

3.4.1 Does PLCζ deletion compromise spermatogenesis and sperm quality parameters?

Utilising CRISPR/Cas9 technology in targeting the coding sequence of mouse PLCζ showed how effective this tool in creating permanent frameshift mutations and protein loss of function in both of the $Cas9^{wt}$ and the Nickase approaches. However, this technology as any current technology also hold number of disadvantages, most importantly here is the reported off-target effect. Thus, two knockout mouse lines were created by employing different Cas9 approaches not only to test the specificity of gRNAs but was also to obtain a better validation on the resulting phenotype that would eventually eliminate any discrepancies through the experimental procedures. Additional point to consider, is due to the testes-specific PLCζ expression in mammals (Saunders *et al.*, 2002), from as early as the round spermatid (Vanden Meerschaut *et al.*, 2013; Aarabi *et al.*, 2012; Yoneda *et al.*, 2006; Yazawa *et al.*, 2000), and since naturally occurring and man-made genetic alterations can easily interfere with the intricate events of spermatogenesis leading to either complete gonadal failure (Wang *et al.*, 2016; Lopes *et al.*, 2013) or formation of spermatozoa harbouring structural changes (Sun *et al.*, 2006), it was crucial therefore in this study to characterise the testicular developmental stages and the sperm functional parameters not in one but in two mouse lines harbouring the same knockout effect. Such high level of validation would be of a great interest not only in underpinning the exact role of PLCζ in egg activation and embryo development, but also if PLCζ expression is involved in additional cellular activities, specifically normal sperm formation and function as reported by several reports.

Starting with histological examination of testicular sections from $PLC\zeta^{em1Jparr}$ and $PLC\zeta^{em2Jparr}$ homozygous males, findings revealed no detrimental effect from lacking the expression of PLCζ on testes spermatogenesis. Morphological examination on tissue sections from the knockout lines showed normal distribution of the germinal cells, meiotic cells, spermatids, and other supporting cells inside the seminiferous tubules. Indicating that spermatogenesis in mammals and the hormonal regulation that supports the sperm formation are both independent on the expression of PLCζ. The finding comes in total disagreement with a preliminary report (Ito *et al.*, 2010), and other clinical reports

associated PLCζ mutations with abnormal sperm formation and characterisation (Heytens *et al.*, 2009; Taylor *et al.*, 2010; Kashir *et al.*, 2013; Escoffier *et al.*, 2015). Remarkably, PLCζ homozygous knockouts provided the first conclusive evidence emphasising the irrelevance of PLCζ expression in testes spermatogenesis and sperm structural development in mammals.

However, testicular tissue sectioning and staining alone usually fail to establish the fertilising ability of the sperm. As being able on generating a sperm is totally different from being able on generating a sperm equipped with the aptitude to bind and fuse with the oocyte. Thus, comprehensive semen analysis on the homozygous mutants is imperative in this sense to eliminate any propositions suggest lacking PLCζ expression might alter the sperm functional parameters and diminishes the fertilising potential of the sperm.

Similarly, one could argue that since PLCζ expression is detectable as early as the round spermatid, lacking the expression from this stage onward would subject the sperm to structural changes across the maturation process in the epididymis. The appropriate response to such claims is to extensively inspect the isolated epididymal sperm for any signs of irregularities such as in sperm viability, sperm motility, and sperm capacity to undergo the acrosome reaction, as well as sperm binding and fusion with oocyte.

Indeed, sperm viability analysis by flow cytometry on samples from $PLC\zeta^{em1Jparr}$ and $PLC\zeta^{em2Jparr}$ homozygous males did not reveal any detectable difference in the total percentage of viable sperm when compared to $PLC\zeta^{wt}$. This strongly signifies that PLCζ protein is not involved in the process of sperm maturation, nor the deletion itself diminished the normal proportion of viable sperms. Evidently, sperm viability findings correlate significantly with sperm's ability in achieving the standard steps in the epididymal spermiogenetic process, such as sperm plasma membrane remodelling and integrity (Jones, 1998c; Hossain *et al.*, 2011), cytoplasmic extrusion (Rengan *et al.*, 2012), and nuclear histone-protamine replacement (Bao and Bedford, 2016), as well as demonstrating high DNA integrity (Samplaski *et al.*, 2015). Moreover, sperm viability studies were also found to identify cases of infertility caused by epididymal spermatozoa maturation arrest, in which sperm show consequential abnormal morphology, and diminished ability to construct the zona pellucida and hyaluronic acid binding sites in mature spermatozoa (Huszar *et al.*, 1997).

In this regard, given the importance of sperm viability analysis on detecting plasma membrane integrity, findings from this technique can also be used to predict sperm motility and sperm ability to undergo capacitation and hyperactivation, under even physiological conditions (Kasimanickam *et al.*, 2006; Hossain *et al.*, 2011). Indeed, CASA analysis has shown no detectable differences in all the studied samples in terms of the characterised types of progressive motility or the ability of the sperm to reach capacitation and hyperactivation, totally confirming the predicted correlation with the findings from sperm viability analysis. Which consequently helped in determining the fertilising ability of PLCζ^{em1Jparr} and PLCζ^{em2Jparr} homozygous males for the following *in vivo* and *in vitro* studies. The finding has also suggested that the pathways involved in utilising the intracellular ATP, cAMP, and Ca^{2+} for stimulating the propulsive flagellar movement is independent of PLCζ expression and function in mouse epididymal sperm.

The fertilising ability of the mammalian spermatozoa also depends upon the sperm's ability to undergo capacitation and the acrosome reaction (AR). This study has investigated whether PLCζ-null spermatozoa are able to undergo the AR in response to physiological and non-physiological stimuli. Such investigation would help to elucidate not only the sperm's ability to undergo the AR when incubated with ionophores, but also to investigate if the natural pathways that is involved in sperm capacitation would exert the same effect when the sperm is treated with progesterone. It has been found that ionophores can initiate AR in non-capacitated sperm without the need to mobilize Ca^{2+} from the internal stores (Harper *et al.*, 2006), whereas progesterone promotes the uptake of Ca^{2+} only by capacitated spermatozoa, and initiates the AR similar to the natural mechanism of a ZP-induced AR (Gupta, 2015; Avella *et al.*, 2013). The findings from this part of the study would be of great interest not only in determining the ability of PLCζ-null spermatozoa to undergo the AR, but also to elucidate if the two pathways can promote the same results. Moreover, the findings here would also help in understanding if PLCζ protein is involved in capacitation and AR besides being the best candidate for oocyte activation, as several studies have localized PLCζ in the acrosomal segment of the sperm (Fujimoto *et al.*, 2004; Young *et al.*, 2009; Escoffier *et al.*, 2015; Heytens *et al.*, 2009; Grasa *et al.*, 2008; Yoon *et al.*, 2008; Ferrer-Vaquer *et al.*, 2016; Bi *et al.*, 2009).

The current data did not show any observable difference between PLCζ-null and wildtype groups in inducing the AR in response to incubation with either ionomycin (10 µM) or progesterone (20 µM) following the studied time intervals. This leads to an overall

conclusion that PLCζ-null spermatozoa did not inherit any structural abnormalities in the acrosomal area as a result of the PLCζ deletion, nor has the loss of sperm-PLCζ affects the ability of the sperm to undergo capacitation and AR under physiological and non-physiological conditions.

Another factor was examined in this part of the study is the sperm's ability to penetrate the natural barriers surrounding the oocyte, ZP and oolemma, as well as the sperm's ability to fuse and incorporate into the cytoplasm following IVF. Sperm DNA staining and 3-D images projections acquired with the aid of confocal microscopy confirmed no detectable differences in the rate of sperm penetration and fusion between the PLCζ mutant groups and the wildtypes. Signifying the importance of the sperm functional parameters in predicting the fertilising ability of a sperm from one side, and from another side confirmed the irrelevance of PLCζ expression on affecting sperm's formation and performance in mammals.

In conclusion, PLCζ homozygous knockouts have provided for the first time direct and conclusive evidence showing that mammalian spermatogenesis and mature spermatozoa functional parameters are completely independent of PLCζ expression, and PLCζ-deficient mice are still able to generate spermatozoa with normal sperm parameters, contradicting a number of previous reports.

Importantly, however, normal sperm parameters are often very central to predict levels of fertilisation and pregnancy in all mammals, given the importance of PLCζ in initiating the Ca^{2+}oscillations that triggers egg activation, PLCζ-null sperm are expected to profoundly abrupt egg activation and embryo formation even with the reported normal semen profile. Thus, it is worth noting here that even with the appeared normal sperm parameters in this study, general semen analysis does not always reflect the fertilising ability of a sperm. This has been demonstrated not only in this experimental approach, but also in clinical studies of fertile oligozoospermic men, and of men with normal sperm parameters suffering (unexplained) male infertility (Wang and Swerdloff, 2014; Escoffier *et al.*, 2016). It is vital, therefore, to include PLCζ expression analysis in every routine assessment for fertility both experimentally and clinically as semen quality analysis alone would not always reflect the fertilising potentials of a sperm.

3.4.2 Does the lack of PLCζ expression abolish the sperm's ability to induce Ca^{2+} rise post-fertilisation?

As mentioned earlier, all the Ca^{2+} imaging studies following IVF or ICSI procedures with PLCζ-null and $PLC\zeta^{wt}$ sperm have been performed by our collaborators in Ghent and Massachusetts.

At Petra de Sutter's lab, Ca^{2+} imaging studies of mouse oocyte fertilised with PLCζ-null sperm showed complete absence of Ca^{2+}oscillations post ICSI when compared to $PLC\zeta^{wt}$ sperm injections. Similar findings were obtained from Rafael Fissore's lab have provided a further confirmation to the findings from de Sutter's, that PLCζ-null sperm lacks the ability to generate Ca^{2+}oscillations post ICSI. This defect in initiating Ca^{2+} transients was confirmed by rescuing the phenotype with injecting the full length of PLCζ cRNA into the mouse oocytes. Both labs have showed definite experimental reproducibility of the findings based on the results generated under the experimental conditions and procedures mentioned in the Materials and Methods section of this chapter.

This work presents the first direct evidence that sperm-PLCζ is the physiological trigger that initiate the standard Ca^{2+} oscillations when injected into the mouse oocytes. Thus, this part of the study comes in total agreement with findings from several studies regarding the physiological relevance of PLCζ in initiating Ca^{2+} oscillations in mammalian oocyte (Saunders *et al.*, 2002; Fujimoto *et al.*, 2004; Knott *et al.*, 2005; Kouchi *et al.*, 2005; Kurokawa *et al.*, 2005; Swann *et al.*, 2006; Parrington *et al.*, 2007).

Importantly, however, one could argue that utilising ICSI in these setups might have led to misleading results because of some negative effect on the ability of these sperm to induce the Ca^{2+} oscillations, that was related to the fact that sperm immobilization is required prior to ICSI (Yanagida *et al.*, 2001). Similarly, sperm injection is evidently different from natural fertilization, where ICSI does not involve sperm-oocyte interaction which in this case might leave open possibility that some aspect of normal sperm-oocyte integration leads to a limited degree of Ca^{2+} rise. Therefore, it was imperative to perform Ca^{2+} imaging studies following IVF with PLCζ-null sperm to confirm the findings from ICSI procedures. The results from fertilising mouse oocytes *in vitro* with PLCζ-null sperm

also showed absence of the Ca^{2+} oscillations apart from a single Ca^{2+} increase that was recorded in one of the oocytes.

Although Ca^{2+} imaging in this part of the study has confirmed that PLCζ is the physiological trigger of the sperm-induced Ca^{2+} oscillations, a few oocytes that were fertilized by PLCζ-null sperm *in vitro* and *in vivo* were able to develop to embryonic stages and produced viable and healthy pups. This rather surprising findings led us to propose the existence of an alternative pathway in egg activation that is completely independent of the sperm factor PLCζ. Here, the true identity of this factor is still a mystery, however, membrane interactions between gametes were found to be responsible in triggering this pathway. On the other hand, expression analysis of PAWP as one of the candidates for the sperm factor in egg activation has excluded any contribution from this factor in rescuing the PLCζ-related phenotype, as PAWP RNA levels and protein expression analysis were found to be unaffected by either the CRISPR mutation, or by the absence of PLCζ expression, although, PAWP mRNA expression was slightly greater in the PLCζ-null sperm.

Findings from this part of the study indicate that natural mating and fertilization without the standard physiological trigger of oocyte activation in mammals can still initiate embryogenesis, albeit at much reduced efficiency and after a significant delay. The live birth of animals in the complete absence of sperm PLCζ would seem to challenge several previous reports that highlighted the primary importance of PLCζ in inducing the Ca^{2+} oscillations that drives exit MII pathways, CGE, the block to polyspermy and early embryonic gene expression (Ducibella and Fissore, 2008; Rogers *et al.*, 2006; Madgwick *et al.*, 2005; Larman *et al.*, 2004; Hyslop *et al.*, 2004; Halet *et al.*, 2004; Dumollard *et al.*, 2004; Ozil *et al.*, 2006; Dale *et al.*, 1985; Ducibella, 1996). In fact, the finding is not quite as surprising as it first appears given that previous studies have shown that ovulated, unfertilized hamster and mouse oocytes left to reside in the oviduct for extended periods of times *in vivo* can undergo spontaneous oocyte activation (Yanagimachi and Chang, 1961; Whittingham and Siracusa, 1978). Further analysis has suggested that these oocytes showed a spontaneous decrease in the activities of histone H1 and MAPK (Xu et al., 1997). However, such parthenogenetic embryos are incapable of development to term due to absence of the paternal DNA. Importantly, the live offspring generated from crosses between PLCζ mutant males and wildtype females are the first to be generated

through natural mating in the absence of the sperm-PLCζ induced Ca^{2+} oscillations that normally trigger mammalian development.

Recently Nozawa *et al.* (2018) reported creating a mouse model lacking PLCζ with a very similar phenotype to PLCζ knockouts generated in this study (Hachem *et al.*, 2017). However, the report came with a notable difference. Nozawa and colleagues found that PLCζ-null sperm can still induce number of delayed and atypical Ca^{2+} (2 to 3) spikes that is only observed following IVF, not ICSI, whereas a single Ca^{2+} rise was only recorded in one oocyte in our study. A possible explanation for the differences between the two observations is probably due to the potential adverse effects of cryopreservation on the semen samples that we collected and sent to our collaborators. Freeze-thawing can cause structural abnormalities in the sperm head and tail affecting a number of factors during fertilization (Sztein *et al.*, 2000; Liu *et al.*, 2009; Schachter-Safrai *et al.*, 2017), which then could have contributed to the reduction of the sperm's ability to induce the atypical Ca^{2+} spikes. Thus, further analysis is still required to understand the potential role of membrane integrity in the initiation of the atypical Ca^{2+} rise and egg activation in fresh *vs* cryopreserved sperm samples.

Together, findings from both of the published studies of PLCζ-null sperm mice have suggested that sperm-oocyte binding and interaction through natural fertilisation in mammals can mediate Ca^{2+} transients and oocyte activation in the absence of prime sperm factor PLCζ, albeit at a greatly reduced efficiency and with an observable effect from cryopreservation on the integrity of this process.

3.5 Conclusion

To conclude the findings from this chapter, PLCζ deletion in mice did not cause any detrimental defects in spermatogenesis nor did affect sperm functional parameters. Although, PLCζ knockout sperm injected into the oocyte failed to trigger the standard Ca^{2+} oscillations in the oocytes, a rescue experiment with PLCζ cRNA injection have successfully restored the standard phenotype. The findings provide the first direct evidence that PLCζ is the physiological trigger of the sperm-induced Ca^{2+} oscillations that trigger oocyte activation in mammals. Unexpectedly however, oocytes which were fertilised with the knockout sperm can still develop to the blastocyst stage and producing live offspring, albeit at much reduced efficiency and after a significant delay. This suggests a yet-to-be identified PLCζ-independent route following oocyte activation that is dependent on sperm-oocyte membrane interaction.

4 Polyspermy and Juno shedding

4.1 Background

In mammals, successful fertilisation occurs when a single sperm binds and fuses with the oocyte, together they provide the diploid number of chromosomes for the zygote's normal development. One of the abnormal forms of fertilisation in mammals is when more than one sperm bind and fuses with the oocyte leading to perturbation of fertilisation and cessation of development (Wang *et al.*, 2003). Thus, mammals have adopted several mechanisms to ensure successful insemination with a single sperm per oocyte, such as sperms filtration through the physical barriers of the female genital tract, and egg-based blocking mechanisms (Gardner and Evans, 2006).

Despite all the blocking mechanisms in mammals and human, the incidence of polyspermy *in vivo* is still observable around 1-2 % for every fertilisation event (Baumer *et al.*, 2000), and the reasons behind this observation is yet to be understood. However, number of factors were found to contribute to increase the incidence of polyspermy, such as, high sperm concentration (Fukuda and Chang, 1978), delayed postovulatory oocyte fertilisation (Ducibella and Buetow, 1994), and species-specific related phenomena as in porcine oocytes (Hunter, 1991). All have been reported to cause a reduction in the fertilisation rate, and stagnation of the first embryonic cell division.

In mammals, the oocyte contributes to block polyspermy through two mechanisms: first is the cortical and zona reaction to prevent sperm penetration to the glycoprotein layer surrounding the oocyte (zona pellucida (ZP)), and second is the oocyte's plasma membrane blocking mechanism (Dale and DeFelice, 2011). The oocyte's first defence mechanism against polyspermy occurs by altering the sperm-binding residues that facilitate sperm binding and penetration of ZP layers (Florman and Fissore, 2014). According to the molecular structure of the ZP, it can be distinguished as three layers: ZP3, ZP2, ZP1. The outermost layer, ZP3, was found to be responsible for inducing the acrosome reaction in capacitated sperm, thus exposing the species-specific binding sites that are located underneath the acrosomal segment, and then facilitates sperm binding to specific residues on ZP2 which here acting as a secondary sperm receptor (Gupta *et al.*, 2012; Inoue *et al.*, 2005).

It has been found that fertilisation alters the receptivity of the ZP layers to bind and fuse with additional sperm, via triggering CGE from the cortex of the oocyte to the outside

surroundings (Miyazaki *et al.*, 1993). The enzymatic activities of the CGs was found responsible for cleaving the sperm-docking sites on ZP2, and blocks sperm binding and penetration (Burkart *et al.*, 2012). Disrupting the CGE artificially by buffering the actions of the Ca^{2+} rise following fertilisation, blocks all oocyte activation events including the ZP blocking mechanism (Deng *et al.*, 2003). Likewise, abnormal Ca^{2+} transients associated with post-ovulatory aged oocytes have also been reported to induce similar effects (Wortzman and Evans, 2005; Jones and Whittingham, 1996). Taken together the findings, show that the cortical and zonal reactions are very important in ZP block and prevent polyspermy, and the process is strongly dependent on Ca^{2+} transients that follow fertilisation.

On the other hand, the oocyte's second defence mechanism corporates the plasma membrane blocking mechanism for additional sperm to fuse with the oocyte. This is based on the finding that *in vitro* fertilisation with ZP-free oocytes most of the oocytes were still found monospermic even in situations included insemination with relatively large number of sperms. In addition, challenging the same oocytes with a second wave of insemination, hardly any of the additional sperms found a way inside the oocytes, revealing that the fertilised membrane is somehow different from the membrane of the unfertilised oocyte (Gardner and Evans, 2006; Gardner *et al.*, 2007b). In contrast, fertilised oocytes *in vitro* in the presence of a Ca^{2+} buffering compound were found to be polyspermic, indicating the involvement of the plasma membrane in the blocking mechanism firstly, and secondly Ca^{2+} rise is both essential and efficient to preventing supernumerary sperm entry (Florman and Fissore, 2014; Maluchnik and Borsuk, 1994).

Surprisingly, however, activating the oocytes artificially either by ICSI, parthenogenetically, or by sperm extract injections, did not show to trigger the establishment of membrane block, even in the accompanied Ca^{2+} rise following these conditions. Suggests involvement of a Ca^{2+}-independent event that is to some extent contributing to the cellular cues that govern plasma membrane block establishment. This event might be a part of the membrane interaction between gametes that is prelude to the Ca^{2+} rise but still contribute to the post-fertilisation membrane block to polyspermy. Such a model of membrane interaction between gametes may include a signalling event that triggered by the binding of an extracellular sperm ligand to an oocyte receptor.

Recently, Bianchi and colleagues (2014) identified a folate receptor 4 glycophosphatidylinositol (GPI)-anchored protein (named Juno) on the oocyte's plasma membrane as a good candidate for sperm-oocyte recognition, and as a potential factor in membrane establishment. They showed that this protein is essential for sperm binding and fertilisation, and a mouse model lacks Juno expression was found to be infertile. Further evidences for the importance of this protein in membrane establishment came from the shedding property of Juno, 30-45 min after fertilisation, which was proposed to constitute the membrane block to polyspermy. These findings placed Juno as one of the best candidates for mediating gamete interaction in mammals, and also as a key molecule that might be involved in the membrane block to polyspermy.

Juno's shedding mechanism is not fully resolved. However, it appears that the shedding mechanism occurs upon sperm-binding, and not after sperm injection or parthenogenetic activation, surprisingly similar to the process of membrane establishment in mammals (Maleszewski *et al.*, 1996). In addition, binding of Juno with the sperm counter-receptor protein (Izumo1) was found to be transient, and not permanent. This suggests that Juno works firstly as a sperm binding site on the oocyte, and secondly as a mediatory to a yet-to-be identified protein which is considered to have the capacity to neutralise the strong repulsive forces of the membranes (sperm and oocyte) for the later fusion step (Inoue, 2017; Bianchi and Wright, 2015). Yet, the detailed molecular mechanism of sperm fusion still remains largely unknown despite the identification of Juno. Targeted deletion studies have revealed that at least two additional proteins are necessary for sperm-oocyte binding and fusion, CD9 on the oocyte and SPACA6 on the spermatozoon (Kaji *et al.*, 2000; Lorenzetti *et al.*, 2014).

This study took into consideration the fact that there have been no published reports indicating the direct role of the sperm PLCζ in preventing polyspermy in mammalian oocytes. The animal models that we have developed lacking expression of PLCζ would provide a perfect tool to address this notion via a series of experiments designed to unravel the internal mechanism that which controls incidents of polyspermy. Thus, this part of the thesis will firstly focus on the effects of lacking the expression of PLCζ on the oocyte's ability to block polyspermy, and secondly will study if Juno is truly capable on initiating the membrane establishment block to polyspermy in the absence of the standard Ca^{2+} oscillations, as proposed by several studies.

4.2 Materials and methods

4.2.1 *In vivo* fertilized eggs and sperm DNA staining

3 – 4-week old C57Bl/6J female mice (Charles River UK) were injected intraperitoneally with 5 IU of PMSG (Intervet) and 48 hours later with 5 IU of hCG (Intervet), and paired with male mice from either wildtype or PLCζ-null. Zygotes were retrieved from oviductal ampullae at 18 hours post-hCG. Cumulus-enclosed zygotes were denuded by exposure to 1 mg/ml hyaluronidase (Sigma) in modified HTF (Zenith Biotech) for 3 – 6 minutes, washed through fresh modified HTF, and cultured in KSOMaa in the presence of 5 % CO_2 at 37 °C. For assessment of polyspermy, the zygotes were then placed in fresh modified HTF containing 1μg/ml Hoechst 33342 and incubated for 20 – 30 minutes, then were washed in fresh modified HTF and imaged using a fluorescence microscope.

4.2.2 *In vitro* fertilized eggs immunostaining against Juno and sperm DNA

C57BL/6J female mice at 3–4 weeks old were stimulated using 5 IU of PMSG (Folligon, Intervets). Ovulation was induced 46–48 hours later using 5 IU hCG (Chorulon, Intervet). Oocyte-granulosa cell complexes (MII) were collected 13–14 hours following hCG administration in a complete pre-warmed HTF medium (Zenith Biotech). The oocytes were then inseminated with pre-capacitated sperm from either wildtype or PLCζ-null at a final concentration of 1 x 10^6 sperm/ml, under mineral oil (Zenith Biotech) at 37°C and 5% CO_2.

Six hours post IVF, oocytes were collected and washed three times in PBS supplemented with 4% BSA, and then fixed in 3.7% paraformaldehyde for 30 minutes. Non-specific protein binding sites were blocked by incubating the cells in 4% BSA, before overnight incubation at 4°C with anti-Juno polyclonal antibody (1:100) (a gift from Dr Enrica Bianchi) in blocking buffer. Secondary antibody (Alexa fluor 546) was applied at room temperature for 45 minutes along with Hoechst 33342 DNA staining, whilst being protected from light. Cells were then washed and air-dried on superfrost plus slides (Fisher

Scientific, USA), then mounted by ProLong Gold Antifade Mountant (Thermofisher) under a coverslip.

Immunofluorescence was examined on a LSX8 Leica confocal scanning laser microscope with a 20x objective. Juno's expression on the oolemma was detected by the Alexa Fluor 546 dye at 556/573 (excitation/emission) laser line, while sperm and oocyte DNA were detected at 358/461 (ex/em.). A high-resolution image series was acquired in 2D for studying Juno expression in oocytes. Multiple images on the z plane were generated at the same time in order to build 3-dimensional (3D) projections of the embryos for counting of sperm heads inside the oocytes by the DNA staining method. The settings on the laser power, sensitivity of detectors and pinhole size (1 airy units) were adjusted until no fluorescence was observed in the negative control group and subsequently kept the same for the same set of experiments. Images were analysed and processed using imageJ/Fiji software (NIH, USA).

4.3 Results

1.1.1 Increased polyspermy in oocytes fertilized *in vivo* by PLCζ-null sperm

Progress made in understanding polyspermy has only been achieved by using calcium ionophores and Ca^{2+} chelating agents to create conditions mimicking the early fertilisation events, making it possible to dissect and analyse each event separately for better understanding. However, utilising such agents could generate non-physiological responses which in turn create a non-natural cellular behaviour. An animal model whose sperm lack the ability to generate Ca^{2+} oscillations following fertilisation, would provide a perfect tool to study ZP structural remodelling, oocyte membrane establishment, and CGE in mammals.

Indeed, investigating the levels of polyspermy in wildtype mouse oocytes from females fertilized *in vivo* by $PLC\zeta^{wt}$ and PLCζ-null males showed a significant increase in polyspermy among oocytes fertilized by $PLC\zeta^{em1Jparr}$: 21/111 and $PLC\zeta^{em2Jparr}$: 19/82, versus oocytes fertilized by $PLC\zeta^{wt}$ males (3/37) (figure 4-1). These findings indicate that PLCζ-null sperms are normal regarding their ability to penetrate the oocytes (result section 3.2.8), however, the mechanism that is responsible for ZP block and membrane establishment seems as if it was not engaged in a timely fashion. Whether or not this failure is limited to cortical granule release is unknown in this study, it appears, however, that the current phonotype is dependent on PLCζ expression and the standard Ca^{2+} oscillations.

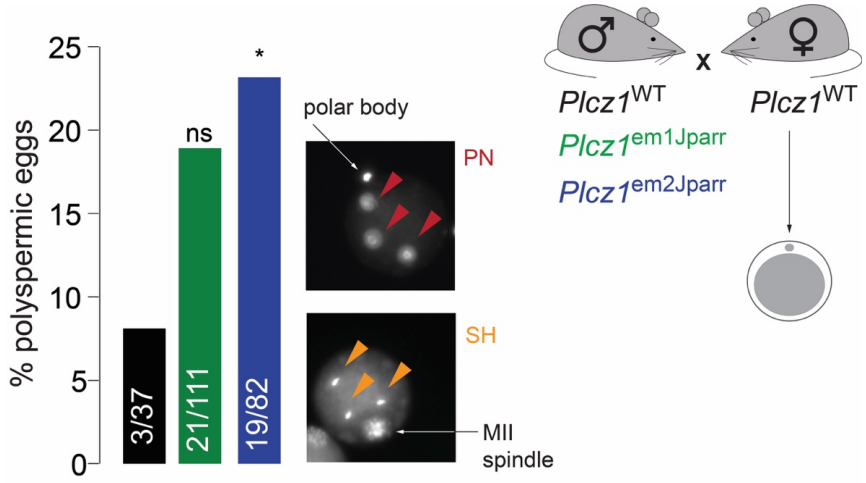


Figure 4-1: Polyspermic oocytes produced with natural mating

Number of polyspermic oocytes derived from super-ovulated wildtype females fertilized *in vivo* by homozygote PLCζ^{wt}, PLCζ^{em1Jparr} or PLCζ^{em2Jparr} males. Oocytes were stained with Hoechst 18 hours post hCG treatment of females, for visualization of abnormal number of pronuclei (>2 PN) or sperm heads (>1 SH). Data are presented as percentage of total oocytes examined from combined experiments: (PLCζ^{wt}: 37 oocytes, 2 males; PLCζ^{em1Jparr}: 111 oocytes, 3 males; PLCζ^{em2Jparr}: 82 oocytes, 2 males) and statistical analysis performed using a 2x2 contingency table followed by a Fisher's exact test. Exemplar fertilized oocytes showing polyspermy are shown.

1.1.2 Increased polyspermy in oocytes fertilized *in vitro* by PLCζ-null sperm

The mouse line PLCζ^{em1Jparr} was used to investigate the incidents of polyspermy following *in vitro* fertilisation. The inseminated oocytes with PLCζ^{wt} and PLCζ^{em1Jparr} sperm samples were collected and washed to remove any excess attached sperm to the zona pellucida, then Hoechst DNA staining was performed for sperm head localisation. Images from laser confocal microscopy on z-plane series were used to create three-dimensional constructions for oocytes, and individual sperm DNA was pin-pointed inside each oocyte with the aid of image-J software.

This part of the study confirmed the findings from the *in vivo* fertilisation, and the results were very conclusive regarding the role of the standard Ca^{2+} rise from PLCζ^{wt} in blocking polyspermy. In contrast, fertilisation with PLCζ^{em1Jparr} spermatozoa showed a significant increase in the number of sperm heads inside oocytes (PLCζ^{em1Jparr}:69.8% to 17.9% with PLCζ^{wt}). In addition, the ZP layers surrounding the oocytes that inseminated with PLCζ^{em1Jparr} showed to contain a greater number of incorporated sperms when compared with oocytes inseminated with PLCζ^{wt}. The reason behind this might be due to an abnormal or complete absence of the CGE which could lead to failure in establishing the ZP block (figure 4-3). Thus, leading for more sperm to penetrate the ZP, and more sperm to inter the perivitelline space.

Findings from (Nozawa *et al.*, 2018) confirmed our data regarding the association between lacking the expression of PLCζ and the incidents of polyspermy. In addition, they showed a significant delay in the mechanism that control ZP blocks and membrane establishment in oocytes fertilised with PLCζ-null sperm, and the observed results coincide with the delayed Ca^{2+} rise. Together, PLCζ expression post fertilisation is essential for triggering the standard Ca^{2+} oscillations, that governs the natural mechanism of ZP block and membrane establishment in mammals.

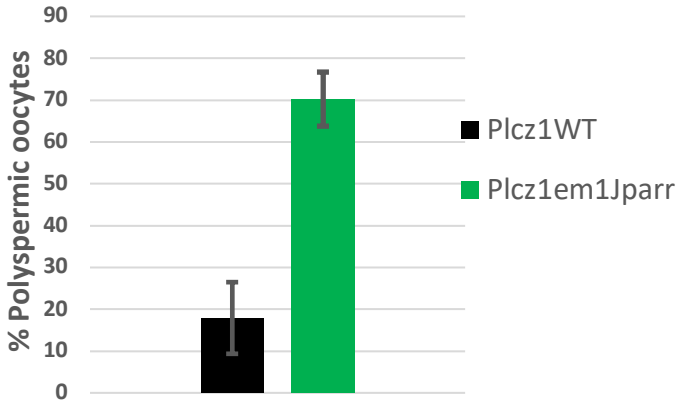


Figure 4-2: Increased polyspermy in oocytes fertilized by PLCζ^{em1Jparr} sperm

Show mean percentage of oocytes showing abnormal number (>1) of sperm heads in individual oocytes.

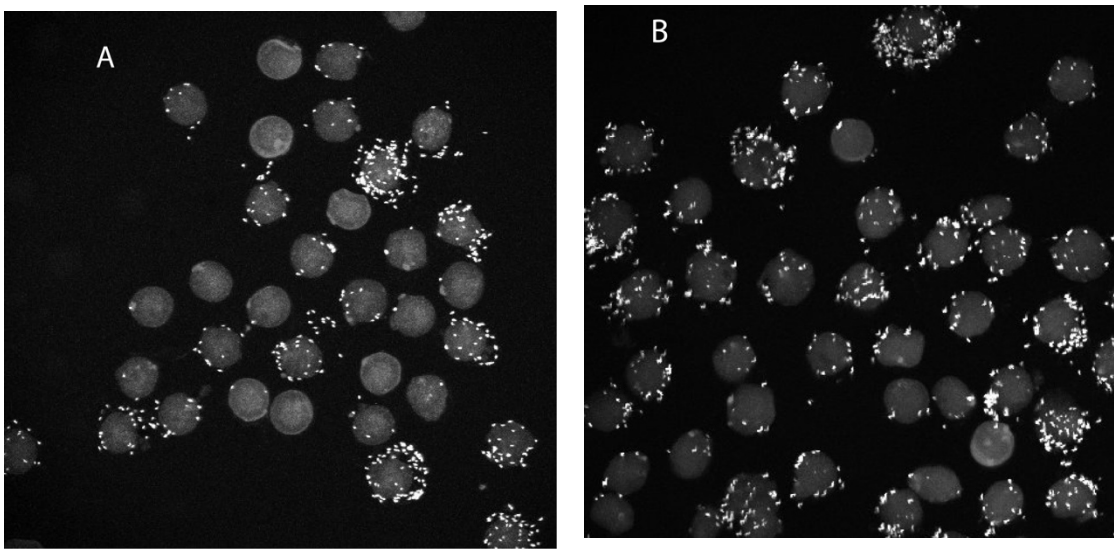


Figure 4-3: Presents oocytes inseminated *in vitro* with (A) PLCζ^{wt} and (B) PLCζ^{em1Jparr} spermatozoa

Oocytes were collected six hours post fertilisation and washed three time with HTF medium before staining with Hoechst DNA staining.

1.1.3 Juno shedding post fertilisation is PLCζ-independent

Although, it is well documented that ZP blocks is dependent on the Ca^{2+} rise that follows fertilisation, the exact mechanism that triggers the membrane establishment in mammalian oocytes is still largely unknow. Folate receptor 4 (Juno) protein on the oolemma showed potential characteristics for sperm binding and fusion with the oocyte, and the observed shedding property post fertilisation has been proposed to ensure monospermic fertilisation (Inoue, 2017; Ohto *et al.*, 2016; Bianchi *et al.*, 2014). Therefore, including Juno expression analysis in this chapter of analysis was imperative in order to have a better understanding on the role of sperm-PLCζ on oocyte membrane establishment firstly, and secondly if the shedding mechanism is either PLCζ dependent or not dependent.

Indeed, following immunostaining with anti-Juno monoclonal antibody of unfertilised oocytes, and those that fertilised with $PLC\zeta^{wt}$ or $PLC\zeta^{em1Jparr}$ spermatozoa, the following was observed:

In unfertilised oocytes, Juno was found to be highly expressed on the oolemma of MII oocytes, and the expression pattern is consistent with the reported findings from Bianchi *et al.* (2014) and Ohto *et al.* (2016). Interestingly, Juno was also expressed on the first polar body membrane, suggesting Juno was also expressed at the GV stage before the first polar body extrusion (figure 4.4 A).

Following fertilisation with $PLC\zeta^{wt}$ sperm, all the fertilised oocytes exhibited a strong reduction in Juno expression, suggesting sperm entry kick starts the shedding process. However, number of areas on the oolemma were still observed to have small patches of persistent staining against Juno which was found to be unevenly distributed even after 6 hours of insemination, including the polar body membrane (figure 4.4 B).

Further examination following insemination with $PLC\zeta^{em1Jparr}$ spermatozoa, revealed shedding of Juno in oocytes similar to that seen with oocytes fertilised with $PLC\zeta^{wt}$. Most of the Juno expression had disappeared from the oolemma, except for the unfertilised oocytes where the expression level was strongly visible as a ring-like form surrounding the oocyte. A very interesting observation following fertilisation with $PLC\zeta^{em1Jparr}$ sperm was that most of the persistent Juno expression patches witnessed with $PLC\zeta^{wt}$ sperm were

completely absent in this condition, apart obviously from the polar body membrane where Juno is still expressed at this site (figure 4.4 C). This might be due to the relatively large number of sperms that have reached the perivitelline space as a result of the absence of the standard Ca^{2+} oscillations and the lack of a ZP block. The presence of supernumerary sperm in the perivitelline space would facilitate more interaction between Izumo and Juno leading to extensive shedding and loss of the expression as observed in figure 4.4 C.

Although Bianchi and colleagues (2014) proposed a role for Juno in the membrane block to polyspermy, the findings from this part of the study contradict this proposal. Juno shedding mechanism appears to have no contribution in the block of polyspermy following fertilisation with PLCζ-null sperm.

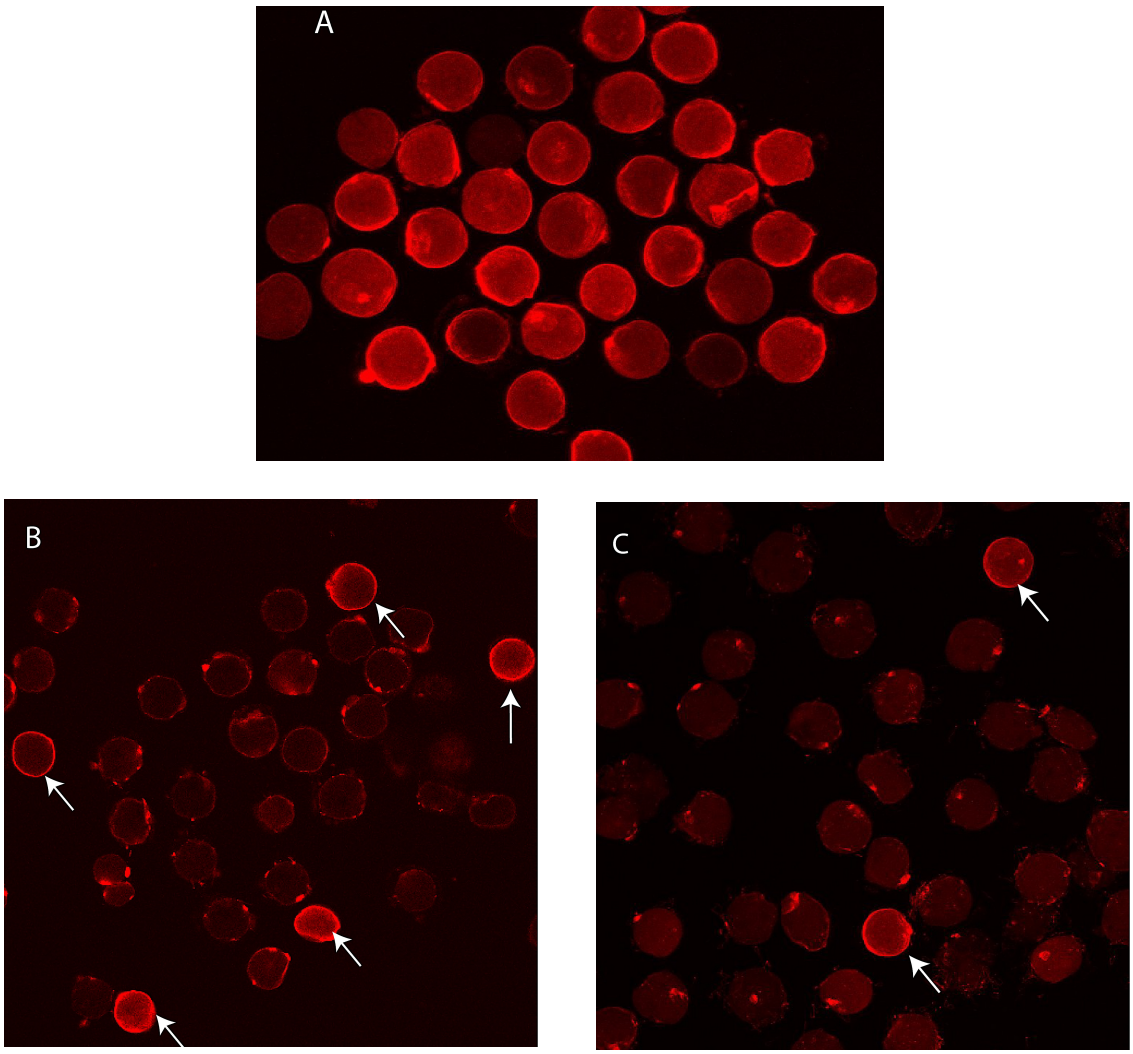


Figure 4-4: Representative confocal images of mouse oocytes exhibiting characteristic localisation of Juno proteins on the oolemma before and after incubation with sperm

A) Juno is highly expressed on the oolemma of unfertilised oocytes.
B) Juno shedding post insemination with PLCζ^{wt} sperm (arrow indicates unfertilised).
C) Juno shedding post insemination with PLCζ^{em1Jparr} sperm (arrow indicates unfertilised).

4.4 Discussion

4.4.1 Does sperm PLCζ contribute to block polyspermy?

Physiological polyspermy or penetration of the oocyte by more than a single sperm occurs in numerous species of animals including insects, reptiles, and birds (Iwao, 2012). However, this type of fertilisation in mammals is considered abnormal, and can lead to developmental failure and spontaneous abortion in humans. The pathological effect of supernumerary fertilisation comes from misgoverning one of the vital developmental process in mitosis, the sperm's centrosome microtubule-organising centre (Snook *et al.*, 2011). Thus, mammalian females have adopted several mechanisms to prevent fertilisation with multiple sperms, yet, the incidents are still around 1-2% in mammals, including human (Baumer *et al.*, 2000; Wang *et al.*, 2003). Although, number of factors have shown a direct contribution to polyspermic fertilisation, the exact molecular trigger has always been a mystery for a very long time (Abbott and Ducibella, 2001; Miao and Williams, 2012).

Repetitive Ca^{2+} oscillations following sperm entry has shown to trigger all the events that lead to egg activation, including ZP blocks and membrane establishment in mammals. These oscillations are dependent primarily upon the hydrolysis of PIP_2 by sperm PLCζ and the subsequent generation IP_3, and DAG in oocytes. Cortical granule exocytosis from the cortex of the oocyte has been found to be triggered by the first Ca^{2+} rise that occurs within 5-10 minutes following sperm entry (Kline and Stewart-Savage, 1994; Tahara *et al.*, 1996). Further Ca^{2+} oscillations continue to drive more waves of CGE to reach the perivitelline space, results in altering the molecular structure of the ZP to become impenetrable for additional sperm entry (Gupta *et al.*, 2012; Burkart *et al.*, 2012; Ducibella *et al.*, 2002). Although the exact molecular drive that transduce the Ca^{2+} signal to trigger CGE in mammalian eggs have not yet been identified, number Ca^{2+}-dependent downstream mediators, such as CaMKII, PKC isoforms, and actin depolymerizing, showed a potential contribution to ZP block (Gardner *et al.*, 2007a; Jones, 1998b; Cheeseman *et al.*, 2016).

The fact that most of the findings regarding the effects of CGE on ZP block and membrane establishment has been studied via utilizing non-physiological approaches,

such as parthenogenic egg activation, or via buffering the sperm-induced Ca^{2+} rise, has since resulted in many controversies in understanding this mechanism. Therefore, elucidating the Ca^{2+} response pathway in eggs fertilised with the PLCζ-null sperm on ZP blocking and membrane establishment, was fundamental and relevant to both experimental and clinical assisted reproductive techniques.

Indeed, findings from *in vitro* fertilisation and *in vivo* mating with PLCζ knockouts, revealed a strong association between polyspermy and deficient Ca^{2+} oscillations in mammals. The incidents of polyspermy have increased in oocytes by more than threefold following in *in vivo* and *in vitro* fertilisation with PLCζ knockout sperm. It appears that lacking the standard Ca^{2+} oscillations in post fertilisation events produced a defect in the mechanism of CGE affecting ZP block. It has also been noted in this study that the sperm density attached to the zona layers of almost every oocyte fertilised with the knockout sperm has also increased significantly. Indicates that these sperm have incorporated deeply within the layers of ZP, due to the proposed absence of the zona block, that was even difficult to detach these sperms by several washings of fresh medium. The findings come in total agreement with numerous reports highlighted the importance of the Ca^{2+} rise on ZP block; however, this is the first report to show the adverse effect of lacking the sperm-PLCζ on normal fertilisation and development in mammals.

It is worth mentioning that, Nozawa and colleagues (2018) have reported similar observations regarding the ZP block and polyspermy associated with the phenotype of PLCζ knockouts. They reported a delayed and incomplete CGE and ZP block following fertilisation with PLCζ knockout sperm, thus allowing more sperm to reach the perivitelline space and produce polyspermic oocytes. The limited number of Ca^{2+} transients (3 to 4 per oocyte) that have been reported following the alternative pathway in egg activation, failed to trigger the normal activation pathway that ensures single sperm fertilisation (Satouh *et al.*, 2017; Ducibella *et al.*, 2006; Ducibella *et al.*, 2002). In conclusion, this study finds that sperm-PLCζ is required to initiate ZP block to prevent polyspermy. Lacking of the functional activity of PLCζ can lead to supernumerary fertilisation, and stagnation in mammalian embryo development.

4.4.2 Does Juno's shedding mechanism contribute to oocyte membrane establishment?

Although, egg plasma membrane block to polyspermy has been described in several mammalian species such as humans, mice, and rabbits (Horvath *et al.*, 1993; Sengoku *et al.*, 1999; Overstreet and Bedford, 1974), little is known about the mechanism that controls membrane block in mammals. Studies included challenging the fertilised membrane with a second wave of insemination revealed distinct mechanistic in utilising the sperm associated Ca^{2+} rise (Gardner *et al.*, 2007b), indicative that Ca^{2+} signal alone is not sufficient to establish a complete membrane block (Wortzman-Show *et al.*, 2007).

The acquired property of the fertilised membrane appears to be incapable on supporting additional sperm entry in conditions that comprise membrane interaction between gametes. This membrane factor is evidently prelude to the Ca^{2+} rise and CGE, yet, still contribute to the post-fertilisation membrane block to polyspermy. Suggests involvement of fusogen proteins from both ends of the gametes to trigger the signalling cascade for membrane block.

Several studies have proposed a fundamental role for Juno protein on the oolemma in facilitating sperm binding (through Izumo1 protein) and fusion with the oocyte (Ohto *et al.*, 2016; Bianchi *et al.*, 2014). In addition, the shedding mechanism of Juno post fertilisation appears to be important in preventing polyspermy, proposedly through hindering additional gamete interaction and neutralising incoming sperms. However, the mechanism that controls the shedding property remains largely unknown. Moreover, immunogold labelling localised Juno protein in the oocyte's surroundings following GCE, suggests the shedding mechanism is somehow dependent on cortical reaction, while CGE contributes to polyspermy prevention by reducing the number of sperms reaching the perivitelline space that potentially bind with Juno.

In this part of the study we found that the Juno shedding mechanism is PLCζ-independent. Both PLCζ-null and $PLC\zeta^{wt}$ sperms revealed no significant difference in terms of Juno immunostaining post fertilisation. The phenotype, however, showed a clear indication that in the absence of PLCζ, the ZP layers and Juno ectodomain fail to establish

a permanent block to polyspermy and prevent excess sperm binding and fusion with the oocyte.

It is very clear from the phenotype associated with PLCζ knockouts, that PLCζ^{wt} contributes to prevent polyspermy via initiating the standard Ca^{2+} oscillations and ZP block. Although, the sperm-oocyte membrane interactions have been found to generate a typical Ca^{2+} oscillations (Nozawa *et al.*, 2018), the primitive form of this activation still have failed to initiate ZP block and membrane establishment.

4.5 Conclusion

In conclusion, observations presented in this chapter provide strong support for the role of the standard Ca^{2+} oscillations in the processes of ZP blocks and membrane establishment in mammalian eggs. Lacking the expression of PLCζ in sperms found to be significantly increase the incidents of polyspermy following *in vivo* and *in vitro* fertilisation. Examining the shedding process that controls Juno expression on mouse oocyte, found no observable contribution from Juno in preventing polyspermy post fertilisation with sperms lacking the expression of PLCζ. Thus, contradicting number of studies highlighted the proposed role of Juno as an essential factor both in sperm binding and a factor that regulate membrane establishment in mammals.

5 General discussion

5.1 CIRPSR/Cas9 approach and creating the first PLCζ knockouts

One of the many challenges that faced those investigating the physiological relevance of PLCζ in mammals, was the lack of an animal model deficient in PLCζ gene expression. Generation of a PLCζ knockout was essential to unravel the exact molecular mechanisms that governs oocyte to embryo transitions. A novel approach in targeting eukaryotes' genomes by editing first appeared in 2013 through harnessing the bacterial adaptive immune system CRISPR-associated protein 9. This tool has provided a much simpler and more economic method for gene-targeted modifications in any living organism. The simplicity of this tool comes from the its ability to target any genomic sequence by introducing a short-guide RNA along with the prokaryotic Cas9 protein or recombinant RNA into the cells of interest, leading to targeting of the specific sequence with double-strand breaks, and indels formation as a result of the NHEJ activity at the repair site. One of the major advancements this tool offered to the scientific community, was the capacity for applying desired genetic modifications in one-cell stage embryos, that has ultimately led to revolutionisation of speed and versatility in generating genetically modified animals.

Although the editing efficiency and the outcome of CRISPR-aided mutagenesis has been questioned by several reports, following well-defined approaches in limiting the off-target effects, reducing alleles complexity, and increasing the capacity for characterising the transgenic animals to sufficient standards, further studies have practically addressed every concern. Therefore, this study applied CRISPR/Cas9 in two separate approaches, the wildtype Cas9 with a single guide RNA, and the mutant nickase with a pair of guide RNAs, targeting the coding sequence of PLCζ for mutagenesis as a first attempt in creating a mouse model lacking the expression of PLCζ in sperm cells.

Introducing CRISPR/Cas9 constructs into mouse zygotes in this study has successfully altered the wildtype genomic sequence of the PLCζ gene in a number of animals. However, genomic-based analysis found that the outcome of the allele complexity in each clone can drastically be increased in cases where more than one sgRNA was introduced

with the mutant nickase. Decoding the allele complexity in each clone of the founders (F0) was essential in determining the desired allele that eventually needed to be transmitted to a subsequent progeny for the ultimate formation of homozygous males. Indeed, this study revealed that most of the founders have one or two alleles that were altered by the mutation, although the possibility of additional undetected alleles in these animals cannot be dismissed. Such findings would be considered as disadvantageous and tricky to analyse; however, the documented on-target effect of utilising two guide RNAs and the nickase has outweighed any likely disadvantages.

In fact, it was found that sub-cloning of PCR products and trace sequencing to disentangle the alleles' complexity, was very important and required in cases of clones with difficult to deconvolute traces. Findings from this part of the study helped to identify two potential candidates that were fitted to the selection criteria with high likelihoods for transmitting the desirable alleles to the next generation. Crossing between the selected female founders and wildtype males generated a number of heterozygous animals (F1) following each approach, which were used to generate the PLC^{em1Jparr} and PLCζ$^{+/em2Jparr}$ homozygous mouse lines, that each harbour a PLCζ knockout mutation. Genotyping-based studies, PLCζ mRNA expression, and immunoblot protein analysis all confirmed the frameshift mutation and loss of function of sperm-PLCζ protein in both of the mutant mouse lines.

All in all, utilising CRISPR/Cas9 in this study for target site mutagenesis has proven how powerful this novel tool is for making precise, targeted changes to the genome of embryonic cells, that has ultimately led to the generation of stable transgenic mouse lines harbouring the desired mutations in the PLCζ gene. Harnessing CRISPR/Cas9's full capabilities require extensive amount of knowledge, in terms of knowing the limitations of this approach, and the concerns that are needed to be taken into account before application. CRISPR/Cas9 has revolutionized genomics research in every aspect of biological research and will continue to do so for years to come.

5.2 The role of PLCζ in mammalian fertility

Findings demonstrated in this study show that absence of functional PLCζ does not compromise spermatogenesis and sperm quality parameters such as viability, motility, hyperactivity, and ability to undergo the acrosome reaction. This is in contrast to a previous preliminary report which claimed that PLCζ knockout male mice were defective in the spermatogenic process (Ito *et al.*, 2010). However, calcium imaging analysis following fertilisation with cryopreserved PLCζ-null sperm, showed that these lacked the ability to induce Ca^{2+} oscillations in the oocyte. Thus, we provide the first direct evidence that PLCζ is the physiological trigger of Ca^{2+} oscillations in mouse oocytes, and probably in oocytes of all mammals. Remarkably, few oocytes fertilized by PLCζ-null *in vivo* and *in vitro* with fresh sperm can still develop to the blastocyst stage. Additionally, natural mating of PLCζ knockout males with wild type females resulted in low rates of oocyte activation that nevertheless can lead to development to term. Importantly, this is the first demonstration in mammals that natural mating and fertilization without the prime physiological trigger of oocyte activation can result in offspring. These findings are significant because PLCζ-null sperm and the following generated embryos offer a way to test the efficacy and safety of activation stimuli used in clinical IVF and will make it possible for the first time to ascertain the impact of Ca^{2+} oscillations on gene expression in the early embryo and on the health of offspring.

A key role of the sperm-induced Ca^{2+} oscillations is to downregulate, via a signalling pathway involving CamKIIγ and Emi2, MPF, which is responsible for the metaphase II arrest of the oocyte (Sanders and Swann, 2016; Sobinoff *et al.*, 2013). A later decline in MAPK activity correlates with the formation of pronuclei and entry into interphase of the first cell cycle. Importantly, MPF levels can be reduced artificially in various ways, even without a Ca^{2+} stimulus, triggering oocyte activation and development to blastocyst *in vitro* (Miao *et al.*, 2012; Suzuki *et al.*, 2010b; Knott *et al.*, 2006; Phillips *et al.*, 2002).

This mode of oocyte activation, without Ca^{2+} release, may explain the spontaneous activation observed *in vivo* in ovulated, hamster and mouse oocytes left to reside in the oviduct for extended periods of time in the absence of fertilization ((Xu *et al.*, 1997; Whittingham and Siracusa, 1978; Yanagimachi and Chang, 1961). Moreover, oocytes

from the C57BL/6 strain, the strain used in this studies, have been shown to have a particularly high susceptibility to spontaneous activation during *in vitro* maturation (Cheng *et al.*, 2012). Thus, it is possible that a related mechanism might be responsible for the activation we observe. In the situation described here, the self-activation that aging, unfertilized oocytes experience that normally results in fragmentation or embryonic arrest, is rescued by the PLCζ-null fertilizing sperm. It remains to be seen if these findings have relevance for other mammals, including humans, besides mice.

One other possibility is that PLCζ-null sperm are inducing an atypical Ca^{2+} signal in the oocyte. However, we failed to detect any form of Ca^{2+} response following ICSI with PLCζ-null sperm. Lastly, a final formal possibility is that sperm factors other than PLCζ might be involved in oocyte activation in this instance. The postacrosomal sheath WW domain-binding protein (PAWP) has been suggested to play a role in oocyte activation (Aarabi *et al.*, 2014). However, sperm from PAWP-null ($Wbp2nl^{-/-}$) mice have no defect in oocyte activation capacity (Satouh *et al.*, 2015), arguing against a role in this process. Future studies will be required to uncover which of these potential alternative mechanisms is allowing oocyte activation to occur in the absence of the normal physiological trigger. There has been considerable debate about the importance of Ca^{2+} oscillations for optimal oocyte activation and subsequent embryo development. Although it is possible to bypass the Ca^{2+}-dependent route *in vitro* in various ways (Miao *et al.*, 2012; Kuroda *et al.*, 2006; Phillips *et al.*, 2002), altering the number and frequency of Ca^{2+} transients can subtly affect embryonic gene expression and developmental potential (Ozil *et al.*, 2005; Ducibella *et al.*, 2002). This is of important clinical significance given that currently infertility in men whose sperm fail to induce oocyte activation, can be treated by inducing oocyte activation artificially with mechanical, electrical, or chemical stimuli (Vanden Meerschaut *et al.*, 2014; Sfontouris *et al.*, 2015). However, the long-term effects of such treatments on human development remain far from clear, an issue of some concern given that the Ca^{2+}signals induced by these treatments are highly non-physiological (Sfontouris *et al.*, 2015; Vanden Meerschaut *et al.*, 2014). Findings here are important in this respect in two main ways. First, our demonstration that PLCζ-null mouse males can still conceive offspring *in vivo*, albeit at a reduced efficiency, seemingly in the absence of the normal sperm-induced Ca^{2+}oscillations, will allow us to study whether these offspring differ from those resulting from a normal oocyte activation dependent on Ca^{2+} signals. Second, the availability of PLCζ-null sperm now makes it

possible to assess in a mouse model, how artificial egg activation stimuli, used in the clinic, might affect embryonic gene expression and offspring growth, metabolism and behaviour. Importantly, it will provide a way to test the efficacy and safety of recombinant PLCζ protein as an alternative therapeutic agent to treat infertility caused by oocyte activation deficiency.

5.3 The role of PLCζ in ZP blocks and membrane establishment

In mammals, the oocyte to embryo transition requires modifications of the zona pellucida and plasma membrane that prevent polyspermy, as an essential part in the process of oocyte activation and embryonic development. The initial Ca^{2+} release that is associated with hydrolysis of phosphoinositide by the enzymatic actions of the sperm PLCζ governs the CGE post fertilisation, and can be observed within the first few minutes of the first Ca^{2+} transient after fertilization (Abbott and Ducibella, 2001). Further oscillations drive further waves of release of the contents of the CGs into the oocyte surroundings, so that the number of CGs remaining in the egg continues to decrease with time after fertilization (Ducibella *et al.*, 2002). However, the exact mechanism that transduce the Ca^{2+} signal to cause CG exocytosis have not yet been identified. The Ca^{2+}-dependent downstream mediators, such as CaMKII, PKC isoforms, and actin filament-based mechanisms all have been shown to contribute to the process (Cheeseman *et al.*, 2016; Gardner *et al.*, 2007a).

Waves of CG contents that extrude into the perivitelline space results in biochemical modifications on the zona pellucida to block further sperm binding and penetration (Burkart *et al.*, 2012). In contrast, the influence of Ca^{2+} oscillations on membrane establishment is not well-understood. It appears that the membrane block is a graded response to Ca^{2+} signals, more effective in oocytes that show higher numbers of Ca^{2+} oscillations, and that the entire mechanism of membrane establishment is based on sperm-egg membrane contact (Gardner *et al.*, 2007b; Wortzman *et al.*, 2006). Indeed, injecting sperm directly by ICSI, or activating the oocyte parthenogenetically do not form a membrane block to polyspermy in free-zona oocytes, suggesting that sperm-oocyte fusion provides an essential signal to the plasma membrane and/or cortical cytoskeleton that, along with Ca^{2+}, is required for establishment of the membrane block (Miao and Williams, 2012).

Applying PLCζ-null sperm to the study of the ZP block and membrane establishment post fertilisation provides a novel platform for examining the level of contribution of the standard Ca^{2+} oscillations in preventing supernumerary fertilisation. Indeed, the incidents of polyspermy have increased in oocytes fertilised with PLCζ-null sperm by

more than threefold following in *in vivo* and *in vitro* fertilisation. It appears that the lack of the standard Ca^{2+} oscillations as mediators of post fertilisation events produced a defect in the mechanism of CGE affecting ZP block. Nozawa and colleagues (2018) have also reported similar observations regarding the ZP block and polyspermy that are associated with the phenotype of the PLCζ knockout. The limited number of atypical Ca^{2+} transients per oocyte that have been reported following the alternative pathway of oocyte activation, failed to trigger the normal activation pathway that ensures single sperm fertilisation, thus allowing more sperm to reach the perivitelline space and produce polyspermic oocytes.

On the other hand, several reports have highlighted the role of the shedding mechanism of Juno post fertilisation in preventing polyspermy, supposedly through hindering additional gamete interaction and neutralising incoming sperm. However, both PLCζ-null and $PLC\zeta^{wt}$ sperm revealed no significant differences in terms of Juno immunostaining post fertilisation. The phenotype, however, showed a clear indication that in the absence of PLCζ, the ZP layers and Juno ectodomain fail to establish a permanent block to polyspermy and prevent excess sperm binding and fusion with the oocyte.

Although, the sperm-oocyte membrane interactions have been found to generate atypical and delayed Ca^{2+} oscillations (Nozawa *et al.*, 2018), the primitive form of this activation still failed to initiate the ZP block and membrane establishment. In fact, CGE is considered as an early activation event following sperm fusion, thus a delay in initiating this process would compromise the mechanism of prevention of multiple sperm entry and fusion, and sperm PLCζ is essential in this sense firstly to initiate the blocking mechanism, and secondly to trigger the late events in oocyte activation and embryo formation.

5.4 Theories of the alternative pathway in egg activation.

To understand the mechanism by which the unknown factor contributes to egg activation in mammals, two questions have been raised and needed to be answered to a satisfactory level:

1. How can such few Ca^{2+} spikes manage to activate the oocyte in the absence of the standard Ca^{2+} oscillations?

2. Why do Ca^{2+} rises require a longer duration of time (est. one-hour) to appear after PLCζ-null sperm binding and fusion?

Addressing the first question requires going through previous studies that have provided a number of pieces of evidence for an oocyte activation process in similar situations where Ca^{2+} spikes were either artificially decreased to a certain limit, or introduced at lower numbers than that physiologically normal. Indeed, a single Ca^{2+} rise was found to be efficient in inducing oocyte activation in pigs (Speybroeck *et al.*, 2012), mouse (Miao *et al.*, 2012; Gardner *et al.*, 2007b; Lawrence *et al.*, 1998), rat (Ben-Yosef *et al.*, 1995), and human (Yamaguchi *et al.*, 2017). Artificially, oocyte activation can be achieved by inducing a variety of stimuli ranging from calcium ionophore, ethanol, and strontium, leading to Ca^{2+} signals of a non-physiological nature. This has led to a considerable debate about whether the precise pattern of Ca^{2+} signals at fertilization is important. Moreover, it has even been possible to bypass the Ca^{2+} rise at fertilization by bypassing this normal physiological signal and inducing Zn^{2+}-dependent exit from meiosis, resulting in development to term, albeit 50% less efficiently (Suzuki *et al.*, 2010b). However, against the idea that the precise nature of the Ca^{2+} signal at fertilization is not important, studies by Ozil and colleagues have shown that the number and frequency of Ca^{2+} transients affect both embryonic gene expression and development to term (Ozil *et al.*, 2006). Addressing this issue is not only important from the point of view of understanding a fundamental developmental process, but it also has practical implications (Vanden Meerschaut *et al.*, 2014).

One important consequence of having generated PLCζ-null sperm is that for the first time this will allow us to study the effect of different oocyte activation stimuli upon development of the embryo, foetus, and subsequent development following birth. The artificial oocyte activation approaches used in clinical ART have proven successful in allowing men who produce sperm that are deficient in their ability to activate their partner's oocytes, to conceive. However, important questions have been raised about the implications of using such approaches for the health of human individuals produced in this way since the Ca^{2+} signals generated by such stimuli show important differences compared to those induced physiologically by normal human sperm. This is particularly a concern given that studies of mouse parthenogenetic embryos generated by different patterns of artificially induced Ca^{2+} transients, and those generated from fertilized mouse eggs whose endogenous Ca^{2+} oscillations have been inhibited or hyper-stimulated leading to changes in the number and frequency of Ca^{2+} transients, indicate that such embryos have subtle differences in embryonic gene expression. In response to such concerns, recombinant human PLCζ has been proposed as an alternative, more physiological AOA agent (Nomikos *et al.*, 2013). Now for the first time, PLCζ-null sperm make it possible to employ these as a null background to test the efficacy and biosafety of various AOA approaches, including recombinant PLCζ, in a mouse model. Correspondingly, the demonstration that PLCζ-null males can produce offspring despite the inability of PLCζ sperm to trigger the standard Ca^{2+} release in the oocyte, offers a way to study offspring apparently conceived *in vivo* without the normal Ca^{2+} oscillatory signal.

Addressing the possible mechanisms that contribute to the delayed Ca^{2+} rises following the alternative pathway of oocyte activation, requires initially paying attention to the following points:

First, since the atypical Ca^{2+} rise has only been witnessed in situations involving fertilisation with sperm lacking the expression of PLCζ, this might suggest that the alternative pathway of oocyte activation is only active following the absence of the standard Ca^{2+} oscillations, which in this sense would act as a fail-safe mechanism for PLCζ loss. Thus, the standard Ca^{2+} oscillations might be responsible for upregulation or downregulation of certain effectors within the oocyte or the sperm to antagonise the generation of any erratic calcium spikes (the atypical Ca^{2+} spikes) that might disturb the dynamics of the PLCζ-induced Ca^{2+} oscillations. This hypothesis is actually supported by the fact that the pattern of every normal Ca^{2+} oscillatory behaviour in oocytes has been

observed as consistent transients through time, that were not interrupted by either an abrupt increase in the frequency, nor a visible reset in the oscillatory dynamics following fertilisation. See (Sneyd *et al.*, 2006; Swann and Yu, 2008) for more information.

Second, triggering Ca^{2+} release in mammalian oocytes is solely maintained by recruiting the phosphoinositide signalling pathway and IP_3 production intracellularly (Turner *et al.*, 1984; Swann and Whitaker, 1986; Swann *et al.*, 1989; Miyazaki *et al.*, 1990; Fissore *et al.*, 1995; Halet *et al.*, 2002; Saunders *et al.*, 2002; Clapham, 2007). However, due to the obscure identity of the alternative factor, it could also be involving Ca^{2+} release via an IP_3-independent mechanism through cADPR, nitric oxide, or NAADPH stimulation (Galione *et al.*, 1993b; Lee *et al.*, 1996; Hyslop *et al.*, 2001). Therefore, in order to understand the cues that governs the delayed activation, it is essential in the future to disentangle whether the alternative pathway follows the standard mechanism of Ca^{2+} release, or the alternative factor recruits a novel mechanism in mammalian oocyte activation.

Subsequently, three possible scenarios might contribute to the generation of a delayed response based on the mode of action: The first scenario is based on a sperm-borne factor that requires a relatively longer time to be released into the oocyte in a process might include a specific RNA translation, protein synthesis, or a form of post-translational modification inside the oocyte, then ultimately to reach a certain threshold level before acting on initiating the first global Ca^{2+} transient (figure 5-1 B). Whether the mechanism is controlled by a novel sperm factor or by one of the other sperm-borne candidates such as PAWP, Tr-kit, or citrate synthase (Aarabi *et al.*, 2014; Muciaccia *et al.*, 2010; Sette *et al.*, 2002), a theory based on protein synthesis and intracellular modification would chronologically fit in the witnessed time interval between sperm fusion and the first recorded Ca^{2+} transient, and could theoretically explain the observed delay following the absence of the sperm prime factor.

However, findings from whole sperm injections tend to argue against the likelihood of the proposed mechanism. It was found that fertilising the oocytes with the injected PLCζ-null sperm failed to cause any Ca^{2+} rises within the cytosol after hours of injection, suggesting a mechanism that is independent of sperm content for egg activation. Nevertheless, injecting a whole sperm by ICSI together with the plasma membrane proteins and the acrosomal contents might inhibit or perturb the alternative factor activation in oocytes

(Morozumi *et al.*, 2006; Morozumi and Yanagimachi, 2005). Such possible inhibitors would naturally be eliminated when a sperm passes through the biological barriers of the oocyte as following natural fertilisation. Thus, further examination is required to examine if any of the sperm contents could produce adverse effects on triggering the alternative pathway in egg activation when injected into the oocyte.

The second scenario is based on a sperm-oocyte membrane interaction that triggers a downstream cascade of events leading to the initiation of a delayed rise in Ca^{2+}. The proposed mechanism is centred on the fact that all the witnessed events of oocyte activation and embryo formation in this study and in the Nozawa *et al* (2018) study were only observed in situations involving freshly collected PLCζ-null sperm that interacted with the oocyte membrane, as in the IVF procedure and natural mating. Additional validation to the proposal came from our observation of the adverse effects of sperm cryopreservation on triggering the alternative pathway, which might indicate the involvement of gametes' membrane interaction in this mechanism that is somehow partially disrupted by cryopreservation. It is well-documented by electron microscopy and by sperm functional parameters that sperm freezing-thawing yields a remarkable alteration in membrane factors, including phospholipid composition and cholesterol content, as well as membrane hydraulic permeability and osmotic tolerance limits (Sieme *et al.*, 2015). The required physical membrane contact between gametes to trigger the alternative pathway may suggest an involvement of a receptor-ligand interaction that could recruit one of the Ca^{2+} releasing mechanisms in the process. The finding also highlights the potential importance of the oolemmal protein(s) to trigger the activation, and the best candidate for this hypothesised route could be a protein that is functioning as a site for sperm binding with signal transduction properties (figure 5-1 C). Although a model based on sperm-oocyte receptors interaction was a dominant proposition for a very long time, several studies have casted significant doubts over this proposal (Swann *et al.*, 1989; Miyazaki *et al.*, 1990; Crossley *et al.*, 1991; Swann, 1992; Swann and Ozil, 1994; Galione *et al.*, 1994; Machaty *et al.*, 1997; Williams *et al.*, 1998; Mehlmann *et al.*, 1998; Carroll *et al.*, 1999; Shearer *et al.*, 1999; Lawrence *et al.*, 1997; Palermo *et al.*, 2017).

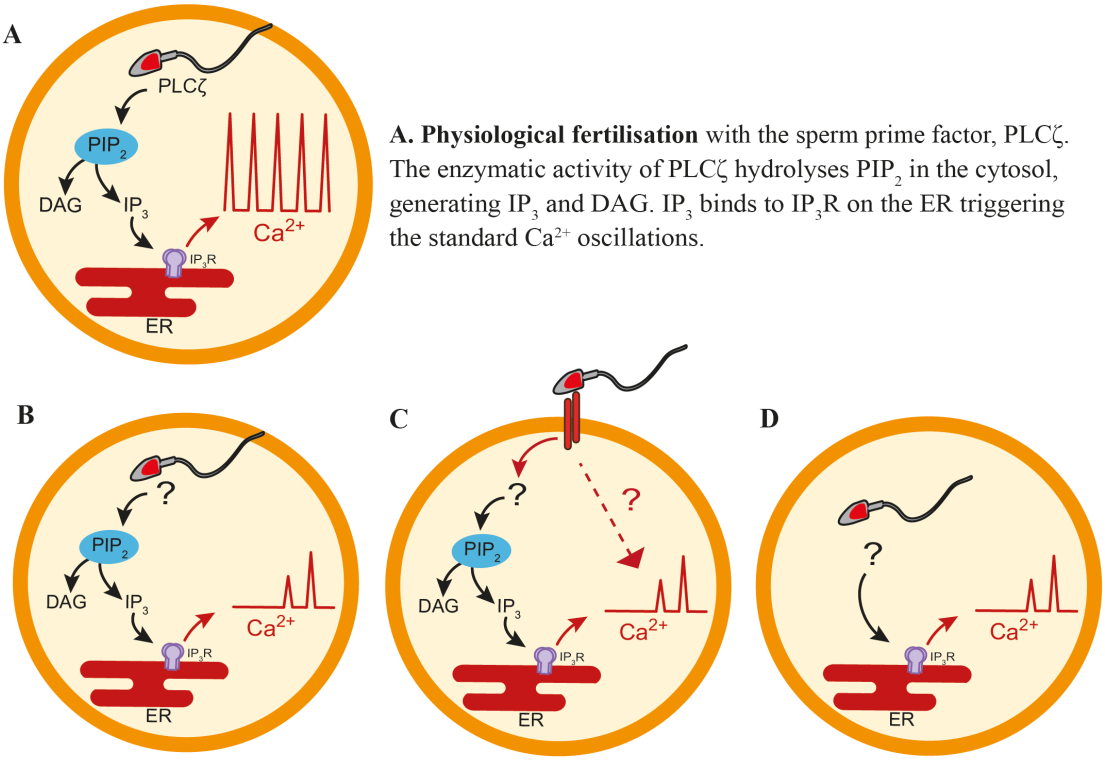
On the other hand, a sperm ligand interaction could mediate Ca^{2+} influx via stimulation of a channel opening on the surface of the oocyte promoting a cytosolic Ca^{2+} increase. Several Ca^{2+} channels have been found and reported to have direct contribution to the Ca^{2+} dynamics and the persistence of the oscillations following fertilisation (Stricker,

1996; Gomez-Fernandez *et al.*, 2009; Lee *et al.*, 2012; Carvacho *et al.*, 2013; Bernhardt *et al.*, 2015; Zhang *et al.*, 2018). However, stimulating the gating mechanism of these channels would always induce a robust Ca^{2+} influx that would contribute to egg activation. Nevertheless, lack of any scientific report describing a delayed channel response, similar to that observed following fertilisation with PLCζ-null sperms, challenges the existence of such a mechanism under the current understanding.

The third scenario is based on one of the oocyte's internal organelles contributing to spontaneous Ca^{2+} release from the ER. This phenomenon has been previously described in many excitable and non-excitable isolated cell types (Jaconi *et al.*, 1988; Williams *et al.*, 1992; Johnston *et al.*, 2005; Wang *et al.*, 2006; Verkhratsky and Shmigol, 1996), and it has also been reported during *in vitro* maturation of mouse oocytes (Carroll *et al.*, 1994; Carroll and Swann, 1992). Although the molecular trigger and the function of these oscillations are still unclear, it is generally believed that these oscillations regulate a large number of processes during oocyte maturation that may be necessary for the acquisition of meiotic competence (Carroll *et al.*, 1994). Remarkably, spontaneous Ca^{2+} rises cease to exist as the oocyte matures to MII, indicates developing a tighter control over Ca^{2+} realising routes and higher sensitivity towards the triggering mechanism for the repetitive cytosolic Ca^{2+} rises at fertilization (Jones *et al.*, 1995; Mehlmann and Kline, 1994). This is essential for better regulation of MII cell cycle and to prevent any premature CGE that might hinder sperm binding and penetration prior to fertilisation. Although the molecular component that ensures prevention of the spontaneous Ca^{2+} rise in mature MII is still unknown, a slight modification of the ER gating mechanism following fertilisation with PLCζ-null sperm could contribute to a delayed Ca^{2+} rise as part of the alternative pathway of oocyte activation (figure 5-1 D). The fact that Sr^{2+} and adenophostin induce Ca^{2+} rises similar to those generated with PLCζ^{wt} sperm, indicate the likelihood of Ca^{2+} release from the ER that is completely independent of IP_3 production (Kline and Kline, 1992; Swann *et al.*, 1989).

Undoubtedly the mechanism of oocyte activation in mammals is mainly dependent on the sperm PLCζ. However, additional factors appear that are yet-to-be identified can be associated with triggering oocyte activation following the absence of the standard Ca^{2+} oscillations. Although, the standard oscillations have been shown to regulate a plethora of cellular mechanism in the oocyte, production of healthy mice pups from sperm lacking PLCζ casted significant doubts on the physiological necessity of this protein.

Notwithstanding, PLCζ expression has a significant impact on blocking polyspermy and ensuring diploid fertilisation. Thus, it would appear then that mammals have acquired the expression of PLCζ in their genome following millions of years of evolution as an important way of preventing supernumerary fertilisation, which mammalian oocytes seem to be extremely weak in dealing with as a phenomenon.



A. Physiological fertilisation with the sperm prime factor, PLCζ. The enzymatic activity of PLCζ hydrolyses PIP_2 in the cytosol, generating IP_3 and DAG. IP_3 binds to IP_3R on the ER triggering the standard Ca^{2+} oscillations.

Figures B. C. & D. represent the proposed mechanism of egg activation following the absence of the sperm- PLCζ:

B. Sperm introduces a factor that requires transcriptional activities by the oocyte to generate IP_3 and the delayed Ca^{2+} rise.
C. Sperm contacts with the oolemmal membrane mediates the delayed Ca^{2+} rise either via a novel factor that catalyses PIP_2 or via sperm binding activating a Ca^{2+} channel opening.
D. Delayed spontaneous Ca^{2+} rise from the ER via a sperm factor that modulates the ER's gating mechanism.

Figure 5-1: Schematic represents the proposed mechanisms of egg activation following fertilisation with PLCζ-null sperm.

5.5 General conclusion

Activation of the egg by the sperm is a key developmental event that in mammals, is triggered by sperm-induced Ca^{2+} oscillations. Phospholipase C ζ has been put forward as a key candidate for the trigger of these oscillations. Despite advances in the general understanding of the signalling pathways that lie downstream of the sperm-induced Ca^{2+} oscillations, exactly how the sperm triggers such Ca^{2+} response to sperm entry into the oocyte has remained controversial. Following this aim, this study successfully created the first PLCζ knockout mouse by utilising CRISPR/Cas9 approaches, making it possible to definitely address a key outstanding issue in mammalian fertilisation. Phenotypic analysis showed PLCζ knockout males are able to produce viable sperm with physiologically normal sperm parameters, contradicting a previous study claimed PLCζ was essential for spermatogenesis. However, fertilization with cryopreserved PLCζ knockout sperm failed to trigger the standard Ca^{2+} oscillations following *in vitro* fertilization and ICSI.

Interestingly, however, eggs fertilized by *in vivo* and *in vitro* with fresh PLCζ knockout sperm, but not by ICSI, still trigger oocyte activation and embryo formation, albeit at greatly reduced efficiency and with a significant time delay. This suggests that some membrane-related unidentified factor may act to compensate for the lack of the sperm prime factor, PLCζ. In line with absence of the standard Ca^{2+} oscillations, polyspermy was increased significantly following *in vivo* and *in vitro* fertilization, signifying the importance of PLCζ protein on triggering the ZP block in mammals. Juno expression analysis post fertilization revealed no significant contribution in membrane establishment contradicting number of studies.

Finally, living offspring can be conceived by PLCζ knockout males, showing for the first time that natural conception can occur in the absence of the standard Ca^{2+} oscillations. It will be of great importance to study these offspring since oocyte activation failure in humans is currently treated by the use of Ca^{2+} ionophores which activates the oocyte in a very non-physiological manner. PLCζ knockout mice make it now possible to study the importance of Ca^{2+} oscillations for development, and the long-term safety of this clinical approach for treating infertility, in a mouse model.

6 Reference list

Aarabi, M., Balakier, H., Bashar, S., Moskovtsev, S. I., Sutovsky, P., Librach, C. L. & Oko, R. (2014). Sperm-derived WW domain-binding protein, PAWP, elicits calcium oscillations and oocyte activation in humans and mice. *FASEB J,* 28**,** 4434-40.

Aarabi, M., Qin, Z., Xu, W., Mewburn, J. & Oko, R. (2010). Sperm-borne protein, PAWP, initiates zygotic development in Xenopus laevis by eliciting intracellular calcium release. *Mol Reprod Dev,* 77**,** 249-56.

Aarabi, M., Yu, Y., Xu, W., Tse, M. Y., Pang, S. C., Yi, Y. J., Sutovsky, P. & Oko, R. (2012). The testicular and epididymal expression profile of PLCzeta in mouse and human does not support its role as a sperm-borne oocyte activating factor. *PLoS One,* 7**,** e33496.

Abbott, A. L. & Ducibella, T. (2001). Calcium and the control of mammalian cortical granule exocytosis. *Front Biosci,* 6**,** D792-806.

Agarwal, A., Ozturk, E. & Loughlin, K. R. (1992). Comparison of semen analysis between the two Hamilton-Thorn semen analysers. *Andrologia,* 24**,** 327-9.

Amdani, S. N., Jones, C. & Coward, K. (2013). Phospholipase C zeta (PLCzeta): oocyte activation and clinical links to male factor infertility. *Adv Biol Regul,* 53**,** 292-308.

Arrotéia, K. F., Garcia, P. V., Barbieri, M. F., Justino, M. L. & Pereira, L. V. (2012). The epididymis: embryology, structure, function and its role in fertilization and infertility. *In:* PEREIRA, L. V. (ed.) *Embryology - Updates and Highlights on Classic Topics.* First edition ed.: InTech.

Arur, S. (2017). Signaling-Mediated Regulation of Meiotic Prophase I and Transition During Oogenesis. *Results Probl Cell Differ,* 59**,** 101-123.

Avella, M. A., Xiong, B. & Dean, J. (2013). The molecular basis of gamete recognition in mice and humans. *Mol Hum Reprod,* 19**,** 279-89.

Bao, J. & Bedford, M. T. (2016). Epigenetic regulation of the histone-to-protamine transition during spermiogenesis. *Reproduction,* 151**,** R55-70.

Bassett, A. & Liu, J. L. (2014a). CRISPR/Cas9 mediated genome engineering in Drosophila. *Methods,* 69**,** 128-36.

Bassett, A. R. & Liu, J. L. (2014b). CRISPR/Cas9 and genome editing in Drosophila. *J Genet Genomics,* 41**,** 7-19.

Bassett, A. R., Tibbit, C., Ponting, C. P. & Liu, J. L. (2014). Highly Efficient Targeted Mutagenesis of Drosophila with the CRISPR/Cas9 System. *Cell Rep,* 6**,** 1178-1179.

Baumer, A., Balmer, D., Binkert, F. & Schinzel, A. (2000). Parental origin and mechanisms of formation of triploidy: a study of 25 cases. *Eur J Hum Genet,* 8**,** 911-7.

Bedford-Guaus, S. J., Mcpartlin, L. A., Xie, J., Westmiller, S. L., Buffone, M. G. & Roberson, M. S. (2011). Molecular cloning and characterization of phospholipase C zeta in equine sperm and testis reveals species-specific differences in expression of catalytically active protein. *Biol Reprod,* 85**,** 78-88.

Ben-Yosef, D., Oron, Y. & Shalgi, R. (1995). Low temperature and fertilization-induced Ca2+ changes in rat eggs. *Mol Reprod Dev,* 42**,** 122-9.

Bernhardt, M. L., Kim, A. M., O'halloran, T. V. & Woodruff, T. K. (2011). Zinc requirement during meiosis I-meiosis II transition in mouse oocytes is independent of the MOS-MAPK pathway. *Biol Reprod,* 84**,** 526-36.

Bernhardt, M. L., Kong, B. Y., Kim, A. M., O'halloran, T. V. & Woodruff, T. K. (2012). A zinc-dependent mechanism regulates meiotic progression in mammalian oocytes. *Biol Reprod,* 86**,** 114.

Bernhardt, M. L., Padilla-Banks, E., Stein, P., Zhang, Y. & Williams, C. J. (2017). Store-operated Ca2+ entry is not required for fertilization-induced Ca2+ signaling in mouse eggs. *Cell Calcium,* 65**,** 63-72.

Bernhardt, M. L., Zhang, Y., Erxleben, C. F., Padilla-Banks, E., Mcdonough, C. E., Miao, Y. L., Armstrong, D. L. & Williams, C. J. (2015). CaV3.2 T-type channels mediate Ca(2)(+) entry during oocyte maturation and following fertilization. *J Cell Sci,* 128**,** 4442-52.

Berridge, M. J. (1981). Phosphatidylinositol hydrolysis and calcium signaling. *Adv Cyclic Nucleotide Res,* 14**,** 289-99.

Berridge, M. J. (1997). Elementary and global aspects of calcium signalling. *J Physiol,* 499 (Pt 2)**,** 291-306.

Berridge, M. J. & Galione, A. (1988). Cytosolic calcium oscillators. *FASEB J,* 2**,** 3074-82.

Berridge, M. J., Lipp, P. & Bootman, M. D. (2000). The versatility and universality of calcium signalling. *Nat Rev Mol Cell Biol,* 1**,** 11-21.

Bi, Y., Xu, W. M., Wong, H. Y., Zhu, H., Zhou, Z. M., Chan, H. C. & Sha, J. H. (2009). NYD-SP27, a novel intrinsic decapacitation factor in sperm. *Asian J Androl,* 11**,** 229-39.

Bianchi, E., Doe, B., Goulding, D. & Wright, G. J. (2014). Juno is the egg Izumo receptor and is essential for mammalian fertilization. *Nature,* 508**,** 483-7.

Bianchi, E. & Wright, G. J. (2015). Cross-species fertilization: the hamster egg receptor, Juno, binds the human sperm ligand, Izumo1. *Philos Trans R Soc Lond B Biol Sci,* 370**,** 20140101.

Borges, E., Jr., De Almeida Ferreira Braga, D. P., De Sousa Bonetti, T. C., Iaconelli, A., Jr. & Franco, J. G., Jr. (2009). Artificial oocyte activation with calcium ionophore A23187 in intracytoplasmic sperm injection cycles using surgically retrieved spermatozoa. *Fertil Steril,* 92**,** 131-6.

Brucker, C., Kassner, G., Loser, C., Hinrichsen, M. & Lipford, G. B. (1994). Progesterone-induced acrosome reaction: potential role for sperm acrosome antigen-1 in fertilization. *Hum Reprod,* 9**,** 1897-902.

Burkart, A. D., Xiong, B., Baibakov, B., Jimenez-Movilla, M. & Dean, J. (2012). Ovastacin, a cortical granule protease, cleaves ZP2 in the zona pellucida to prevent polyspermy. *J Cell Biol,* 197**,** 37-44.

Busa, W. B. & Nuccitelli, R. (1985). An elevated free cytosolic Ca2+ wave follows fertilization in eggs of the frog, Xenopus laevis. *J Cell Biol,* 100**,** 1325-9.

Caldecott, K. W. (2008). Single-strand break repair and genetic disease. *Nat Rev Genet,* 9**,** 619-31.

Capecchi, M. R. (2005). Gene targeting in mice: functional analysis of the mammalian genome for the twenty-first century. *Nat Rev Genet,* 6**,** 507-12.

Carroll, D. (2011). Genome engineering with zinc-finger nucleases. *Genetics,* 188**,** 773-82.

Carroll, D. J., Albay, D. T., Terasaki, M., Jaffe, L. A. & Foltz, K. R. (1999). Identification of PLCgamma-dependent and -independent events during fertilization of sea urchin eggs. *Dev Biol,* 206**,** 232-47.

Carroll, J. & Swann, K. (1992). Spontaneous cytosolic calcium oscillations driven by inositol trisphosphate occur during in vitro maturation of mouse oocytes. *J Biol Chem,* 267**,** 11196-201.

Carroll, J., Swann, K., Whittingham, D. & Whitaker, M. (1994). Spatiotemporal dynamics of intracellular [Ca2+]i oscillations during the growth and meiotic maturation of mouse oocytes. *Development,* 120**,** 3507-17.

Carroll, M., Levasseur, M., Wood, C., Whitaker, M., Jones, K. T. & Mcdougall, A. (2003). Exploring the mechanism of action of the sperm-triggered calcium-wave pacemaker in ascidian zygotes. *J Cell Sci,* 116**,** 4997-5004.

Carvacho, I., Lee, H. C., Fissore, R. A. & Clapham, D. E. (2013). TRPV3 channels mediate strontium-induced mouse-egg activation. *Cell Rep,* 5**,** 1375-86.

Casser, E., Israel, S., Witten, A., Schulte, K., Schlatt, S., Nordhoff, V. & Boiani, M. (2017). Totipotency segregates between the sister blastomeres of two-cell stage mouse embryos. *Sci Rep,* 7**,** 8299.

Castagna, M., Takai, Y., Kaibuchi, K., Sano, K., Kikkawa, U. & Nishizuka, Y. (1982). Direct activation of calcium-activated, phospholipid-dependent protein kinase by tumor-promoting phorbol esters. *J Biol Chem,* 257**,** 7847-51.

Celik, O., Celik, N., Gungor, S., Haberal, E. T. & Aydin, S. (2015). Selective Regulation of Oocyte Meiotic Events Enhances Progress in Fertility Preservation Methods. *Biochem Insights,* 8**,** 11-21.

Cheeseman, L. P., Boulanger, J., Bond, L. M. & Schuh, M. (2016). Two pathways regulate cortical granule translocation to prevent polyspermy in mouse oocytes. *Nat Commun,* 7**,** 13726.

Chen, H. I. & Sudol, M. (1995). The WW domain of Yes-associated protein binds a proline-rich ligand that differs from the consensus established for Src homology 3-binding modules. *Proc Natl Acad Sci U S A,* 92**,** 7819-23.

Cheng, Y., Zhong, Z. & Latham, K. E. (2012). Strain-specific spontaneous activation during mouse oocyte maturation. *Fertil Steril,* 98**,** 200-6.

Cho, S. W., Kim, S., Kim, Y., Kweon, J., Kim, H. S., Bae, S. & Kim, J. S. (2014). Analysis of off-target effects of CRISPR/Cas-derived RNA-guided endonucleases and nickases. *Genome Res,* 24**,** 132-41.

Chu, V. T., Weber, T., Wefers, B., Wurst, W., Sander, S., Rajewsky, K. & Kuhn, R. (2015). Increasing the efficiency of homology-directed repair for CRISPR-Cas9-induced precise gene editing in mammalian cells. *Nat Biotechnol,* 33**,** 543-8.

Ciapa, B. & Arnoult, C. (2011). Could modifications of signalling pathways activated after ICSI induce a potential risk of epigenetic defects? *Int J Dev Biol,* 55**,** 143-52.

Clapham, D. E. (2007). Calcium signaling. *Cell,* 131**,** 1047-58.

Clift, D. & Schuh, M. (2013). Restarting life: fertilization and the transition from meiosis to mitosis. *Nat Rev Mol Cell Biol,* 14**,** 549-62.

Cong, L., Ran, F. A., Cox, D., Lin, S., Barretto, R., Habib, N., Hsu, P. D., Wu, X., Jiang, W., Marraffini, L. A. & Zhang, F. (2013). Multiplex genome engineering using CRISPR/Cas systems. *Science,* 339**,** 819-23.

Cooney, M. A., Malcuit, C., Cheon, B., Holland, M. K., Fissore, R. A. & D'cruz, N. T. (2010). Species-specific differences in the activity and nuclear localization of murine and bovine phospholipase C zeta 1. *Biol Reprod,* 83**,** 92-101.

Coward, K., Campos-Mendoza, A., Larman, M., Hibbitt, O., Mcandrew, B., Bromage, N. & Parrington, J. (2003). Teleost fish spermatozoa contain a cytosolic protein factor that induces calcium release

in sea urchin egg homogenates and triggers calcium oscillations when injected into mouse oocytes. *Biochem Biophys Res Commun,* 305**,** 299-304.

Coward, K., Ponting, C. P., Chang, H. Y., Hibbitt, O., Savolainen, P., Jones, K. T. & Parrington, J. (2005). Phospholipase Czeta, the trigger of egg activation in mammals, is present in a non-mammalian species. *Reproduction,* 130**,** 157-63.

Coward, K., Ponting, C. P., Zhang, N., Young, C., Huang, C. J., Chou, C. M., Kashir, J., Fissore, R. A. & Parrington, J. (2011). Identification and functional analysis of an ovarian form of the egg activation factor phospholipase C zeta (PLCzeta) in pufferfish. *Mol Reprod Dev,* 78**,** 48-56.

Cox, L. J., Larman, M. G., Saunders, C. M., Hashimoto, K., Swann, K. & Lai, F. A. (2002). Sperm phospholipase Czeta from humans and cynomolgus monkeys triggers Ca2+ oscillations, activation and development of mouse oocytes. *Reproduction,* 124**,** 611-23.

Crossley, I., Whalley, T. & Whitaker, M. (1991). Guanosine 5'-thiotriphosphate may stimulate phosphoinositide messenger production in sea urchin eggs by a different route than the fertilizing sperm. *Cell Regul,* 2**,** 121-33.

Cuthbertson, K. S. & Cobbold, P. H. (1985). Phorbol ester and sperm activate mouse oocytes by inducing sustained oscillations in cell Ca2+. *Nature,* 316**,** 541-2.

Dacheux, J. L., Castella, S., Gatti, J. L. & Dacheux, F. (2005). Epididymal cell secretory activities and the role of proteins in boar sperm maturation. *Theriogenology,* 63**,** 319-41.

Dale, B. & Defelice, L. (2011). Polyspermy prevention: facts and artifacts? *J Assist Reprod Genet,* 28**,** 199-207.

Dale, B., Defelice, L. J. & Ehrenstein, G. (1985). Injection of a soluble sperm fraction into sea-urchin eggs triggers the cortical reaction. *Experientia,* 41**,** 1068-70.

Dam, A. H., Feenstra, I., Westphal, J. R., Ramos, L., Van Golde, R. J. & Kremer, J. A. (2007). Globozoospermia revisited. *Hum Reprod Update,* 13**,** 63-75.

Day, M. L., Mcguinness, O. M., Berridge, M. J. & Johnson, M. H. (2000). Regulation of fertilization-induced Ca(2+)spiking in the mouse zygote. *Cell Calcium,* 28**,** 47-54.

Dedkova, E. N., Sigova, A. A. & Zinchenko, V. P. (2000). Mechanism of action of calcium ionophores on intact cells: ionophore-resistant cells. *Membr Cell Biol,* 13**,** 357-68.

Deguchi, R. & Osanai, K. (1994). Repetitive intracellular Ca2+ increases at fertilization and the role of Ca2+ in meiosis reinitiation from the first metaphase in oocytes of marine bivalves. *Dev Biol,* 163**,** 162-74.

Deguchi, R., Shirakawa, H., Oda, S., Mohri, T. & Miyazaki, S. (2000). Spatiotemporal Analysis of Ca2+ Waves in Relation to the Sperm Entry Site and Animal–Vegetal Axis during Ca2+ Oscillations in Fertilized Mouse Eggs. *Developmental Biology,* 218**,** 299-313.

Deng, M., Kishikawa, H., Yanagimachi, R., Kopf, G. S., Schultz, R. M. & Williams, C. J. (2003). Chromatin-mediated cortical granule redistribution is responsible for the formation of the cortical granule-free domain in mouse eggs. *Dev Biol,* 257**,** 166-76.

Doudna, J. A. & Charpentier, E. (2014). Genome editing. The new frontier of genome engineering with CRISPR-Cas9. *Science,* 346**,** 1258096.

Dow, L. E. (2015). Modeling Disease In Vivo With CRISPR/Cas9. *Trends Mol Med,* 21**,** 609-21.

Ducibella, T. (1996). The cortical reaction and development of activation competence in mammalian oocytes. *Hum Reprod Update,* 2**,** 29-42.

Ducibella, T. & Buetow, J. (1994). Competence to undergo normal, fertilization-induced cortical activation develops after metaphase I of meiosis in mouse oocytes. *Dev Biol,* 165**,** 95-104.

Ducibella, T. & Fissore, R. (2008). The roles of Ca2+, downstream protein kinases, and oscillatory signaling in regulating fertilization and the activation of development. *Dev Biol,* 315**,** 257-79.

Ducibella, T., Huneau, D., Angelichio, E., Xu, Z., Schultz, R. M., Kopf, G. S., Fissore, R., Madoux, S. & Ozil, J. P. (2002). Egg-to-embryo transition is driven by differential responses to Ca(2+) oscillation number. *Dev Biol,* 250**,** 280-91.

Ducibella, T., Schultz, R. M. & Ozil, J. P. (2006). Role of calcium signals in early development. *Semin Cell Dev Biol,* 17**,** 324-32.

Duesbery, N. S. & Vande Woude, G. F. (1998). Cytoplasmic control of nuclear behavior during meiotic maturation of frog oocytes. *Biol Cell,* 90**,** 461-6.

Dumollard, R., Marangos, P., Fitzharris, G., Swann, K., Duchen, M. & Carroll, J. (2004). Sperm-triggered [Ca2+] oscillations and Ca2+ homeostasis in the mouse egg have an absolute requirement for mitochondrial ATP production. *Development,* 131**,** 3057-67.

Duncan, F. E., Que, E. L., Zhang, N., Feinberg, E. C., O'halloran, T. V. & Woodruff, T. K. (2016). The zinc spark is an inorganic signature of human egg activation. *Sci Rep,* 6**,** 24737.

Dupont, G., Mcguinness, O. M., Johnson, M. H., Berridge, M. J. & Borgese, F. (1996). Phospholipase C in mouse oocytes: characterization of beta and gamma isoforms and their possible involvement in sperm-induced Ca2+ spiking. *Biochem J,* 316 (Pt 2)**,** 583-91.

Ebner, T., Montag, M., Oocyte Activation Study, G., Montag, M., Van Der Ven, K., Van Der Ven, H., Ebner, T., Shebl, O., Oppelt, P., Hirchenhain, J., Krussel, J., Maxrath, B., Gnoth, C., Friol, K., Tigges, J., Wunsch, E., Luckhaus, J., Beerkotte, A., Weiss, D., Grunwald, K., Struller, D. & Etien, C. (2015). Live birth after artificial oocyte activation using a ready-to-use ionophore: a prospective multicentre study. *Reprod Biomed Online,* 30**,** 359-65.

Eisen, A. & Reynolds, G. T. (1984). Calcium transients during early development in single starfish (Asterias forbesi) oocytes. *J Cell Biol,* 99**,** 1878-82.

Escoffier, J., Lee, H. C., Yassine, S., Zouari, R., Martinez, G., Karaouzene, T., Coutton, C., Kherraf, Z. E., Halouani, L., Triki, C., Nef, S., Thierry-Mieg, N., Savinov, S. N., Fissore, R., Ray, P. F. & Arnoult, C. (2016). Homozygous mutation of PLCZ1 leads to defective human oocyte activation and infertility that is not rescued by the WW-binding protein PAWP. *Hum Mol Genet,* 25**,** 878-91.

Escoffier, J., Yassine, S., Lee, H. C., Martinez, G., Delaroche, J., Coutton, C., Karaouzene, T., Zouari, R., Metzler-Guillemain, C., Pernet-Gallay, K., Hennebicq, S., Ray, P. F., Fissore, R. & Arnoult, C. (2015). Subcellular localization of phospholipase Czeta in human sperm and its absence in DPY19L2-deficient sperm are consistent with its role in oocyte activation. *Mol Hum Reprod,* 21**,** 157-68.

Esfandiari, N., Javed, M. H., Gotlieb, L. & Casper, R. F. (2005). Complete failed fertilization after intracytoplasmic sperm injection--analysis of 10 years' data. *Int J Fertil Womens Med,* 50**,** 187-92.

Eshre. 2012. *World's number of IVF and ICSI babies has now reached a calculated total of 5 million.* [Online]. ScienceDaily. Available: ScienceDaily. www.sciencedaily.com/releases/2012/07/120702134746.htm [Accessed January, 8 2018].

Evans, J. P. & Kopf, G. S. (1998). Molecular mechanisms of sperm-egg interactions and egg activation. *Andrologia,* 30**,** 297-307.

Farrell, P. B., Presicce, G. A., Brockett, C. C. & Foote, R. H. (1998). Quantification of bull sperm characteristics measured by computer-assisted sperm analysis (CASA) and the relationship to fertility. *Theriogenology,* 49**,** 871-9.

Ferrer-Vaquer, A., Barragan, M., Freour, T., Vernaeve, V. & Vassena, R. (2016). PLCzeta sequence, protein levels, and distribution in human sperm do not correlate with semen characteristics and fertilization rates after ICSI. *J Assist Reprod Genet,* 33**,** 747-56.

Fissore, R. A., Pinto-Correia, C. & Robl, J. M. (1995). Inositol trisphosphate-induced calcium release in the generation of calcium oscillations in bovine eggs. *Biol Reprod,* 53**,** 766-74.

Florman, H. M. & Fissore, R. (2014). Fertilization in Mammals. *In:* PLANT, T. & ZELEZNIK, A. (eds.) *Knobil and Neill's Physiology of Reproduction.* 4 ed. San Diego, United States: Academic Press.

Freour, T., Barragan, M., Torra-Massana, M., Ferrer-Vaquer, A. & Vassena, R. (2017). Is there an association between PAWP/WBP2NL sequence, expression, and distribution in sperm cells and fertilization failures in ICSI cycles? *Mol Reprod Dev*.

Fujimoto, S., Yoshida, N., Fukui, T., Amanai, M., Isobe, T., Itagaki, C., Izumi, T. & Perry, A. C. (2004). Mammalian phospholipase Czeta induces oocyte activation from the sperm perinuclear matrix. *Dev Biol,* 274**,** 370-83.

Fukuda, Y. & Chang, M. C. (1978). Relationship between sperm concentration and polyspermy in intact and zona-free mouse eggs inseminated in vitro. *Arch Androl,* 1**,** 267-73.

Galione, A., Mcdougall, A., Busa, W. B., Willmott, N., Gillot, I. & Whitaker, M. (1993a). Redundant mechanisms of calcium-induced calcium release underlying calcium waves during fertilization of sea urchin eggs. *Science,* 261**,** 348-52.

Galione, A., Swann, K., Georgiou, P. & Whitaker, M. (1994). Regenerative and non-regenerative calcium transients in hamster eggs triggered by inositol 1,4,5-trisphosphate. *J Physiol,* 480 (Pt 3)**,** 465-74.

Galione, A., White, A., Willmott, N., Turner, M., Potter, B. V. & Watson, S. P. (1993b). cGMP mobilizes intracellular Ca2+ in sea urchin eggs by stimulating cyclic ADP-ribose synthesis. *Nature,* 365**,** 456-9.

Gardner, A. J. & Evans, J. P. (2006). Mammalian membrane block to polyspermy: new insights into how mammalian eggs prevent fertilisation by multiple sperm. *Reprod Fertil Dev,* 18**,** 53-61.

Gardner, A. J., Knott, J. G., Jones, K. T. & Evans, J. P. (2007a). CaMKII can participate in but is not sufficient for the establishment of the membrane block to polyspermy in mouse eggs. *J Cell Physiol,* 212**,** 275-80.

Gardner, A. J., Williams, C. J. & Evans, J. P. (2007b). Establishment of the mammalian membrane block to polyspermy: evidence for calcium-dependent and -independent regulation. *Reproduction,* 133**,** 383-93.

Garrido, N., Martinez-Conejero, J. A., Jauregui, J., Horcajadas, J. A., Simon, C., Remohi, J. & Meseguer, M. (2009). Microarray analysis in sperm from fertile and infertile men without basic sperm analysis abnormalities reveals a significantly different transcriptome. *Fertil Steril,* 91**,** 1307-10.

Gerlai, R. (2016). Gene Targeting Using Homologous Recombination in Embryonic Stem Cells: The Future for Behavior Genetics? *Front Genet,* 7**,** 43.

Geyer, C. B., Inselman, A. L., Sunman, J. A., Bornstein, S., Handel, M. A. & Eddy, E. M. (2009). A missense mutation in the Capza3 gene and disruption of F-actin organization in spermatids of repro32 infertile male mice. *Dev Biol,* 330**,** 142-52.

Gomez-Fernandez, C., Pozo-Guisado, E., Ganan-Parra, M., Perianes, M. J., Alvarez, I. S. & Martin-Romero, F. J. (2009). Relocalization of STIM1 in mouse oocytes at fertilization: early involvement of store-operated calcium entry. *Reproduction,* 138**,** 211-21.

Gonzalez-Garcia, J. R., Bradley, J., Nomikos, M., Paul, L., Machaty, Z., Lai, F. A. & Swann, K. (2014). The dynamics of MAPK inactivation at fertilization in mouse eggs. *J Cell Sci,* 127**,** 2749-60.

Grasa, P., Coward, K., Young, C. & Parrington, J. (2008). The pattern of localization of the putative oocyte activation factor, phospholipase Czeta, in uncapacitated, capacitated, and ionophore-treated human spermatozoa. *Hum Reprod,* 23**,** 2513-22.

Griswold, M. D. (2016). Spermatogenesis: The Commitment to Meiosis. *Physiol Rev,* 96**,** 1-17.

Gupta, S. K. (2015). Role of zona pellucida glycoproteins during fertilization in humans. *J Reprod Immunol,* 108**,** 90-7.

Gupta, S. K., Bhandari, B., Shrestha, A., Biswal, B. K., Palaniappan, C., Malhotra, S. S. & Gupta, N. (2012). Mammalian zona pellucida glycoproteins: structure and function during fertilization. *Cell Tissue Res,* 349**,** 665-78.

Hachem, A., Godwin, J., Ruas, M., Lee, H. C., Buitrago, M. F., Ardestani, G., Bassett, A., Fox, S., Navarrete, F., De Sutter, P., Heindryckx, B., Fissore, R. & Parrington, J. (2017). PLCzeta is the physiological trigger of the Ca2+ oscillations that induce embryogenesis in mammals but offspring can be conceived in its absence. *Development*.

Halet, G., Tunwell, R., Balla, T., Swann, K. & Carroll, J. (2002). The dynamics of plasma membrane PtdIns(4,5)P(2) at fertilization of mouse eggs. *J Cell Sci,* 115**,** 2139-49.

Halet, G., Tunwell, R., Parkinson, S. J. & Carroll, J. (2004). Conventional PKCs regulate the temporal pattern of Ca2+ oscillations at fertilization in mouse eggs. *J Cell Biol,* 164**,** 1033-44.

Harada, Y., Kawazoe, M., Eto, Y., Ueno, S. & Iwao, Y. (2011). The Ca2+ increase by the sperm factor in physiologically polyspermic newt fertilization: its signaling mechanism in egg cytoplasm and the species-specificity. *Dev Biol,* 351**,** 266-76.

Harada, Y., Matsumoto, T., Hirahara, S., Nakashima, A., Ueno, S., Oda, S., Miyazaki, S. & Iwao, Y. (2007). Characterization of a sperm factor for egg activation at fertilization of the newt Cynops pyrrhogaster. *Dev Biol,* 306**,** 797-808.

Harper, C. V., Barratt, C. L., Publicover, S. J. & Kirkman-Brown, J. C. (2006). Kinetics of the progesterone-induced acrosome reaction and its relation to intracellular calcium responses in individual human spermatozoa. *Biol Reprod,* 75**,** 933-9.

Heindryckx, B., De Gheselle, S., Gerris, J., Dhont, M. & De Sutter, P. (2008). Efficiency of assisted oocyte activation as a solution for failed intracytoplasmic sperm injection. *Reprod Biomed Online,* 17**,** 662-8.

Heindryckx, B., Van Der Elst, J., De Sutter, P. & Dhont, M. (2005). Treatment option for sperm- or oocyte-related fertilization failure: assisted oocyte activation following diagnostic heterologous ICSI. *Hum Reprod,* 20**,** 2237-41.

Heytens, E., Parrington, J., Coward, K., Young, C., Lambrecht, S., Yoon, S. Y., Fissore, R. A., Hamer, R., Deane, C. M., Ruas, M., Grasa, P., Soleimani, R., Cuvelier, C. A., Gerris, J., Dhont, M., Deforce, D., Leybaert, L. & De Sutter, P. (2009). Reduced amounts and abnormal forms of phospholipase C zeta (PLCzeta) in spermatozoa from infertile men. *Hum Reprod,* 24**,** 2417-28.

Heytens, E., Schmitt-John, T., Moser, J. M., Jensen, N. M., Soleimani, R., Young, C., Coward, K., Parrington, J. & De Sutter, P. (2010). Reduced fertilization after ICSI and abnormal phospholipase C zeta presence in spermatozoa from the wobbler mouse. *Reprod Biomed Online,* 21**,** 742-9.

Homa, S. T. & Swann, K. (1994). A cytosolic sperm factor triggers calcium oscillations and membrane hyperpolarizations in human oocytes. *Hum Reprod,* 9**,** 2356-61.

Horvath, P. & Barrangou, R. (2010). CRISPR/Cas, the immune system of bacteria and archaea. *Science,* 327**,** 167-70.

Horvath, P. M., Kellom, T., Caulfield, J. & Boldt, J. (1993). Mechanistic studies of the plasma membrane block to polyspermy in mouse eggs. *Mol Reprod Dev,* 34**,** 65-72.

Hossain, M. S., Johannisson, A., Wallgren, M., Nagy, S., Siqueira, A. P. & Rodriguez-Martinez, H. (2011). Flow cytometry for the assessment of animal sperm integrity and functionality: state of the art. *Asian J Androl,* 13**,** 406-19.

Hsu, P. D., Lander, E. S. & Zhang, F. (2014). Development and applications of CRISPR-Cas9 for genome engineering. *Cell,* 157**,** 1262-78.

Hsu, P. D., Scott, D. A., Weinstein, J. A., Ran, F. A., Konermann, S., Agarwala, V., Li, Y., Fine, E. J., Wu, X., Shalem, O., Cradick, T. J., Marraffini, L. A., Bao, G. & Zhang, F. (2013). DNA targeting specificity of RNA-guided Cas9 nucleases. *Nat Biotechnol,* 31**,** 827-32.

Hunter, R. H. (1991). Oviduct function in pigs, with particular reference to the pathological condition of polyspermy. *Mol Reprod Dev,* 29**,** 385-91.

Huszar, G., Sbracia, M., Vigue, L., Miller, D. J. & Shur, B. D. (1997). Sperm plasma membrane remodeling during spermiogenetic maturation in men: relationship among plasma membrane beta 1,4-galactosyltransferase, cytoplasmic creatine phosphokinase, and creatine phosphokinase isoform ratios. *Biol Reprod,* 56**,** 1020-4.

Hyslop, L. A., Carroll, M., Nixon, V. L., Mcdougall, A. & Jones, K. T. (2001). Simultaneous measurement of intracellular nitric oxide and free calcium levels in chordate eggs demonstrates that nitric oxide has no role at fertilization. *Dev Biol,* 234**,** 216-30.

Hyslop, L. A., Nixon, V. L., Levasseur, M., Chapman, F., Chiba, K., Mcdougall, A., Venables, J. P., Elliott, D. J. & Jones, K. T. (2004). Ca2+-promoted cyclin B1 degradation in mouse oocytes requires the establishment of a metaphase arrest. *Developmental Biology,* 269**,** 206-219.

Inoue, N. (2017). Novel insights into the molecular mechanism of sperm-egg fusion via IZUMO1. *J Plant Res,* 130**,** 475-478.

Inoue, N., Ikawa, M., Isotani, A. & Okabe, M. (2005). The immunoglobulin superfamily protein Izumo is required for sperm to fuse with eggs. *Nature,* 434**,** 234-8.

Ito, J., Parrington, J. & Fissore, R. A. (2011). PLCzeta and its role as a trigger of development in vertebrates. *Mol Reprod Dev,* 78**,** 846-53.

Ito, M., Nagaoka, K., Kuroda, K., Kawano, N., Yoshida, K., Harada, Y., Shikano, T., Miyado, M., Oda, S. & Toshimori, K. 2010. Arrest of spermatogenesis at round spermatids in PLCZ1-deficient mice (abstract). 11th International Symposium on Spermatology.

Ito, M., Shikano, T., Oda, S., Horiguchi, T., Tanimoto, S., Awaji, T., Mitani, H. & Miyazaki, S. (2008). Difference in Ca2+ oscillation-inducing activity and nuclear translocation ability of PLCZ1, an egg-activating sperm factor candidate, between mouse, rat, human, and medaka fish. *Biol Reprod,* 78**,** 1081-90.

Iwao, Y. (2012). Egg activation in physiological polyspermy. *Reproduction,* 144**,** 11-22.

Jaconi, M. E., Rivest, R. W., Schlegel, W., Wollheim, C. B., Pittet, D. & Lew, P. D. (1988). Spontaneous and chemoattractant-induced oscillations of cytosolic free calcium in single adherent human neutrophils. *J Biol Chem,* 263**,** 10557-60.

Jaffe, L. F. (1983). Sources of calcium in egg activation: a review and hypothesis. *Dev Biol,* 99**,** 265-76.

Javadian-Elyaderani, S., Ghaedi, K., Tavalaee, M., Rabiee, F., Deemeh, M. R. & Nasr-Esfahani, M. H. (2016). Diagnosis of genetic defects through parallel assessment of PLCzeta and CAPZA3 in infertile men with history of failed oocyte activation. *Iran J Basic Med Sci,* 19**,** 281-9.

Jellerette, T., He, C. L., Wu, H., Parys, J. B. & Fissore, R. A. (2000). Down-regulation of the inositol 1,4,5-trisphosphate receptor in mouse eggs following fertilization or parthenogenetic activation. *Dev Biol,* 223**,** 238-50.

Jiang, F. & Doudna, J. A. (2017). CRISPR-Cas9 Structures and Mechanisms. *Annu Rev Biophys,* 46**,** 505-529.

Jinek, M., East, A., Cheng, A., Lin, S., Ma, E. & Doudna, J. (2013). RNA-programmed genome editing in human cells. *Elife,* 2**,** e00471.

Johnston, L., Sergeant, G. P., Hollywood, M. A., Thornbury, K. D. & Mchale, N. G. (2005). Calcium oscillations in interstitial cells of the rabbit urethra. *J Physiol,* 565**,** 449-61.

Jones, K. T. (1998a). Ca2+ oscillations in the activation of the egg and development of the embryo in mammals. *Int J Dev Biol,* 42**,** 1-10.

Jones, K. T. (1998b). Protein kinase C action at fertilization: overstated or undervalued? *Rev Reprod,* 3**,** 7-12.

Jones, K. T. (2004). Turning it on and off: M-phase promoting factor during meiotic maturation and fertilization. *Mol Hum Reprod,* 10**,** 1-5.

Jones, K. T. (2005). Mammalian egg activation: from Ca2+ spiking to cell cycle progression. *Reproduction,* 130**,** 813-23.

Jones, K. T. (2007). Intracellular calcium in the fertilization and development of mammalian eggs. *Clin Exp Pharmacol Physiol,* 34**,** 1084-9.

Jones, K. T., Carroll, J. & Whittingham, D. G. (1995). Ionomycin, thapsigargin, ryanodine, and sperm induced Ca2+ release increase during meiotic maturation of mouse oocytes. *J Biol Chem,* 270**,** 6671-7.

Jones, K. T., Cruttwell, C., Parrington, J. & Swann, K. (1998). A mammalian sperm cytosolic phospholipase C activity generates inositol trisphosphate and causes Ca2+ release in sea urchin egg homogenates. *FEBS Lett,* 437**,** 297-300.

Jones, K. T., Matsuda, M., Parrington, J., Katan, M. & Swann, K. (2000). Different Ca2+-releasing abilities of sperm extracts compared with tissue extracts and phospholipase C isoforms in sea urchin egg homogenate and mouse eggs. *Biochem J,* 346 Pt 3**,** 743-9.

Jones, K. T. & Nixon, V. L. (2000). Sperm-induced Ca(2+) oscillations in mouse oocytes and eggs can be mimicked by photolysis of caged inositol 1,4,5-trisphosphate: evidence to support a continuous low level production of inositol 1, 4,5-trisphosphate during mammalian fertilization. *Dev Biol,* 225**,** 1-12.

Jones, K. T. & Whittingham, D. G. (1996). A comparison of sperm- and IP3-induced Ca2+ release in activated and aging mouse oocytes. *Dev Biol,* 178**,** 229-37.

Jones, R. (1998c). Plasma membrane structure and remodelling during sperm maturation in the epididymis. *J Reprod Fertil Suppl,* 53**,** 73-84.

Kadamur, G. & Ross, E. M. (2013). Mammalian phospholipase C. *Annu Rev Physiol,* 75**,** 127-54.

Kaji, K., Oda, S., Shikano, T., Ohnuki, T., Uematsu, Y., Sakagami, J., Tada, N., Miyazaki, S. & Kudo, A. (2000). The gamete fusion process is defective in eggs of Cd9-deficient mice. *Nat Genet,* 24**,** 279-82.

Kamel, R. M. (2013). Assisted reproductive technology after the birth of louise brown. *J Reprod Infertil,* 14**,** 96-109.

Kashir, J., Heindryckx, B., Jones, C., De Sutter, P., Parrington, J. & Coward, K. (2010). Oocyte activation, phospholipase C zeta and human infertility. *Hum Reprod Update,* 16**,** 690-703.

Kashir, J., Jones, C., Mounce, G., Ramadan, W. M., Lemmon, B., Heindryckx, B., De Sutter, P., Parrington, J., Turner, K., Child, T., Mcveigh, E. & Coward, K. (2013). Variance in total levels of phospholipase C zeta (PLC-zeta) in human sperm may limit the applicability of quantitative immunofluorescent analysis as a diagnostic indicator of oocyte activation capability. *Fertil Steril,* 99**,** 107-17.

Kashir, J., Konstantinidis, M., Jones, C., Lemmon, B., Lee, H. C., Hamer, R., Heindryckx, B., Deane, C. M., De Sutter, P., Fissore, R. A., Parrington, J., Wells, D. & Coward, K. (2012). A maternally inherited autosomal point mutation in human phospholipase C zeta (PLCzeta) leads to male infertility. *Hum Reprod,* 27**,** 222-31.

Kashir, J., Nomikos, M. & Lai, F. A. (2017). Phospholipase C zeta and calcium oscillations at fertilisation: The evidence, applications, and further questions. *Advances in Biological Regulation.*

Kashir, J., Nomikos, M., Lai, F. A. & Swann, K. (2014). Sperm-induced Ca2+ release during egg activation in mammals. *Biochem Biophys Res Commun,* 450**,** 1204-11.

Kashir, J., Nomikos, M., Swann, K. & Lai, F. A. (2015). PLCzeta or PAWP: revisiting the putative mammalian sperm factor that triggers egg activation and embryogenesis. *Mol Hum Reprod,* 21**,** 383-8.

Kasimanickam, R., Nebel, R. L., Peeler, I. D., Silvia, W. L., Wolf, K. T., Mcallister, A. J. & Cassell, B. G. (2006). Breed differences in competitive indices of Holstein and Jersey bulls and their association with sperm DNA fragmentation index and plasma membrane integrity. *Theriogenology,* 66**,** 1307-15.

Kennedy, C. E., Krieger, K. B., Sutovsky, M., Xu, W., Vargovic, P., Didion, B. A., Ellersieck, M. R., Hennessy, M. E., Verstegen, J., Oko, R. & Sutovsky, P. (2014). Protein expression pattern of PAWP in bull spermatozoa is associated with sperm quality and fertility following artificial insemination. *Mol Reprod Dev,* 81**,** 436-49.

Kim, A. M., Bernhardt, M. L., Kong, B. Y., Ahn, R. W., Vogt, S., Woodruff, T. K. & O'halloran, T. V. (2011). Zinc sparks are triggered by fertilization and facilitate cell cycle resumption in mammalian eggs. *ACS Chem Biol,* 6**,** 716-23.

Kim, A. M., Vogt, S., O'halloran, T. V. & Woodruff, T. K. (2010). Zinc availability regulates exit from meiosis in maturing mammalian oocytes. *Nat Chem Biol,* 6**,** 674-81.

Kim, J. W., Kim, S. D., Yang, S. H., Yoon, S. H., Jung, J. H. & Lim, J. H. (2014). Successful pregnancy after SrCl2 oocyte activation in couples with repeated low fertilization rates following calcium ionophore treatment. *Syst Biol Reprod Med,* 60**,** 177-82.

Kline, D. & Kline, J. T. (1992). Repetitive calcium transients and the role of calcium in exocytosis and cell cycle activation in the mouse egg. *Dev Biol,* 149**,** 80-9.

Kline, D. & Stewart-Savage, J. (1994). The timing of cortical granule fusion, content dispersal, and endocytosis during fertilization of the hamster egg: an electrophysiological and histochemical study. *Dev Biol,* 162**,** 277-87.

Knott, J. G., Gardner, A. J., Madgwick, S., Jones, K. T., Williams, C. J. & Schultz, R. M. (2006). Calmodulin-dependent protein kinase II triggers mouse egg activation and embryo development in the absence of Ca2+ oscillations. *Dev Biol,* 296**,** 388-95.

Knott, J. G., Kurokawa, M., Fissore, R. A., Schultz, R. M. & Williams, C. J. (2005). Transgenic RNA interference reveals role for mouse sperm phospholipase Czeta in triggering Ca2+ oscillations during fertilization. *Biol Reprod,* 72**,** 992-6.

Kono, T., Jones, K. T., Bos-Mikich, A., Whittingham, D. G. & Carroll, J. (1996). A cell cycle-associated change in Ca2+ releasing activity leads to the generation of Ca2+ transients in mouse embryos during the first mitotic division. *J Cell Biol,* 132**,** 915-23.

Kouchi, Z., Fukami, K., Shikano, T., Oda, S., Nakamura, Y., Takenawa, T. & Miyazaki, S. (2004). Recombinant phospholipase Czeta has high Ca2+ sensitivity and induces Ca2+ oscillations in mouse eggs. *J Biol Chem,* 279**,** 10408-12.

Kouchi, Z., Shikano, T., Nakamura, Y., Shirakawa, H., Fukami, K. & Miyazaki, S. (2005). The role of EF-hand domains and C2 domain in regulation of enzymatic activity of phospholipase Czeta. *J Biol Chem,* 280**,** 21015-21.

Kouranova, E., Forbes, K., Zhao, G., Warren, J., Bartels, A., Wu, Y. & Cui, X. (2016). CRISPRs for Optimal Targeting: Delivery of CRISPR Components as DNA, RNA, and Protein into Cultured Cells and Single-Cell Embryos. *Hum Gene Ther,* 27**,** 464-75.

Krisher, R. L. 2013. *Oocyte physiology and development in domestic animals,* Ames, Iowa, Wiley-Blackwell.

Kumar, N. & Singh, A. K. (2015). Trends of male factor infertility, an important cause of infertility: A review of literature. *J Hum Reprod Sci,* 8**,** 191-6.

Kuroda, K., Ito, M., Shikano, T., Awaji, T., Yoda, A., Takeuchi, H., Kinoshita, K. & Miyazaki, S. (2006). The role of X/Y linker region and N-terminal EF-hand domain in nuclear translocation and Ca2+ oscillation-inducing activities of phospholipase Czeta, a mammalian egg-activating factor. *J Biol Chem,* 281**,** 27794-805.

Kurokawa, M., Sato, K., Wu, H., He, C., Malcuit, C., Black, S. J., Fukami, K. & Fissore, R. A. (2005). Functional, biochemical, and chromatographic characterization of the complete [Ca2+]i oscillation-inducing activity of porcine sperm. *Dev Biol,* 285**,** 376-92.

Kyono, K., Kumagai, S., Nishinaka, C., Nakajo, Y., Uto, H., Toya, M., Sugawara, J. & Araki, Y. (2008). Birth and follow-up of babies born following ICSI using SrCl2 oocyte activation. *Reprod Biomed Online,* 17**,** 53-8.

Lander, E. S. (2016). The Heroes of CRISPR. *Cell,* 164**,** 18-28.

Larman, M. G., Saunders, C. M., Carroll, J., Lai, F. A. & Swann, K. (2004). Cell cycle-dependent Ca2+ oscillations in mouse embryos are regulated by nuclear targeting of PLCzeta. *J Cell Sci,* 117**,** 2513-21.

Lawrence, Y., Ozil, J. P. & Swann, K. (1998). The effects of a Ca2+ chelator and heavy-metal-ion chelators upon Ca2+ oscillations and activation at fertilization in mouse eggs suggest a role for repetitive Ca2+ increases. *Biochem J,* 335 (Pt 2)**,** 335-42.

Lawrence, Y., Whitaker, M. & Swann, K. (1997). Sperm-egg fusion is the prelude to the initial Ca2+ increase at fertilization in the mouse. *Development,* 124**,** 233-41.

Lee, B., Yoon, S. Y., Malcuit, C., Parys, J. B. & Fissore, R. A. (2010). Inositol 1,4,5-trisphosphate receptor 1 degradation in mouse eggs and impact on [Ca2+]i oscillations. *J Cell Physiol,* 222**,** 238-47.

Lee, H. C., Yoon, S. Y., Lykke-Hartmann, K., Fissore, R. A. & Carvacho, I. (2016). TRPV3 channels mediate Ca(2)(+) influx induced by 2-APB in mouse eggs. *Cell Calcium,* 59**,** 21-31.

Lee, K., Wang, C. & Machaty, Z. (2012). STIM1 is required for Ca2+ signaling during mammalian fertilization. *Dev Biol,* 367**,** 154-62.

Lee, S. J., Christenson, L., Martin, T. & Shen, S. S. (1996). The cyclic GMP-mediated calcium release pathway in sea urchin eggs is not required for the rise in calcium during fertilization. *Dev Biol,* 180**,** 324-35.

Lee, S. J., Madden, P. J. & Shen, S. S. (1998). U73122 blocked the cGMP-induced calcium release in sea urchin eggs. *Exp Cell Res,* 242**,** 328-40.

Liu, J., Nagy, Z., Joris, H., Tournaye, H., Smitz, J., Camus, M., Devroey, P. & Van Steirteghem, A. (1995). Analysis of 76 total fertilization failure cycles out of 2732 intracytoplasmic sperm injection cycles. *Hum Reprod,* 10**,** 2630-6.

Liu, L., Nutter, L. M., Law, N. & Mckerlie, C. (2009). Sperm freezing and in vitro fertilization in three substrains of C57BL/6 mice. *J Am Assoc Lab Anim Sci,* 48**,** 39-43.

Liu, L. & Yang, X. (1999). Interplay of maturation-promoting factor and mitogen-activated protein kinase inactivation during metaphase-to-interphase transition of activated bovine oocytes. *Biol Reprod,* 61**,** 1-7.

Lockyer, E. J. (2016). The potential of CRISPR-Cas9 for treating genetic disorders. *Bioscience Horizons: The International Journal of Student Research,* 9**,** hzw012-hzw012.

Lopes, A. M., Aston, K. I., Thompson, E., Carvalho, F., Goncalves, J., Huang, N., Matthiesen, R., Noordam, M. J., Quintela, I., Ramu, A., Seabra, C., Wilfert, A. B., Dai, J., Downie, J. M., Fernandes, S., Guo, X., Sha, J., Amorim, A., Barros, A., Carracedo, A., Hu, Z., Hurles, M. E., Moskovtsev, S., Ober, C., Paduch, D. A., Schiffman, J. D., Schlegel, P. N., Sousa, M., Carrell, D. T. & Conrad, D. F. (2013). Human spermatogenic failure purges deleterious mutation load from the autosomes and both sex chromosomes, including the gene DMRT1. *PLoS Genet,* 9**,** e1003349.

Loren, J. & Lacham-Kaplan, O. (2006). The employment of strontium to activate mouse oocytes: effects on spermatid-injection outcome. *Reproduction,* 131**,** 259-67.

Lorenzetti, D., Poirier, C., Zhao, M., Overbeek, P. A., Harrison, W. & Bishop, C. E. (2014). A transgenic insertion on mouse chromosome 17 inactivates a novel immunoglobulin superfamily gene potentially involved in sperm-egg fusion. *Mamm Genome,* 25**,** 141-8.

Lu, Y., Reddy, R., Ferrer Buitrago, M., Vander Jeught, M., Neupane, J., De Vos, W. H., Van Den Abbeel, E., Lierman, S., De Sutter, P. & Heindryckx, B. (2018). Strontium fails to induce Ca2+ release and activation in human oocytes despite the presence of functional TRPV3 channels. *Human Reproduction Open,* 2018**,** hoy005-hoy005.

Ma, H., Marti-Gutierrez, N., Park, S. W., Wu, J., Lee, Y., Suzuki, K., Koski, A., Ji, D., Hayama, T., Ahmed, R., Darby, H., Van Dyken, C., Li, Y., Kang, E., Park, A. R., Kim, D., Kim, S. T., Gong, J., Gu, Y., Xu, X., Battaglia, D., Krieg, S. A., Lee, D. M., Wu, D. H., Wolf, D. P., Heitner, S. B., Belmonte, J. C. I., Amato, P., Kim, J. S., Kaul, S. & Mitalipov, S. (2017). Correction of a pathogenic gene mutation in human embryos. *Nature,* 548**,** 413-419.

Ma, S. F., Liu, X. Y., Miao, D. Q., Han, Z. B., Zhang, X., Miao, Y. L., Yanagimachi, R. & Tan, J. H. (2005). Parthenogenetic activation of mouse oocytes by strontium chloride: a search for the best conditions. *Theriogenology,* 64**,** 1142-57.

Machaty, Z. (2013). Oocyte Calcium Homeostasis. *In:* KRISHER, R. L. (ed.) *Oocyte Physiology and Development in Domestic Animals.* 1st ed. New Delhi, India: John Wiley & Sons, Inc.

Machaty, Z. (2016). Signal transduction in mammalian oocytes during fertilization. *Cell Tissue Res,* 363**,** 169-83.

Machaty, Z., Mayes, M. A., Kovacs, L. G., Balatti, P. A., Kim, J. H. & Prather, R. S. (1997). Activation of porcine oocytes via an exogenously introduced rat muscarinic M1 receptor. *Biol Reprod,* 57**,** 85-91.

Madgwick, S., Levasseur, M. & Jones, K. T. (2005). Calmodulin-dependent protein kinase II, and not protein kinase C, is sufficient for triggering cell-cycle resumption in mammalian eggs. *J Cell Sci,* 118**,** 3849-59.

Maleszewski, M., Kimura, Y. & Yanagimachi, R. (1996). Sperm membrane incorporation into oolemma contributes to the oolemma block to sperm penetration: evidence based on intracytoplasmic sperm injection experiments in the mouse. *Mol Reprod Dev,* 44**,** 256-9.

Maluchnik, D. & Borsuk, E. (1994). Sperm entry into fertilised mouse eggs. *Zygote,* 2**,** 129-31.

Marangos, P., Fitzharris, G. & Carroll, J. (2003). Ca2+ oscillations at fertilization in mammals are regulated by the formation of pronuclei. *Development,* 130**,** 1461-72.

Masui, Y. & Markert, C. L. (1971). Cytoplasmic control of nuclear behavior during meiotic maturation of frog oocytes. *J Exp Zool,* 177**,** 129-45.

Mcdougall, A. & Levasseur, M. (1998). Sperm-triggered calcium oscillations during meiosis in ascidian oocytes first pause, restart, then stop: correlations with cell cycle kinase activity. *Development,* 125**,** 4451-9.

Mehlmann, L. M., Carpenter, G., Rhee, S. G. & Jaffe, L. A. (1998). SH2 domain-mediated activation of phospholipase Cgamma is not required to initiate Ca2+ release at fertilization of mouse eggs. *Dev Biol,* 203**,** 221-32.

Mehlmann, L. M., Chattopadhyay, A., Carpenter, G. & Jaffe, L. A. (2001). Evidence that phospholipase C from the sperm is not responsible for initiating Ca(2+) release at fertilization in mouse eggs. *Dev Biol,* 236**,** 492-501.

Mehlmann, L. M. & Kline, D. (1994). Regulation of intracellular calcium in the mouse egg: calcium release in response to sperm or inositol trisphosphate is enhanced after meiotic maturation. *Biol Reprod,* 51**,** 1088-98.

Mehlmann, L. M., Terasaki, M., Jaffe, L. A. & Kline, D. (1995). Reorganization of the endoplasmic reticulum during meiotic maturation of the mouse oocyte. *Dev Biol,* 170**,** 607-15.

Mejia-Flores, I., Chiquete-Felix, N., Palma-Lara, I., Uribe-Carvajal, S. & De Lourdes Juarez-Mosqueda, M. (2017). During capacitation in bull spermatozoa, actin and PLC-zeta undergo dynamic interactions. *Zygote,* 25**,** 558-566.

Menkveld, R., Wong, W. Y., Lombard, C. J., Wetzels, A. M., Thomas, C. M., Merkus, H. M. & Steegers-Theunissen, R. P. (2001). Semen parameters, including WHO and strict criteria morphology, in a fertile and subfertile population: an effort towards standardization of in-vivo thresholds. *Hum Reprod,* 16**,** 1165-71.

Miao, Y. L., Stein, P., Jefferson, W. N., Padilla-Banks, E. & Williams, C. J. (2012). Calcium influx-mediated signaling is required for complete mouse egg activation. *Proc Natl Acad Sci U S A,* 109**,** 4169-74.

Miao, Y. L. & Williams, C. J. (2012). Calcium signaling in mammalian egg activation and embryo development: the influence of subcellular localization. *Mol Reprod Dev,* 79**,** 742-56.

Miyazaki, S., Hashimoto, N., Yoshimoto, Y., Kishimoto, T., Igusa, Y. & Hiramoto, Y. (1986). Temporal and spatial dynamics of the periodic increase in intracellular free calcium at fertilization of golden hamster eggs. *Dev Biol,* 118**,** 259-67.

Miyazaki, S. & Ito, M. (2006). Calcium signals for egg activation in mammals. *J Pharmacol Sci,* 100**,** 545-52.

Miyazaki, S., Katayama, Y. & Swann, K. (1990). Synergistic activation by serotonin and GTP analogue and inhibition by phorbol ester of cyclic Ca2+ rises in hamster eggs. *J Physiol,* 426**,** 209-27.

Miyazaki, S., Shirakawa, H., Nakada, K. & Honda, Y. (1993). Essential role of the inositol 1,4,5-trisphosphate receptor/Ca2+ release channel in Ca2+ waves and Ca2+ oscillations at fertilization of mammalian eggs. *Dev Biol,* 158**,** 62-78.

Miyazaki, S., Yuzaki, M., Nakada, K., Shirakawa, H., Nakanishi, S., Nakade, S. & Mikoshiba, K. (1992). Block of Ca2+ wave and Ca2+ oscillation by antibody to the inositol 1,4,5-trisphosphate receptor in fertilized hamster eggs. *Science,* 257**,** 251-5.

Mizushima, S., Takagi, S., Ono, T., Atsumi, Y., Tsukada, A., Saito, N. & Shimada, K. (2009). Phospholipase Czeta mRNA expression and its potency during spermatogenesis for activation of quail oocyte as a sperm factor. *Mol Reprod Dev,* 76**,** 1200-7.

Montag, M., Koster, M., Van Der Ven, K., Bohlen, U. & Van Der Ven, H. (2012). The benefit of artificial oocyte activation is dependent on the fertilization rate in a previous treatment cycle. *Reprod Biomed Online,* 24**,** 521-6.

Moos, J., Xu, Z., Schultz, R. M. & Kopf, G. S. (1996). Regulation of nuclear envelope assembly/disassembly by MAP kinase. *Dev Biol,* 175**,** 358-61.

Morozumi, K., Shikano, T., Miyazaki, S. & Yanagimachi, R. (2006). Simultaneous removal of sperm plasma membrane and acrosome before intracytoplasmic sperm injection improves oocyte activation/embryonic development. *Proc Natl Acad Sci U S A,* 103**,** 17661-6.

Morozumi, K. & Yanagimachi, R. (2005). Incorporation of the acrosome into the oocyte during intracytoplasmic sperm injection could be potentially hazardous to embryo development. *Proc Natl Acad Sci U S A,* 102**,** 14209-14.

Mortimer, D. & Mortimer, S. T. (2013). Computer-Aided Sperm Analysis (CASA) of sperm motility and hyperactivation. *Methods Mol Biol,* 927**,** 77-87.

Mortimer, S. T., Van Der Horst, G. & Mortimer, D. (2015). The future of computer-aided sperm analysis. *Asian J Androl,* 17**,** 545-53.

Muciaccia, B., Sette, C., Paronetto, M. P., Barchi, M., Pensini, S., D'agostino, A., Gandini, L., Geremia, R., Stefanini, M. & Rossi, P. (2010). Expression of a truncated form of KIT tyrosine kinase in human spermatozoa correlates with sperm DNA integrity. *Hum Reprod,* 25**,** 2188-202.

Nasr-Esfahani, M. H., Deemeh, M. R. & Tavalaee, M. (2010). Artificial oocyte activation and intracytoplasmic sperm injection. *Fertil Steril,* 94**,** 520-6.

Nikolettos, N., Kupker, W., Demirel, C., Schopper, B., Blasig, C., Sturm, R., Felberbaum, R., Bauer, O., Diedrich, K. & Al-Hasani, S. (1999). Fertilization potential of spermatozoa with abnormal morphology. *Hum Reprod,* 14 Suppl 1**,** 47-70.

Nikolic, A., Volarevic, V., Armstrong, L., Lako, M. & Stojkovic, M. (2016). Primordial Germ Cells: Current Knowledge and Perspectives. *Stem Cells Int,* 2016**,** 1741072.

Niu, Y., Shen, B., Cui, Y., Chen, Y., Wang, J., Wang, L., Kang, Y., Zhao, X., Si, W., Li, W., Xiang, A. P., Zhou, J., Guo, X., Bi, Y., Si, C., Hu, B., Dong, G., Wang, H., Zhou, Z., Li, T., Tan, T., Pu, X., Wang, F., Ji, S., Zhou, Q., Huang, X., Ji, W. & Sha, J. (2014). Generation of gene-modified cynomolgus monkey via Cas9/RNA-mediated gene targeting in one-cell embryos. *Cell,* 156**,** 836-43.

Nomikos, M., Blayney, L. M., Larman, M. G., Campbell, K., Rossbach, A., Saunders, C. M., Swann, K. & Lai, F. A. (2005). Role of phospholipase C-zeta domains in Ca2+-dependent phosphatidylinositol 4,5-bisphosphate hydrolysis and cytoplasmic Ca2+ oscillations. *J Biol Chem,* 280**,** 31011-8.

Nomikos, M., Elgmati, K., Theodoridou, M., Calver, B. L., Nounesis, G., Swann, K. & Lai, F. A. (2011a). Phospholipase Czeta binding to PtdIns(4,5)P2 requires the XY-linker region. *J Cell Sci,* 124**,** 2582-90.

Nomikos, M., Elgmati, K., Theodoridou, M., Georgilis, A., Gonzalez-Garcia, J. R., Nounesis, G., Swann, K. & Lai, F. A. (2011b). Novel regulation of PLCzeta activity via its XY-linker. *Biochem J,* 438**,** 427-32.

Nomikos, M., Sanders, J. R., Kashir, J., Sanusi, R., Buntwal, L., Love, D., Ashley, P., Sanders, D., Knaggs, P., Bunkheila, A., Swann, K. & Lai, F. A. (2015). Functional disparity between human PAWP and PLCzeta in the generation of Ca2+ oscillations for oocyte activation. *Mol Hum Reprod,* 21**,** 702-10.

Nomikos, M., Sanders, J. R., Theodoridou, M., Kashir, J., Matthews, E., Nounesis, G., Lai, F. A. & Swann, K. (2014a). Sperm-specific post-acrosomal WW-domain binding protein (PAWP) does not cause Ca2+ release in mouse oocytes. *Mol Hum Reprod,* 20**,** 938-47.

Nomikos, M., Theodoridou, M., Elgmati, K., Parthimos, D., Calver, B. L., Buntwal, L., Nounesis, G., Swann, K. & Lai, F. A. (2014b). Human PLCzeta exhibits superior fertilization potency over mouse PLCzeta in triggering the Ca(2+) oscillations required for mammalian oocyte activation. *Mol Hum Reprod,* 20**,** 489-98.

Nomikos, M., Yu, Y., Elgmati, K., Theodoridou, M., Campbell, K., Vassilakopoulou, V., Zikos, C., Livaniou, E., Amso, N., Nounesis, G., Swann, K. & Lai, F. A. (2013). Phospholipase Czeta rescues failed oocyte activation in a prototype of male factor infertility. *Fertil Steril,* 99**,** 76-85.

Nozawa, K., Satouh, Y., Fujimoto, T., Oji, A. & Ikawa, M. (2018). Sperm-borne phospholipase C zeta-1 ensures monospermic fertilization in mice. *Sci Rep,* 8**,** 1315.

Nuccitelli, R. (1987). The wave of activation current in the egg of the medaka fish. *Dev Biol,* 122**,** 522-34.

O'donnell, L., Nicholls, P. K., O'bryan, M. K., Mclachlan, R. I. & Stanton, P. G. (2011). Spermiation: The process of sperm release. *Spermatogenesis,* 1**,** 14-35.

Oh, J. S., Susor, A. & Conti, M. (2011). Protein tyrosine kinase Wee1B is essential for metaphase II exit in mouse oocytes. *Science,* 332**,** 462-5.

Ohe, M., Kawamura, Y., Ueno, H., Inoue, D., Kanemori, Y., Senoo, C., Isoda, M., Nakajo, N. & Sagata, N. (2010). Emi2 inhibition of the anaphase-promoting complex/cyclosome absolutely requires Emi2 binding via the C-terminal RL tail. *Mol Biol Cell,* 21**,** 905-13.

Ohto, U., Ishida, H., Krayukhina, E., Uchiyama, S., Inoue, N. & Shimizu, T. (2016). Structure of IZUMO1-JUNO reveals sperm-oocyte recognition during mammalian fertilization. *Nature,* 534**,** 566-9.

Oliver, D., Yuan, S., Mcswiggin, H. & Yan, W. (2015). Pervasive Genotypic Mosaicism in Founder Mice Derived from Genome Editing through Pronuclear Injection. *PLoS One,* 10**,** e0129457.

Overstreet, J. W. & Bedford, J. M. (1974). Comparison of the penetrability of the egg vestments in follicular oocytes, unfertilized and fertilized ova of the rabbit. *Dev Biol,* 41**,** 185-92.

Ozil, J. P., Banrezes, B., Toth, S., Pan, H. & Schultz, R. M. (2006). Ca2+ oscillatory pattern in fertilized mouse eggs affects gene expression and development to term. *Dev Biol,* 300**,** 534-44.

Ozil, J. P., Markoulaki, S., Toth, S., Matson, S., Banrezes, B., Knott, J. G., Schultz, R. M., Huneau, D. & Ducibella, T. (2005). Egg activation events are regulated by the duration of a sustained [Ca2+]cyt signal in the mouse. *Dev Biol,* 282**,** 39-54.

Ozil, J. P., Sainte-Beuve, T. & Banrezes, B. (2017). [Mg2+]o/[Ca2+]o determines Ca2+ response at fertilization: tuning of adult phenotype? *Reproduction,* 154**,** 675-693.

Ozil, J. P. & Swann, K. (1995). Stimulation of repetitive calcium transients in mouse eggs. *J Physiol,* 483 (Pt 2)**,** 331-46.

Palermo, G. D., O'neill, C. L., Chow, S., Cheung, S., Parrella, A., Pereira, N. & Rosenwaks, Z. (2017). Intracytoplasmic sperm injection: state of the art in humans. *Reproduction,* 154**,** F93-F110.

Palermo, G. D., Schlegel, P. N., Colombero, L. T., Zaninovic, N., Moy, F. & Rosenwaks, Z. (1996). Aggressive sperm immobilization prior to intracytoplasmic sperm injection with immature spermatozoa improves fertilization and pregnancy rates. *Hum Reprod,* 11**,** 1023-9.

Pan, Q., Ju, Z., Huang, J., Zhang, Y., Qi, C., Gao, Q., Zhou, L., Li, Q., Wang, L., Zhong, J., Liu, M. & Wang, C. (2013). PLCz functional haplotypes modulating promoter transcriptional activity are associated with semen quality traits in Chinese Holstein bulls. *PLoS One,* 8**,** e58795.

Paronetto, M. P., Venables, J. P., Elliott, D. J., Geremia, R., Rossi, P. & Sette, C. (2003). Tr-kit promotes the formation of a multimolecular complex composed by Fyn, PLCgamma1 and Sam68. *Oncogene,* 22**,** 8707-15.

Parrington, J., Davis, L. C., Galione, A. & Wessel, G. (2007). Flipping the switch: how a sperm activates the egg at fertilization. *Dev Dyn,* 236**,** 2027-38.

Parrington, J., Jones, M. L., Tunwell, R., Devader, C., Katan, M. & Swann, K. (2002). Phospholipase C isoforms in mammalian spermatozoa: potential components of the sperm factor that causes Ca2+ release in eggs. *Reproduction,* 123**,** 31-9.

Parrington, J., Lear, P. & Hachem, A. (2015). Calcium signals regulated by NAADP and two-pore channels--their role in development, differentiation and cancer. *Int J Dev Biol,* 59**,** 341-55.

Phillips, K. P., Petrunewich, M. A., Collins, J. L., Booth, R. A., Liu, X. J. & Baltz, J. M. (2002). Inhibition of MEK or cdc2 kinase parthenogenetically activates mouse eggs and yields the same phenotypes as Mos(-/-) parthenogenotes. *Dev Biol,* 247**,** 210-23.

Phillips, S. V., Yu, Y., Rossbach, A., Nomikos, M., Vassilakopoulou, V., Livaniou, E., Cumbes, B., Lai, F. A., George, C. H. & Swann, K. (2011). Divergent effect of mammalian PLCzeta in generating Ca(2)(+) oscillations in somatic cells compared with eggs. *Biochem J,* 438**,** 545-53.

Que, E. L., Bleher, R., Duncan, F. E., Kong, B. Y., Gleber, S. C., Vogt, S., Chen, S., Garwin, S. A., Bayer, A. R., Dravid, V. P., Woodruff, T. K. & O'halloran, T. V. (2015). Quantitative mapping of zinc fluxes in the mammalian egg reveals the origin of fertilization-induced zinc sparks. *Nat Chem,* 7**,** 130-9.

Ran, F. A., Hsu, P. D., Lin, C. Y., Gootenberg, J. S., Konermann, S., Trevino, A. E., Scott, D. A., Inoue, A., Matoba, S., Zhang, Y. & Zhang, F. (2013). Double nicking by RNA-guided CRISPR Cas9 for enhanced genome editing specificity. *Cell,* 154**,** 1380-9.

Rath, D., Amlinger, L., Rath, A. & Lundgren, M. (2015). The CRISPR-Cas immune system: biology, mechanisms and applications. *Biochimie,* 117**,** 119-28.

Rauh, N. R., Schmidt, A., Bormann, J., Nigg, E. A. & Mayer, T. U. (2005). Calcium triggers exit from meiosis II by targeting the APC/C inhibitor XErp1 for degradation. *Nature,* 437**,** 1048-52.

Rengan, A. K., Agarwal, A., Van Der Linde, M. & Du Plessis, S. S. (2012). An investigation of excess residual cytoplasm in human spermatozoa and its distinction from the cytoplasmic droplet. *Reprod Biol Endocrinol,* 10**,** 92.

Ridgway, E. B., Gilkey, J. C. & Jaffe, L. F. (1977). Free calcium increases explosively in activating medaka eggs. *Proc Natl Acad Sci U S A,* 74**,** 623-7.

Rogers, N. T., Halet, G., Piao, Y., Carroll, J., Ko, M. S. & Swann, K. (2006). The absence of a Ca(2+) signal during mouse egg activation can affect parthenogenetic preimplantation development, gene expression patterns, and blastocyst quality. *Reproduction,* 132**,** 45-57.

Rogers, N. T., Hobson, E., Pickering, S., Lai, F. A., Braude, P. & Swann, K. (2004). Phospholipase Czeta causes Ca2+ oscillations and parthenogenetic activation of human oocytes. *Reproduction,* 128**,** 697-702.

Sadler, T. W. & Langman, J. 2012. *Langman's medical embryology,* Philadelphia, Wolters Kluwer Health/Lippincott Williams & Wilkins.

Samplaski, M. K., Dimitromanolakis, A., Lo, K. C., Grober, E. D., Mullen, B., Garbens, A. & Jarvi, K. A. (2015). The relationship between sperm viability and DNA fragmentation rates. *Reprod Biol Endocrinol,* 13**,** 42.

Sanders, J. R., Ashley, B., Moon, A., Woolley, T. E. & Swann, K. (2018). PLCζ Induced Ca2+ Oscillations in Mouse Eggs Involve a Positive Feedback Cycle of Ca2+ Induced InsP3 Formation From Cytoplasmic PIP2. *Frontiers in Cell and Developmental Biology,* 6.

Sanders, J. R. & Swann, K. (2016). Molecular triggers of egg activation at fertilization in mammals. *Reproduction,* 152**,** R41-50.

Santella, L. & Dale, B. (2015). Assisted yes, but where do we draw the line? *Reprod Biomed Online,* 31**,** 476-8.

Sato, M. S., Yoshitomo, M., Mohri, T. & Miyazaki, S. (1999). Spatiotemporal analysis of [Ca2+]i rises in mouse eggs after intracytoplasmic sperm injection (ICSI). *Cell Calcium,* 26**,** 49-58.

Satouh, Y., Nozawa, K. & Ikawa, M. (2015). Sperm postacrosomal WW domain-binding protein is not required for mouse egg activation. *Biol Reprod,* 93**,** 94.

Satouh, Y., Nozawa, K., Yamagata, K., Fujimoto, T. & Ikawa, M. (2017). Viable offspring after imaging of Ca2+ oscillations and visualization of the cortical reaction in mouse eggs. *Biol Reprod,* 96**,** 563-575.

Saunders, C. M., Larman, M. G., Parrington, J., Cox, L. J., Royse, J., Blayney, L. M., Swann, K. & Lai, F. A. (2002). PLC zeta: a sperm-specific trigger of Ca(2+) oscillations in eggs and embryo development. *Development,* 129**,** 3533-44.

Saunders, C. M., Swann, K. & Lai, F. A. (2007). PLCzeta, a sperm-specific PLC and its potential role in fertilization. *Biochem Soc Symp***,** 23-36.

Schachter-Safrai, N., Karavani, G., Levitas, E., Friger, M., Zeadna, A., Lunenfeld, E. & Har-Vardi, I. (2017). Does cryopreservation of sperm affect fertilization in nonobstructive azoospermia or cryptozoospermia? *Fertil Steril,* 107**,** 1148-1152.

Schmidt, A., Duncan, P. I., Rauh, N. R., Sauer, G., Fry, A. M., Nigg, E. A. & Mayer, T. U. (2005). Xenopus polo-like kinase Plx1 regulates XErp1, a novel inhibitor of APC/C activity. *Genes Dev,* 19**,** 502-13.

Schmidt, T., Patton, C. & Epel, D. (1982). Is there a role for the Ca2+ influx during fertilization of the sea urchin egg? *Developmental Biology,* 90**,** 284-290.

Schrimpf, R., Dierks, C., Martinsson, G., Sieme, H. & Distl, O. (2014). Genome-wide association study identifies phospholipase C zeta 1 (PLCz1) as a stallion fertility locus in Hanoverian warmblood horses. *PLoS One,* 9**,** e109675.

Sengoku, K., Tamate, K., Takaoka, Y., Horikawa, M., Goishi, K., Okada, R., Tsuchiya, K. & Ishikawa, M. (1999). Requirement of sperm-oocyte plasma membrane fusion for establishment of the plasma membrane block to polyspermy in human pronuclear oocytes. *Mol Reprod Dev,* 52**,** 183-8.

Senthilkumaran, B. (2011). Recent advances in meiotic maturation and ovulation: comparing mammals and pisces. *Front Biosci (Landmark Ed),* 16**,** 1898-914.

Sette, C., Bevilacqua, A., Bianchini, A., Mangia, F., Geremia, R. & Rossi, P. (1997). Parthenogenetic activation of mouse eggs by microinjection of a truncated c-kit tyrosine kinase present in spermatozoa. *Development,* 124**,** 2267-74.

Sette, C., Paronetto, M. P., Barchi, M., Bevilacqua, A., Geremia, R. & Rossi, P. (2002). Tr-kit-induced resumption of the cell cycle in mouse eggs requires activation of a Src-like kinase. *EMBO J,* 21**,** 5386-95.

Sfontouris, I. A., Nastri, C. O., Lima, M. L., Tahmasbpourmarzouni, E., Raine-Fenning, N. & Martins, W. P. (2015). Artificial oocyte activation to improve reproductive outcomes in women with previous fertilization failure: a systematic review and meta-analysis of RCTs. *Hum Reprod,* 30**,** 1831-41.

Shah, S. A., Erdmann, S., Mojica, F. J. & Garrett, R. A. (2013). Protospacer recognition motifs: mixed identities and functional diversity. *RNA Biol,* 10**,** 891-9.

Shao, Y., Guan, Y., Wang, L., Qiu, Z., Liu, M., Chen, Y., Wu, L., Li, Y., Ma, X., Liu, M. & Li, D. (2014). CRISPR/Cas-mediated genome editing in the rat via direct injection of one-cell embryos. *Nat Protoc,* 9**,** 2493-512.

Shearer, J., De Nadai, C., Emily-Fenouil, F., Gache, C., Whitaker, M. & Ciapa, B. (1999). Role of phospholipase Cgamma at fertilization and during mitosis in sea urchin eggs and embryos. *Development,* 126**,** 2273-84.

Shimada, K., Ono, T. & Mizushima, S. (2014). Application of intracytoplasmic sperm injection (ICSI) for fertilization and development in birds. *Gen Comp Endocrinol,* 196**,** 100-5.

Sieme, H., Oldenhof, H. & Wolkers, W. F. (2015). Sperm Membrane Behaviour during Cooling and Cryopreservation. *Reprod Domest Anim,* 50 Suppl 3**,** 20-6.

Smedler, E. & Uhlen, P. (2014). Frequency decoding of calcium oscillations. *Biochim Biophys Acta,* 1840**,** 964-9.

Snapgene 2016. SnapGene® software (from GSL Biotech; available at snapgene.com).

Sneyd, J., Tsaneva-Atanasova, K., Reznikov, V., Bai, Y., Sanderson, M. J. & Yule, D. I. (2006). A method for determining the dependence of calcium oscillations on inositol trisphosphate oscillations. *Proc Natl Acad Sci U S A,* 103**,** 1675-80.

Snook, R. R., Hosken, D. J. & Karr, T. L. (2011). The biology and evolution of polyspermy: insights from cellular and functional studies of sperm and centrosomal behavior in the fertilized egg. *Reproduction,* 142**,** 779-92.

Sobinoff, A. P., Sutherland, J. M. & Mclaughlin, E. A. (2013). Intracellular signalling during female gametogenesis. *Mol Hum Reprod,* 19**,** 265-78.

Sousa, M., Mendoza, C., Barros, A. & Tesarik, J. (1996). Calcium responses of human oocytes after intracytoplasmic injection of leukocytes, spermatocytes and round spermatids. *Mol Hum Reprod,* 2**,** 853-7.

Speksnijder, J. E., Corson, D. W., Sardet, C. & Jaffe, L. F. (1989). Free calcium pulses following fertilization in the ascidian egg. *Dev Biol,* 135**,** 182-90.

Speybroeck, N., Williams, C. J., Lafia, K. B., Devleesschauwer, B. & Berkvens, D. (2012). Estimating the prevalence of infections in vector populations using pools of samples. *Med Vet Entomol,* 26**,** 361-71.

Stachecki, J. J. & Armant, D. R. (1996). Transient release of calcium from inositol 1,4,5-trisphosphate-specific stores regulates mouse preimplantation development. *Development,* 122**,** 2485-96.

Steinhardt, R., Zucker, R. & Schatten, G. (1977). Intracellular calcium release at fertilization in the sea urchin egg. *Dev Biol,* 58**,** 185-96.

Steinhardt, R. A., Epel, D., Carroll, E. J., Jr. & Yanagimachi, R. (1974). Is calcium ionophore a universal activator for unfertilised eggs? *Nature,* 252**,** 41-3.

Stricker, S. A. (1996). Repetitive calcium waves induced by fertilization in the nemertean worm Cerebratulus lacteus. *Dev Biol,* 176**,** 243-63.

Stricker, S. A. (1999). Comparative biology of calcium signaling during fertilization and egg activation in animals. *Dev Biol,* 211**,** 157-76.

Stricker, S. A. (2006). Structural reorganizations of the endoplasmic reticulum during egg maturation and fertilization. *Semin Cell Dev Biol,* 17**,** 303-13.

Su, Y. H., Lin, T. Y., Huang, C. L., Tu, C. F. & Chuang, C. K. (2015). Construction of a CRISPR-Cas9 System for Pig Genome Targeting. *Anim Biotechnol,* 26**,** 279-88.

Sun, F., Ko, E. & Martin, R. H. (2006). Is there a relationship between sperm chromosome abnormalities and sperm morphology? *Reprod Biol Endocrinol,* 4**,** 1.

Sun, L., Chai, Y., Hannigan, R., Bhogaraju, V. K. & Machaca, K. (2007). Zinc regulates the ability of Cdc25C to activate MPF/cdk1. *J Cell Physiol,* 213**,** 98-104.

Suzuki, T., Suzuki, E., Yoshida, N., Kubo, A., Li, H., Okuda, E., Amanai, M. & Perry, A. C. (2010a). Mouse Emi2 as a distinctive regulatory hub in second meiotic metaphase. *Development,* 137**,** 3281-91.

Suzuki, T., Yoshida, N., Suzuki, E., Okuda, E. & Perry, A. C. (2010b). Full-term mouse development by abolishing Zn2+-dependent metaphase II arrest without Ca2+ release. *Development,* 137**,** 2659-69.

Swain, J. E. & Pool, T. B. (2008). ART failure: oocyte contributions to unsuccessful fertilization. *Hum Reprod Update,* 14**,** 431-46.

Swann, K. (1990). A cytosolic sperm factor stimulates repetitive calcium increases and mimics fertilization in hamster eggs. *Development,* 110**,** 1295-302.

Swann, K. (1992). Different triggers for calcium oscillations in mouse eggs involve a ryanodine-sensitive calcium store. *Biochem J,* 287 (Pt 1)**,** 79-84.

Swann, K., Igusa, Y. & Miyazaki, S. (1989). Evidence for an inhibitory effect of protein kinase C on G-protein-mediated repetitive calcium transients in hamster eggs. *EMBO J,* 8**,** 3711-8.

Swann, K. & Jones, K. T. (2002). Membrane events of egg activation. *In:* HARDY, D. M. (ed.) *Fertilization.* San Diego: Academic Press.

Swann, K. & Lai, F. A. (2016). Egg Activation at Fertilization by a Soluble Sperm Protein. *Physiol Rev,* 96**,** 127-49.

Swann, K. & Ozil, J. P. (1994). Dynamics of the calcium signal that triggers mammalian egg activation. *Int Rev Cytol,* 152**,** 183-222.

Swann, K., Saunders, C. M., Rogers, N. T. & Lai, F. A. (2006). PLCzeta(zeta): a sperm protein that triggers Ca2+ oscillations and egg activation in mammals. *Semin Cell Dev Biol,* 17**,** 264-73.

Swann, K. & Whitaker, M. (1986). The part played by inositol trisphosphate and calcium in the propagation of the fertilization wave in sea urchin eggs. *J Cell Biol,* 103**,** 2333-42.

Swann, K. & Yu, Y. (2008). The dynamics of calcium oscillations that activate mammalian eggs. *Int J Dev Biol,* 52**,** 585-94.

Sztein, J. M., Farley, J. S. & Mobraaten, L. E. (2000). In vitro fertilization with cryopreserved inbred mouse sperm. *Biol Reprod,* 63**,** 1774-80.

Tahara, M., Tasaka, K., Masumoto, N., Mammoto, A., Ikebuchi, Y. & Miyake, A. (1996). Dynamics of cortical granule exocytosis at fertilization in living mouse eggs. *Am J Physiol,* 270**,** C1354-61.

Takahashi, T., Kikuchi, T., Kidokoro, Y. & Shirakawa, H. (2013). Ca(2)(+) influx-dependent refilling of intracellular Ca(2)(+) stores determines the frequency of Ca(2)(+) oscillations in fertilized mouse eggs. *Biochem Biophys Res Commun,* 430**,** 60-5.

Talansky, B. E., Malter, H. E. & Cohen, J. (1991). A preferential site for sperm-egg fusion in mammals. *Mol Reprod Dev,* 28**,** 183-8.

Tavalaee, M. & Nasr-Esfahani, M. H. (2016). Expression profile of PLCzeta, PAWP, and TR-KIT in association with fertilization potential, embryo development, and pregnancy outcomes in globozoospermic candidates for intra-cytoplasmic sperm injection and artificial oocyte activation. *Andrology,* 4**,** 850-6.

Taylor, S. L., Yoon, S. Y., Morshedi, M. S., Lacey, D. R., Jellerette, T., Fissore, R. A. & Oehninger, S. (2010). Complete globozoospermia associated with PLCzeta deficiency treated with calcium ionophore and ICSI results in pregnancy. *Reprod Biomed Online,* 20**,** 559-64.

Tesarik, J., Rienzi, L., Ubaldi, F., Mendoza, C. & Greco, E. (2002). Use of a modified intracytoplasmic sperm injection technique to overcome sperm-borne and oocyte-borne oocyte activation failures. *Fertil Steril,* 78**,** 619-24.

Tesarik, J., Sousa, M. & Testart, J. (1994). Human oocyte activation after intracytoplasmic sperm injection. *Hum Reprod,* 9**,** 511-8.

Thomas, A. P., Bird, G. S., Hajnoczky, G., Robb-Gaspers, L. D. & Putney, J. W., Jr. (1996). Spatial and temporal aspects of cellular calcium signaling. *FASEB J,* 10**,** 1505-17.

Tsafriri, A., Reich, R. & A.D., A. (1994). The Ovarian Egg and Ovulation. *In:* LAMMING, G. E. (ed.) *Marshall's Physiology of Reproduction.* Fourth edition ed.: Chapman & Hall.

Turner, P. R., Sheetz, M. P. & Jaffe, L. A. (1984). Fertilization increases the polyphosphoinositide content of sea urchin eggs. *Nature,* 310**,** 414-5.

Vanden Meerschaut, F., Nikiforaki, D., De Roo, C., Lierman, S., Qian, C., Schmitt-John, T., De Sutter, P. & Heindryckx, B. (2013). Comparison of pre- and post-implantation development following the application of three artificial activating stimuli in a mouse model with round-headed sperm cells deficient for oocyte activation. *Hum Reprod,* 28**,** 1190-8.

Vanden Meerschaut, F., Nikiforaki, D., Heindryckx, B. & De Sutter, P. (2014). Assisted oocyte activation following ICSI fertilization failure. *Reprod Biomed Online,* 28**,** 560-71.

Verkhratsky, A. & Shmigol, A. (1996). Calcium-induced calcium release in neurones. *Cell Calcium,* 19**,** 1-14.

Verlhac, M. H., Kubiak, J. Z., Clarke, H. J. & Maro, B. (1994). Microtubule and chromatin behavior follow MAP kinase activity but not MPF activity during meiosis in mouse oocytes. *Development,* 120**,** 1017-25.

Wakai, T. & Fissore, R. A. (2013). Ca(2+) homeostasis and regulation of ER Ca(2+) in mammalian oocytes/eggs. *Cell Calcium,* 53**,** 63-7.

Wang, C. & Swerdloff, R. S. (2014). Limitations of semen analysis as a test of male fertility and anticipated needs from newer tests. *Fertil Steril,* 102**,** 1502-7.

Wang, F., Shi, Z., Cui, Y., Guo, X., Shi, Y. B. & Chen, Y. (2015). Targeted gene disruption in Xenopus laevis using CRISPR/Cas9. *Cell Biosci,* 5**,** 15.

Wang, H., Zhao, R., Guo, C., Jiang, S., Yang, J., Xu, Y., Liu, Y., Fan, L., Xiong, W., Ma, J., Peng, S., Zeng, Z., Zhou, Y., Li, X., Li, Z., Li, X., Schmitt, D. C., Tan, M., Li, G. & Zhou, M. (2016). Knockout of BRD7 results in impaired spermatogenesis and male infertility. *Sci Rep,* 6**,** 21776.

Wang, T. F., Zhou, C., Tang, A. H., Wang, S. Q. & Chai, Z. (2006). Cellular mechanism for spontaneous calcium oscillations in astrocytes. *Acta Pharmacol Sin,* 27**,** 861-8.

Wang, W. H., Day, B. N. & Wu, G. M. (2003). How does polyspermy happen in mammalian oocytes? *Microsc Res Tech,* 61**,** 335-41.

Wassarman, P. M., Jovine, L., Qi, H., Williams, Z., Darie, C. & Litscher, E. S. (2005). Recent aspects of mammalian fertilization research. *Mol Cell Endocrinol,* 234**,** 95-103.

Whitaker, M. (1996). Control of meiotic arrest. *Rev Reprod,* 1**,** 127-35.

Whitaker, M. & Irvine, R. F. (1984). Inositol 1,4,5-trisphosphate microinjection activates sea urchin eggs. *Nature,* 312**,** 636.

Whittingham, D. G. & Siracusa, G. (1978). The involvement of calcium in the activation of mammalian oocytes. *Exp Cell Res,* 113**,** 311-7.

Wilkes, S., Chinn, D. J., Murdoch, A. & Rubin, G. (2009). Epidemiology and management of infertility: a population-based study in UK primary care. *Fam Pract,* 26**,** 269-74.

Williams, C. J., Mehlmann, L. M., Jaffe, L. A., Kopf, G. S. & Schultz, R. M. (1998). Evidence that Gq family G proteins do not function in mouse egg activation at fertilization. *Dev Biol,* 198**,** 116-27.

Williams, D. A., Delbridge, L. M., Cody, S. H., Harris, P. J. & Morgan, T. O. (1992). Spontaneous and propagated calcium release in isolated cardiac myocytes viewed by confocal microscopy. *Am J Physiol,* 262**,** C731-42.

World Health Organization. 2010. *WHO laboratory manual for the examination and processing of human semen,* Geneva, World Health Organization.

Wortzman, G. B. & Evans, J. P. (2005). Membrane and cortical abnormalities in post-ovulatory aged eggs: analysis of fertilizability and establishment of the membrane block to polyspermy. *Mol Hum Reprod,* 11**,** 1-9.

Wortzman, G. B., Gardner, A. J. & Evans, J. P. (2006). Analysis of Mammalian sperm-egg membrane interactions during in vitro fertilization. *Methods Mol Biol,* 341**,** 89-101.

Wortzman-Show, G. B., Kurokawa, M., Fissore, R. A. & Evans, J. P. (2007). Calcium and sperm components in the establishment of the membrane block to polyspermy: studies of ICSI and activation with sperm factor. *Mol Hum Reprod,* 13**,** 557-65.

Wu, A. T., Sutovsky, P., Manandhar, G., Xu, W., Katayama, M., Day, B. N., Park, K. W., Yi, Y. J., Xi, Y. W., Prather, R. S. & Oko, R. (2007). PAWP, a sperm-specific WW domain-binding protein, promotes meiotic resumption and pronuclear development during fertilization. *J Biol Chem,* 282**,** 12164-75.

Xu, H., Delling, M., Jun, J. C. & Clapham, D. E. (2006). Oregano, thyme and clove-derived flavors and skin sensitizers activate specific TRP channels. *Nat Neurosci,* 9**,** 628-35.

Xu, Z., Abbott, A., Kopf, G. S., Schultz, R. M. & Ducibella, T. (1997). Spontaneous activation of ovulated mouse eggs: time-dependent effects on M-phase exit, cortical granule exocytosis, maternal messenger ribonucleic acid recruitment, and inositol 1,4,5-trisphosphate sensitivity. *Biol Reprod,* 57**,** 743-50.

Xu, Z., Kopf, G. S. & Schultz, R. M. (1994). Involvement of inositol 1,4,5-trisphosphate-mediated Ca2+ release in early and late events of mouse egg activation. *Development,* 120**,** 1851-9.

Yamaguchi, T., Ito, M., Kuroda, K., Takeda, S. & Tanaka, A. (2017). The establishment of appropriate methods for egg-activation by human PLCZ1 RNA injection into human oocyte. *Cell Calcium,* 65**,** 22-30.

Yanagida, K. (2004). Complete fertilization failure in ICSI. *Hum Cell,* 17**,** 187-93.

Yanagida, K., Katayose, H., Hirata, S., Yazawa, H., Hayashi, S. & Sato, A. (2001). Influence of sperm immobilization on onset of Ca(2+) oscillations after ICSI. *Hum Reprod,* 16**,** 148-152.

Yanagida, K., Katayose, H., Yazawa, H., Kimura, Y., Sato, A., Yanagimachi, H. & Yanagimachi, R. (1999). Successful fertilization and pregnancy following ICSI and electrical oocyte activation. *Hum Reprod,* 14**,** 1307-11.

Yanagimachi, R. (1998). Intracytoplasmic sperm injection experiments using the mouse as a model. *Hum Reprod,* 13 Suppl 1**,** 87-98.

Yanagimachi, R. & Chang, M. C. (1961). Fertilizable life of golden hamster ova and their morphological changes at the time of losing fertilizability. *J Exp Zool,* 148**,** 185-203.

Yang, H., Wang, H. & Jaenisch, R. (2014). Generating genetically modified mice using CRISPR/Cas-mediated genome engineering. *Nat Protoc,* 9**,** 1956-68.

Yazawa, H., Yanagida, K., Katayose, H., Hayashi, S. & Sato, A. (2000). Comparison of oocyte activation and Ca2+ oscillation-inducing abilities of round/elongated spermatids of mouse, hamster, rat, rabbit and human assessed by mouse oocyte activation assay. *Hum Reprod,* 15**,** 2582-90.

Yen, S. T., Zhang, M., Deng, J. M., Usman, S. J., Smith, C. N., Parker-Thornburg, J., Swinton, P. G., Martin, J. F. & Behringer, R. R. (2014). Somatic mosaicism and allele complexity induced by CRISPR/Cas9 RNA injections in mouse zygotes. *Dev Biol,* 393**,** 3-9.

Yeste, M., Jones, C., Amdani, S. N., Patel, S. & Coward, K. (2016). Oocyte activation deficiency: a role for an oocyte contribution? *Hum Reprod Update,* 22**,** 23-47.

Yoda, A., Oda, S., Shikano, T., Kouchi, Z., Awaji, T., Shirakawa, H., Kinoshita, K. & Miyazaki, S. (2004). Ca2+ oscillation-inducing phospholipase C zeta expressed in mouse eggs is accumulated to the pronucleus during egg activation. *Dev Biol,* 268**,** 245-57.

Yoneda, A., Kashima, M., Yoshida, S., Terada, K., Nakagawa, S., Sakamoto, A., Hayakawa, K., Suzuki, K., Ueda, J. & Watanabe, T. (2006). Molecular cloning, testicular postnatal expression, and oocyte-activating potential of porcine phospholipase Czeta. *Reproduction,* 132**,** 393-401.

Yoon, S. Y. & Fissore, R. A. (2007). Release of phospholipase C zetaand [Ca2+]i oscillation-inducing activity during mammalian fertilization. *Reproduction,* 134**,** 695-704.

Yoon, S. Y., Jellerette, T., Salicioni, A. M., Lee, H. C., Yoo, M. S., Coward, K., Parrington, J., Grow, D., Cibelli, J. B., Visconti, P. E., Mager, J. & Fissore, R. A. (2008). Human sperm devoid of PLC, zeta 1 fail to induce Ca(2+) release and are unable to initiate the first step of embryo development. *J Clin Invest,* 118**,** 3671-81.

Yoshida, N., Amanai, M., Fukui, T., Kajikawa, E., Brahmajosyula, M., Iwahori, A., Nakano, Y., Shoji, S., Diebold, J., Hessel, H., Huss, R. & Perry, A. C. (2007). Broad, ectopic expression of the sperm protein PLCZ1 induces parthenogenesis and ovarian tumours in mice. *Development,* 134**,** 3941-52.

Yoshida, N. & Perry, A. C. (2007). Piezo-actuated mouse intracytoplasmic sperm injection (ICSI). *Nat Protoc,* 2**,** 296-304.

Young, C., Grasa, P., Coward, K., Davis, L. C. & Parrington, J. (2009). Phospholipase C zeta undergoes dynamic changes in its pattern of localization in sperm during capacitation and the acrosome reaction. *Fertil Steril,* 91**,** 2230-42.

Yu, Y., Halet, G., Lai, F. A. & Swann, K. (2008). Regulation of diacylglycerol production and protein kinase C stimulation during sperm- and PLCzeta-mediated mouse egg activation. *Biol Cell,* 100**,** 633-43.

Yu, Y., Nomikos, M., Theodoridou, M., Nounesis, G., Lai, F. A. & Swann, K. (2012). PLCzeta causes Ca(2+) oscillations in mouse eggs by targeting intracellular and not plasma membrane PI(4,5)P(2). *Mol Biol Cell,* 23**,** 371-80.

Zegers-Hochschild, F., Adamson, G. D., De Mouzon, J., Ishihara, O., Mansour, R., Nygren, K., Sullivan, E., Vanderpoel, S., International Committee for Monitoring Assisted Reproductive, T. & World Health, O. (2009). International Committee for Monitoring Assisted Reproductive Technology (ICMART) and the World Health Organization (WHO) revised glossary of ART terminology, 2009. *Fertil Steril,* 92**,** 1520-4.

Zhang, L., Chao, C. H., Jaeger, L. A., Papp, A. B. & Machaty, Z. (2018). Calcium oscillations in fertilized pig oocytes are associated with repetitive interactions between STIM1 and ORAI1. *Biol Reprod,* 98**,** 510-519.

Zhang, L., Tang, J., Haines, C. J., Feng, H. L., Lai, L., Teng, X. & Han, Y. (2011). c-kit and its related genes in spermatogonial differentiation. *Spermatogenesis,* 1**,** 186-194.

Zhang, N., Duncan, F. E., Que, E. L., O'halloran, T. V. & Woodruff, T. K. (2016). The fertilization-induced zinc spark is a novel biomarker of mouse embryo quality and early development. *Sci Rep,* 6**,** 22772.

Zhang, X. H., Tee, L. Y., Wang, X. G., Huang, Q. S. & Yang, S. H. (2015). Off-target Effects in CRISPR/Cas9-mediated Genome Engineering. *Mol Ther Nucleic Acids,* 4**,** e264.